University of Huddersfield Repository

Zurgani, Emad. K. A.

Documentation of the Body Transformations during the Decomposition Process: From the Crime Scene to the Laboratory

Original Citation

Zurgani, Emad. K. A. (2018) Documentation of the Body Transformations during the Decomposition Process: From the Crime Scene to the Laboratory. Doctoral thesis, University of Huddersfield.

This version is available at http://eprints.hud.ac.uk/id/eprint/34690/

Documentation of the Body Transformations during the Decomposition Process:
From the Crime Scene to the Laboratory

A Thesis submitted to the University of Huddersfield in partial fulfilment of the requirements for the degree of Doctor of Philosophy

Emad. K. A. Zurgani

School of Applied Sciences

Dec 2017

Copyright statement

Abstract

Forensic science is defined as the application of scientific or technical practices to the recognition, collection, analysis, and interpretation of evidence for criminal and civil law or regulatory issues. A combination of computer science in the field of 3D reconstruction and molecular biology science and techniques were employed in this research aims to document and record a complete picture of the body decomposition process including the changes of the microbiome over the decomposition process.

In this thesis, the possibility to reconstruct the crime scene and the decomposition process was investigated. In addition, a 3D model aiming to integrate the biological and thanatological information was generated. The possibility of utilising Autodesk 123D Catch software as a new tool for 3D reconstruction of a crime scene was thoroughly evaluated.

First experiments demonstrated that the number of photos required to obtain the best result was specified to be from 20 to 30 photos as a minimum. In addition, significant experiments were performed in different conditions of sizes, locations, and different involved materials. The measurements were obtained from the models using the same software were compared with the real measurements of the tested objects. The result of the correlation between real and estimated measurements showed a very strong agreement ranging from 0.994 to 1.000.

With reference to the documentation of the decomposition process, there are different factors, intrinsic and extrinsic, have been reported affecting the decomposition of a carrion/body. These factors mainly interact with the rates of the biological and chemical reaction happening after death. The biological reactions are mainly due to the activity of microorganism and insects. Pigs (*Sus scrofa domesticus*) were used as a model for human studies and the results obtained have been applied to other mammals without considering the effect of fur on the decomposition process and on the insect and microbial colonisation. In order to investigate this point, rabbits (*Oryctolagus cuniculus*) with and without fur were used in two sets of experiments at Huddersfield in summer 2014 and in spring 2015.

The results obtained in this study showed a similarity of the decomposition stages between animals with and without fur. However, the decomposition process was faster during the summer due to the fast of insect colonisation and activity. In addition, the entomological data collected during the summer and spring experiments were demonstrated that the same taxa nearly were present in both seasons, except *Hydrotaea* (Diptera, Muscidae), which was

presented only in the summer experiment, moreover, only one sample of *Lucilia sericata* (Calliphoridae) was detected in the spring season. Differences in colonisation time were observed only in spring experiment; animals without fur were colonised two days before animals with fur. The season could have affected the insect's activity and the spread of the decomposition volatiles.

The microbial communities during the decomposition process were investigated using BIOLOG EcoPlate™ and the hypervariable V1-3 region of 16S rRNA gene was used for their molecular identification based on pyrosequencing. Eurofins Genomic Operon using 454-GS Junior pyrosequencing platform (Roche) carried out these analyses.

The functional diversity of the bacterial communities on all carcasses samples showed a considerable variability depending on the stage of the decomposition and the sampling region (Oral cavity, skin and interface-sand-carrion) in both seasons. Furthermore, over the molecular analyses of bacterial communities at the phylum level, four main phyla of bacteria were detected among analysed carrion during the decomposition process. These phyla were changed significantly during the stages of the decomposition and between sampling regions. While no difference was observed due to presence or absence of fur. On the other hand, the analysis at the family level was able to highlight differences at the temporal scale but as well as carrion with and without fur. The statistical analysis results showed a significant difference in the bacterial community family distribution among the presence of fur and among the decomposition stages, with significant differences among sampling regions and seasons.
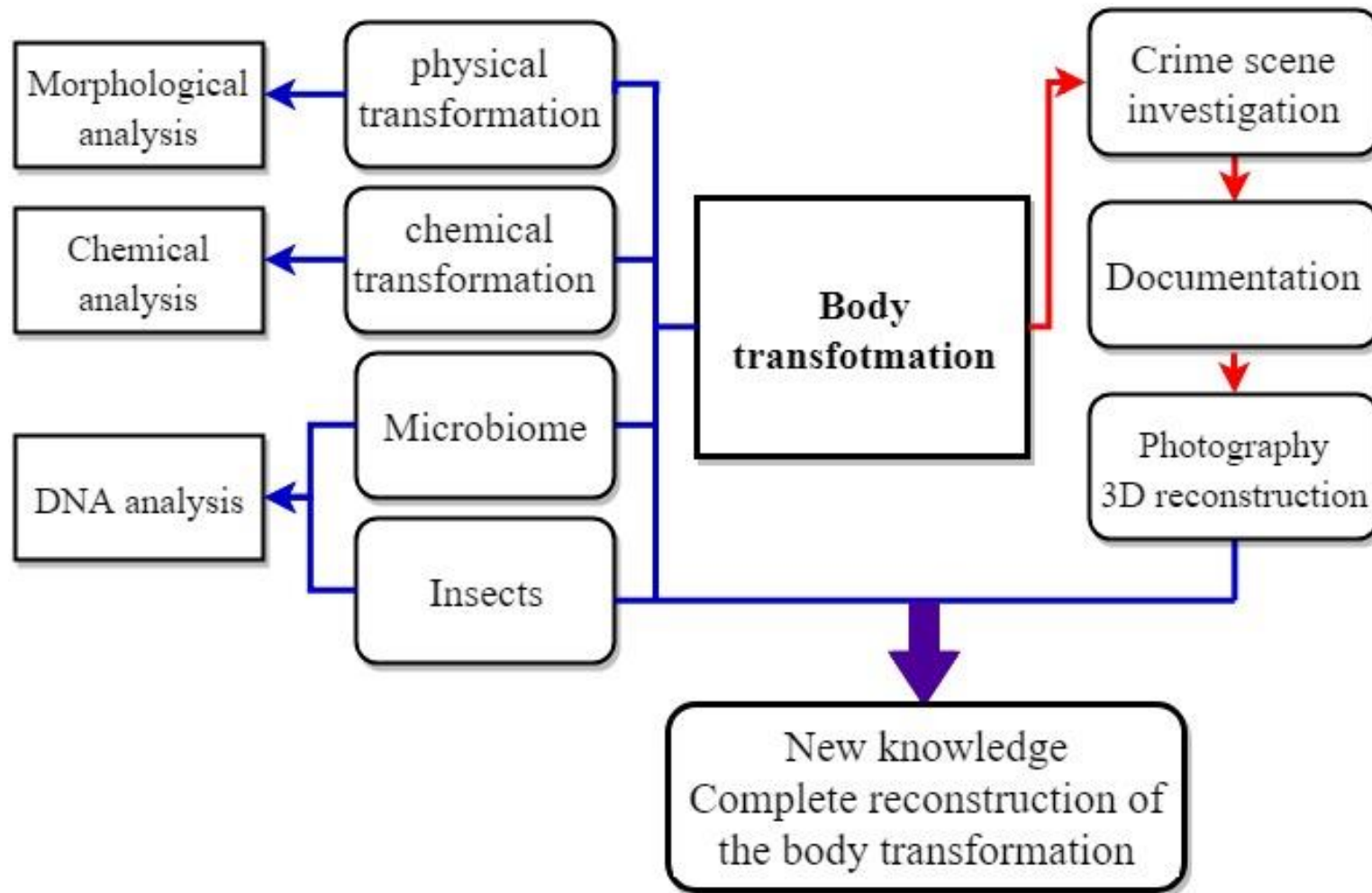
Analysis performed in this thesis

Acknowledgements

I would like to give my special thanks to all who are in one way or another, had helped me finished my research:

- My supervisor, Dr Stefano Vanin, for his guidance and persistent help; for sharing with me his expertise and research insights.

- My family: parents, wife, brothers and sisters for their love and their support continuously in spite of the far distance; and our Almighty God for giving me the strength to face all the challenges in my life and finish this important step.

- All my friends and Huddersfield University staff for their help during the research period.

- Finally, I would like to thank Libyan government for funding my research in this difficult situation.

EMAD. K. ZURGANI

Table of Contents

List of Figures

List of Tables

List of Abbreviations

AAFS	American Academy of Forensic Sciences
ADD	Accumulate Degree Days
ARF	Anthropological Research Facility
ATP	Adenosine triphosphate
AWCD	Average Well Colour Development
CCD	Charge Coupled Device
CI	Colonization Interval
CLPP	Community Level Physiological Profiling
DNA	Deoxyribonucleic Acid
HMP	Human Microbiome Project
ICP	Iterative Closest Points
MCLPPs	Microbial Community Level Physiological Profiles
MMCPs	Microbial Community Metabolic Profiles
mPMI	minimum Post Mortem Interval
NGS	Next Generation Sequencing
OTU	Operational Taxonomic Units
PCA	Principle Components Analysis
PCR	Polymerase Chain Reaction
PH	acidity/alkalinity
PIA	Period of Insect Activity
PMI	Post Mortem Interval
PPi	Pyrophosphate
RH	Relative Humidity
RNA	Ribonucleic Acid
rRNA	Ribosomal Ribonucleic Acid
RT	Reversibly Terminating
SGS	Second Generation Sequencing
SSU	Small Subunit rRNA Database

1. Introduction

1.1 Forensic Sciences

Forensic science comprises applying scientific principles and approaches under the domain of law and legislation aiming for the execution of justice through providing valid evidence that can confirm the location of the committed crime and the scenario that has been followed to commit the crime.

Forensic science is serving two main tasks, analysing the physical evidence, and providing the resultant information to the court (Kirk, 2009). The main principles concerned with the forensic science are the identification and the interpretation of the physical evidence. In fact, the binary combination of science and technology are representing as the independent witness in the criminal or the civil aspects (Saferstein, 2013). Science and technology are having a close term interference, in fact, the most development of the forensic science is depending on the parallel development of the technology in various science fields (Tilstone *et al*. 2013). The provided supporting evidence must be strong and valid enough to be utilised in the legal procedures at an elevated level. The long-standing forms of forensic physical evidence including fingerprints, bloodstains, hairs, fibres, soils, and DNA, which can provide a high degree of the scientific certainty, also, to determine that evidence came from one source. In addition, identifying sampling origin in accordance with the source or sources of a known origin, in order to exclude the rest based on the analysis of evidence (Kiely, 2005).

Physical evidence is having a critical importance throughout the criminal investigation, due to the fact that the information provided by the victims, suspects, and witnesses are considered as incomplete and inaccurate (Council, 2014).

The investigation scheme of the crime scene is including evidence identification, collection, preservation, and transportation, in addition, all the necessary tests that aid in proving or disproving the characteristics of samples. The conducted forensic laboratory analysis might provide a comprehensive platform for characterisation and comparison of the questioned source and the known source samples.

Throughout the investigation process, investigators might provide an alternative interpretation of analyses, with the derivatization of new conclusions (Council, 2014).

According to Klinkner (2009), the basic principles of the forensic science methodological approach are:

- Determination and understanding of the information and evidence that could be spotted at the crime scene.
- Following valid procedures for collecting and recording evidence.
- Implementing the evidence-testing phase according to the standards.
- Providing the evidential requirements for the court judgement (Klinkner, 2009).

1.1.1 The Importance of Forensic Sciences

The forensic science is encompassing a vital part of the reconstruction of the crime scene by using various disciplines including Pathology, Anthropology, Microbiology, Toxicology, Chemistry, etc. The forensic science can provide a supportive evidence in regards to the details of the crime scenario including the crime approach, the location, and the time of the committed crime. Furthermore, the implementation of forensic science approaches and the relevant technology exhibited a remarkable usefulness in investigative cases involving missing people, whether they are crime victims or wanted criminals. Additionally, in regards to the oppression, the mistaken victims, and the relevant forensic cases, the mainstay of issuing the verdicts under the law legislation of attaining justice is based on the forensic scientific evidence in the corresponding crime scene following various scientific and medical approaches (civil and criminal)(Fisher and Fisher, 2012).

Forensic science includes several disciplines from biology to E-crime investigation. A list of some forensic sciences is reported as following:

Forensic Archaeology is concerning the scope of determining the cadaver location and the recovery of the geophysical surveying techniques, moreover, applying photo-documentation and imaging throughout the forensic investigation (White, 2010).

Forensic Anthropology deals primarily with the identification and examination of human skeletal remains (Byers, 2015).

Forensic Ballistics is a scientific domain, which allows the rational application of ballistics for serving scientific purposes, aiming for the attenuation of justice. This heterogeneous discipline of science is availing a major fundamental task which is the restructuring of the fatal or no-fatal

crime scenario associated with gunshot injuries (Karger, 2009). Furthermore, this sector is defined as the science of the projectiles motions, in particular with the crimes committed through the monopolisation of firearms (Warlow, 2016).

Forensic Biology, this scope of science is acting as a layout platform, which permits the intellectual application of the life science knowledge and theories into the forensic investigations sessions. The fundamental attention of this science sector has been directed towards the analysis of the extracted DNA samples and the collected body fluids present at the crime scene (AAFS).

Forensic Computer Science this domain of investigation is concerning the scanning of computers and the suspected devices for the purpose of exploring digital data as a main or supportive investigative evidence (Agarwal *et al*. 2011).

Forensic Entomology is the study of insects, and forensic entomologists use in civil and criminal cases (Amendt *et al*. 2007).

Forensic Engineering is concerning the investigation of the failure analysis, restructuring of accidents, and discovering the origin of combustion and explosions (Saferstein, 2013).

Environmental Forensics is defined as the systematic and scientific evaluation of physical, chemical and historical information for the purpose of developing defensible scientific and legal conclusions regarding the source or age of a contaminant release into the environment (Murphy and Morrison, 2014).

Forensic Graphology is the study and auditing of handwriting, particularly the handwriting associated with characteristic cases such as ransom notes, poison pen letters or blackmail demands (Oliveira *et al*. 2005).

Forensic Odontology is involving the extensive study of teeth aiming for providing information about identification and age estimation. Moreover, this scope of science is concerning the investigation of the bite marks associated crimes (Saferstein, 2013).

Forensic Pathology is applied aiming for investigating the causes of unnatural, unexplained, and brutal death through the implementation of inclusive examination of the body and its remains (Rowlinson, 2015, White, 2010).

Forensic Photography is a fundamental element of crime scene investigation, especially for the documentation purposes. Forensic photographers are responsible for recording the crime scene through photographic techniques and approaches (Osterburg and Ward, 2010).

Forensic Psychology is an area in which the relationship between human behaviour and legal proceedings is examined (Saferstein, 2013).

Forensic Toxicology is the study of the effects of extraneous substances such as poisons and drugs in the body (White, 2010).

Depending on the type of the crime, all these forensic sciences disciplines are functioning collectively aiming for performing a comprehensive investigation and reconstructing various crime scenarios for accomplishing the prime aims, justice restoration and culprit condemnation.

1.1.2 Definition of Crime

A crime is something that is against the law, and it is any an illegal and incorrect action, which is defined by the law as an offence and for which punishment is prescribed. Accordingly, there are four elements which are considered as the base of the crime events, namely, legality, conduct, unlawfulness and guilt (Coetzee, 2009, Douglas *et al*. 2013).

1.1.3 Crime Scene

A primary crime scene is a location where a crime occurred, and where the majority of physical evidence can be found. However, the scene of a crime can be any other places or any other things, which contain physical evidence related to the committed crime. For instance, the vehicle used by the suspects to and from the scene might also contain physical evidence related to the conducted crime, the vehicle will be considered as a necessary area of investigation.

Also, other areas needed to be investigated including the residence place of the suspect, searching for robbed items, weapons, burglary tools, any tools that might be exploited to commit the crime, or any other evidence that can be found, all are defined as a secondary crime scene (Coetzee, 2009).

A secondary crime scene has to be processed in the same way as the primary crime scene to collect the physical evidence. A crime scene can be very small or limited, such as the back seat of the car where the sexual abuse occurred for example, or only one room in the house. Also, it can be wider, like the entire of the house or outside the house (street, garden, etc.) (Dutelle, 2016). The crime scene is the initial starting point for the investigation process to take place, through the collection of the evidence that can aid in the identification of the criminals (LeMay, 2011). Additionally, the comprehensive investigation of the crime scene can allow the logic creation and the reconstruction of the committed crime. Significantly, the investigation process of the crime scene must follow a detailed systematic approach (Bostanci, 2015).

A crime scene can be also classified as following: (Lee and Pagliaro, 2013).

- Type of crime (murder, robbery, sexual assault).
- Physical location (indoor, outdoor).
- Physical condition (buried, underwater).
- The boundaries of the scene (house, computer, car).
- The appearance of the crime scene (organised, disorganised crime scene).
- Activity (active, passive scenes).
- Size of the crime scene (wide, macroscopic, microscopic scene).

1.1.4 Evidence

The evidence is defined as any information or objects submitted legally to the court as a leading proof of the discovery and the confirmation of the truth of any alleged and suspected mater of facts under investigation. Moreover, under the forensic science context, the evidence is synonymous with the exhibit in legal terms. The evidence is defined as any item or sample collected from the crime scene as a result of the investigation process, including any objects, biochemical or chemical substance, marks and traces such as swabs, whole objects, fibre, debris, fingerprint, and footprints or tires, etc. that provide information about the investigated crime (Tilstone *et al*. 2013).

The primary sources of physical evidence are the victim, suspect, and crime scene, in addition, the secondary sources include the residence place or any places related to the suspect (Douglas *et al*., 2013). The exploration and examining of evidence can support the forensic investigation in variable manners; for instance, trace an illegal substance, identification of the remains, or the

reconstruction of the crime scenario. These investigative approaches can be implemented utilising tools and techniques aiming for the identification, collecting, analysis, data interpretation, and evidence preservation. Generally, evidence cites data or items that can be exploited in the court to be considered by the judges and juries(Lee and Pagliaro, 2013).

1.1.4.1 Forensic Evidence

The science area of application in criminal law usually concerns evidence collection, analysis, and interpretation of information. Due to the complexity of the crime scene environment, different scopes of science have to be used simultaneously (Kiely, 2005). In order to reconstruct the criminal events, various kinds of evidence can be collected and thoroughly analysed. In terms of the accepted legal characterisation, forensic science evidence can be divided into two kinds as follows:

- Testimonial evidence, which is the evidence provided in the form of statements made under oath.
- Real evidence, is based on the examination of exhibits, which can be in a wide area such as a house, or small as fibre, or as fleeting as an odour, or as obvious as the explosion scene.

Forensic evidence can be classified depending on their utilisation throughout the investigations (Table. 1) (Tilstone *et al.* 2013).

Table 1.Forensic evidence classification.

Type	Discerption	Example
Inceptive	Refers to the commission of a crime	Identification of the fire cause is it (accident, arson)
Exclusionary	Eliminates something and thus refuse a hypothesis	DNA profiling of semen in a rape crime
Associative	Uses exclusion and confirming to assess the links between people and places	Soil, fingerprint, DNA
Corroborative	Supports a hypothesis but could arise for other reasons	Fibres on the suspect clothing that could come from the victim clothing

Additionally, evidence can be classified into other two essential categories as follows:

Direct evidence; includes eyewitness statements or recorded video by police cameras. In court, direct evidence involves testimony by a witness about what that witness personally saw.

Circumstantial evidence; is an indirect evidence that can be used to reconstruct the criminal event but not in a direct way. Moreover, the circumstantial evidence may provide the relation between the crime scene and the suspect. The nature of this evidence could be physical or biological nature, the physical evidence includes tool marks, or impressions such as fingerprint, footprints, and tire impression (Fig. 1).

Moreover, physical evidence includes fibres, weapons, and bullets, etc. While the biological evidence including body fluids, hairs, parts of plants, and natural fibres. Most of the collected physical evidence, except the fingerprints, is aiding the reduction of the numbers of the suspects. In addition, the biological evidence might usually limit the suspects to a small group, or sometimes reduce them to the most likely individual (Ramsey, 1996).
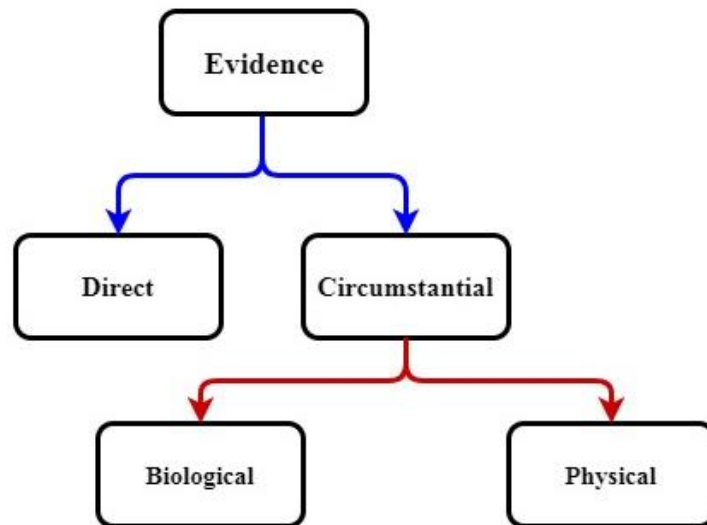
Figure 1. Evidence classification.

List of some common physical evidence with the commonly associated forensic analysis is listed as following: (Kiely, 2005, Layton, 2006, Schiro, 2007).

- Shells (Ballistics).
- Signs of teeth (biting) bite marks.
- Fragments of glass.
- Shoes (footprint).

- The impact of the wheels of vehicles.

- Trace evidence.

- Body fluids (DNA analysis and patterns of blood).

- Paint (Analysis of paint flakes).

- Marks on the tools (analysis crush, scratch and digging).

- Hair (All analyses of hair (human - animal).

- Fibres (All analyses of fibres (natural - Industrial).

- Fingerprints.

- Firearms.

- Documents (Forgery (analysis of documents).

- Soil and dust.

This kind of evidence is questioned by the AAFS validation committee.

1.1.5 Crime Scene Investigation

Crime scene investigation is an important area in forensic science, it is the first step of the criminal investigation process after conducting the crime scene analysis and collection and submission the physical evidence to the relevant forensic laboratories. Crime scene investigation is not a mechanical process, but a sequence of steps that allow the reconstruction of the crime scene. Scene processing is the term applied to describe the sequence of steps and the proper measurements taken to investigate a crime and to reconstruct the circumstances of the crime, through the identification of the events and collect the physical evidence that can lead to the identification of the offenders (Gardner, 2011). Crime investigation usually begins at the place where the crime was committed. The area has to be secured for preventing the destruction of crucial physical evidence and preserve any useful information that can lead investigators to link the perpetrators to the victim. The size of the area to be secured varies with each crime, and a series of protocols prepared to secure and protect evidence should be followed (Fish *et al*. 2013). The crime scene investigation is more than the careful and attentive processing, documentation, collection and packaging of the physical evidence, it is the integration of all the formerly mentioned elements within the forensic processes.

Nevertheless, the crime scene investigator or forensic scientist ability to identify the potential various physical evidence is the foundation and base of all the forensic investigations.

The following recognition of physical evidence besides the identification of the probable source of the evidence is the next step. In fact, the crime scene investigations are the first step towards understanding and establishing what, when, where and how the crime happened as well as the suspects involved in the crime (Lee and Pagliaro, 2013).

1.1.5.1 The Process of Crime Scene Investigation

Processing and managing the crime scene as technical disciplines are considered as major critical aspects of the effective criminal investigations (Julian *et al*. 2012). A crime scene investigation identifies the cascades of events, which have been taken place and led to the committed crime through the careful organisation, documentation, collecting, preserving, interpreting, and reconstructing the physical evidence at the crime scene. Moreover, the objective of the examination of the physical evidence is to provide supportive information to the investigation process. From the intersection and the positive collaboration of these objectives, a proper scientific crime scene investigation can be obtained and accomplished (Julian *et al*. 2012). The investigator processes the scene in a logical order by following the requested various stages (Fig. 2) (Gardner, 2005).

Figure 2. Schematic representation of the process of crime scene investigation.

9

1.1.6 Crime Scene Documentation

Documentation of crime scene is a preliminary step in the crime scene investigation process and the reconstruction of the crime (Fisher and Fisher, 2012). Documenting the scene begins with the first responding officer, for any class of cases, whether it is a burglary, assault, accidental death, etc. The crime scene must be documented after conducting an extensive evaluation by the initial scene survey. Prior to any shifting or moving or even touching of items present in the crime scene, the whole scene must be fully documented to ensure a permanently preserved recording of the scene in the first founded initial condition. Thus, the main aim of the documentation process is to record and to preserve the situation of the crime scene and the relation between the physical evidence found in the scene. Moreover, to link the physical evidence with the crime scene status when it was observed by the examiner (Dutelle, 2010).

The documentation of the crime scene is the most time-consuming activity among the investigation cascade and requires the investigator to remain organised and follow a systematic approach throughout the process for more comprehensive and complete documentation process and more accurate and defensible the reconstruction can be (Scott, 2009).

In the documentation phase for processing the crime scene, all functions have to be in correspondence and to be consistent in depicting the crime scene. Consequently, the fully documented crime scene permits the ability of the investigators to perform the effective reconstruction of the crime event and deliver it to the courtroom. There are different methods to document a crime scene such as description, notes, printed forms, sketch, 2D drawing, 3D-models, photography, and videotapes. The documentation is important to create a detailed record of the scene, evidence recovered, and actions, which have been taken place during the search of the crime scene (Abu Hana *et al*. 2008).

However, the four major steps of the documentation process are noted as recording, videography, photography, and sketching. All of these four steps are necessary to be implemented and none can perform as an adequate substitution for the other. Any type of demonstrative evidence must be verified by authenticity, accuracy and identification (Gardner, 2011). The accurate recording of crime scene details is crucial for several reasons: first, it will provide investigators with unaware information; furthermore, it will provide an assisted in the reconstruction of the scene by the court. Nowadays, high geometric accuracy 3D crime scene

reconstructions techniques are frequently used for forensic investigations, since evidence gathered with topographic and photogrammetric devices can be more compelling for juries and allow investigators to virtually revisit a crime scene (Agosto *et al*. 2008).

Furthermore, to ensure the integrity of all evidence recovered from a crime scene and demonstrate the credibility of a crime scene investigator, it is important to make extensive records. This requires the completion of several interrelated documents for all of the recovered items (Scott, 2009). In the other hand, errors can be raised from the incomplete documentation; therefore, all aspects of the scene have to be documented through the crime scene photography, ensuring that all critical evidence has been documented. Adherence to a systematic photographic technique as well as a standard scene processing model will significantly eliminate possible errors (Gardner, 2011).

However, the purpose of the crime scene documentation is not just to document the physical evidence, but also to document the whole scene. The term entire scene including the unreachable points in the walls, ceilings, and objects. The lack of photo-documentation of these areas may result in claims by lawyers of evidence that was present on the surfaces that the photography "missed." For an accomplishing a successful photographic documentation, the entire scene must be completely documented through photo capturing, in both cases of presence or absence of evidence to prove that nothing was there (Dutelle, 2010).

There are multiple reasons, which confirm the significance of documenting the crime scene, one of the prime reasons is to provide a permanent record of the crime scene in the initial founded state to be used during the investigation, to function as a reminding tool for the investigators or witness, also, in court if the case culminates in a trial. An additional reason is to provide a platform for counting the steps followed during the processing of the crime scene. Furthermore, documenting the degradable physical evidence in which the preservation process is problematic until its recovery from the scene (Jackson *et al*. 2011). In addition, the essential tools which aid in the effective documentation of the crime scene during investigation including Photographs, sketching, videography and the CSI's reports (Fish *et al*. 2014).

1.1.6.1 Reports or Notes

Extensive recording of notes and observation for all physical evidence recovered from the crime scene is considered as a significant aspect, including the location in which the physical evidence

has been discovered, who has collected the evidence, at which time, and a description of the item itself. Additionally, overall notes regarding the scene should be recorded, including the surrounding environmental conditions, and any other relevant details. Sketches are generally utilised to provide an illustration in regard to the locations, dimensions and significant object orientations founded at the scene, also the relevant measurements (Fish *et al*. 2014).

A chronological order for the documented notes and observations is important, and it must be exhibiting the lack of any analytical findings, conclusions, or personal suggestions. Subsequently, the documentation areas of the investigation process are only restricted towards the crime scene observed facts, the documented notes are adaptable to any updates throughout the investigation process. In addition to the observed notes, there are vital factors needed to be recorded such as the date and time indicators (e.g., newspapers, Mail), general descriptions of the scene and surrounding area, open doors and windows, any person who was present at the crime scene, victim and witness statements, odours or any characteristic smell and lighting conditions (Miller, 2013).

1.1.6.2 Sketches

Sketches are utilised along with the images and reports to document the crime scene. A crime scene sketch is a simple drawing that exactly demonstrates the state of a crime scene, the position of the relevant items, and the relationship of the items (Saferstein, 2013). These must include the real measurements, without the urgent need to reach to the architectural drawing scale. Furthermore, for courtroom presentation, the hand-drawn sketches can be converted using computer programs such as CAD, which provide a dynamic, professional appearance to the sketches (Dutelle, 2010).

One of the main advantages of a sketch is that it can cover wide spaces and scenes; also, it can be instantly sketched to give a clear diagram of the scene with the accurate orientation. Sketching acts as a complementary aid to the photographs and videos of the crime location to obtain the proper dimensions of the crime scene as both (pics and videos) can distort those measurements. Usually, the usage of the sketch gives a complete detailed of the crime scene status, whereas the two dimensions' photograph does not show the accurate measurements of objects and between them. Moreover, the sketch is able to represent the whole scene in one paper (Miller, 2013).

Rough sketches and final sketches are the two types of sketches used for documentation of crime scene (Fig. 3) (Saferstein, 2013).
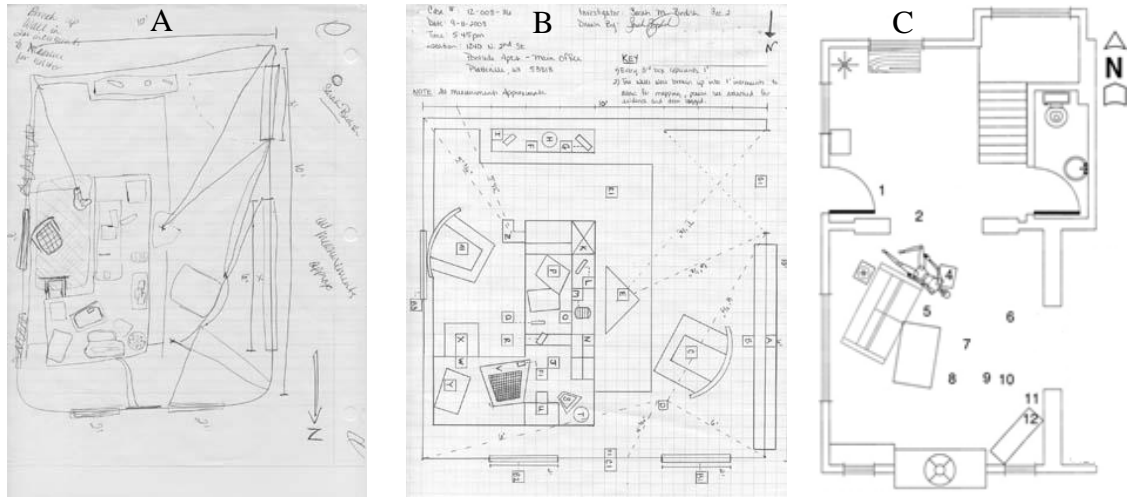
Figure 3. (A) Example of a rough sketch (B) final sketch (C) Example of a final sketch using CAD program.

The sketch is considered as an important aspect of the documentation of the crime scene as it describes the physical facts accurately. It also provides the ability to document the exact site and present the relation between the existing objects and the observed evidence at the crime scene. In addition, it can be a useful tool in the creation of the overall picture of the crime scene for the distanced observers such as judges, juries, witnesses, and others. Furthermore, it can provide a permanent piece of court acceptable record of the crime scene. Additionally, it can thoroughly support the preparation of the investigative reports by the investigators and provide help for the clear presentation in the court by the case presenters (Layton, 2006).

1.1.6.3 Videography

Scene documentation also includes videography, especially in murder cases. Video recordings can provide supportive information for the layout of the crime scene, such as the specific time intervals, which was required to move from one location to the other, and how many turns were presented. Once the investigation has proceeded further, detection of forgotten things and errors (Layton, 2006). Illustratively, during a video walk-through the crime scene, the crime scene investigator captures the whole crime scene and the areas around the scene from all the possible angles and record a continuous audio narrative (Fish *et al*. 2014).

1.1.6.4 Photography

Photography is the most important of the crime scene documentation techniques, by producing a lasting visual record of the crime scene and discovered evidence (Scott, 2009). Photographs capture time in a unique way; they provide a static representation of a scene, reflecting its properties at a specific time interval. The photography is the essential way in the documentation process and an important tool in the field of crime scene investigation. Photos are captured of the overall scene as soon as possible to record the scene as it is observed before anything is handled, moved or added to the scene (Pastra *et al*. 2003).

Photos cover the condition and orientation of the overall scene, the location, and if possible, the relationships between different areas in the scene as well as to the various items of evidence found at the scene (Suboch, 2016). Photo documentation allows the viewer to observe the necessary detail of specific items found in the scene (Miller, 2013).

Collectively, all that can be achieved by three main kinds of photos, which crime scene investigators need for crime scene documentation as follows: (1) Overall scene photos showing the possible view of the scene. (2) Evidence-establishing or mid-range photos presenting the relation between the items. (3) Evidence close-up (Layton, 2006).

Close-up photos are usually captured of the items that include serial numbers or tags. The following photo with the addition of a measuring tool is captured for the same items; these photos help the analytical process. In addition, special techniques of photographs such as panoramic photography are used to capture the large scene (Layton, 2006). The human visual is nearly 180 degrees, but that of a standard 50-mm camera lens is approximately 80 degrees. Photos are taken and merged together using different software to present a complete view (Fisher and Fisher, 2012).

1.1.6.4.1 Capturing Photos of the Scene

The photos can provide supportive evidence and information about the crime scene only when the images capture the whole scene. On the other hand, the images can be misleading due to the type of imaging capture process (perspective projection, lens distortions, etc.).

The main objective of capturing the overall photographs is to recover the general condition and layout of the scene. The photographer always seeks to capture the whole scene including the

most visible landmarks (e.g., doors, furniture, bodies), and the original condition of the scene prior to the significant change. Therefore, overall photographs are always the first photos taken (Suboch, 2016).

Overall photographs normally are used to capture the room or the scene. Usually, it is believed that taking photos from the opposite corners of the scene is a good practice for the overall photographs capturing (Fig. 5). Through repeating this process for each corner of the scene, which is resulting in four photos that provide overlapping coverage of the complete scene. In addition, wide-angle lenses (e.g., 28 mm lens) are often used to allow the photographer to capture a wider view in a single photo. The ability of the photographer to capture wide areas of the crime scene can be enhanced through the utilisation of extreme wide-angle lenses, although, as the field of the view increases, more peripheral distortion might occur. Therefore, a wide-angle lens is not suitable for crime scene and evidence photography (Gardner, 2011).

Figure (4) summarises three different kinds of photos capturing form different scenarios. Panoramic images are also affected by similar problems. In fact, manual modelling of the scene is difficult and may not result in a realistic model (Bostanci, 2015).

| | Interior | Isolated Object | Façade |
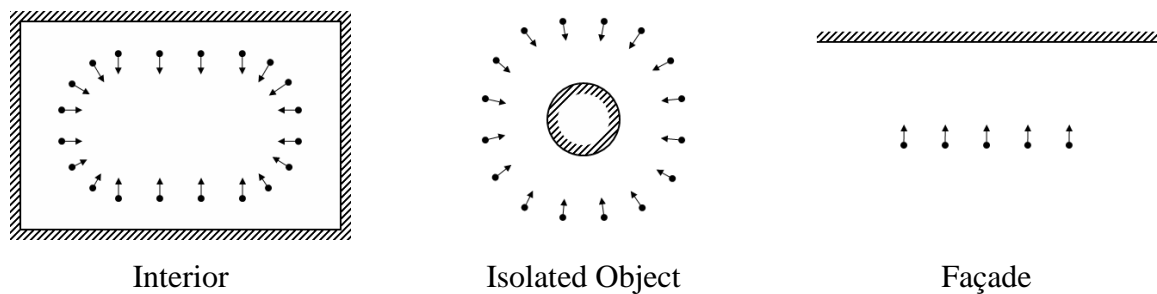
Figure 4. The directions of photos taken for different cases of capturing the object or the scene.
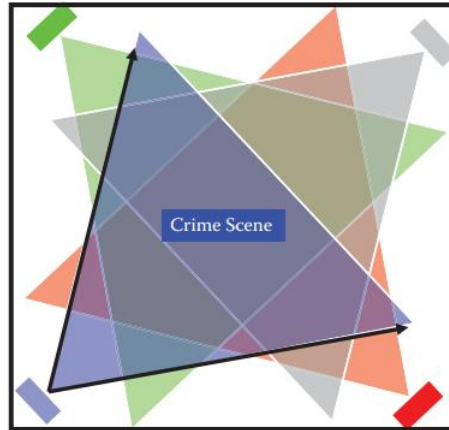
Figure 5. Overall photographs are exposed so they overlap each other. A typical procedure is to go to the corners of a room and take a photograph from each one, looking to the opposite corner.

1.1.6.4.2 Digital Imaging

Digital imaging is recently considered as a powerful new technology utilised in capturing, analysing and recording the crime scene and the associated physical evidence (Fig. 6). This introduced technique utilised as a complementary to the traditional common tools: video, photography and sketches. they all have been utilised collectively in crime scene documentation for criminal investigation (Mennell and Shaw, 2005).

The digital images are featured with superior advantages including the ease of access to the captured images, the simplicity of integration into the common electronic technologies, overcoming the need to the expensive film processing equipment and special rooms. The major drawback of this technique is the vulnerability to the digital manipulation, which can affect the issue of court admissibility. However, implementing policies and written precautions in order to monitor and regulate the use of the digital images can minimise and eliminate the defects and the disadvantages of the technique. As proclaimed and agreed by the law enforcement community, the digital imaging in crime scene documentation can be effectively utilised as a supportive supplemental technique, but not as a complete replacing approach to the traditional common techniques (Bostanci, 2015).

Figure 6. Recording of crime scene and evidence using a handheld digital camera.

1.1.7 Crime Scene Reconstruction

The reconstruction of the crime scene has been developed and evolved during the 1990s as a new aspect of forensic sciences that combines areas from a number of different disciplines. Crime scene reconstruction is the use of scientific methods, physical evidence, and their interrelationships to gain a clear knowledge of the series of events related to the crime (Clemens, 1998). In general, the crime scene examinations are recommended to be performed as quickly as possible, although in some exceptional circumstances a delay in the investigations is approved. This is a result of the nature of the evidence, as it is usually ephemeral and lasts for a very short time. Moreover, the scenes of crime might present a variation in the evidence. This variation stands as an enormous challenge facing the investigators and forensic examiners efforts to record and document the scene details for subsequent analysis. This typically includes detailed measurements by means of photography and videography. Subsequently, investigators create scale drawings of the scene, and in some cases, they make physical models. The main purpose of reconstructing a crime scene is to obtain accurate information describing the cascade of events surrounding the committed crime using physical evidence, scientific methods, and their interrelationships. Both the evidence found at the crime scene and the evidence collected during the time of the crime, contribute the reconstruction of the crime scene in four dimensions: width, depth, height and time (Knox, 2012).

Crime scenes can be reconstructed using various levels of detail is correlated with the aim of investigations. A crime scene reconstruction is a process of determining or eliminating the actions that happened at the crime scene by the analysis of the crime scene pattern, in addition,

the location and position of the physical evidence, and the result of the laboratory examination of the physical evidence (Lee *et al*. 2001).

Throughout the recent years, the persistent improvements in technology are followed by a parallel interest in implementing this technological technique to ease the forensic investigation, these techniques such as designing computer graphics software which can simulate the crime scene. This approach can offer several advantages in comparison to the traditional methods, including the creation of a partial realistic view of the scene from different positions and angles, additionally, combining forensic with the computer modelling. Until now, most of the crime scene reconstruction provide adjustable 2D and 3D views of Cad models, rendered using standard local illumination techniques. While such systems can be of substantial benefit to investigators, they are not primarily concerned with creating reconstructions that attempt to be realistic (Howard *et al*. 2000).

The overall all documentation process, including the pictures capturing, recording measurements and notes of the crime scene is considered as a problematic process. Therefore, it is required to assign updated approaches featured with accuracy, details oriented, fast, and capable of preserving, viewing, and preserving the crime scene to the jury. As an out to date example, one of the advances in the useful recent technology in law enforcement is the developing and the adaptation of the high-resolution cameras that poses the ability to capture multiple images during a short period of time. This technique can aid in cataloguing the entire crime scene and documenting most of the details present in the crime scene, thus, considering it as a useful tool for the investigator and for court the presentation. Some cameras are designed to able to capture images in 360 degrees, these cameras are offering a massive ease of utilisation and great flexibility. Furthermore, the laser scanners are more precise in the investigative scene. A permanent visualising record of the entire crime scene can be digitally created through this technology. Additionally, it permits the investigator to review the image immediately after capturing it and allows the proper adjustment to the captured photo. Consequently, the reconstruction of the crime scene has been evolved during the recent years, and becomes an implementation area for imposing the high and sophisticated technologies, such as Total Stations, Panoramic cameras and now 3D Scanners (Fig. 7), instead of the outdated techniques, such as the tape measure and recording information and data in a paper forms (Keith, 2015).

The process of crime scene reconstruction should be performed optimally in a short period of time, thus, time management and arrangement is a problematic factor in the investigation.

Additionally, the crime scene is vital entity can provide supportive perception in regards to the crime event cascade, which has been taken place in a specific time interval, and in accordance time unit, second, minutes, hours, and even days or more. Therefore, the prolong recording time can inform about the magnitude of evidence which has been observed and collected thoroughly, also, the sequence of recording is considered as a vital aspect through the documentation (Knox, 2012).
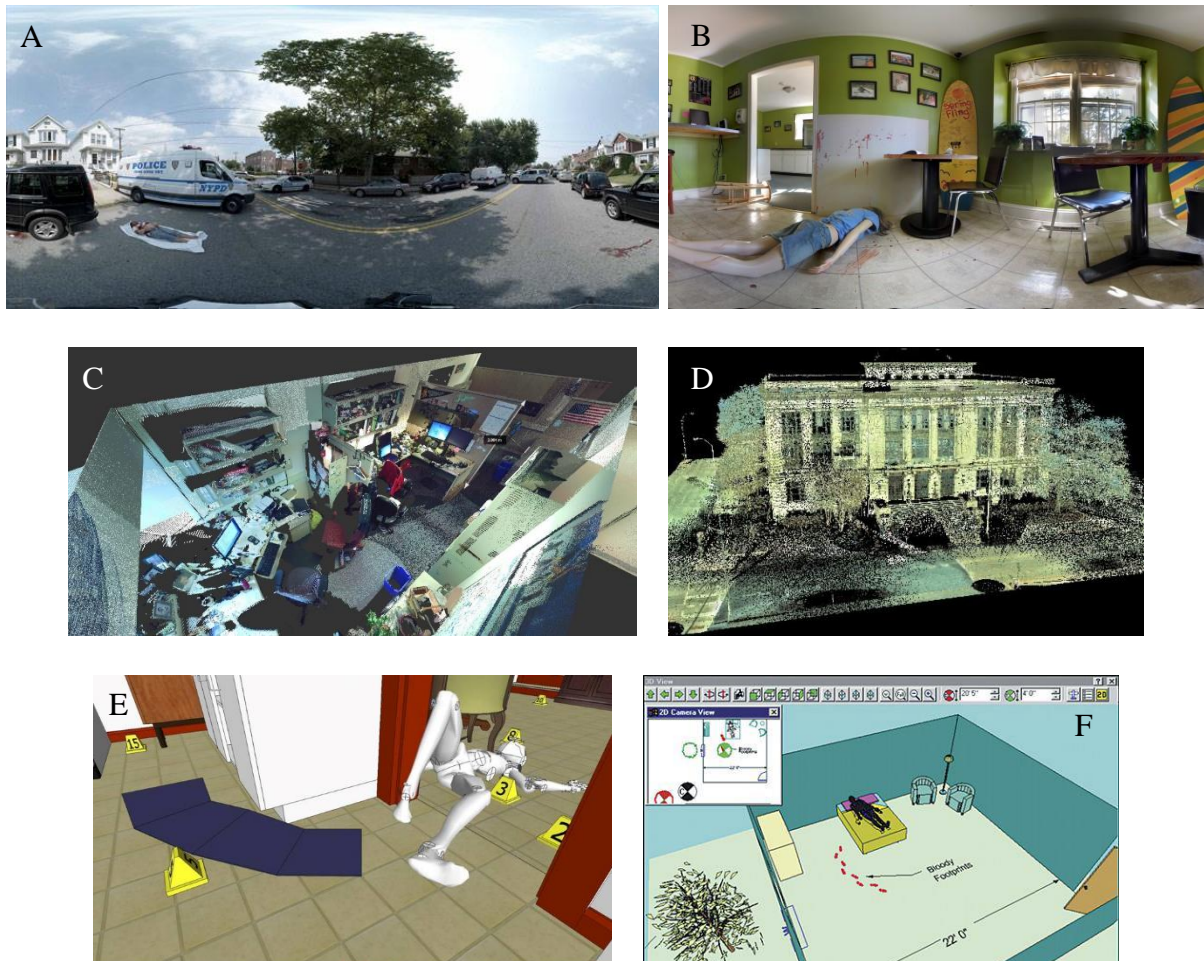
Figure 7. Different approaches used for capture a crime scene. (A, B) outdoor and indoor panoramic images. (C, D) outdoor and indoor Laser scanner generated point clouds (E, F) Sketch up and 3D modelling.

1.1.7.1 Importance of Crime Scene Reconstruction

The accurate recording of crime scene details is crucial for several reasons; providing the investigators with visual information that they may not otherwise have known about. Furthermore, it will support the scene investigation and the clear presenting to the court

(Chisum, 2006). Nowadays, high geometric accurate 3D crime scene reconstructions are frequently used for forensic investigations. This is due to the fact that evidence collection with photogrammetric devices can be more compelling for juries and allows the investigators to virtually "revisit" the crime scene (Agosto *et al*. 2008).

One of the most useful ways to find out the real scenario of the crime is to limit the possibilities that created the crime scene or the evidence as found. The integrity of the crime scene is the main driver for reconstructing the crime (Lee *et al*. 2001). Moreover, the reconstructing of the crime scene is one of the major ways to preserve the integrity of a crime scene. It is different from re-creation or criminal profiling. Recreation is by replacing the essential things or activities at the scene of a crime according to the original scene documentation. Whereas, re-enactment is by re-ordering the scene of a crime by suspect, witness or another individual depending on their information about the crime. Criminal profiling depends on psychological and statistical analysis of the scene in order to identify the attributes of the suspect, which can be considered as a supportive aspect of the forensic investigation. In spite of that, these analyses are not commonly used in solving crimes. Reconstruction is established on the capability of imposing the accurate observations at the scene, the scientists ability to observe physical evidence and using the logical routes to formulate the theory (Miller, 2013).

1.1.8 3D Reconstruction

In the last years, the generation of 3D models for objects has become a topic of interest for several researchers. Particular attention has also been paid to the reconstruction of realistic human models, which could be employed in a wide range of applications (Pollefeys, 1999). Compared with a conventional photography, the 3D reconstruction of the crime scene is not restricted to the idea of acquiring an album of photographs with a 360-degree image of view, but it is an integrative process composing of a variety of scene elements, which shows the actual place where the crime occurred (Liao *et al*. 2015).

Crime scene investigation in the three dimensions can be an effective means to a more comprehensive understanding of the details of the crime (Ma *et al*. 2010). In addition, 3D is a highly effective tool for communicating complex scenarios to a jury and aiding counsel in describing and presenting a situation. Repeatedly this has proved to be an intriguing communication tool by enhancing the concentration of the jury, clearer descriptions and detail

can be retained. In addition, 3D crime scene reconstruction can be considered as a cost-effective approach through the elimination of the unnecessary site visits (Se and Jasiobedzki, 2005).

A crime scene reconstruction in three dimensions is developed as an extension of current techniques of crime scene investigation. Developing an accurate 2D model of the crime scene is the first step in a crime scene reconstruction; also, crime scene photography is a basic and important driver to create 3D models. In addition, crime scene investigators collect other data including measurements to help create accurate 3D models. A 3D model is an accurate mathematical representation of the actual crime scene (Sauter, 2011).

Obtaining three-dimensional reconstructions of scenes or objects from images has been recently considered as an interesting area of research in relevance to the computer field and other concerned domains, which are interested in the aspect of the 3D modelling. However, in all cases, accuracy is the basis that needed to be obtained through exploiting sophisticated devices with high technology, with drawbacks of affordability and the requiring of high expertise specialists (Pollefeys *et al.* 2000). Nevertheless, obtaining realistic models considered as a laborious and costly task, in plus to the on-site measurements, the manual restructure of the whole site, the correction, and the utilisation of the additional software can all be a time-consuming task. Although, a consensus of agreements in regards to the best technique which can be implanted for the 3D reconstruction. In general, a supportive range of sensors, laser scanners, presents throughout many applications, the combination and the integration of different recording techniques, in particular when surveying large and complex sites, is the optimum method to be followed, which can ensure the accuracy, the portability, and the low-cost, fast acquisition, and flexibility (Remondino, 2011).

Accuracy: Precision and reliability are key factors of metric surveying unless the work is performed for simple and quick visualisation.

Portability: the portable techniques are superiorly appropriate due to accessibility issues through many sites, particularly in the absence of electricity, location constraints, etc.

Low cost: with the limited budgets that documentation missions have. The relatively inexpensive 3D methods such as photogrammetry using a digital camera can obtain high-quality information.

Fast acquisition: most sites have limited time for documentation.

Flexibility: Due to the variety and the dimensions of both locations and objects, the used technique should be adaptable to a variety of scales and it should be applicable in various conditions (Remondino, 2011).

1.1.8.1 Methodology of 3D Reconstruction

Reconstruction of three-dimensional models is needed for various applications utilising various techniques and technologies, although, it considered as a complex process. The reconstructed 3D models can be used in virtual environments for visualising applications, classification and analysis. Some methods of 3D reconstruction are presented as following:

1.1.8.1.1 Handheld Devices

Several applicable techniques that can impose throughout the crime scene to aid in defining the location, recording and recovering the physical evidence. The urge of using the technology to aid the investigation is raising throughout the years, in parallel with the introduction and the upgrading of the digital cameras. The utilisation of the specialised digital cameras, as previously mentioned, can support the investigation through documenting the crime scene, briefing purposes, or to create a 3D model (Mennell and Shaw, 2005).

The order of photos captured with a digital camera used to create 3D models, and the camera motion is recovered by comparing the key features in the image sequence. Dense stereo matching is performed between the sequential frames. The input photos are used as a surface texture to obtain photorealistic 3D models. However, it requires a prolonged processing time and the outputs of a scaled version of the original object. Another device is a self-referenced sensor, which consists of two cameras and a cross-hair laser light projector. Frame to frame registration is achieved using a set of fiducials projected with an additional stationary laser system. The system requires a long acquisition time as it can capture only sparse 3D data for each frame and the 3D models do not have a photo-realistic appearance. Additionally, a real-time 3D modelling approach that enables the user to rotate an object and observe a continuous and updated model as the object is scanned. It consists of a 60Hz structured-light rangefinder and a real-time variant of ICP (iterative closest points) for alignment. It is limited to the outside-looking-in case and does not acquire colour. In addition, the Model Camera, which is a low-cost hand-held scene-modelling device. It consists of a digital video camera with 16 laser

pointers attached to it. Model Camera acquires 16 depth samples per frame and registers the frames using depth and colour information. The surfaces are approximated with a few quadratics and this approach only works for smooth continuous surfaces ISM utilises stereo cameras to gain 3D data, detect the camera motion and record successive frames together. The resulting models are fully calibrated (allow Euclidean measurement) and have a photo-realistic appearance. The data acquisition and processing takes minutes (Se and Jasiobedzki, 2006).

1.1.8.1.2 3D Laser Scanner

The 3D laser scanner is a technique that is majorly oriented for scanning the physical objects by projecting the adjustable laser beam directly to a targeted object in a closely spaced grid of points. Through measuring the time of the laser light projection, which is the required time for the laser beam to pass from the scanner to the physical objects and reverse back to the scanner, the establishment of positioning in three-dimensional space of each scanned point on the object required. Consequently, the representation of the obtained data will be in the cloud form of collective points, which consists of nearly a thousand points in three-dimensional space that is accurately correlated to represent the existing object. The concluded information can be feasibly converted into a 3D CAD model that can be modified and manipulated with ease exploiting CAD software, in which the structure and the design of the new equipment can be efficiently added (Arayici *et al*. 2004, Gasser *et al*. 2001).

Terrestrial laser scanners are commonly been used in the constructing objects from buildings and natural environments due to the efficiency in acquiring high data rate, high accuracy and high spatial data density. Considering the variability of parameters from one instrument to the other, the acquisition rates can vary from 1 to 6 kHz, ranging accuracy varies from 5mm to 25mm (Arayici, 2007). Nevertheless, the problem with a 3D laser scanner is that laser beams projected from the device may not always reflect back to the sensor properly due to the difference in surfaces types. Furthermore, additional parameters to be considered in relevance to the affordability of the devices and the cost-effectiveness, the range of existing prices deemed to be expensive, in addition, specialists to run these devices properly are needed (Bostanci, 2015).

The essential technical characteristics of laser scanner are listed in table 2. In addition, several required accessories (i.e. laptop, tripod, batteries, and marks) are also shown in Figure 8 (Fernandez-Sarria *et al*. 2013).

Figure 8. Laser scanner accessories required. (A) Leica scan station (B) Aiming mark on a tripod (C) Scanned target.

Table 2. Main characteristics of the Leica Scan Station Laser scanner (Fernandez-Sarria *et al*. 2013).

Instrument type	Pulsed, dual-axis compensated, very-high-speed laser scanner, with survey grade accuracy, range, and field-of-view
User interface	Notebook or Tablet PC
Camera	Integrated high-resolution digital camera
Accuracy of single measurement	6 mm Position 4 mm Distance Angle (horizontal/vertical) 60 µrad/60 µrad (3.8 mgon/3.8 mgon)
Laser spot size	From 0 – 50 m: 4 mm (FWHH-based); 6 mm (Gaussian-based)
Modelled surface precision/noise	2 mm
Target acquisition	2 mm std. deviation
Dual-axis compensator	Resolution 1 ", dynamic range +/- 5
Data integrity monitoring	Periodic self-check during operation and start-up
Laser scanning system	Range 300 m @ 90 %; 134 m @18 % albedo. Scan rate Maximum instantaneous: up to 50,000 points/sec. Average: dependent on specific scan density and field-of-view Scan density <1 mm max, through full range; fully selectable horizontal and vertical spacing; single point dwell capability
Laser class	3R (IEC-60825-1), visible green
Lighting	Fully operational between bright sunlight and complete darkness
Power supply	36 V; AC or DC; hot-swappable
Field of view (horizontal/ vertical)	360/270
Scanning optics	Single mirror, from an upper window design
Integrated colour digital imaging	User-defined pixel resolution; low, medium, high

1.1.8.1.3 Other Methods

A computer software is available to present the crime scenes in two and three-dimensional. In addition, some computer programs have the ability to draw crime scenes to the required scale and have been used to impose drawing movement in shooting scenes to be utilised in the

reconstruction of the crime scenes. Moreover, some programs are able to describe the scene in three dimensions similar to video slices, which can provide a simulated, experience for the viewer to create the crime scene utilising computer graphics. These systems have been used in the courtroom to project the video image onto a screen and to provide an explanation to a jury in regards to the condition and the sequence of events in the crime scene. The software also can be used to describe the crime scene in drawn format depending on the victim or the suspect scenarios (Fisher and Fisher, 2012).

1.1.8.1.4 3D Reconstruction Using Photogrammetry

Butnariu *et al*. (2013) described the process to formulate the proposed methodology for image-based 3D reconstruction of an object (Fig. 9) to cover the following steps:

Acquire a set of images: The first essential step in geometric reconstruction using principles of photogrammetry is to obtain a set of images of the object that is intended to be reconstructed. The way in which photographs are acquired is a very important aspect greatly reflected in the quality of the final reconstruction. The object is photographed from different angles, spatially arranged in a circle or arc around the object and each photo must contain about 70-80% of previously captured image content.

Generate a point cloud data from the images: The images from the data set are used to identify the points of interest, and to obtain the 3D coordinates of the object. The process is carried out using a specific framework. Because is a compute-intensive process, using a standalone software framework require a powerful computing system. For obtaining a better sits of results, a cloud of web service has been utilised for serving the scope.

Generate a 3D mesh model: On this step, the resulted point will use to generate a textured 3D mesh, for these step, the free software MeshLab® can be used.
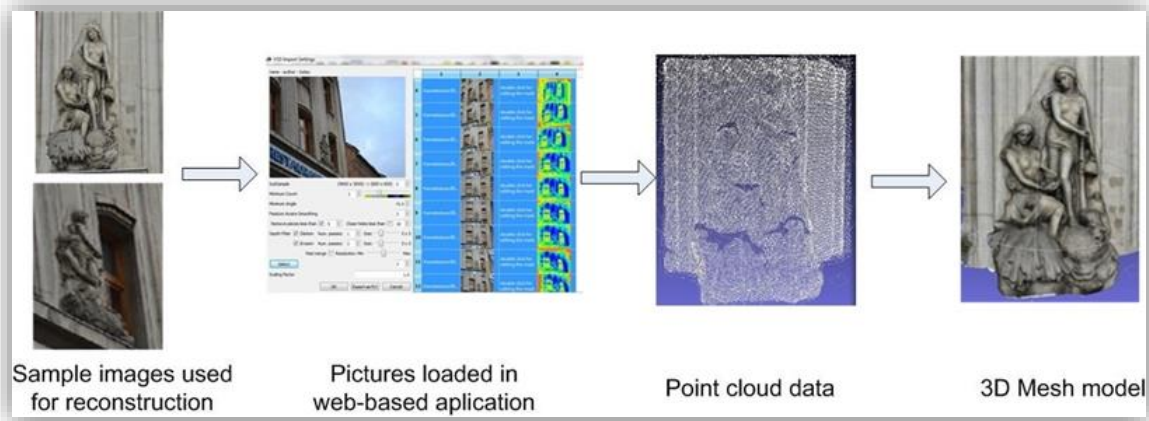
Figure 9. Methodology for virtual reconstruction.

Many modelling tools have a very steep learning curve, so the time required to invest in learning a tool to get even a simple result is often prohibitive. Among all the web-services packages actually available, 123D Catch by Autodesk is the software that is allowing obtaining 3D scene reconstruction through the manual stitching of matching points on triplets of images and the resubmission of the scene to the service. The used approach underlying 123D Catch technology is well described by (Hsu *et al*. 2009).

A technique like 123D Catch is undoubtedly helpful and it provides the scientists with a good tool for an accurate result. Indeed, there is evidence that 123D Catch technique is capable of producing the same size of data sets, which are comparable to laser scanning. This is significant as these high-resolution data sets are generated at lower costs and with reduced data collection times. In addition, it should be recognised that image-based methods do require significant image texture to be effective and accurate. However, nearly most of the photogrammetry services are very fast and easy to use (Erickson *et al*. 2013).

1.1.8.2 Comparing of Some 3D reconstruction Web Service Methods with Autodesk 123D Catch

Due to the development of cloud computing in the last years, several frameworks have developed reconstruction. This review shows the most actual frameworks and compares their features and capabilities (Table. 3) (Butnariu *et al*. 2013).

1.1.8.2.1 Autodesk 123D Catch

Autodesk 123D Catch is a free service offered by Autodesk that uses cloud computing for the reconstruction of 3D objects from images, which is managed through software downloaded from (www.123dapp.com/catch). The management of data is made through a standalone software application installed on the user PC (Chandler and Fryer, 2013). This application allows uploading images, downloading the results, rendering the processed 3D point cloud or mesh, export the result using several 3D formats (DWG, FBX, RZI, OBJ, IPM, LAS). This service can process automatic up to 70 photos in a short time (Butnariu *et al*. 2013). Furthermore, it is possible to set the origin and the axes of a global reference system. The result of the reconstruction process is a triangulated surface, which can be achieved in three different resolutions: mobile (fast medium resolution mesh), standard (high-resolution texture mesh) and maximum (very high-density mesh). Recently two kinds of applications are available: the web application that allows computing the 3D scene directly online, and the application for the smartphones, iPad or PC which enables the creation and the review of the 3D scene (Bostanci, 2015).

1.1.8.2.2 ARC3D

ARC3D is a free web service that provides a standalone software application for uploading photos to the server system. The application delivers valid results when a number of photos about 70 are used. After processing the images, the results are received by a notification email containing links to the files generated. It contains two types of reconstruction data: pixel maps in a V3D format that can be used for the manual reconstruction of 3D. Mesh from a generated point cloud using MeshLab software of a 3D textured mesh in OBJ format processed by the ARC3D server application (but not accurate), and a low result model for online viewing (Schoning and Heidemann, 2015, Butnariu *et al*. 2013).

1.1.8.2.3 Hypr3D

Hypr3D (www.hypr3d.com) is a free web service similar to ARC3D that provides only a web interface to upload and download the files. The best results are obtained when 70-80 images are used. The advantage of this approach, compared with ARC3D, is the reduced time of delivering the reconstruction results (about 3-4 hours). The web service delivers two types of

geometry: low resolution meshes in a 3D format with JPG textures and a point cloud in PLY format. Also, a high-resolution mesh in STL format can be obtained, but without textures applied (Butnariu *et al*. 2013).

1.1.8.2.4 My 3D Scanner

My 3D Scanner (www.my3dscanner.com) is a free web service. This service can process up to 100 photos but for a long time up to 25 hours. The advantage of this application is the high-resolution mesh delivered (up to 1000000 triangles). The drawback is the missing of textures applied to the mesh because it contains only colour information. The result delivered by the application contains an object file for the 3D mesh and a ply for the point cloud *(Butnariu et al*. 2013).

Table 3. Comparison between some photogrammetry services.

	ARC3	Hypr3D	My 3D Scanner	Autodesk 123D
Price	Free	Free	Free	Free
User interface	Web-based + standalone	Web-based	Web-based	Software standalone
Processing time	4 – 5 hours	3 – 4 hours	10 – 24 hours	1 – 2 hours
Cloud processing	Yes	Yes	Yes	Yes
Maximum number of images	70	200	100	70
Point cloud output	Yes	Yes	Yes	Yes
3D mesh output	Yes	Yes	Yes	Yes
Texture output	Yes	Yes	Yes	Yes
Apply automatic	Yes	Yes	Yes	Yes
Maximum number of mesh triangles	10000	200000	1900000	150000
Native 3D files format	OBJ, jpg or v3d, jpg	Ply, STL, jpg	Ply, OBJ	3dp

In addition, some open source reconstruction software has a standalone application as following:

1.1.8.2.5 Photosynth

Microsoft Live Labs developed Photosynth successfully into a web application; it is a web service that is accessible through a Windows Live account on the Photosynth website.

Photosynth is a photo visualisation tool that uses the same underlying data (camera positions and points) (Snavely *et al*. 2008). Users can upload their images to Microsoft's server and the server will return point clouds. Photosynth enables to create two kinds of 3D products: creating panorama views and synths. The former stitch a set of images together taken from the same point to create a panoramic picture; it creates a view that allows browsing from photo to another photo by using a set of overlapping images. However, it is also able to create a point cloud of the object. By using some toolkits and the results can be exported in different formats (PLY, OBJ, VRML, and X3D) (http://synthexport.codeplex.com) (Brutto and Meli, 2012).

1.1.8.2.6 Agisoft PhotoScan

Agisoft PhotoScan is a low-cost software from Agisoft LLC (www.agisoft.ru) to obtain automatically high-quality textured 3D models, using digital photos of scenes (Agisoft, 2012). The software is based on Multi-view 3D Reconstruction technology and can operate with calibrated and uncalibrated images in both controlled and uncontrolled conditions. PhotoScan has two versions for sale: $179 for a standard version (low-cost) or $3499 for a professional version. This program is executable under Windows operating systems (Kersten and Lindstaedt, 2012). In addition, all data will remain with the users on their personal computers, this software could be operated for the large projects that need around 100 images or more, and the model can be exported for editing in external software. All the processes can be performed at different levels of accuracy and many parameters can be set to improve the final result (Brutto and Meli, 2012).

1.1.8.9.3 Previous studies of 3D reconstruction

The 3D modelling or 3D reconstruction has attracted the interests and the intention of the relevant researchers in the forensic domain during the last few years. A demonstrative review of some previous related studies on the 3D modelling and the 3D reconstruction section have been elucidating in table 4.

Table 4. Several studies of 3D reconstruction using different methods.

Title	Software or system	Reference
The reliability and validity of measurements of human dental casts made by an intra-oral 3D scanner, with conventional hand-held digital callipers as the comparison measure	Use of intra-oral 3D scanners in forensic investigations	(Rajshekar *et al*. 2017)
Virtual animation of victim-specific 3D models obtained from CT scans for forensic reconstructions: Living and dead subjects	Specialized 3D modelling and animation techniques	(Villa *et al*. 2017)
The hiatus in crime scene documentation: Visualisation of the location of evidence	Total Station (TS), Geographic Information System (GIS) (ArcGIS 10.3 application)	(de Leeuwe, 2017)
3D modelling of building indoor spaces and closed doors from imagery and point clouds	Laser Scanner (TLS); model Riegl LMS Z-390i (RIEGL Laser Measurement Systems GmbH, Horn, Austria), Sketchup and Nikon D200 camera.	(Diaz-Vilarino *et al*. 2017)
How Technology is Revolutionising Crime Scene Capture and Presentation Visualising a Crime Scene using Novel Crime Scene Documentation Technology	Digital Imaging Technology; Panoramic Imaging; Spherical Photography, Laser Scanning.	(Sheppard *et al*. 2016)
Application of multi-resolution 3D techniques in crime scene documentation with bloodstain pattern analysis	3D scanning, Laser scanning	(Hołowko *et al*. 2016)
Multi-camera system for 3D forensic documentation	Botscan multi-camera system and PhotoScan software	(Leipner *et al*. 2016)
Low-cost crime scene mapping: reviewing emerging freeware, low-cost methods of 3D mapping and applying them to crime scene investigation and forensic evidence	Kinect sensors	(Colwill, 2016)
3D Modeling of Building Indoor Spaces and Closed Doors from Imagery and Point Clouds	A pipeline of techniques used for the reconstruction and interpretation of building interiors based on point clouds and images. (Imagery and Point Clouds)	(Diaz-Vilarino *et al*. 2015)
3D Reconstruction of Crime Scenes and Design Considerations for an Interactive Investigation Tool	Sophisticated computer vision techniques	(Bostanci, 2015)

Building 3D event logs for video investigation	using a semi-interactive method that builds the model from panoramas (video frames to a 3D model of the scene)	(Dang *et al*. 2015)
Progressive 3D Model Acquisition with a Commodity Hand-held Camera	Real-time scanning	(Kang and Medioni, 2015)
Accident or homicide – Virtual crime scene reconstruction using 3D methods	The non-contact optical 3D digitising system GOMATOS	(Buck *et al*. 2013)
Towards a three-dimensional cost-effective registration of the archaeological heritage	PhotoScan software package	(De Reu *et al*. 2013)
Worth a thousand words – Photogrammetry for archaeological 3D surveying	The photogrammetry and 3D mapping applications	(Remondino, 2013)
An Introduction to Building 3D Crime Scene Models Using Sketch Up	Sketch Up	(Clair *et al*. 2012)
3D bloodstain pattern analysis: Ballistic reconstruction of the trajectories of blood drops and determination of the centres of origin of the bloodstains	Digital close-range photogrammetry system and a laser scanner	(Buck *et al*. 2011)
A semi-interactive panorama based 3D reconstruction framework for indoor scenes	Panoramas	(Dang *et al*. 2011)
Kinect Fusion: Real-time 3D Reconstruction and Interaction Using a Moving Depth Camera	Kinect Fusion	(Izadi *et al*. 2011)
Building Rome on a Cloudless Day (ECCV 2010)	3D reconstruction from unregistered Internet-scale photo collections of images within the span of a day on a single PC ("cloudless")	(Raguram *et al*. 2010)
Web-Based Presentation of Semantically Tagged 3D Content for Public Sculptures and Monuments in the UK	Combination of graphical APIs and semantic technologies in order to integrate 3D content with semantic tags in a web browser	(Rodriguez-Echavarria *et al*. 2009)
A Stereo-Based System with Inertial Navigation for Outdoor 3D Scanning	A 3D scanning system consisting of a stereo camera combined with an inertial navigation system	(Byczkowski and Lang, 2009)
Three-Dimensional Assessment of Skin Wounds Using a Standard Digital Camera	Approach to building 3-D models of skin wounds from colour images	(Treuillet *et al*. 2009)
Crime Scene Reconstruction Using a Fully Geomatic Approach	Total station surveying, photogrammetry and laser scanning	(Agosto *et al*. 2008)

Stereo-Vision Based 3D Modeling and Localization for Unmanned Vehicles	Creating photo-realistic 3D models using onboard sensors on unmanned vehicles	(Se and Jasiobedzki, 2008)
Reverse Engineering from 3D optical acquisition: application to Crime Scene Investigation	3D optical instrumentation for the contactless acquisition of crime scenes.	(Cavagnini *et al*. 2007)
Animating and Interacting with Graphical Evidence: Bringing Courtrooms to Life with Virtual Reconstructions	Digital and mobile technologies	(Schofield, 2007)
Photo-realistic 3D Model Reconstruction	Instant Scene Modeller (iSM), a 3D imaging system creates 3D models using a hand-held stereo camera	(Se and Jasiobedzki, 2006)
VIRTOPSY—Scientific Documentation, Reconstruction and Animation in Forensic: Individual and Real 3D Data Based Geo-Metric Approach Including Optical Body/Object Surface and Radiological CT/MRI Scanning	Photogrammetry, optical surface and radiological	(Thali *et al*. 2005)
Instant Scene Modeller for Crime Scene Reconstruction	Instant Scene Modeller (iSM). A 3D imaging system creates 3D models using a hand-held stereo camera.	(Se and Jasiobedzki, 2005)
Analysis of patterned injuries and injury-causing instruments with forensic 3D/CAD supported photogrammetry (FPHG): an instruction manual for the documentation process	3D / CAD program	(Brüschweiler *et al*. 2003)
Improved vision in forensic documentation: forensic 3D/CAD-supported photogrammetry of bodily injury external surfaces combined with volumetric radiologic scanning of bodily injury internal structures provides more investigative leads and stronger forensic evidence	Photogrammetric technique, RolleiMetric multi-image evaluation system And 3D/CAD-supported Photometry	(Thali *et al*. 2000)
Modelling and Rendering for Scene of Crime Reconstruction	Computer graphics modelling and rendering techniques for the construction of a virtual environment corresponding to a real crime scene	(Murta *et al*. 1998)

Crime scene often deals with cadavers, thus, the reconstruction of the criminal events is always depending on the analysis of the scene as well as the body.

Considerably, there are various elements associated with the concept of the crime scene platform, significantly, the presence of cadavers and the associated remnants. Therefore, the reconstruction of the crime scene is not restricted to the documentation of the events cascades and the physical evidence, the comprehensive perception in regards to the carcass must be conducted through implementing the proper analytical procedures and concerning selective elements to be examined and tested thoroughly.

1.2 Body Transformations

The death actually a process and not an event, it starts at the point where the heart stops, and the oxygen does not reach the cells. After several minutes of death, the decomposition process begins within an autolysis process. This begins usually in the liver, where the richness of the enzymes, and in the brain, which has high water content. Furthermore, the internal organs are usually free of microbes. Without the functioning of the immune system, which stops working soon after death, the microbes will spread freely through the body organs. In addition, insects will be attracted to the decomposing tissue. Thusly, a comprehension of the decomposition and the role of insects and microbial communities during the decomposition process is necessary and important for accurate estimating of post-mortem interval PMI. Because they all have an essential effect on the rate of decomposition (Costandi, 2015).

1.2.1 Decomposition and other Body Post-mortem Transformations

Decomposition begins approximately 4 minutes after death has occurred (Vass, 2001). Also, it is a natural process occurs for every organism that has died (Hau *et al*. 2014). In fact, the body undergoes major chemical and physical changes. Forensic pathologists can use these changes in order to estimate the minimum Post Mortem Interval (mPMI) (Gunn, 2011).

Decomposition is a fundamental process and important to nutrient cycling and energy flow in most ecosystems (Finley *et al*. 2015). Thus, understanding this process has broad application to ecological and environmental science and also in entomology when arthropods are collected and interpreted as evidence (Benbow *et al*. 2013).

The decomposition characteristics such as the variability, the dynamic nature, the ecological aspect, and the biochemical processing are all depending on the biotic factors, including the scavenging, insects' activity, and microbial community, and the abiotic factors, such as temperature, moisture that is variable in accordance with the seasons, the geographic sites, and the preventative barriers (Carter *et al*. 2015). Furthermore, in order to provide a comprehensive understanding of the decomposition changes, it is necessary for deeply understand the sequence of the decomposition process, stages, and factors affecting the decomposition process. The temperature and the humidity degrees are the two main environmental factors which can affect significantly the degradation of the body components and the microbial activity (Carter *et al*. 2015). Decomposition changes are dependent upon temperature, humidity, insect activity and condition of the body at death. (Gunn, 2011).There are a series of early changes in the body that result in a specific change in the physical nature or appearance of the body before and during the decomposition process. These changes have traditionally been used in estimations of the PMI, they are as follows: (Gardner and Bevel, 2009, Gunn, 2011).

- Greenish discolouration. The first change is discolouration to the green of the abdomen, and then the discolouration spreads throughout the body.
- The body begins to swell due to the gas of the bacterial formation that is promoted in warm weather and retarded in cold weather. Tissues swell and the eyes.
- Skin slippage. As the body becomes bloated, the skin begins sliding and form blisters, and the blood starts to degrade.
- Decomposed blood and body fluids, appearing dark brown and stinking smell, come out of the body orifices, due to gas push the fluid in the least resistance path.
- Lastly, skeletonisation may take weeks or months depending on the environment. Many bodies are discovered in partial skeletonisation.
- Exposed parts of the body decompose faster. The internal parts of the body (i.e., abdomen, chest, and head) also decompose fast. In addition, when a body part is exposed to injury, that part tends to decompose faster.

Mummification is a natural process or artificial conservation, which consists of the dehydration and exsiccation (the process of drying up) of tissues. It may be partial and coexist with other forms of conservation and/or putrefaction. It extends more easily to the whole body than other processes, such as saponification (Goff, 2009). It is characterised by dryness and brittle, torn skin on the prominences (cheeks, forehead, sides of the back, and hips), generally brown in colour, though coexisting with white, green, or black zones because of colonisation by fungus.

As for the internal organs, the process varies in relation to the time of death, and they may be partially mummified, putrefied, with adiopocere, or even absent (Pinheiro, 2006).

The whole body or parts of the body in a dry weather, have a large surface area to mass ratio will desiccate. The low level of humidity will serve to stop bacterial action and usually exclusion of insects and other scavengers from the body.in this type of situation. The temperatures will be very high or very low. The dried tissues and skin will survive for a long time with a little change, also will take a leathery appearance. Mummification can occur within a period of several weeks in hot, dry conditions or in areas that have very low humidity, such as in arctic regions or deserts (Vass, 2001, Goff, 2009).

Saponification (formation of soap from fat under high pH levels) or it is the process of hydrolysis of fatty tissues in wet, anaerobic situations, such as submersion or in flooded burials. The tissues take a yellow, greasy, waxy appearance and consistency. This process requires a period of several months to complete (Vass, 2001, Goff, 2009).

1.2.2 Decomposition stages

There are several stages of cadaver decomposition are ranging from two to eight stages, the basis of the remains physical appearance and the arthropod deposition patterns. Considerably, the six stages, namely fresh, bloated, active decay, advanced decay, dry and remains (Payne, 1965, Carter *et al*. 2007). Whereas Campobasso *et al*. (2001) divided the stages of decomposition into four stages, although there are more sub-stages involved, based on the physical appearance of the remains and associated arthropod arrival patterns *(*Campobasso *et al*. 2001, Reed Jr, 1958).

On the other hand, decomposition stages have been divided into five main stages: fresh, bloat, active decay, advanced decay and putrid dry stage (Fig. 10), depending on the arrival and departure of the insects follow these stages as the breakdown of the cadaver proceeds. Each stage is attractive to different species and each stage of decay provides an ideal habitat species to lay eggs and feed. Thus, this leads to series of insects' species (Carter *et al*. 2007, Gill, 2005, Goff, 1993, Hewadikaram and Goff, 1991, Matuszewski *et al*. 2010). Also, *(*Matuszewski *et al*. 2008) demonstrated that five stages of decomposition were observed: fresh stage, bloated stage, active decay stage, advanced decay stage, and remains stage. This is could be a generalised pattern that can be easily applied to most existing studies.

Figure 10. The five basic stages of the decomposition process. (A) Fresh, (B) Bloat, (C) Active decay, (D) Advanced decay and (E) Dry stage (Parkinson, 2009).

Fresh stage

The fresh stage is the first stage of decomposition due to the inability of the heart to beat the blood. The blood is not circulated around the body. Thus, the blood settles at the bottom of the body due to the effect of gravity and results in the appearance of a dark red skin colour, this phenomenon is also known as livor mortis. Next, oxygen molecules depletion leads to cellular autolysis as a consequence of the aerobic metabolism antagonism along with the cellular enzymatic destruction. The fresh stage begins at the moment of death and continues until the carcass begins to bloat (Finley *et al*. 2015).

During the procreation intervals, certain species of flies such as the blowflies and flesh flies with the nomenclatures of Calliphoridae and Sarcophagidae, respectively are a deposit and then proliferate and colonise on the cadaver tissues in order to select a suitable location for offspring incubation. In the case of the absence of the scavengers, the driving force, which governs the removal of the soft tissues, is the establishment of the maggot activity upon the ovipositional of the flies. Furthermore, carbon dioxide CO_2–C evolution, which is a descriptor index for the microbial introducing activity to the cadaver tissues within 24 hours, positively influences the soil microbes' proliferation; particularly the zymogenous -strategist bacteria (Honeycutt, 2012). Moreover, the exhaustion of the internal oxygen concentration can provide proactively a suitable ambient environment for the anaerobic species of microbes, such as Clostridium and Bacteroides, which is introduced originally from the gastrointestinal tract and the respiratory airways, to propagate and spread to the internal organs. The cellular anaerobiosis reactions

include the alteration of the primary building blocks of carbohydrates, lipids and proteins, by the microorganisms as anaerobic converting mechanisms, into organic acids (such as propionic and lactic acid), as well as into gasses (such as methane, hydrogen sulphide and ammonia). (Gennard, 2012).

Bloat stage

The bloat stage is the second stage of the decomposition that occurs due to the microbial metabolic activity of bacteria in the gut and other areas of the body that produce gases. The produce gases as a side product of the anaerobiosis are responsible for the colour changes, the liberation of odour, and the bloating of the cadaver. This causes the abdomen of the carrion to be inflated and manifest the body with the balloon-shape (Gunn, 2011), which can attract or repel certain insect taxa to the carcass (Finley *et al*. 2015).

As an accompanied consequence of the resultant reaction products and the cadaver putrefaction during the first stage, the next stage 'Bloated' is started. During this stage, the internal purging fluids have been forced to diffuse into the surrounding soil through the cadaveric orifices cavities, mouth, nose, and anus commonly, the fluids escape take place due to the accumulation of the resultant anaerobic gasses, compelling the spontaneous occurrence of this process. There is a limited knowledge regarding the ecological effect of the purging fluids on the natural chemistry of the below ground. However, an earlier established perception is that the escaping fluids can aid in the microbial biomass flush, shifting the nature of the faunal communities present in the soil, carbon atom mineralisation based on the CO_2–C evolution, and the elevation of the soil nutrients richness (Honeycutt, 2012). Thus, the mentioned cascade of putrefactive bloating and maggot feeding processes aid in the laceration of the cover skin, which can permit the re-oxygenation of the internal tissues into a larger surface area, which in hand provide a suitable incubation area for the fly larvae and aerobic microbial to establish their proliferative activities (Tsokos, 2005).

Active decay stage

Active decay' stage is the third process of the decomposition following the bloating stage as a result of insects activity (Finley *et al*. 2015). In addition, it is the stage where the body's gas is no longer kept under the skin. Therefore, the body collapses in on itself, and the most of the skin is lost at this stage of the decomposition (Gunn, 2011). Moreover, the re-oxygenation

designates the initiation of the 'Active Decay' stage; this stage is featuring with a rapid mass loss as a result of the establishment of the maximum maggot activity and the peak liberation of the fluids during the active decay, the nutrients and the microbial community's status and account. Nevertheless, the Bornemissza (1957) has observed the quantitative elevation of some soil faunal communities such as Calliphoridae, Histeridae, Ptiliidae, Staphylinidae) and a reduction in the numbers of Collembola and Acari beneath a guinea pig (*Cavia porcellus L.*) cadaver (~620 g) throughout the 'Active Decay' (Bornemissza, 1957). This decomposition phase is named as "Black Putrefaction", the persistence of the 'Active Decay' is sequenced until the maggots are completely migrated from the cadaver to pupate (Gennard, 2012, Gunn, 2011).

Advanced decay stage

Advanced Decay stage is characterised by a decrease in entomological activity as the resource is consumed (Finley *et al*. 2015), and it is providing an illustration of this phenomenon. The cadaver size, the extent of the maggot mass, and the soil texture control the lateral range of the cadaver decomposition. Particularly, the soil texture along with the cadaver size influence the vertical range of the cadaver decomposition. It is important to note that identification of the sequenced transition from the advanced decay to dry to remains is complicated (Payne, 1965).

Dry remains stage

Dry remains stage is the final step of the decomposition process, when bones, dry skin, and hair only remain from the decomposed carcass (Finley *et al*. 2015). At this point in the decomposition, most of the soft tissues are removed, by natural causes, and the hard structures of the body, such as fingernails and skeleton remain (Gunn, 2011). In addition, the elevation of the plant growth around the borders of the cadaver decomposition act as an indicator for the initiation of the Dry stage. The rise in the plant growth within the cadaver decomposition can act as an indicator for determining the remains stage. The depletion of the available nutrients and moisture during the final decomposition stages facilitate the establishment of the second phase which includes the slow process of the cadaver mass lost (Carter *et al*. 2007).

1.2.3 Factors Affecting the Rates of Decomposition Process

A multitude of factors can affect each stage of the decomposition process, either accelerating the process or slowing it down, depending on the specific agent at work (Dautartas, 2009). The natural preservation of a cadaver is highly dependent on the surrounding environment, and a number of factors that play important roles in this phenomenon including temperature, humidity, insects, and the activities of microorganisms such as bacteria (Jordan and Tomberlin, 2017). It is well known that various stages of decomposition can attract different species of insects that also depends on other factors such as temperature, weather and season. When the body is fresh, blowfly and flesh fly and their first instar larvae will most likely be found on the body as well as adult burying beetles. Several factors can affect the rate of a body decomposition and at which insects can colonise it (Campobasso *et al*. 2001). Thus, the environment is a major determinant of the process of decomposition (Dix and Graham, 1999). It is reported that the presence of insecticides on, in or near the body may also serve to delay the onset of insect activity for a period of time (Goff, 2009). In addition, if the carcass has any open wounds, they can also affect the rate of the decomposition according to the Anthropological Research Facility (ARF) at the University of Tennessee. They have suggested that penetrating injury impacts on the decomposition because an open wound can provide easy access for insects and bacteria (Cross and Simmons, 2010, Mann et al., 1990).

Further, the age of the persons, their physical build, and their previous activities affect the decomposition rate. For example, the fatty bodies decompose fast because bacteria have access to tissue with a good supply of water. People who have a low level of muscle tissue or who are very weak show a faster rate of the active decay and a faster rate of decomposition. Active decay is much slower in elderly people and in babies; so overall decomposition will be correspondingly slow (Gennard, 2012). Thus, the complexity of decomposition demonstrates the impact multiple variables have on each other. Given the interrelation among all of those factors, one must be careful, in collecting data on all relevant variables, especially temperature, or else risk inaccuracies in estimating PMI (Guerra, 2014). The most important factors can be summarised as follows:

1.2.3.1 Temperature

Temperature is influenced by seasons, altitude, latitude, burial depth, the presence of water, air movement, vegetation, wrappings or clothing, etc. Temperature and the rate of decomposition linked by Van't Hoff's Law that also called the law of 10 or Q10. It states that the speed of chemical reactions (enzymatic or catalytic decomposition, etc.) increases two or more times with each 10 °C rise in temperature (Vass, 2011). Johnson and colleagues. (2013) state that the temperature can accelerate the rate of the decomposition; in contrast, low temperatures can reduce the rate of the decomposition (Johnson *et al*. 2013). Temperature determines the speed of many of the processes on which minimum post-mortem interval estimations are based on both Pathologies and in Entomology (Campobasso *et al*. 2001). Temperature has a direct impact on the decomposition processes; very low or very high temperatures slow down organic matter decay, inhibit bacterial increase and preserving cadaver tissues longer. Temperature also impacts directly on the insect activity and in the rate of insect development (Goff, 1993). Decomposition that occurs in an environment with temperatures between 15-35 °C is fast because the bacterial growth and cell division occur best under these conditions. However, once temperatures begin dropping under the optimal range for bacteria growth, reproduction of bacteria becomes greatly retarded and then stopping completely. As temperatures continue to fall, the degree of desiccation required for preservation becomes reduced (Micozzi, 1996, Sorg and Haglund, 1996). In fact, in temperatures between 0-5 °C, bacterial multiplication stop and insect activity become greatly retarded. In temperatures below freezing, insect activity stops altogether. Flies are noted to act efficiently at a maximum and minimum temperature range, visiting a carcass and laying eggs in conditions as cold as the mid-40s °F (Mann *et al*. 1990). Temperatures dropping below this, especially past the freezing point, can kill both fly eggs as well as maggot larvae if left exposed to the environment. In fact, a study evaluating the most effective PMI estimation techniques noted that the freezing point is the lowest developmental threshold for insects, with PMI estimates decreasing in precision when the developmental threshold was raised (Vanlaerhoven, 2008).

Warm temperature aids in accelerating the decomposition process of the corpse because it can provide the suitable conditions which can help the elevation of insect activity and increase in insects numbers and the microorganisms and their related energy-producing chemical reactions produce faster degradation (Campobasso *et al*. 2001, Carter *et al*. 2015). Although claims have been made that insect activity is the most important variable in regards to the rate of

decomposition. However, without the best conditions guided by temperature, insect activity can be greatly retarded or stop altogether (Carter *et al*. 2015).

In addition, the hot and dry climates can prevent bacterial growth, limiting the bacterial decay and further preserving the body. Under such conditions, moisture can evaporate from the skin and mummification can occur faster. The internal organs may be preserved, though they will typically undergo a small level of decomposition (Jordan and Tomberlin, 2017). Therefore, without knowledge of the temperatures and environmental factors to which a corpse has been exposed, not much can be said regarding time since death. Importantly, the temperature has been demonstrated to be related to a number of factors known to change decomposition, in the end, to guide the speed at which the decay process progresses (Simmons *et al*. 2010).

In summary, recognising how temperature affects decomposition on its own, but by standardising time and temperature and making accumulated degree-days the variable to be predicted, insect activity is left as the primary factor in decomposition, whose effects are reflected in the total body score. This new approach removes temperature as a variable used to explain the decomposition changes observed in relation to time and instead combines it with time to become the unit to be predicted, i.e. ADD. Thus, overall temperature is still the guiding force in decomposition, but when standardised to become the dependent variable, insect activity is shown to play the central role in the rate of decay (Guerra, 2014).

1.2.3.2 Humidity

Humidity is an important environmental factor that can mediate the biological activities (Metcalf *et al*. 2016). Bacterial growth occurs more rapidly, with the outcome depending on the relative humidity. Microbial and biochemical activities results in a series of decomposition stages that are associated with a reproducible microbial succession across animals, and human corpses (Guerra, 2014, Micozzi, 1996). The most of the microorganisms require at least 60% relative humidity (RH), though some microorganisms can survive and multiply in >20% RH. Thus, reducing the relative humidity creates a less appropriate environment for microorganisms' growth. One indicator of microbial response is their taxonomic classification. For example, Gram-negative bacteria are generally more sensitive to low water activities than Gram-positive bacteria (Jordan and Tomberlin, 2017). Insect activity is greatly retarded because it requires moisture in order to oviposit eggs (Haskell *et al*. 1997). Bacterial growth occurs more rapidly depending on the relative humidity (Micozzi, 1996). Also, changes in the microbial

communities structure under altered humidity conditions suggest differential sensitivity to humidity (Jordan and Tomberlin, 2017).

Moreover, the surrounding humidity plays a vital role in the deposition of the eggs from the females' flies on the cadaver tissues and there is A direct relationship between the humidity degree and the egg deposition ability through the cadaver tissues. The eggs are usually present near to the holes and wounds of the cadaver. In addition, the deposition variabilities are strongly related to the seasonal surrounding aspects as reported in a recent related study by Carter *et al*., (2015). Clear variation based on the seasonal aspect has been noticed throughout the carcases decomposition process (Carter *et al*. 2015).

1.2.3.3 Rainfall

The presence of water that is supplied from rainfall, humidity, or the body itself also exert profound effects on the rate of decomposition. The important attributes that are associated with water include: (a) a high specific heat that stabilizes temperatures; (b) buffering capacity that moderates the effects of local pH changes; (c) sources of H+ required for numerous biochemical reactions; (d) its effect as a diluent; and (e) its ability to act as a solvent for polar molecules. PH (acidity/alkalinity) is yet another parameter that affects intracellular chemical reactions and the catalytic ability of enzymes. Proteolysis (aerobic surface decomposition) typically forms alkaline environments (well over pH 9.0 on the surface) whereas anaerobic burials tend to be acidic due to bacterial fermentation and the liberation of organic acids. These large changes in pH affect not only the microbial flora but also the growth of vegetation as well as the chemical reactions (Vass, 2011).

Microorganisms, like all living organisms, require available water to grow and to function. Different types of fungi and bacteria need varying amounts of water to reproduce and to grow, and the production of enzymes and other metabolites may be sensitive to alterations (Jordan and Tomberlin, 2017). However, rainfall does not produce a considerably large effect on the rate of decay. Since the large role of the humidity in the deterioration process, it is expected that rainfall can accelerate or disturb the decomposition process. According to Mann *et al*., (1990), rainfall does not even retard the activity of maggot. Most of the larvae can use the cavities of the body as shelter from the rain and continue feeding on the corpse. However, they do point out that during moderate to heavy rainfall, fly activity and thus egg laying can be reduced or stopped altogether. This can push time since death estimates back, allowing only

minimum PMI determinations to be made so as to accommodate the effects of unknown confounding variables (Mann *et al*. 1990).

Since rainfall is not identified as a critical factor as with the most variables involved in the decomposition process, it has the potential to affect the roles that are played by other important factors including aridity, humidity, insect activity, adipocere (grave wax) formation, disarticulation, bone mineralization, and so forth. Because of its tight relationship with aridity and relative humidity, precipitation, in the form of rainfall is an important variable to capture, especially if reliable sources regarding daily humidity rates are not available for the particular area under study (Guerra, 2014).

1.2.3.4 Clothing and Body Wrapping

Clothing and body wrappings are particularly interesting variables that can complicate scenes and estimations of time since death. Covering (Clothing) can have an effect on the rate of the body decomposition as shown in the investigation performed by (Centeno *et al*. 2002, VanLaerhoven, 2008, Stuart and Ueland, 2017). In addition, Capobianco (2017) also demonstrated that the clothing generally slowed the rate of decomposition in human cadavers placed on the same site. (Capobianco and Christensen, 2017).

A study was done by Sharanowski *et al*., (2008) demonstrated that the clothes protect the insects from predators and also prevent the carcases from drying out as quickly as they otherwise would (Sharanowski *et al*. 2008). Other study conducted using clothed, wrapped, unclothed, and unwrapped bodies, demonstrated that the clothed and wrapped bodies had larger maggots mass, and all of the wrapped carcases have taken longer to dry out (Kelly *et al*. 2009). Furthermore, research regarding the relationship between insect activity and the presence of clothing appeared to suggest that clothing affects the rate of decay by providing insects with suitable environments within which to consume tissues. After laying eggs at the natural holes of the body, once large numbers of flies colonised remains and thus crowded areas, they would begin using folds in the clothing to lay their eggs. Then, the maggots could process the tissues and thus speed up the rate of decay (Mann *et al*. 1990).

The clothing helps in increasing the number of insects feeding on the body, thus increasing the rate of decomposition. However, the clothing can slow the rate of decomposition in the covered areas (Lowe *et al*. 2013). Therefore, the effects of types of coverage as natural fibres, especially

wool carpet and cotton clothing, followed by wool clothing and materials produced by synthetic fibres. The main points from this study were the importance of the absorbing ability of natural fibres compared to synthetic materials, removing decomposition products, retaining moisture, and disrupt the decomposition process. However, the results also demonstrate that regardless of material type, clothing, wrappings, and coverings function to preserve remains more so than unclothed bodies (Notter and Stuart, 2012).

On the other hand, there is a statistically significant difference between the decomposition rates of clothed and unclothed cadavers, which is relatively faster. In general, the overall rate of the decomposition is similar, and there is no need for different formulae to determine PMI. Moreover, it has been suggested that clothing can provide additional colonisation locations for the blow flies (Card *et al*. 2015).

1.2.3.5 Soil Type

It is well known that the soil environment is an important factor that affects decomposition rates in the underground (Tumer *et al*. 2013). The soil is noted to exert an efficient barrier to solar radiation and thus declined of temperatures with soil depth. There are another two aspects of soil environment that are known to affect the rates of decomposition; humidity content and the presence of the organisms in the soil both plant and animal (Finley *et al*. 2015). The presence of groundwater or clay type soils that retain humidity produces an environment conducive to adiopocere formation. It is important to know that the soil may be the main source of the microbial decomposer community, although soil type is not important (Metcalf *et al*. 2016). However, the change of the physical and chemical properties of soil leads to the change in the structure of the microbial community is that the bacterial community facilitates the proliferation of certain eukaryotes. A high level of moisture, alkalinity (8–9 pH), and an abundance of anaerobic and facultative aerobic bacteria are characteristic of early stages of carcass decomposition (Carter *et al*. 2015).

In addition, the type and particle size of the soil are also the most important factors that affect the decomposition rate of cadavers in soil (Finley *et al*. 2015).

1.2.3.6 Carcass Body Size

The size of carcass does not play an important role in the rate of decomposition. There are no size-related variations were observed between carcases with respect to the composition of the arthropod fauna or patterns of succession (Sutherland *et al*. 2013). It is noted that a greater number of arthropods are attracted to the large carcases, and the rate of decomposition is more rapid than the small size carcases (Hewadikaram and Goff, 1991). However, Komar and Beattie (1998) noted that the smaller carcases were decayed significantly faster than the medium and large carcases and reaching dry skeletal remains in as little as 13 days (Komar and Beattie, 1998).

1.2.3.7 Insects' activity

1.2.3.7.1 The Role of Arthropods in the Breakdown of Corpses

The effect of carrion insects rather than that of large vertebrates highlights the significant and influential role of large numbers of small animals in the functioning of ecosystems (Barton, 2015). It is indicated that the access of insects to the decomposed body is the second most important variable that affects the decomposition rate after temperature which feeds on decaying matter (saprophagous) (Campobasso *et al*. 2001). The death of advanced decay body can be easily dated seasonally using entomological data. A variable number of arthropods that belong to various taxa can be colonising the cadaver, which provides altogether helpful tools for forensic investigation. However, not all insects actually feed on decomposing tissues (the so-called necrophagous species). Only a few species of insects can directly participate in the breakdown of a cadaver and then accelerate the rate of decay. It is reported that Diptera and Coleoptera are important two orders of insects of forensic interest (Campobasso *et al*. 2001).

Other insect orders such as Lepidoptera, Hymenoptera (e.g. ants), and non-insect orders such as Arachnida and Nematoda, can be simply cadaver hosts or more frequently predators of necrophagous species, whose number and distribution on body remains they somehow control. All species associated with the body remains should be collected, identified and preserved according to their time of arrival (Campobasso *et al*. 2001). The carrion decomposition is noted for reintroduces important and essential nutrients such as nitrogen, potassium, calcium and magnesium into an ecosystem (Parmenter and MacMahon, 2009).

A study performed by Vasconcelos *et al*. (2013) investigated the different kinds of insects and their development on the body at different stages of decomposition, using a decomposing pig. This study suggested that at least 10 species completing their larval cycle on carrion in rainforest fragments in Brazil (Vasconcelos *et al*. 2013).

In addition, a study by Pechal *et al*., (2014) indicated that there were differences found between the carcases allowed insect access decomposition compared to carcases with delayed insect access. For instance, in 2010, the cadavers with insects access were close to the dry stage with Calliphoridae larval presence on two cadavers (B and E), whereas the cadaver (F) demonstrated a larval spread since the end of the fifth day (Fig. 11). Meantime, carcases with insect exclusion (A, C, and D) were in the bloat stage of decomposition on the fifth day (Fig. 11). In 2010, the decomposition to dry stage for cadavers with insect's access occurred between the sixth day and the seventh day of the decomposition. Whereas, the cadavers reached the dry stage within five days in 2011 trials. In general, for both 2010 and 2011 trials, cadavers without insect's access approached the dry stage on the ninth day of decomposition, which matched with the fourth day of post-exclusion insect activity. This finding suggests that once insects were allowed to colonise the carrion it had an accelerated decomposition progress (Pechal *et al*. 2014).

Figure 11. Images of carcases on the fifth day of decomposition. Insect exclusion cages were removed from the carcases on this day. (a) Carcasses with insect access (B, E, and F) were at active or advanced decay while (b) insect exclusion carcases (A, C, and D) were still at the bloat stage (Pechal *et al*. 2014).

Further, Simmons *et al*. (2010) noted the role of insect activity in the decomposition process. The cadavers with no insect exposure were decomposed much slower than other cadavers that were exposed to insect activity, coupled with the faster rate of decay seen in continuously exposed remains versus those buried after exposure. They conclude that the presence of insect is the primary agent that affect the rate of decomposition (Simmons *et al*. 2010).

1.2.3.7.2 The Use of Forensic Entomology in Forensic Investigation

Forensic Entomology is the study of the application of insects and other arthropods in a criminal investigation. Insects or arthropods are found in a decomposing vertebrate corpse or carrion. These insect colonisers can be used to estimate the time of death. It is a time interval between death and corpse discovery that is also called PMI (Loucao, 2017). It is possible for the forensics to use data that are based on insects and their larvae morphology, growth histories, species distribution and toxic contents in their tissue in a criminal investigation. The rate of decomposition of the body and the interpretation of PMI is influenced by the arthropods, including insects, that visit and colonise the decomposing body (Goff, 1993).

It is important to know that insects attracted to the body or to other insects that are already on the body can be collected and studied by an entomologist. The entomologist can identify the various types of insects as well as their stages of development. Since each developmental stage lasts for a reasonably predictable time, the entomologist can calculate how long the various insects have been on the body. If live larvae and pupae are available, the entomologist can then let them develop in the laboratory for more accurately define for the length of their developmental stages under prescribed conditions. Potential effects of differences between laboratory conditions and the conditions of the body were exposed to in the environment on the development of the insects must be taken into account during estimation of PMI. The time frame developed by the entomologist represents the minimum time the body has been dead because a body may have been dead for some period of time prior to insect infestation. The entomologist is also able to determine what insects are active at particular times of the year and how long it typically takes particular insects to invade the body. By identifying the insects on the body that are not part of the local population, the entomologist can identify if the body has been moved and, potentially, where it originated (Dix and Graham, 1999). Taxonomic identification of the insects found on corpses is essential to the reconstruction of events surrounding criminal cases involving death. In addition, feeding larvae can be collected for the

potential use of insects as alternative samples for detecting drugs and toxins substances in or on a dead body. The drugs and toxins can also affect their rate of development (Amendt *et al*. 2011, Byrd and Castner, 2009). For example, cocaine and heroin significantly increase the rate of development of larvae and thereby affect the accuracy of PMI if not taken into account (Byrd and Castner, 2009).

1.2.3.7.3 Indicators of Time of Death

Besides the changes involving the body, other information from the scene may help in estimating the time of death. Some of this information involves the body and other details do not (Dix and Graham, 1999). Historically the determine time since a death was based on the condition of the cadaver itself and its physical features such as the decrease in body temperature. The medical information over 72 hours of the dead time is less available to correlate PMI. However, forensic entomology can provide an estimate of the minimum PMI, using the life cycle stages of particular fly species recovered from the cadaver, or from the succession of insects found on the body. This estimate can be used once the normal pathological features are no longer working to determine time since death. The post-mortem interval is believed to start when the first fly starts to lay their eggs on the body and to ends when the body is found. The summation of the time in the individual life stages taken to calculate the insect life stage, which recovered from the body, the relation to its particular stage of decay, gives a good estimation of the probable length of time the person has been dead. Indeed, this may be the best estimate of the time since death that is available (Gennard, 2012).

1.2.3.8 Microbial Communities

Microbial communities and insects are the major driving force for the decomposition process and progress over the time (Metcalf *et al*. 2013) (Fig. 12). Few studies are performed in order to study the microbiome decomposition activity (Hyde *et al*. 2013). However, American groups have been working on this topic in the last years (Gunn and Pitt, 2012, Hyde *et al*. 2013, Metcalf *et al*. 2013, Pechal *et al*. 2013a). It is established that the breakdown of the tissues is primarily a result of autolysis and bacterial decay (Rodriguez, 1996). Although the bacterial communities associated with a decomposing cadaver have been found to be complex, it was found that bacterial communities diverse and varied considerably between individuals. Some researchers

indicate that the analysis of the microbiome has some potential to become a PMI estimation tool (Parkinson, 2009).

The forensic ability of the microbial analysis is becoming increasingly strong as a consequence of advances in molecular sciences and genomics, that increased the evidence that humans have (microbiome) that could use to determine ethnicity, country of origin, and even personal identity (Gunn and Pitt, 2012).

Development of other forensic tools using bacterial communities is strong and helpful for forensic investigators which are could dramatically enhance forensic death investigations by reducing the time and monetary costs required. Furthermore, to determine whether a decomposition process has occurred in a particular place, also in cases where bodies have been moved by perpetrators or by scavenging animals. There are specific organisms such as Enterococcus that can also establish whether that decomposition event was caused by a human body or another large mammal (Parkinson, 2009). Following death, the environmental conditions affect the speed of microbial movement through the body; also, the presence of wounds on the body will aid the entry of microbes. In addition, if the body is immediately frozen after death, then there is no movement of microorganisms and thereby, decomposition does not occur (Gunn and Pitt, 2012). Jordan and Tomberlin (2017) divided the factors affect the microbial activity and that could influence the arthropod activity associated with the decomposing body into abiotic factors, which include (nutrition, temperature, humidity, pH and salinity), and biotic factors, which include (competition, predation, commensalism and pathogens).
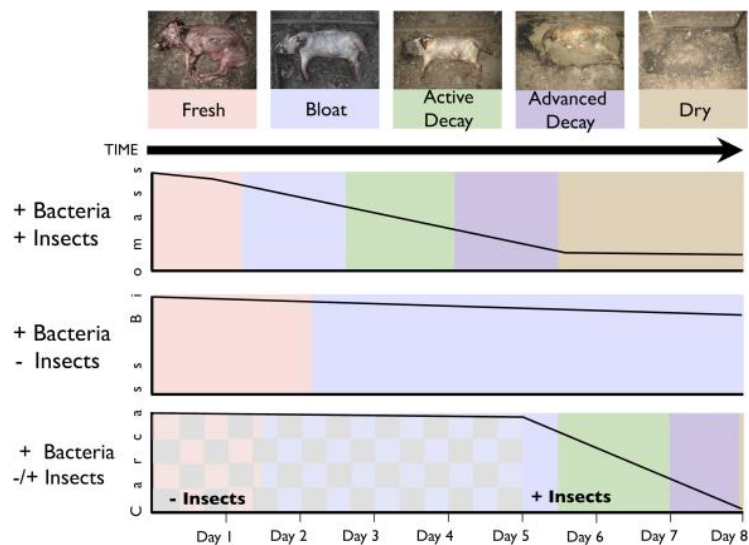
Figure 12. Biodiversity of microbe and arthropod communities instruct cadaver decomposition (Pechal *et al*. 2014).

1.2.3.8.1 The Role of Microbial Communities in the Decomposition Process, and Necrobiome, Epinecrobiome and Thanatomicrobiome Communities

The forensic microbiology is considered recently as one of the main areas of forensic science, which concerns in the inclusive addressing of the role of the microbial communities and the soil inhabitants in several aspects not only restricted to the cadaver decomposition. A dead mammalian cadaver is theorised as a high-quality elemental resource, such as carbon, nitrogen and rich water content, which can liberate an intense and focused pulse of carbon and nutrients into the soil during the decomposition process (Sorg and Haglund, 1996).

In spite of that, about 5000 kg of cadavers can be placed in a square kilometre of terrestrial ecosystem every year, the cadaver decomposition process still considered as a neglected microsphere of forensic. Numerous researchers having a concern regarding the cadaver decomposition process are conducted under the guise of forensic taphonomy, which is defined as a branch of palaeontology that can connect the concerned analysis of the perimortem to the post-mortem periods. It possesses the ability to describe and elaborate all events which affect the organism from the pre-agony and death until the structural conservation and the subsequent transfer from the biosphere to the lithosphere (Haglund and Sorg, 2001, Magni *et al*. 2008).

The forensic taphonomic studies are focusing on the recovery and the collection of the protocols reports which have documented various aspects such as investigations on the death causes, interpretation of the events that led to the cadaver discovery, understanding the post-death alterations which have conducted on the soft tissue, muscles, and bones (Magni *et al*. 2008). This branch of science was developed aiming for obtaining a comprehensive understanding of the decomposition site ecology, tackling the effect of the ecological changes upon introducing the remains of plants and animals, addressing the factors that influence the decomposition process of these natural materials (Carter *et al*. 2007).

 Recently, these stated objectives were consolidated and merged within the forensic science, in order to obtain the comprehensive understanding of the human cadaver decomposition process. Which can lead to the provision of the firm basis for estimating the post-mortem and the post-burial interval. Furthermore, these outlined objectives can assist in determining death causes and its corresponding manner, which can then lead to the identification of the exact locations and positions of clandestine graves. These specified goals can be achieved through the extensive study of the environmental factors that can affect the cadaver decomposition process, such as temperature fluctuation, moisture degree changes, insects' activities, and most importantly the

microbial communities. Which have emerged from the pre-existing cadaver living flora, from the human microbiome, and from the environmental microbial communities in the soil which have diffused from the fallen carrion or have transported through the moving insects (Carter *et al*. 2007).

In fact, by theorising to the cadaver through the context of the ecosystem and from the incubation perception of bacterial, fungal colonies, and insects' communities, have repositioned the cadaver term to be far away from dead system considerations and definitions. The decomposition stage is considered as a mosaic system, which structured with a close association between biotic and abiotic factors with a specified function for each one. Additionally, the ecosystem alterations, for example, the insects' exclusion or burial, might drive to a special pattern of the decomposition; consequently, make the potential for obtaining irregular findings. Thus, the complete understanding of these effective factors is compulsory and essential by the concerned forensics (Hyde *et al*. 2013).

In forensic sciences, the bacterial communities are specified as a prime agent for the initiation and the completion of the cadaver decomposition process along with the human remains degradation. Furthermore, the importance of the soil microbial biomass has been recognised and defined as 'the eye of the needle' which all organic type of material passes through eventually (Jenkinson, 1977). Recent studies elucidated that the microbial communities are following the succession pathways through imposing the modifications and the metabolism of the natural resources through selecting their degree of the usability in comparison to other colonising microorganisms (Benbow *et al*. 2013).

Various terms have been exploited in the forensic in order to refer to decomposition organisms and post-mortem microbiome (Fig 13) to define accurately the corpse's decomposition process:

Necrobiome, from the ancient Greek terminology; nekrò, which means the dead body, the corpse, or the dead person. This term is referring to the various communities of species, whether they were prokaryotic or eukaryotic, also, if they were unicellular or multicellular. This term is defining the correlation between the microbial species and the decomposition process of the heterotrophic biomass remains, which includes the human cadaver and the animals' corpses (Benbow *et al*. 2013).

Epinecrotic bacterial community, from the ancient Greek terminology, which is defined as a branch of the necrobiome which includes the residing or moving microorganism on the

decomposing remains surface, such as the skin or the mucous membrane of the mouth cavity (Pechal *et al*. 2013a).

Thanatomicrobiome, from the ancient Greek terminology; thanatos, which means death, was initially introduced by Can *et al*.,(2014) This term is defining the microbiomes, which are incubated at the surface of the cadaver. In addition, this terminology identified by the authors for providing a description of microorganisms present within the internal organs of the host, for instance, spleen, brain, and heart. The difference between the necrobiome and the thanatomicrobiome is that the necrobiomes comprise various groups of microorganisms' species, insects, arthropods, and larger organisms, which have devoted their function to degrading corpses. While the thanatomicrobiome is, referring to the microorganisms, which can conduct the decomposition process within and through the surface of the cadaver body and the decomposing remains (Fig. 13).

In fact, the majority of the internal organs, such as the brain, heart, liver, and spleen are devoid of microorganisms as a result of the eradicative function of the competent immune system of the healthy adult. Conversely, in regards to the human body post-death scenario, the immune system loses its viability, which leads to the proliferation of the microorganisms throughout the whole body, initially from the ileocecal segment of the intestine and spreading to the vital organs such as the spleen and liver, thereafter, the brain and the heart. The spreading approach followed by the bacteria for the purposes of body system invasion is through the microbial diffusion exploit the lymphatic and the vascular capillary system by the infestation through the lining mucous membrane of the respiratory system track. The environmental atmosphere and the surrounding conditions do not critically affect the internal organs associated microorganisms, moreover, they exhibit a relative resistance to the gastric microorganism proliferation post-death influence, in comparison with the external organs corresponding microorganisms, which are usually incubated in the outer surface of the skin and the oral cavity epithelial tissues. The monopolisation of the internal organ tissues for applying the thanatomicrobiome operation is providing merits countenances superior to other sampling candidates' sites. Dialectically after death, the microorganisms tend to invade and colonise within the tissues of the cadaver's internal organs (Javan *et al*. 2016a).
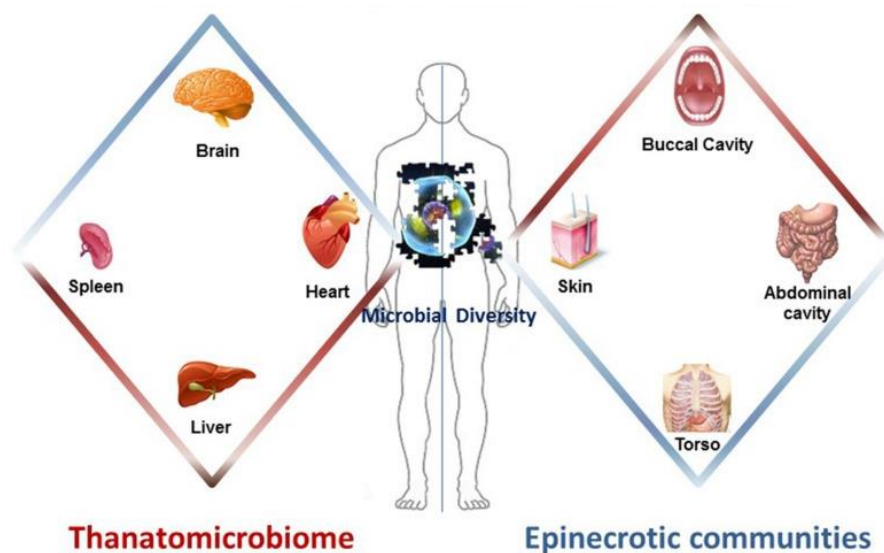
Figure 13. Human post-mortem microbiome (Javan *et al*. 2016a).

From a forensic domain perspective, exploring these signalize microorganisms is an essential manoeuvre, studying and screening the presence or absence of a certain bacterial species can be considered as an indicative tool for evaluating the post-death elapsed time duration. Which, denominated as the post-mortem interval (PMI), in relevance to the related studies implanted in mouse and swine species (Metcalf *et al*. 2013, Pechal *et al*. 2013a). Referring to the related studies, the yielded results from the autopsy microbiology, which is exploited as a confirmatory tool for the presence of a potential ante-mortem infection, identifying and indicating the infection in the scenarios of the anonymous death causes, or assessing the antibiotic therapeutic range of efficacy in inhibiting or eradicating the infectious pathogens (Can *et al*. 2014).

Furthermore, the post-mortem microbiome is utilised for providing a generalised description of the microorganisms' communities associated with the corpse, expressed with indicative terms including the necrobiome, the epinecrobiome and the thanatomicrobiome. The post-mortem microbiome terminology is utilised by the concerned authors in a context where they try to address and estimate the post-mortem interval PMI based on the forensic microbiology purposes (Javan *et al*. 2016a).

1.2.3.8.3 The Use of Forensic Microbiology in Forensic Investigation

Essentially, full recognition and examination of all dimensions of the crime scenes are necessary. Otherwise, some evidence may not get discovered for a while such as the evidence of physical assault, disease and their factor detection, and intentional incidents. There is a

structural similarity between the forensic microbiological investigations and other standards of forensic investigations, involving crime scenes investigations. Which custody practices, evidence collection, samples handling and their proper preservation, evidence transport, evidence analysis, obtained results interpretation, and court comprehensive representation (Budowle *et al*. 2005). Microbes have been in a recognisable position in the field of medicine, fermentation science, and ecology, however, recently microbial science has been introduced in the field of forensics. The continues of advances in the molecular sequencing and computational techniques have revolutionised the involvement of the microbial approach in the forensic field (Gunn and Pitt, 2012).

The widespread and diversity of microbes can legalise confirmed their exploitation as a forensic evidence. Consequently, the microbial forensics has been indicated to illustrate the role of microorganisms in assisting the forensic investigations, in addition, the existence of microbes could permit to identify the individuals, objects, organisms, or locations. In fact, there is a strong proofing that the human is a carrier for a highly diverse microbiome, which might prove its applicability in indicating personal characterisation, ethnicity, and country of origin. Moreover, the human microbiome exhibit variations within body regions, a feature that can be exploited for determining the origin of stains which can be caused by different human fluids, such as saliva and vaginal fluids. In addition, it provides a possibility of imposing a linkage between the residual station and the corresponding person responsible for it. Referring to the same concept, the microbiome composition present in the soil sample might act as an indicator of the geographical origin or a specific location. The high spreadability and diffusivity of the microbes require the proper linkage of the accused and the plaintiff toward a specific strain. Furthermore, the preservation of microbial forensic samples is differing based on the microbial metabolism diversity of the organic and inorganic materials, which can be utilised as preservation media. Not to mention, the human corpse can be a major source for transmitting infectious microorganisms, therefore, requiring the careful handling of minimising the risks of contagious disease exposure (Gunn and Pitt, 2012).

The applications of microbial communities' analysis aid in forming an advance improve an area of forensic science domain, i.e. forensic microbiology. The microbial forensic attribution can be stated as the comprehensive characterisation of microorganisms present in the collected sample, and classify them on the basis of their species or strain level followed by the specific isolation and culturing. Furthermore, scientific attribution can exclude other isolated suspects or sources as much as possible, also, helps investigations and legal procedures. Indeed, the

microbial forensic practice requirements and standards exhibit lower defining borders than other well-established human forensic domains. Nevertheless, the validity establishment of the microbial forensic methods in terms of utilisation and interpretation contributes to several factors including the admissibility, acceptance, confidence, value, and the weight of the obtained evidence in the investigation procedures (Budowle *et al*. 2014).

1.2.3.8.4 Microbial Communities Variation in Human Body

Microorganisms are the most abundant and genetically diverse living organisms, which ubiquitously inhabit the environment including many extremely adverse environments.

The microbial communities associated with human body have a high level of variability among individuals in everybody and between the body regions including the gut, skin, and oral cavity, and relative stability within individuals (Fig. 14)(Costello *et al*. 2009). On the other hand, many similarities of the microbial communities have been found in the different body region, armpits and foot soles also share similar biota (Barley, 2009).

Until a few years ago, the lack of population-scale data detailing their composition and function represented a big obstacle for the scientific community in investigating the microbes that inhabit the human body, soils and elsewhere.

Since 2008, the US NIH-funded Human Microbiome Project Consortium (HMP) has been gathering a broad collection of scientific approaches and expertise to explore defined microbial communities and their links to the corresponding human hosts. The development of molecular biology technologies coupled with new bioinformatic tools are allowing this type of investigations. Microbiome investigations from this cohort involved several complementary analyses, including 16S ribosomal RNA (rRNA) gene sequencing and taxonomic profiles, whole-genome shotgun (WGS) or metagenomic sequencing of whole community DNA. Researchers concerning in HMPC described the thousands of samples obtained from 15 or 18 distinct body sites from 242 donors (18-40 years old) over multiple time points that were processed at two clinical centres, Baylor College of Medicine (BCM) and Washington University School of Medicine. A set of 5,298 samples were collected from 242 adults, from which 16S and WGS data were generated for a total of 5,177 taxonomically characterized communities. (16S) from a collection of 11,174 biological specimens and 681 WGS samples describing the microbial communities from habitats within the human body regions like oral

cavity, skin, gut and vagina and the distribution as seen in (Fig. 14) (Methe *et al*. 2012, Costello *et al*. 2009, Huttenhower *et al*. 2012).
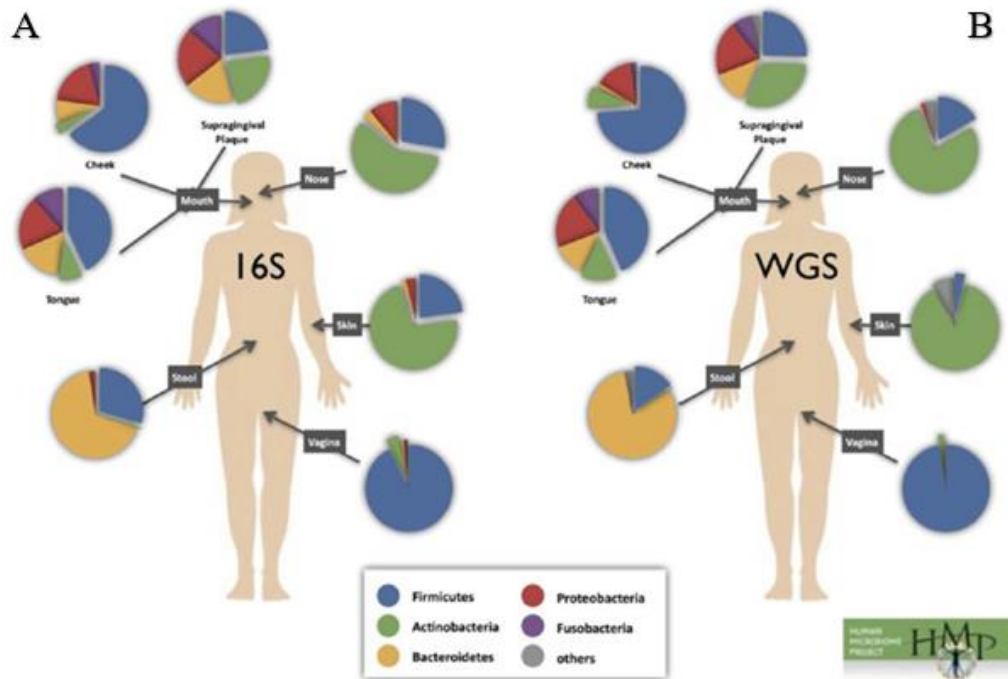
Figure 14. Phylum abundances per body region. (HMP, 2012). For each of the body sites studied by both 16S ribosomal RNA (rRNA) gene sequencing (A) and WGS whole genome shotgun sequencing (B), the five most abundant phyla are Firmicutes, Actinobacteria, Bacteroidetes, Proteobacteria and Fusobacteria.

1.2.3.8.5 Epinecrotic Communities in the Forensic Investigations Contexts

Numerous recent forensic studies have focused on finding a firm correlation between the human bacterial communities, which came from a dead or alive body. Also, from the corresponding crime scene (Fierer *et al*. 2010b, Hyde *et al*. 2013). In order for researchers to perform that aim, several analytical methods have been applied at different stages. In comparison with the previous applications of the microbial community analysis for forensic purposes, the attentions were restricted towards identifying the microbe type obtained and cultured from the crime scene understated environmental circumstances (Gunn and Pitt, 2012).

The forensic investigations are following the formal procedures of exploratory process, starting with the precise locating of the cadaver and the remains, followed by the sampling from the buccal cavity and the skin, for example, by utilizing sterile cotton swabs. This procedure is to provide key investigational for describing and quantifying the viable bacterial communities'

profile present on the cadaver or the remaining at the time of the forensic discovery. Samples collected should be stored individually at a low temperature, approximately −20 °C, in order to be applicable and fertile for further analysis. Thereafter, the metagenomics sequencing analysis is performed after the successful retrieving and processing of the extracted DNA from each collected samples. Posteriorly, assess the overall bacterial communities through the relative determination of the taxon abundance at the preferred context of the taxonomic resolution using a classification of the DNA sequences. The importance of these obtained data is arising from their applicability in aiding the estimation the decomposition time and the physiological interval. Subsequently, a comparison between the identified bacterial communities from the collected samples and the identical reference data from the environment is conducted, the comparison based on the taxon abundance and the relative richness, known ratios of the dominant taxa during composition can be compared with the relative abundance of the identified bacterial community. Afterwards, an estimation of the physiological time range can be obtained based on the analysed bacterial communities which are calculated under the support of the weather station relevant data (Fig. 15) (Pechal *et al*. 2013a).
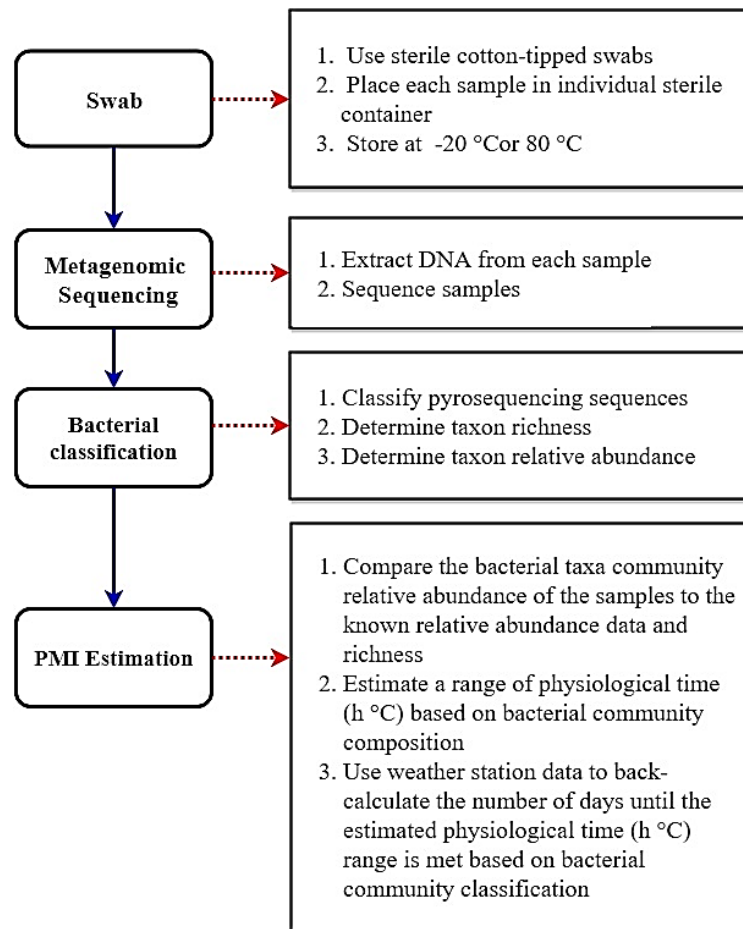
Figure 15. Framework for utilizing bacterial communities to estimate PM (Pechal *et al*. 2013a)

The epinecrotic bacterial communities have unique shifting profiles, restricted to one day for the decomposition process completion, this feature might be helpful in forensic where the conclusive evidence is absent in the crime, for example, when the critical insects are not colonised through the remains at the discovery time. As a future perspective, exploiting the epinecrotic bacterial communities as a forensic analytical tool is take a potential spot for simplifying the investigational measurements. Furthermore, these obtained data are contributing majorly to the rising forensic knowledge based on the general dynamic of the decomposition ecological science and the necrobiome. The critical identification of the communities' interaction can be executed based on connecting the necrobiome to decomposition ecology, in significance to the decomposition process, the attraction controlling the mechanism of the non-microbes to the cadaver, also, the impact of the natural decomposition process along with the forensic suitability and the appropriate applications (Pechal *et al*. 2013a).

1.2.3.8.6 Soil Microbes as Forensic Indicators

For many purposes, the soil microorganisms can be considered as a single group of living soil organic matter (the soil microbial biomass) (Brookes, 2001). The soil surrounding the cadaver plays a crucial role in legal investigations as a tool for providing physical trace evidence that might act as a critical key for linking the victim or suspect to the crime scene, identifying the unknown cadaver and determining whether the cadaver has been moved from the actual crime location or not. The traditional forensic analysis of soil is usually depending on its physical properties and chemical composition examining features such as soil type, colour, and particle size. In addition, its elemental, mineral, and organic content, the factors that can cause the limitation of this analyst procedure is the lack of the reasonable amount of the materials and substrates. Also, the lack of soil databases (Meyers and Foran, 2008).

Soils are considered as a dense environment of various microbial communities. Considerably, the soil microbes could exhibit a forensic significance, particularly in the later stages of decays when the abundance of the insects has been reduced. Also, the differences in the carcass quality were found to affect the soil microbial communities and following decomposition processes (Hawlena *et al*. 2012). From the investigative and a perception of evidence, the acquisition of more data has a direct relationship with the robustness of the forensic case. The microbial communities present in the soil located in contact with the corpses are tending to undergo

substantial biochemical shifting, as consequent results of the fluids, nutrient, microbe movement into the grave soil. The potential changes in the soil microbial communities are providing an advantageous investigative tool that can be exploited for estimating the PMI or identifying the clandestine grave exact sites. The effect of soil water content on the microbial communities' composition was most clearly in the flooded cases, as might be expected since the prevailing electron acceptors strongly affect microbial community structure. Although flooding changed microbial community composition, the response was most pronounced in the organic carbon-amended samples. Without organic carbon inputs, the microbial community most likely lacked sufficient organic carbon and energy sources to grow and ''replace'' itself with a new community. Another potential impact of carbon additions may have been the development of anoxic conditions in carbon-amended microcosms, in contrast to unamended microcosms that more likely remain aerobic in the absence of a strong oxygen demand (Drenovsky *et al*. 2004).

1.2.3.8.7 The two prime areas of microbial communities' applications in forensic studies

- The dynamic analysis, defined as the exploitation of the microbial communities as a biological clock for estimating the PMI in the forensic investigations.
- The static analysis, defined as the utilisation of the microbial community as a fingerprint during the forensic investigation at the crime scene.

1.2.3.8.8 Research Models of the Microbiome Characterisation

Many post-mortem microbiological studies use animal models such as swine (Pechal, Carter, Crippen, Levran and Finley 2016, Benbow *et al*. 2015, Howard *et al*., 2010) or juvenile rodents, Mouse corpses (Metcalf, and Jessica 2016, Carter *et al*. 2008). Pigs could be a suitable alternative because of a high degree of similarity in the decomposition processes comparing to human. Whereas, other studied were performed by (Hyde, Can, Pechal, Sing, Crippen, and Gulnaz T. Javan 2016, Hyde *et al*. 2013, 2015, Metcalf *et al*. 2016) using human cadavers, which they are frequently obtained through field experiments using willed body donation or autopsied cadavers in criminal cases. In addition, Salmon carrions (Pechal and Benbow. 2016). Summary of some research studies about the analysing of the microorganisms that colonise cadaver is listed in table 5.

Table 5. Summary of some research studies showing that the microorganisms can colonise the cadaver in an expected pattern and they can be used for forensic purposes.

Article title	Carrion used	DNA analysis	Statistical and other analysis	Reference
Forensic identification using skin bacterial communities	Human skin Individual objects	Amplified 16S rRNA genes using primer: 27 F and 338 R 454 pyrosequencing	ANOSIM	(Fierer *et al*. 2010a)
The living dead: Bacterial Community Structure of a Cadaver at the Onset and End of the Bloat Stage of Decomposition	Human cadavers	Amplification of V3-5 regions of 16S rDNA gene Primers used: 357 F, 926 R 454-FLX Pyrosequencing	QIIME version 1.7.0, an open-source software package	(Hyde *et al*. 2013)
The potential use of bacterial community succession in forensics as described by high throughput metagenomics sequencing	Swine carcasses	Amplification of V1-3 regions of 16S rDNA Primers used: Gray 28 F, Gray 519 R 454-FLX Pyrosequencing	PERMANOVA	(Pechal *et al*. 2013b)
Microbial Community Functional Change during Vertebrate Carrion Decomposition	Swine carcasses	Biolog EcoPlates™ for Microbial community function Amplification of V1-3 regions of 16S rDNA gene Primers used: Gray 28 F, Gray 519 R 454-FLX Pyrosequencing	PERMANOVA	(Pechal *et al*. 2013a)
A microbial clock provides an accurate estimate of the post-mortem interval in a mouse model system	Mouse	sequenced ~100 base pairs of both 16S and 18S amplicons at a depth of millions of sequences using the Illumina HiSeq platform 16S rRNA variable region 4 (V4) using a primer set 515F/806R 18S primers Euk1391f/ EukBr	PERMANOVA	(Metcalf *et al*. 2013)

		Amplification of V1-9 regions of 16S	Analysis of similarity	
Microbial communities associated with human decomposition and their potential use as post-mortem clocks	Mice corpses	rDNA gene. 454 pyrosequencing for soil 16S rRNA gene sequencing on the Illumina HiSeq platform using prokaryotic 515 F and 806 R primers.	(ANOSIM) and nonmetric multidimensional scaling (MDS) analyses	(Finley *et al.* 2014)
Initial insights into bacterial succession during human decomposition	Human cadavers	454 pyrosequencing and analysis of variable regions 3–5 of the bacterial 16S ribosomal RNA (16S rRNA) gene.	Non-parametric t-tests using 999 Monte Carlo permutations	(Hyde *et al.* 2015)
Seasonal variation of pos-tmortem microbial communities	Swine carcasses	Amplification of V4 region of 16S rRNA gene using 515 F and 806 R primer set. Amplification of 18S rRNA gene using Euk139 F and EukBr primer set Sequencing via Illumina HiSeq and MiSeq platform	PERMANOVA	(Carter *et al.* 2015)
Evaluating variation in human gut microbiota profiles due to DNA extraction method and inter-subject differences	human	V4 region of the 16S rRNA gene was amplified	PERMANOVA	(Mackenzie *et al.* 2015)
Microbial ecology of the salmon necrobiome: evidence salmon carrion decomposition influences aquatic and terrestrial insect microbiomes	Salmon fish	Amplification of variable region 4 of the 16SrRNA gene Primers used: 515 F/ 806 R Illumina MiSeq	PERMANOVA	(Pechal and Benbow, 2016)
Human Thanatomicrobiome Succession and Time Since Death	Swine	16S rRNA genes were amplified by universal primers for the V4 region (515 F–806R) Microbial sequencing was performed on the MiSeq platform (Illumina)	ANOVA measures of microbial diversity differences using ADONIS	(Javan *et al.* 2016b)

Microbial Signatures of Cadaver Grave soil During Decomposition	Human cadavers	The V4 region of 16S rRNA genes was amplified with region-specific 515 F/806 R primers European Bioinformatics Institute Sequence Read Archive (PRJEB9166).	Shannon-Wiener Diversity non-parametric one-way analysis of variance Kruskal-Wallis tests using Prism 5 (GraphPad Software)	(Finley *et al.* 2016)
The Thanatomicrobiome: A Missing Piece of the Microbial Puzzle of Death	Swine	16S rRNA gene amplicon-based sequencing approaches have made significant progress in opening up new lines of inquiry	PERMANOVA and ANOSIM	(Javan *et al.* 2016a)
Microbial community assembly and metabolic function during mammalian corpse decomposition	Mouse and human corpses	amplicon-based sequencing of 16*S* ribosomal RNA (rRNA) genes (archaeal and bacterial community)	Excel and ANOVA	(Metcalf *et al.* 2016)
Dynamics of Necrophagous Insect Species and Bacteria from Swine Carcasses During the Warm Season in Conference Paper	swine carcasses	Denaturing Gradient Gel Electrophoresis (DGGE) analysis of the 16S ribosomal RNA (rRNA) gene fragments.	Comparing the result in Excel	(Iancu *et al.* 2016)
Dynamics of Necrophagous Insect and Tissue Bacteria for Pos-tmortem Interval Estimation During the Warm Season in Romania	swine carcasses	Amplification of Bacterial 16S rRNA gene using primer: F 357 and R 518	MS Excel principal component analysis (PCA)	(Iancu *et al.* 2016)
Post-mortem succession of gut microbial communities in human cadavers	Human Gut Microflora	16S rRNA gene libraries (V4 region) amplicon sequencing Illumina MiSeq platform	SIMPER analysis NMDS analysis of Bray	(DeBruyn and Hauther, 2017)

1.2.4 Estimation of Post Mortem Interval (PMI)

In terms of the physical evidence, the establishment of the approximate time estimation of death until the cadaver discovery moment can exhibit a major source of difficulties in forensic investigations, precisely, speculation of the time period where the corpse was exposed to the surrounding environment, which is known as the post-mortem interval (PMI). It belongs to one of the thanatocronological parameters which used for analysing death time. In death investigations, the accurate assessment of PMI is critically important because it can facilitate the conclusive identification of suspects and victims, also, it can simplify the acceptance or rejection of alibis against the suspects, the death certificates distribution, and the allocation confirmation of assets stated in wills. The determination of the PMI time ranges and indicating the precise time window and locations of both the witness and the decedent are substantial inclusion and exclusion parameters of suspects aiding in defining the assaulting circumstances.

As previously addressed, PMI has exhibited some establishment difficulties, attributed to the relatively limited understanding of the gradual decomposition of the corpse which majorly affected by several surrounding variables. In the early period of the post-mortem, which is the first 48-80 hours after death, the estimation of PMI through the precise measuring of the temperature is considered as the duty of the medical examiner, forensic pathologist, or the coroner. Therefore, this estimation is prone to be affected by several variables and the investigational evaluation is compromised by the thanatological events. However, the applicability of PMI time might be limited in some extremes assaulting cases, for instance, corpse dismemberment, concealment, explosions, and burning, hence, there is no standardised approach for deriving the exact death time in these forensics scenarios (Vanin *et al*. 2013).

Taking into consideration the variability of cadaver's decomposition pathways, there are specific factors that can dependently affect these pathways including biotic, abiotic, or microenvironmental factors. These factors, which initiate the decomposition process, should be extensively studied in order to obtain an approximate estimation of PMI, examples of these decomposition methods including concentrating of potassium in the vitreous humour, livor mortis, and forensic entomology. Unfortunately, the low applicability of these methods in many conventional forensic scenarios and the limited accuracy in measuring the PMI have provoked the need for seeking better alternatives. Considerably, the entomological discipline is an approach, which concerned in insects' knowledge and its applications in the civil proceedings and criminal trials fields. The estimation of the dead time is well known as the cadaveric fauna,

which is widely accepted method for supporting the histological and chemical analysis and aid in police investigational procedures. This method studies the decomposition process as a time-specific function for estimating the PMI belongs to the vertebrate remains, utilising the biotic signatures which are associated with different decomposition stages, for instance, the development rate of blowfly larvae succession correlated with insects which induce changes in the biochemistry of corpse 'grave soil'. The insects are forming the majority of invertebrate fauna which can be found in the corpses, particularly, the flesh flies and beetles which named as the Diptera and Coleoptera respectively. These are known to be selectively attracted the corpse decomposition status and are able to form insects' communities within necrophagous and their parasites, predators, parasitoids (Turchetto and Vanin, 2004).

The insect's viability and their proliferation capacity throughout the cadaver depend on several factors including the ambient temperature of the environment and the contact degree with the corpse (e.g. presence or lack of clothes).

The Period of Insect Activity (PIA), which is the period of time when the depositions of the eggs or larva occur until the discovery of the corpse, is considered different than the term PMI. While, minimum Post Mortem Interval (mPMI) is defined as the eggs elapsing time by Diptera and Coleoptera and the cadaver discovery (Fig. 16) (Lewis and Benbow, 2011). Unfortunately, there are lacks in methodologies for the real experimental measurement of PMI, knowingly; the shorter the time of cadaver finding by the flies will eventually lead to a shorter difference between the PMI and mPMI. Colonisation Interval (CI) is a term suggested by Benecke, in order to minimise the confusion between the PMI and mPMI terms. CI is majorly related to mPMI, and it exhibits more appropriateness for describing entomological forensic purposes (Magni *et al*. 2008).
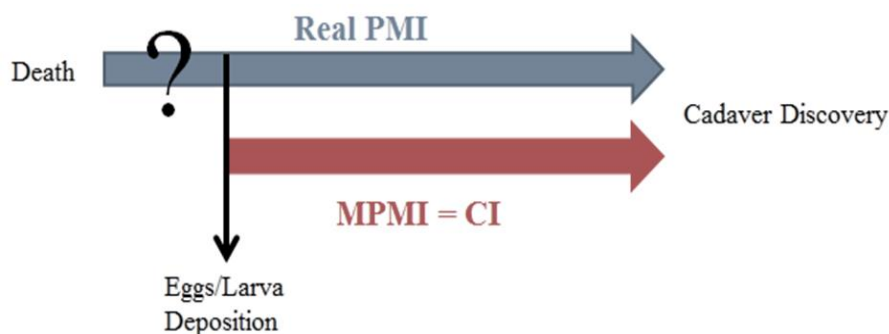
Figure 16. Shown the real period of the pos-tmortem interval (Magni *et al*. 2008).

The cadaver accessibility degree will determine the number of flies attracted and consequently prolonging the egg deposition time. The surrounding barriers and the cadaver location could definitely affect the insects' accessing time to the corpses. Accordingly, the corpse's detectability by the insects is affected by the degree of odour diffusion, and the inherent difficulty in reaching the concealed corpses.

The insect's colonisation process is influenced by two overlapping parameters including gases escaping and the cadaver surface approached by the insects. However, the entomological strategy for estimating PMI is encountering some limitations due to the persistent uncertainty in measuring the time interval between death and insects egg deposition on the cadaver. On the other hand, the entomological approach exhibiting a prime advantage versus the other standard methods in determining the early PMI, the arthropods have the ability to produce a precise measurement in the later phases when the other classical forensics pathologic methodology reach a failure stage. On the other hand, a chemical analysis of various components of blood, cerebrospinal fluid, and vitreous have been studied as a means to determine the time of death. Unfortunately, none of these studies has yielded conclusive means to identify when someone died. The concentration and rate of potassium in the vitreous fluid have received the most attention over the years. Its use is limited because of wide individual variation.

1.2.4.1 An accurate Estimating of PMI using the Microbial Clock

The ecological perspective has been combined into the forensic science in order to optimise the ability to estimate the PMI associated with the terrestrial ecosystem (Metcalf *et al*. 2013).

The ubiquitous microorganisms in the environment are associated with ante-mortem and pos-tmortem manifestations of human beings, as a point of the defect; microorganisms have been underexploited and underutilised as biological indicators for estimating the length of death time. Until now, there is a limited knowledge of understanding the post-mortem microbiology and its involvement in the human cadavers' microbiological diversity (Pechal *et al*. 2015).

The corpse decomposition follows several defined forensic phases depending on the nutrients recycling process performed by the microorganisms' communities as decomposers agents, the phases are including the pre-decomposition fresh phase, the active decay phase which constitutes of bloating and rupturing, and the advanced decay phase (Metcalf *et al*. 2013).

Finley *at al*., (2014) demonstrated that the microbial communities might offer a novel and more precise means of estimating the PMI. Because of this more continuous rather than separate processes. According to the recent studies, the microorganisms' communities are exhibiting a dynamic nature during the post-mortem phase in the screened microbial models, in particular, the indigenous residing of the microbial succession in the human body during the decomposition (Pechal *et al*. 2015).

Considerably, the rapid modifications of the epi-necrotic microbial communities can be invested as a "microbial clock" which can be used as a basis for the approximate estimation of the post-mortem interval (PMI), having the ability to overcome the typical obstacles of the forensic entomology. Recently, collaborative forensics researchers have been conducted towards establishing animals' surrogates instead of human cadavers, intended for studying and accurately estimating the mPMI ranges followed by the statistical extrapolation to the human mPMI, examples of these animals are swine and mouse. The forensic microbiology prime objective concerning this research domain is reaching the optimum description for the decomposition process as a function of the temperature, taking into the consideration the cadaver exposing factors during a period rather than concerning the time as an individual predisposing factor. The metagenomics and the necrobiomic community's analysis are the fundamental basis for provoking these forensics studies. Referring to a recent study, pigs have been used as surrogates for human cadavers, aiding in the clear representation of the bacterial communities' necrobiomic induced changes during the decomposition phases among different seasons. The assessed cascades of the obvious decomposition changes can be utilized in designing a map for estimating death time to be applied feasibly in forensic investigations (Metcalf *et al*. 2013).

Hyde *et al*., (2013) have conducted one of the initial exploratory investigations into the internal microbiome of the human cadavers. In this study, two human cadavers have been placed intentionally in outdoor in order to induce the natural environmental decomposition; the decomposition process has been observed and studied carefully followed by an establishment of metagenomics techniques catalogue of microbiological species involved during the human decomposition bloat stage. The overall result of this study is the successful demonstration of the microbial signature variabilities among the complete human body and sample specific regions within the human body. In addition, it produced a representation of the bacterial shift from the aerobic to the anaerobic state during the interval time between the initial points and the endpoints of the bloat phase with the tested sample (Hyde *et al*. 2013).

Several relevant studies have succeeded in generating an investigational model based on the microbial sequence changing patterns, which can be implemented for the post-mortem intervals estimation. Accordingly, Pechal *et al.*, (2013a) demonstrated that the bacterial communities incubated in the skin and mouth can undergo some drastic changes during the decomposition process. The microbial community changes during the decomposition process in a mouse model confirmed to be measurable, repeatable, and dramatic (Metcalf *et al.* 2013).

1.2.5 Techniques of Microbial Communities' Analysis

The analysis of the microbial forensic is conducted in the context of a criminal investigation, which shapes the differences between its technologies and best practices that used for clinical examination and public health. The analytical differences factors between microbial forensics and other sectors are legal requirements that must meet regarding (1) sample type, (2) level of characterisation, and (3) interpretation and reporting (Garland and Mills, 1991).

Investigators must have confidence in their results and the procedures they have used when reporting to a court. In addition, Investigators must consider reasonable alternative explanations. Furthermore, they must provide known error rates and detection limits when possible for judges. These factors inform the choice of analytical techniques to be used. Traditional microbiology and culture is the current standard in clinical diagnostics, but it is not always possible or practical to culture microbes in a forensic investigation (Council, 2014).

In every ecosystem the microbial a play an important role in the decomposition of organic matter, however, there is no complete information about the functional activity of the microbial communities associated with carrion, and little is known about it. Microbial communities are existing in all environments and they are usually the first organisms to respond to the physical and chemical changes in the environment. Microbial communities provide valuable information about environmental change. The microbial communities' changes are often a sign of changes in the health and viability of the environment as a whole. The changes in the cadaver microbial community functional profiles during the decomposition process and the effects of the environmental conditions, season and the presence of insect were examined using Biolog EcoPlates. Utilising 31 different carbon sources during the cadaver decomposition process (Pechal *et al.* 2013a).

The information about which microbial species may play a role in the decomposition process is limited. There have been no comprehensive studies of the microbial ecology of human decomposition. This could be from the restrictions of classical microbiological methods and the number of microbial species expected to be involved in the decomposition process (Parkinson, 2009).

1.2.5.1 Analysis of the Microbial Communities Evolution

The evolution of the microbial communities on a dead body can be analysed from an ecological point of view studying the carbon sources used by the different bacterial communities that develop during the decomposition on and in the body. This approach has been mainly investigated using the EcoPlate.

EcoPlates were created with recommendations of microbial ecologists specifically for community analysis and microbial ecological studies, to provide a sensitive and reliable index of spatial and temporal environmental change in microbial communities (Boilog, 2012).

- Measure the metabolism of 31 carbon sources per test.
- Each test panel tests in triplicate.
- Simple colourimetric readout.
- Readable with any microplate reader.

The other approach to study the microbiome is based on the DNA sequencing. DNA can be used to identify the organism in what is called molecular identification.

Genomic DNA is extracted directly from dead or alive bacterial colonies grown under any conditions. The 16S rRNA gene (for bacterial identifications) is amplified using universal primers (Microbe Inotech Laboratories, 2009). It may even be possible to use stored DNA extracts from old or cold cases for microbial analyses (Benschop *et al*. 2012). Molecular analysis is often used for studying bacterial phylogeny and taxonomy by using 16S rRNA gene sequences for identification and classification of microbes within complex biological mixture samples. The 16S rRNA gene is a tremendously protected element of the transcriptional machinery of all DNA-based life forms (Patel, 2001), thusly it is the most targeted gene for DNA sequencing in the complex samples containing a huge number of species. The ability to design universal PCR primers, which conserve the regions of 16S gene, makes amplifying the gene easier for a sample containing the variety of microorganisms. Conveniently, the 16S

rRNA gene consists of both conserved and variable regions. Since the conserved regions facilitate the universal amplifying, the variable regions sequencing discriminates between different organisms like archaea and eukaryotic microorganism (Wintzingerode *et al*. 1997). Pyrosequencing used to describe the bacterial communities structure and identify the associated taxa with community functional changes (Pechal *et al*. 2013a).

1.2.5.2 Functional Characterisation of Microbial Communities

Referring to the related studies, BIOLOG Microplates were basically optimised for performing a high through output identification of the isolated bacteria through utilising the sole carbon resource in the analysis, by the means of inoculating 95 singular carbon source additionally with water as a reference control on the 96th well plate. The plates were screened in a specific time interval between 24 and 72 hours' post-inoculation using a pre-grown isolate. As a result of the substrates metabolism in each well, formazan was produced, which induces the colour shifting in the tetrazolium dye. Hence, this method provides a metabolic fingerprint, which might identify the individual species by observing the colour alteration on each plate. Unfortunately, the plate's technique is lacking the ability to yield more comprehensive sets or results that can be generalised, this is due to the limited uniformity of the bacteria and fungi specious in reducing the tetrazolium dye which has introduced bias to this technique. The BIOLOG Microplates are available in different range of types containing variable substrates, for allowing the simple and direct comparison (Preston-Mafham *et al*. 2002).

Functional diversity is the most important parameter for characterisation and exploitation of microbial cultures. Depending upon the target use of the organism, they have been given different names which indicate their major functions in nature or under defined conditions (Ahmad *et al*. 2011). Microorganisms are considered as the first organisms, which exhibit physicochemical alterations in correspondence to the environmental interactions, hence, the microbes, which present virtually in the environment are the prime source of information reflecting the positive and the negative environmental changes. The Biolog EcoPlate™ was designed specifically for analysing the microbial community and for conducting the microbial ecological studies. Originally, the invention of this system was started by the request of the microbial ecologists' group, which they were using the Biolog GN MicroPlate™ without a panel, which can provide sets of replicate tests. Garland and Mills initially addressed the Biolog Microplates for the microbial community analysis in 1991. According to this study, the

inoculation of a mixed culture of microorganisms in the Biolog GN Microplates system, followed by time-specific measurements of fingerprints produced in correspondence to the microbial communities could assure and confirm the proposed characteristic of each scanned communities (Garland and Mills, 1991).

This technique, which named as the community–level physiological profiling, has been elucidated to be applicable aiming for spotting the two-dimensional temporal and spatial changes in the microbial communities. In the ecological aspect, the Microplates has two research functions which include providing an examination of the normal population stability and for detecting and evaluating the changes caused by the environmental changes. The Biolog The BIOLOG EcoPlates™ contains 31 different carbon sources (Fig. 17), (Table 6) which can be utilised by microbial communities depending on their metabolic abilities as growth sources. The set of substrates were chosen similar to many nutrients found in natural environments so that the microbial functional diversity can be evaluated. Each one of the 31 carbon sources is present in triplicate in a 96 well plate. In addition, three blank wells of water acting as a negative control. Which is provide a representative approach to acting as surrogate metabolic signatures for allowing the functional diversity of the evacuated communities. The triplet repetitions of these 31 carbons assure accuracy by performing scientific replications of the resultant data (Chojniak *et al*. 2015). The obtained of metabolic fingerprint profiles, which named as the microbial community level physiological profiles (MCLPPs), can act as a source of ecological data upon temperature and genomic sequencing calibration which enable the prediction of the duration needed to initiate and complete the corpse decomposition. The advantage of CLPP over both classic cell culturing and molecular level RNA/DNA amplification-based techniques is its relatively simple protocol and ease of use (Weber and Legge, 2010). The community-level physiological profile is assessed by the formation of purple colour occurring when the isolate microbes are able to use the specific carbon source contained in the well and begin to respire it. The colour development is directly proportional to the metabolism of each carbon source so the development of formazan can be followed over time. The community-level physiological profiling (CLPP) is considered a functional indicator for the evaluation of microbial community function as well as the functional diversity in the aquatic and terrestrial environments (Button *et al*. 2016).

A1 Water	A2 β-Methyl-D-Glucoside	A3 D-Galactonic Acid γ-Lactone	A4 L-Arginine	A1 Water	A2 β-Methyl-D-Glucoside	A3 D-Galactonic Acid γ-Lactone	A4 L-Arginine	A1 Water	A2 β-Methyl-D-Glucoside	A3 D-Galactonic Acid γ-Lactone	A4 L-Arginine
B1 Pyruvic Acid Methyl Ester	B2 D-Xylose	B3 D-Galacturonic Acid	B4 L-Asparagine	B1 Pyruvic Acid Methyl Ester	B2 D-Xylose	B3 D-Galacturonic Acid	B4 L-Asparagine	B1 Pyruvic Acid Methyl Ester	B2 D-Xylose	B3 D-Galacturonic Acid	B4 L-Asparagine
C1 Tween 40	C2 i-Erythritol	C3 2-Hydroxy Benzoic Acid	C4 L-Phenylalanine	C1 Tween 40	C2 i-Erythritol	C3 2-Hydroxy Benzoic Acid	C4 L-Phenylalanine	C1 Tween 40	C2 i-Erythritol	C3 2-Hydroxy Benzoic Acid	C4 L-Phenylalanine
D1 Tween 80	D2 D-Mannitol	D3 4-Hydroxy Benzoic Acid	D4 L-Serine	D1 Tween 80	D2 D-Mannitol	D3 4-Hydroxy Benzoic Acid	D4 L-Serine	D1 Tween 80	D2 D-Mannitol	D3 4-Hydroxy Benzoic Acid	D4 L-Serine
E1 α-Cyclodextrin	E2 N-Acetyl-D-Glucosamine	E3 γ-Hydroxybutyric Acid	E4 L-Threonine	E1 α-Cyclodextrin	E2 N-Acetyl-D-Glucosamine	E3 γ-Hydroxybutyric Acid	E4 L-Threonine	E1 α-Cyclodextrin	E2 N-Acetyl-D-Glucosamine	E3 γ-Hydroxybutyric Acid	E4 L-Threonine
F1 Glycogen	F2 D-Glucosaminic Acid	F3 Itaconic Acid	F4 Glycyl-L-Glutamic Acid	F1 Glycogen	F2 D-Glucosaminic Acid	F3 Itaconic Acid	F4 Glycyl-L-Glutamic Acid	F1 Glycogen	F2 D-Glucosaminic Acid	F3 Itaconic Acid	F4 Glycyl-L-Glutamic Acid
G1 D-Cellobiose	G2 Glucose-1-Phosphate	G3 α-Ketobutyric Acid	G4 Phenylethyl-amine	G1 D-Cellobiose	G2 Glucose-1-Phosphate	G3 α-Ketobutyric Acid	G4 Phenylethyl-amine	G1 D-Cellobiose	G2 Glucose-1-Phosphate	G3 α-Ketobutyric Acid	G4 Phenylethyl-amine
H1 α-D-Lactose	H2 D,L-α-Glycerol Phosphate	H3 D-Malic Acid	H4 Putrescine	H1 α-D-Lactose	H2 D,L-α-Glycerol Phosphate	H3 D-Malic Acid	H4 Putrescine	H1 α-D-Lactose	H2 D,L-α-Glycerol Phosphate	H3 D-Malic Acid	H4 Putrescine

FIGURE 1. Carbon Sources in EcoPlate

Figure 17. Carbon sources triplicate distribution in 96 wells Ecoplates by BIOLOG.

The reaction cascades of the microbial communities are subjected to a standard analytical procedure through a specific time interval between two to five days. The pattern alterations have undergone statistical analysis and comparison through specialised software. The Principal Components Analysis (PCA) is considered the most dominant method for data analysis of the average well colour development data (AWCD); however, an alternative technique may provide superior advantages. The observed alteration of the fingerprint pattern can offer a valuable source of data concerning the changes carried out in the microbial populations during a specific time interval (Button *et al*. 2016).

The Biolog Microplates have been exposed to a set of comparisons against other approaches, for instance, the phospholipid fatty-acid analysis devised for monitoring the ecological alterations in the microbial communities. The Microplates featured with high sensitivity towards environmental changes and particularly in more determinants changes in water and surrounding temperature (Weber and Legge, 2010).

71

Table 6. The 31 individual carbon sources utilisation on the Biolog EcoPlate

Well Number	Carbon Source	Compound Group
A1	Water	
B1	Pyruvic acid methyl ester	Carbohydrates
C1	Tween 40	Polymers
D1	Tween 80	Polymers
E1	α-Cyclodextrin	Polymers
F1	Glycogen	Polymers
G1	D-Cellobiose	Carbohydrates
H1	α-D-Lactose	Carbohydrates
A2	β-Methyl-D-glucoside	Carbohydrates
B2	D-Xylose	Carbohydrates
C2	i-Erythritol	Carbohydrates
D2	D-Mannitol	Carbohydrates
E2	N-Acetyl-D-glucosamine	Carbohydrates
F2	D-Glucosaminic acid	Carboxylic and ketonic acids
G2	Glucose-1-phosphate	Carbohydrates
H2	D, L-α-Glycerol phosphate	Carbohydrates
A3	D-Galactonic acid-γ-lactone	Carboxylic and ketonic acids
B3	D-Galacturonic acid	Carboxylic and ketonic acids
C3	2-Hydroxybenzoic acid	Carboxylic and ketonic acids
D3	4-Hydroxybenzoic acid	Carboxylic and ketonic acids
E3	γ-Hydroxybutyric acid	Carboxylic and ketonic acids
F3	Itaconic acid	Carboxylic and ketonic acids
G3	α-Ketobutyric acid	Carboxylic and ketonic acids
H3	D-Malic acid	Carboxylic and ketonic acids
A4	L-Arginine	Amino acids
B4	L-Asparagine	Amino acids
C4	L-Phenylalanine	Amino acids
D4	L-Serine	Amino acids
E4	L-Threonine	Amino acids
F4	Glycyl-L-glutamic acid	Amino acids
G4	Phenylethylamine	Amines/amides
H4	Putrescine	Amines/amides

1.2.6 Microbial Community Molecular Analysis

Most of the microbial communities in nature have not been cultured in the laboratory. Therefore, the primary source of information for these uncultured but viable organisms is their biomolecules including nucleic acids, lipids, and proteins. Culture-independent nucleic acid approaches include analyses of whole genomes or selected genes such as 16S and 18S rRNA (ribosomal RNA) for prokaryotes and eukaryotes, respectively. According to the comparative analysis of rRNA signatures, cellular life has been classified into three primary domains: one eukaryotic (Eukarya) and two prokaryotic (Bacteria and Archaea) (Hugenholtz, 2002).

Over the last few decades, the microbial ecology field has seen great improvement and massive development in molecular techniques in order to describe and characterise the phylogenetic and functional diversity of the microorganisms. These techniques have been classified into two major categories depending on their capability of revealing the microbial diversity structure and function: (1) partial community analysis approaches and (2) whole community analysis approaches. Throughout the forensic history, the utilisation of the microbial communities, responsible for the cadaver decomposition, for estimating the post-death elapsed time has been ignored, the difficulty in identifying each microbe associated with the decomposition is referred to the scientific lack of attention. The conventional way of the microbial culturing is associated with the high selectivity and the elevated restrictiveness to a limited class and components of the microbial communities. In addition, the other common microbial culture-independent methods can investigate the overall microbial communities, for instance, the microbial fatty acid analysis is providing a limited perception of the taxonomy of microbial communities. Consequently, the positive lab experimentation is only restricted to the microbes that can be cultured, or for achieving the purpose of identifying changes in the microbial community structure without knowing the taxa involved.

The importance of the usage of the microorganisms as a physical evidence has been elevated, as a result of the development of novel technologies and methods that can facilitate quantifying and describing the generalise post-mortem microorganism. Recently, the high throughput screening and the sequencing methodology can permit the investigation of the microbial communities that present in the screened samples. The microorganism can now be collected from the death scene and identified used RNA genes, 16S and 18S particularly.

This specified microorganism can be classified into phylum and family level; however, it is applicable to identify the microbial overall species with elevated availabilities, which can reach

up to 97%. The progression in understanding the function and structure of microbes under the context of the overall ecosystem, such as the identified human remains in nature, can be furtherly investigated, manipulated, validated, and then positively exploited through the forensic investigations. Predominantly, the recent approaches *(Darling et al. 2014,* Thomas *et al*. 2012, Rastogi and Sani, 2011, Land *et al*. 2015) utilised in the microbial analysis are derived from the metagenomics term context, which is defined as the genomic DNA sequencing directly isolated from the environment. This approach has been implemented routinely throughout a wide range of applications. Regarding the microorganisms' studies, the metagenomics sequencing has been applied to several environmental scenarios, where the microbes have been identified from the plants, animals, and every entity of natural or synthetic environment throughout the globe. The analytical approach of the metagenomics sequencing has assisted in focus on the diversity of the microbes and their roles among the ecosystems. In the beginning, exploiting the known culturing techniques, the utilisation of the metagenomics was limited only to the area of providing the genomic informative data for the corresponding screened microorganism. Following the scientific progression, the cost and the complexity of the metagenomics sequencing have been reduced, that has resulted in the rise of using this analytical technique for exploring a broad range of microbial community, regardless of its cultivability intrinsic feature. One of the significant features of the metagenomics sequencing technique has been perceived from the applicability of sampling the organism genomes to an approximately uniform environmental condition. This impact is obtained from the "shotgun" randomise sequencing method, which is used in the de novo genome sequencing of individualising microorganisms. A random DNA shotgun sequence data, which is isolated from the environmental collected samples, makes the identification of the organism present in the sample is possible, additionally, their functions. Furthermore, through imposing a comparison based on the shotgun metagenomics obtained data across the tested samples, a larger range of issues can be solved, such as the ecology and the biogeography. In addition, linking a specific organism or a function with the "metadata" relevant to the samples, for instance, health status, nutrient cycling rates. A further advantage is the minimization of the inherent errors that can be introduced during culturing, including the contamination, population, population bottlenecks, and taxonomic bias. Thus, the metagenomics sequencing can be perceived as an extenuation of the ribosomal RNA gene "culture-independent" surveys. The elevated potentiality of the novel perception towards the microbial communities has provoked applying the metagenomics approaches into the concerned researcher's fields, such as the agriculture, the law enforcement, the biodefense, the ecology, the evolution, and the industry (Darling *et al*. 2014).

Traditional microbiological techniques involved in laboratory culturing-systems are highly selective and limited to a small component of the microbial communities. Only 1% of bacteria are actually cultivable. The inability to identify or detect the microorganisms associated with a specific environment had also a negative impact on several fields such as forensic microbiology. Historically importance of microorganisms has been ignored in decomposition ecology and their application in estimating the time since the death of human remains due to the lack of effective techniques and protocols. In the last years, molecular techniques have been developed and used to study the necrobiome in a qualitative and quantitative way. These technologies have enhanced the importance of microbes as physical evidence. Today microbial communities can be investigated, monitored, potentially modelled, validated and then used for forensic purposes. Identification of the collected microorganisms from a death scene by high-throughput and sequencing techniques is now possible. Molecular targets such as 16S and 18S RNA genes, for bacteria and eukaryotes respectively, are commonly used. Microorganisms can be typically identified at phylum and family level, and the identification of microbial species with a high degree of reliability is also possible. The critical change in this kind of investigation has been provided by the development of Next Generation Sequencing (NGS) methods. The analysis of the microbiome for the forensic purpose become important for various research groups around the world (Land *et al*. 2015).

The main purposes of these studies are associated with the estimation of the time since death (PMI), the 'microbial fingerprint' and the possibility to identify the geographical origin of the suspect or of the primary crime scene. In addition to research performed in the USA human death facilities (e.g. Tennessee University 'body farm'), animals have been widely used as an alternative to human cadavers for this kind of study (Steussy *et al*. 2015).

However, any consideration was never done before on the role of the fur on the decomposition process, insects and microorganism colonisation.

1.2.6.1 Microbial Community Characterisation Using Bacterial 16S rRNA Gene

Utilising the 16S rRNA gene sequences in studying the bacterial phylogeny and taxonomy is the most frequent housekeeping genetic marker for several reasons: Firstly, 16S rRNA gene exists in all bacteria, as either a multigene family or operons. Secondly, its unchanging function over time, thereby random sequence changes are a precise measurement of time (evolution). Finally, its large sequence around 1,500 base pairs (bp) makes it suitable for informatics resolution. The most attractive potential uses of 16S rRNA gene analysis are to provide genus and species identification for isolates that do not fit any recognised biochemical profiles, for strains generating only a 'low likelihood' or 'acceptable' identification according to commercial systems. It is also used for taxa that are rarely associated with human infectious diseases (Janda and Abbott, 2007). Carl Richard was the first researcher to define important properties of 16S rRNA gene. After observing its behaviour as a molecular chronometer and noticed the conservation degree resulting from the importance of the 16S rRNA as an essential constituent of the cell function. Despite many cellular enzymes whose mutation can be more tolerated by the cells replacing them with other forms, 16S rRNA as part of the ribosomal complex had to keep at a high degree of conservation because of the impossibility to replace it according to an evolutionary point of view. Despite that the precise rate of change in the sequence of 16S rRNA gene is unknown, it is evident that it marks both the evolutionary distance and the relatedness of organisms (Clarridge, 2004).

The 16S rRNA gene sequence is about 1,550 bp long and is composed of both highly conserved regions and nine hypervariable regions (V1-V9) that constitute the most informative portions of the gene sequence for use in taxonomic classification providing distinguishing and statistically valid measurements. Universal primers are usually designed to be complementary to the conserved regions. This allows for the amplification and sequencing of the hypervariable regions in order to provide the taxonomic information. The sequences in the database might comprise a variety of length, however, 500 and 1500 bp are the most popular length for sequencing and comparison (Table. 7) (Singh and Crippen, 2015, Clarridge, 2004).

According to Human Microbiome Project Consortium (HMP), three to five variable regions (V35) of the 16S rRNA gene were selected as the target for 4,879 samples. The sequence of the V13 included as well as a subset of 2,971 samples aiming to get a complete picture of the taxonomic profiles (Consortium, 2012). The majority of the sample collection was targeted for

16S sequencing using the Roche-454 FLX Titanium based technology, which further and precise information will be given in this dissertation.

Table 7. 16S rRNA gene PCR primers. Different primers combination can be used in order to amplify specific 16S rRNA gene regions and sequencing them via NGS.

Pyrosequencing PCR Primers	Covered region	Region Length	References
28 FW 5`TTTGATCNTGGCTCAG 3`	V1-V3	~500 bp	Benbow *et al*. 2014; Pechal *et al*. 2014
519 RV 5`GTNTTACNGCGGCKGCTG 3`			Crippen *et al*. 2014; Sing *et al*. 2014
357 FW 5`CCTACGGGAGGCAGCAG 3	V3-V5	~570 bp	Can *et al*. 2014
926 RV 5`ACTRAAAMGAATTGACGG 3'			
27 FW 5'AGAGTTTGATCMTGGCTCAG 3'	V1-V8	~1460 bp	Hyde *et al*. 2013 ; Hyde *et al*. 2014
1492 RV 5'TACCTTG TTACGACTT3'			

The clinical investigations based on the 16S rRNA bacterial gene and 18S rRNA gene suggest a shift in both the microbial taxonomic and the functional profiles or identifying a species that was not appearing in healthy groups but present in the illness conditions. While the roles played by many of these microorganisms have yet to be identified, it is known that they contribute to the health and well-being of their host by metabolising indigestible compounds, producing essential vitamins, and preventing the growth of harmful bacteria. The importance of healthy microbiota and the association between human microbiome and diseases were shown in colon cancer obesity and type II diabetes (Finley *et al*. 2014). Findings of the HMP also reveal that human bacterial community structure often displays only minor variability during an adult lifespan. By the way, it does vary significantly among individuals giving the possibility to use microbes as a potential marker of identification not only for human health purposes. One of the innovative applications actually involves forensic criminal investigations.

1.2.7 Sequencing Technology

The recent developments in the sequencing methodologies opened the door for several applications; such as population genetics based on the complete genomic sequences of a vast group of individuals (Table 8). In addition, sequencing of complete genomes from samples with a high level of contamination, for example, DNA samples of ancient human beings or other species. The current SGS systems development is increasing without any pauses, the essential

improvements were in 2011from Illumina and SOLiD platforms. SGS is not commonly implied in forensic genetics, although several studies highlight the arising opportunities. The lower sequencing costs and the compact equipment's facilitate the possibility to perform a complete genome sequencing easily for any sample size by any research group on a bench scale instruments (Berglund *et al*. 2011).

Determining the DNA sequence is one of the most comprehensive methods of obtaining information about the genome of any living organism. By utilising the fluorescence labelling of terminating nucleotides and electrophoresis, Sanger has been considered the best standard sequencing method. In fact, Sanger early impact in the microbial genomic field was the novel complete bacterial *Haemophilus influenza* in 1995.

In terms of applications, there are two major types of projects, de novo sequencing, and resequencing. The de novo sequencing is for the sequencing of organism genome for the first time. Whereas, resequencing requires an available sequence reference for the genome or parts of it. The difference between the two applications should be considered when choosing sequencing strategy. The resequencing approach is widely used in human forensics and population genetics, while both de novo sequencing and resequencing are required in microbial forensics (Berglund *et al*. 2011).

1.2.7.1 Second-Generation of Sequencing Technologies

Commonly, there are three major SGS systems used in many laboratories; the first one is Genome Sequencer from 454 Life Sciences (Branford, CT, USA) (acquired by Roche in 2005) Dr James D. Watson successfully sequenced a complete human genome for the first time using this sequencer. The second system is the Genome Analyser (launched in 2006), which was firstly designed by Solexa and enhanced by Illumina (San Diego, CA, USA). The third system is the SOLiD system (launched in 2007), which was conceived by Applied BioSystems which is part of Life Technologies (Carlsbad, CA, USA). The three systems share the same steps of sequencing; preparing and amplifying of template DNA, distributing the templates on a solid support, sequencing and imaging, base calling, quality control and data analysis (Fig. 18) (Berglund *et al*. 2011, Heather and Chain, 2016).
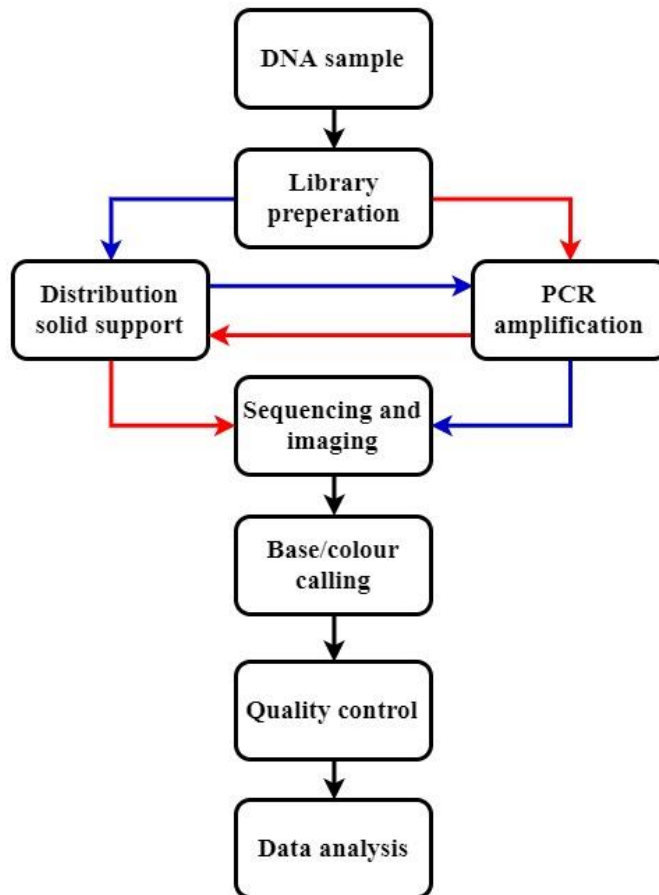
Figure 18. The common steps between all the SGS techniques are drawn in black arrows, whereas steps of illumine system are in blue arrows and the Roche 454 and SOLiD systems in red (Heather and Chain, 2016).

1.2.7.2 Next Generation Sequencing (NGS)

The fast development and wide applications of the next-generation sequencing (NGS) technologies, genomic sequence information became within reach to be used in some fields. SOLiD/Ion Torrent PGM typically represents NGS systems from Life Sciences, Genome Analyser/HiSeq 2000/MiSeq from Illumina, and GS FLX Titanium/GS Junior from Roche. Beijing Genomics Institute (BGI), which possesses the world's biggest sequencing capacity, has multiple NGS systems including 137 HiSeq 2000, 27 SOLiD, one Ion Torrent PGM, one MiSeq, and one 454 sequencing (Buermans and Den Dunnen, 2014).

The Maxam-Gilbert and Sanger sequencing are comprehensively understood as the first generation sequencing. Recently, the newly evolved sequencing approaches have found a foothold among the old strategies, thusly, named as the next generation sequencing (NGS) approaches (Fig. 19). The main key merit of NGS approach is the capability of producing high

throughputs of numerous sequencing simultaneously. Consequently, the microbial taxa can be identified by exploiting the resultant sequencing, these microbial taxa including the uncultivable organisms and those exist in small numbers. The NGS possess the capability to provide an optimum storage capacity for all of the microbial operons and genes expressed under variable analytical conditions through a specific range of applications (Nikolaki and Tsiamis, 2013). The microbial ecology has been revolutionising through imposing the NGS approaches and recently exploited for screening several ecosystems. Moreover, the NGS approaches have eased the initiation of more optimisation and the introduction of new high throughputs technologies, such as the metagenomics, the genomics, the transcriptomics, and the met transcriptomics. In comparison to the basic culture-independent approaches, the NGS strategies are capable of conducting a comprehensive analysis of a numerous number of the sequenced nucleic acid, allowing the complete description and demonstration of the ecosystems microbial constituents. These new techniques can be implemented in two distinct ways, the shotgun sequencing, which is the overall microbial nucleic acids sequencing, and the targeted sequencing, concerned in the gene-specific sequencing. In regards to the targeted sequencing pathway, the polymerase chain reaction (PCR) has been utilised in amplifying segments of the conserved DNA or cDNA sequences with the exploitment of universal primers. Concerning the phylogenetic composition, a massive generation of information can be obtained as a result of Shotgun sequencing approach, aiding the provision of firm concepts in regards to the numbers of potential genes functions within the communities.

Under the platform of NGS, the generation of a vast genome-scale dataset can be obtained as a result of performing relevant technologies. However, minor substantial differences can be expressed associated with engineering, chemical sequencing, accuracy, cost-effectiveness, and the output, including the sequence number and the read length.

Furthermore, more examples of the third generation approach has been effectively listed, such as the heliscope single molecule sequencing, the DNA nanoball sequencing, sequencing of the Nanopore DNA, tunnelling current DNA sequencing, microscopic techniques, and spectrometry-based mass sequencing, are all exposed to the expected ongoing revolution and development (Buermans and Den Dunnen, 2014, Nikolaki and Tsiamis, 2013).
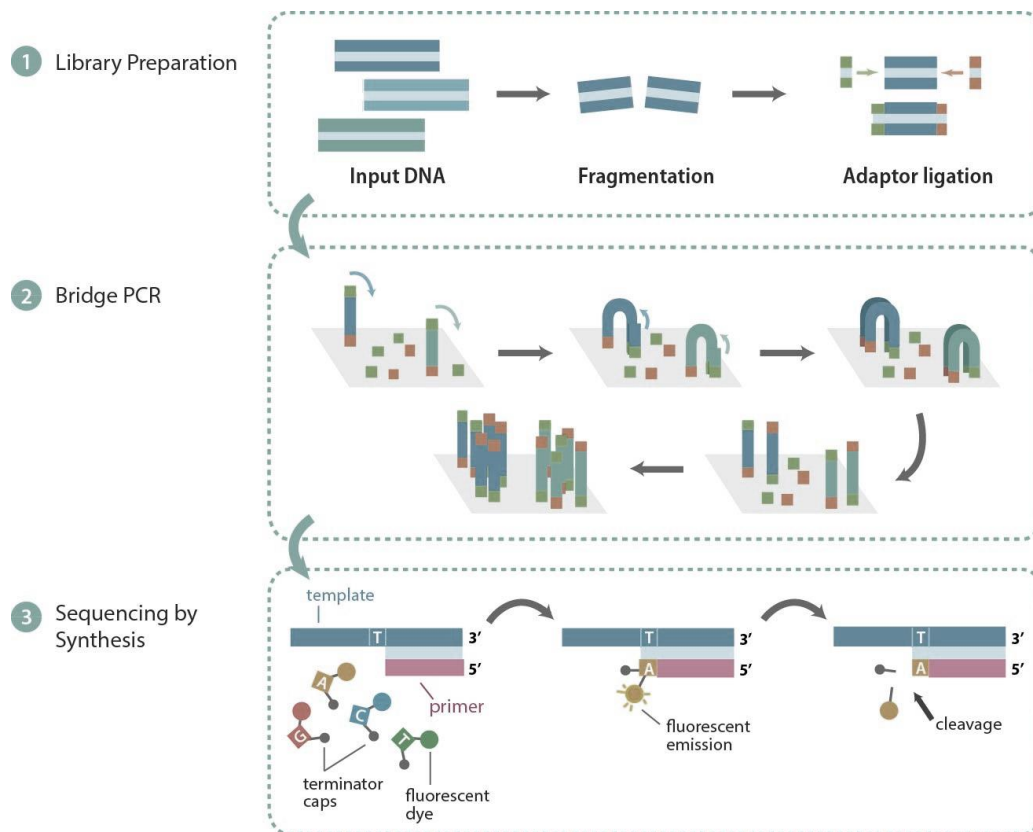
Figure 19. Next Generation Sequencing method (NGS) (Buermans and Den Dunnen, 2014)

1.2.7.3 The Roche 454 Pyrosequencing

The first array of the 454-pyrosequencing system, constructed by Roche in 2004, was the initiative core of the new ear of the NGS. Through implementing this approach, double-stranded DNA fragments are linked to a specialised adaptor diluted and occupied into small beads, one molecule per bead. The ligated DNA is cloned through PCR into millions of copies exploiting different primers such as the biotinylated in the oil/water emulsion. The storage of the formulated beads has been accomplished in separate picotiter-size wells, for the allowances of the non-biotinylated strands to be denatured and washed away. The structure of the plate array is composed of around one million wells, and independent type of reactions, which can result in sequencing, which can separately occur within each well. Post primer addition the pyrosequencing reaction has completed by the DNA synthesis exploiting the single-stranded DNA molecules as a leading template. Sequencing of the reaction is monitored by a detecting light, which is generated through luciferase-mediated conversion of luciferin to oxyluciferin upon primer extension. Currently, the 454 pyrosequencing can provide reads which are longer than 1000 bp, along with a high sequence output, around one megabase (Mb) in the case of the

454 GS FLX+ system. The defined drawbacks of the 454 platform, is the homopolymer stretching complexity in sequencing and the higher cost per Mb *(Berglund et al. 2011, Liu et al. 2012, Quince et al. 2009)*.

1.2.7.4 Pyrosequencing

Pyrosequencing type of sequencing is generated based on the sequencing-by-synthesis theory; it is considered as the first substitution to the classic Sanger technique the Novo DNA sequencing. It depends on the pyrophosphate luminometric detection, which has liberated during the primer-directed DNA polymerase reaction, which is facilitated by the nucleotide involvement. The Pyrosequencing technique has built on the theory of sequencing-by-synthesis fundamentals and based on the released detection of the Pyrophosphate (PPi) through the DNA synthesis. It can recruit four enzymes series in order to accuracy impose the nucleic acid detection sequencing throughout the synthesis. In particular, during the pyrosequencing, the sequencing primer is hybridised to a single-stranded DNA following the biotin labelled template. This is treated with several enzymes such as DNA polymerase, ATP sulfurylase, luciferase, apyrase, the substrates adenosine 5' phosphosulfate (APS), and the luciferin. Four deoxynucleotide triphosphates (dNTPs) cycles are introduced to the parts of the reaction medium in replicates. The cascades are triggered along with the initiation of the nucleic acid polymerization reaction in which an inorganic Pyrophosphate (PPi) is liberated as a yield product of the nucleotide incorporated through the polymerase. In fact, each event involving the incorporation of the nucleotide is leading to the liberation of the PPi in a quantity equivalent to the incorporated nucleotide. Considerably, the liberated PPi is exposed to a quantitative conversion to ATP under the effect of the sulfurylase and the presence of APS *(Ahmadian et al. 2006, Fakruddin et al. 2012)*.

The generated ATP is able to facilitate the luciferin (luciferase-mediated) transforming into oxyluciferin, which in turn helps the emission of visible light (of 560-nanometer wavelength) with correlated intensity to the amount of ATPs. Then, the emitted light can be detected and measured photon detection devices such as the A Charge Coupled Device (CCD) camera or the photomultiplier. The Apyrase is considered as a nucleotide degrading enzyme, which can persistently degrade the ATP and the non-incorporated dNTPs in the reaction media. Usually, the time interval between each nucleotide neglected is 65 seconds, which facilitate an optimum degrading process. The dNTP addition is implanted once at a time since the added nucleotide

is well known; therefore, the sequencing of the template can be determined. Through the pyro gram, the generated light has been observed as a peak signal, in correspondence to the electropherogram in dideoxy sequencing, and proportional to the number of the incorporated nucleotides, accordingly, triple dGTP incorporation can produce a triple higher peak. Throughout the synthesis cascades, the DNA strand is extended by the integral nucleotides, and then the DNA sequence is demonstrated by the p08. The stranded pyrosequencing is utilising the Klenow fragment of Escherichia coli DNA Pol (Fakruddin *et al*. 2012).

The sequencing is initially started with the nitrogen base located near to the annealed primer, which can facilitate the flexible design of the methodology. Sampling and preparing the single-strand DNA process is considered as a fast operation, needs around 15 minutes approximately. For the Sanger sequencing, the sample preparation usually performed in 4 hours, namely; PCR cleaning up takes 60 minutes, cyclic amplification takes about 3-4 hours and about 15 minutes for cleaning up the dye. The sequencing of short stretches of DNA costs relatively less than the currently available methods. The pyrosequencing technique has numerous key merits in comparison to the other DNA sequencing technologies. As an example of these advantages, the order of the dispensed nucleotide can simply be organised and modifications in the pyro gram scheme can reveal mutations, removal, and insertion. Furthermore, this approach is conducted in the real-time, for each sample, the nucleotide incorporations and the base callings can all be observed persistently. Additionally, the Pyrosequencing strategy can be implanted in automation for the large scaling screening (Fakruddin and Chowdhury, 2012).

The Pyrosequencing approach can allow the profound exploring of the living microbiome incubated normally in the humans, and providing a demonstration that the human can hold a high degree of taxon variability and richness. For instance, the microbial samples pyrosequencing, which has been collected from several body regions, around 27 parts such as the forehead, the foot sole, the oral cavity and the gut, resulting in producing 4949 species grades phylotypes out of an overall of 250000 16S rRNA sequences (Pechal *et al*. 2013b).

1.2.7.5 The Illumina Platform

In this method, primers with specific adaptor integral to those presented in the DNA are connected to the primers through the slide building a bridge like structure. After the sequencing process, complementary primers for imposes adaptation during the synthesis, moreover, four kinds of reversibly blocked terminating nucleotides (RT nucleotides). Thereafter, the non-

incorporated RT nucleotides are washed away, chemical displacement of the pigment and the terminal 3' blocker from the DNA, which allows the incorporation, detecting, and the initiation of the next sequencing cycle. Contrariwise, an extra nucleotide is added to the DNA chains in the pyrosequencing for an extra nucleotide at a time.

The technology is requiring the exploitment of the DNA polymerase as an opposed to multiple, expensive enzymes are required to be available to perform these strategies. Furthermore, a delay in accruing images can consider as associated consequences of the nucleotide incorporation, which might be a consecutive result of the presence of a large array of DNA groups to be demonstrated in the sequential images when utilised a single camera. Recently, the Illumina approach is capable of producing standard reads of 150-300 bp; this can be elevated to 300-600 bp by using "paired-end" sequencing both ends of the same DNA cluster. The major prime feature of this new technology is the relative cost-effectiveness of the high output sequencing per run (up to 3000 Mb for the HiSeq) (Reuter *et al*. 2015, Sinclair *et al*. 2015).

Table 8. Comparison of sequencing techniques. Sanger sequencing to Roche 454 GS FLX, Illumina MiSeq, and Ion Torrent Personal Genome Machine (PMG) platforms adapted (Ari and Arikan, 2016, Goodwin *et al*. 2016).

Methodology	Sanger Chain termination	Roche 454 GS FLX Pyrosequencing	Illumina MiSeq Sequence by Synthesis	Ion Torrent PGM (318 chip) Ion semiconductor sequencing
Accuracy	99.9 %	99.9 %	99.9 %	98.3 %
Read length	~1,000 bp	700 bp	2.1-2.4 Gb	600Mb-1Gb
Reads per run	1	1 million	14 - 16 million	4- 5.5 million
Runtime	Up to 3 h	23 h	17 h	4 h
US $/1 million bases	$2,400	$9.50	$200-300	$450-800
Error profile		1%	1%	1%
Advantages	Long individual reads.	Long read size. Relatively fast.	High sequence yield.	High sequence yield. Relatively fast.
Disadvantages	Unfeasible and very expensive for larger microbial diversity determination.	Expensive. Homopolymer errors.	Equipment can be very expensive. Requires high concentrations of DNA.	Homopolymer errors.

1.3 Aims

The documentation of the crime scene is one of the most important aspects of any crime scene investigation. The documentation process provides the accurate record of the evidence found at the scene and all the observations of the scene itself at the time of discovery by using more than one method of documentation: like notes, photographs and sketches.

The quality of the scene documentation is an essential and extremely valuable aspect of the entire investigation and care must be exercised to procure the best documents and photographs.

Occasionally, the crime scene photographer may have to work quickly, due to the circumstance of crime, weather, or oncoming darkness. Thus, the inaccurate documentation can lead to inadmissible evidence in a court of law or missed evidence that may allow a guilty party to get away with a crime against persons or property.

Three-dimensional documentation of the crime scene is believed to be an effective means to provide a deeper understanding of the details of the crime and to improve the quality of the crime scene investigations. Especially for communicating complicated scenarios to the jury and keep clearer descriptions and detail. In addition, 3D crime scene reconstruction saves time and money by eliminating further site visits.

At the moment, there is a lack of a tool able to integrate from a visual point of view the cadaver transformation with all the biological organism responsible for the transformation (e.g. Bacteria and Insects). This tool would provide a further level of knowledge to understand the body transformations, but as well to reconstruct the body decomposition. In order to try developing this tool, we operate in two phases.

Therefore, the aim of the first part of this research was to explore the use of modern low-cost technologies to provide a forensic tool for the 3D documentation of crime scene. This method would deliver a high quality and cost-effective technique to create accurate records of the crime scene in three dimensions, measurements could be taken from the 3D model using Autodesk 123D catch software as a relatively cheap and easy-to-use.

One of the most difficult elements of a crime scene to be documented is the cadaver and its transformation during the decomposition process. The possibility of linking the parameters and elements that affect the body transformation with a specific case is fundamental both in the

investigative and trial phases. In the last one, the possibility to present the decomposition events in an effective way can play a very important role in the judgement process.

Among the factors affecting the cadaver decomposition, the microbiome plays a critical role contributing to the transformation of it in energy and nutrient for the ecosystem.

Several studies have been performed in the last years on this topic especially in the United State. Humans and animals (mice, rats and pig, etc.) were used to follow the microbe variations on the body during the time. In this research, rabbits were used as a model for economical, spatial and ethical reasons. However, this model allows for further investigations.

To date, there is a lack in the literature about the effect of fur on the functional activity of epinecrotic microbial communities associated with carrion and on the taxonomy of bacterial communities' changing during the decomposition stages.

Therefore, the aim of the second part of the research was to investigate the microbial communities associated with exposed decomposing rabbit carcasses and to assess whether changes in this community have the potential to be used in the estimating of a time since death in forensic investigations. In addition, to use the characterization of the microbial communities developed on decomposing carrion in order to provide a geographic and seasonal microbial database as a forensic tool. Moreover, to study the effect of fur on the decomposition process and on the insect and microbial colonisation. Furthermore, data obtained in this work can be applied not only on crimes against people but also on the Forensic Veterinary field.

2. Materials and Methods

2.1 3D Crime Scene Reconstruction Experimental Setup

In order to obtain good quality pictures and to validate 3D reconstruction methods, a Nikon D3100 digital camera was used in auto mode during the acquisition (Fig. 20, Table. 9). To create a 3D model out of an object using 123D Catch software, a computer with the specifications reported in table 10 was used. 123D Catch software can assemble up to 70 individual photos into one 3D model.

Different objects were used for this study. Objects with different shapes, sizes, and colours were used to evaluate how the software works under different conditions. The size of the objects was <50 cm for small scenes and >50cm for large scenes. Pictures were collected at outdoor and indoor conditions.

Table 9. Nikon D3100 camera specifications.

Full model name	Nikon D3100
Resolution	14.20 Megapixels
Sensor size	APS-C (23.1mm x 15.4mm)
Kit Lens	3.00 x zoom 18-55mm (27-83mm eq.)
Viewfinder	Optical / LCD
Native ISO	100 - 3200
Extended ISO	100 - 12,800
Shutter	1/4000 - 30 seconds
Max Aperture	3.5 (kit lens)
Dimensions	4.9 x 3.8 x 2.9 in. (125 x 97 x 74 mm)
Weight	27.4 oz (777 g) includes batteries, kit lens
Manufacturer	Nikon
Full specs	Nikon D3100 specifications

Figure 20. Nikon D3100 Camera.

Table 10. Minimum and recommended hardware and software specifications for Windows platforms.

System component	Recommended
CPU speed	2 GHz
Main memory (RAM)	4 GB
Virtual memory	4 GB
Web browser	Internet Explorer
Video viewer	Adobe Flash Player
Disk space	At leas1.0 – 2.0 GB free disk space for installation
Operating System	Windows 7 (64-bit edition)

Autodesk 123D Catch is a free service offered by Autodesk that uses cloud computing for the reconstruction of 3D objects from digital images (Chandler and Fryer., 2013); the software is available for downloaded from www.123dapp.com/catch. Autodesk 123D Catch is an App for Android and Windows operating systems. Photos taken from different angles and positions are combined in order to virtualize an object. Photos should shoot in a circular ring from another angle that is at least 50 degrees lower or higher than the previous circular ring. The management of data is made through a standalone software application installed on the PC or through an online service. This application allows uploading images, downloading the results, and exporting the result using several 3D formats (DWG, FBX, OBJ, IPM, LAS). The result of the reconstruction process can be achieved in three different resolutions: mobile (fast medium resolution mesh), standard (high-resolution texture mesh) and maximum (very high-density mesh).

2.1.1 Methodological Approach

The basic idea behind Autodesk 123D Catch is that by taking a series of photos of an object from different positions and angles, 3D modelling software located in the cloud identifies unique points on the surface of the object. The software uses photogrammetry to reconstruct the relative positions from which the photos were taken, and from the information that was obtained. Also, to triangulate measurements within 3D space by finding common points of reference amongst a series of photos of the object (Autodesk, 2012, Butnariu *et al*. 2013).

The software generates a 3D mesh of points for the object from the images to create a photorealistic rendering of the model in 3D, which can then be manipulated in a computer graphics program like AutoCAD or 3DS Max. The model can be exported into OBJ or IPM format to be used with CAD software, Maya or Autodesk 123D for further analysis and measurement if required (Venkatesh *et al*. 2012).

2.1.1.1 Creating a New Model

To create a 3D model out of the object, Autodesk 123D Catch software was downloaded on the computer however as well the online service can be used. Autodesk 123D Catch application requires internet access to connect to the Autodesk servers and startup. Once the application is started, it can be created a new model by clicking on "create a new photo scene" icon on the main face of the application.

Step1: photos shooting and collection

Autodesk 123D Catch requires 20-30 photos, should be taken from various angles, to create a 3D model of the object. A digital camera Nikon D3100 was used to take the photographs. All photos were taken in Auto mode, walking around the object to take photos at all possible angles. Special care was taken to ensure good exposure and good focus depending on the lighting conditions. The pictures were taken randomly from any angle to obtain a full capture of the object surfaces, but it should be ensured to get adequate overlap between adjacent photos (Fig. 21).

The following attentions were paid to the photos collection:

- Pictures captured all sides of the target object, both all the way around and top and bottom.
- The object did not move during capture, and lighting remained consistent.
- The target object was taken up most of the frame by getting close to the object or zooming in.
- Consistent diffuse lighting all around the object was prepared.
- The accurate focus was important to remove any out of focus shots.
- Measuring the distance from the object during the capture of photos was not necessary.
- Photos were stored in a specific folder with a label.
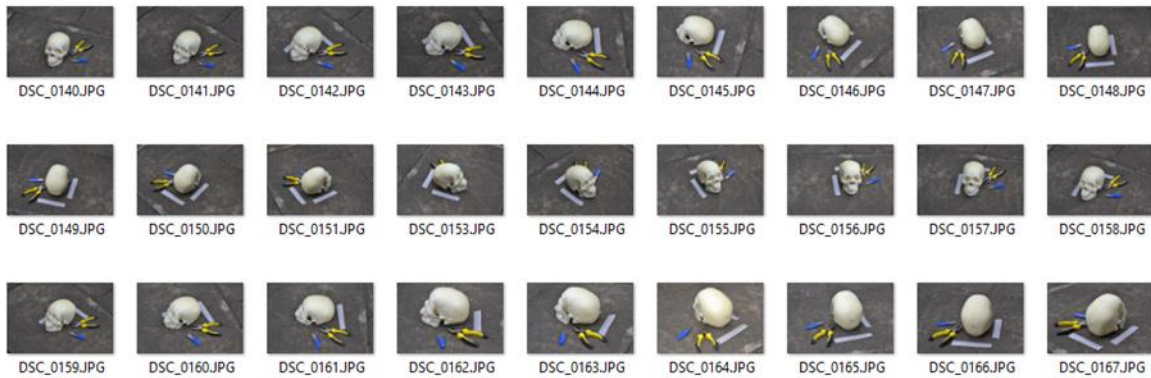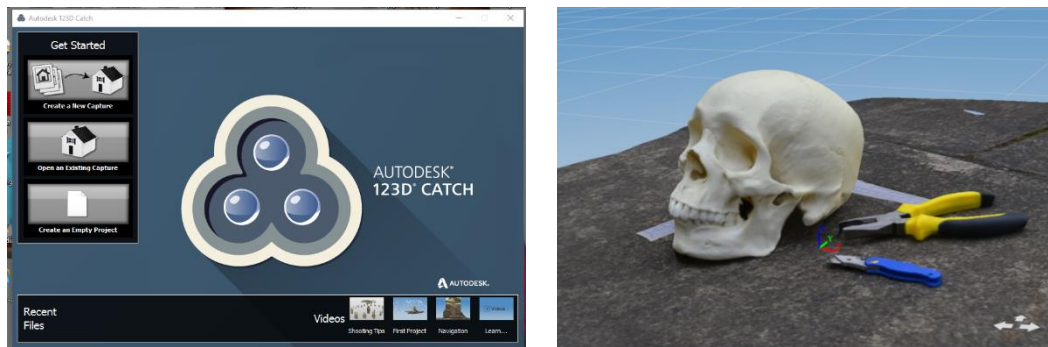
Figure 21. Autodesk 123D Catch software and a collection of photos used to create a 3D model of the skull.

Step 2: Create photo scene in 123D Catch (Fig. 22)

The images were imported onto to the desktop application without any need of manually calibrating or tagging the images with each other. This is one of the biggest advantages of the 123D Catch when compared with other modelling software which they require the use of manual calibration or another method to determine the camera orientation and position.

The software computed the images and uploaded them to the Autodesk server.

- Photos were uploaded to the 123D Catch software, to create a photo scene.
- A 123D Catch application was opened and creates a new photo scene as it used new capture tool, and then images file selected.
- The scene loading took some time, approximately 15 to 20 minutes.
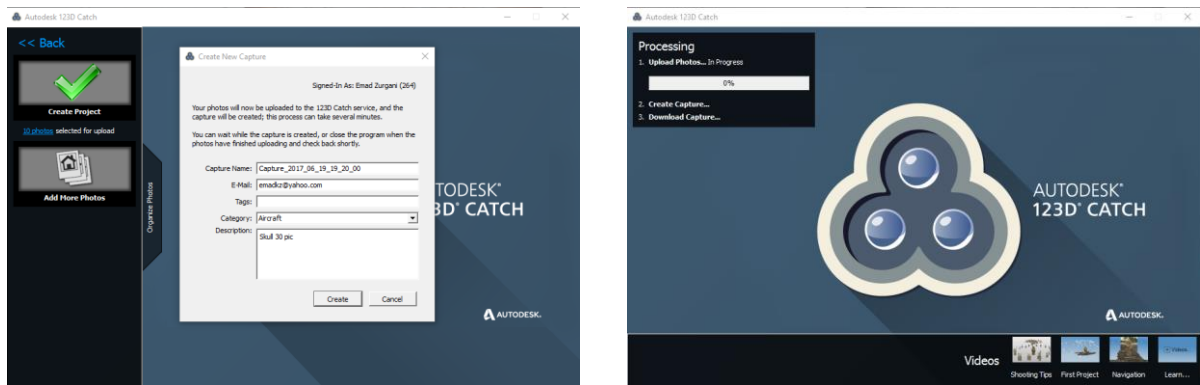
Figure 22. Example of submission of the photos to the 123D Catch service, to create a photo scene.

Step 3: Download, review and clean up the scene (Fig. 23)

When the model was finished, it came straight away on the main face of the software. To present better of 3D model of the scene some elements were erased by selecting them with the lasso or square tools. The 3D model that was obtained can rotate, viewed and analysed from any side.
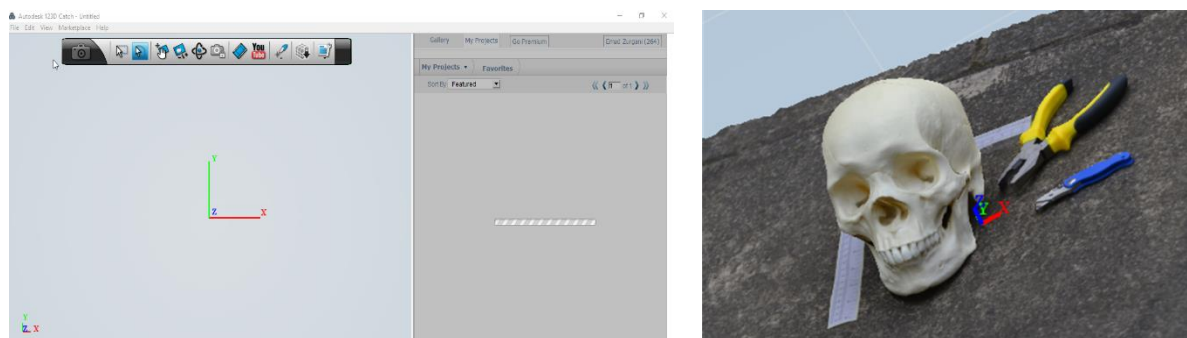
Figure 23. Downloading and 3D presentation of the reconstructed object.

2.1.2 Validation Method

It is essential that the precision and accuracy of 3D models reconstructed using Autodesk 123D Catch is evaluated if those models are going to be used in any practical applications especially in the forensic context (Boisvert *et al*. 2013).

In order to use the proposed method in the forensic context, it is essential to make sure of the quality of the reconstruction method followed. Additionally, measuring the 3D errors between the real and the obtained measurements, and how the errors might affect the quality of the 3D reconstructed models.

91

The Autodesk 123D Catch is a high-quality software that allows the creation of models in different conditions, and it allows measuring them within a few minutes. To evaluate the accuracy of the reconstructed models, significant experiments were run out to investigate the validity of the software.

The first experiments were performed to identify the minimum number of photos needed for good and complete model start with 5,10,15,20 and 30 photos. A box was used as a standard object with the straight edges.

Another experiment was performed to evaluate the accuracy of the models, which is reconstructed by the 123D Catch, serving the purposes of investigating the suitability of the already specified numbers of photos in the previous experiment with different objects under investigation core. In addition, the possibility to collect accurate measurements directly from the 3D reconstruction models was explored. The experiment was run and a skull was selected to be reconstructed and three areas on the skull were identified to be measured (two teeth and nose bone). The measurements of these areas were taken and compared with the real dimensions to investigate the error rate and the validity of the software (Fig. 32).

Furthermore, significant experiments were performed specifically for small-scale scenes <50 cm and large-scale scenes >50 cm. The measurements of the objectives at the scene and the distances between specific points were taken to compute the difference between the same measurements on the models obtained using 123D Catch software three times. All objects had a different shape, size, and colour to evaluate how the method works under different conditions.

In addition, the experiments were performed outdoor and indoor in the University crime scene facility. After this step was positively performed, the difference between real measurements and estimated measurements from the 3D models were statistically evaluated (Figs. 39, 40), (Table. 30).

2.1.3 Comparison with other Software Packages

The validation was performed by comparing the 3D model of a skull; generated using 123D Catch to the model of the same skull generated using: 1) Agisoft Photoscan; and 2) Photosynth. The comparison to Agisoft Photoscan and Photosynth survey methodology were selected, as they are both standalone application software and widely accepted in the field of reconstruction. The comparison took into account the level of accuracy and the processing time. Experiments

were performed on four datasets, each dataset is a sequence of (10, 20, 35, and 50) images of the same object (skull) captured using digital Nikon D3100 camera. The geometry of this object allows evaluating the quality of reconstructing at surfaces and angles.

Photosynth

Photosynth Technology Preview released by Microsoft Live Labs, is a web service, which is accessible through a Windows Live account on the Photosynth website https://photosynth.en.softonic.com/.It requires the installation of an application to allow the uploading of the images to the server. Photosynth enables to create two kinds of 3D products: panoramas and synths. The former stitch a set of images together taken from the same point to create a seamlessly panoramic picture. The latter creates a view that allows browsing from photo to another photo by using a set of overlapping images. However, it is also able to create a point cloud of the object. The images exterior orientation parameters and the point cloud can be exported through Synth Export applications (http://synthexport.codeplex.com) in different formats (Brutto and Meli, 2012). Photosynth is a photo visualisation tool that uses the same underlying data (camera positions and points) (Snavely *et al*. 2008).

There are different steps to create a new 3D model with Photosynth software:

- After installing the Photosynth, software and logged into Photosynth click the "Upload" button up top and then the "Create Synth" button on the next page.
- Drag the photos into the Photosynth window, and choose a name your new Photosynth.
- Click "Synth" in the bottom right corner, which may take a long time.
- Export results and save.

Minimum hardware specifications requirements for Photosynth:

- 1.4 GHz 64-bit processor
- Windows XP or later
- 512 MB of RAM
- Storage disk space requirements 32 GB

Agisoft PhotoScan

Agisoft PhotoScan is a low-cost commercial 3D reconstruction software from Agisoft LLC (www.agisoft.ru). The software is based on Multiview 3D Reconstruction technology, which automatically builds precise textured 3D models using digital photos. The model can be exported for editing in external software. PhotoScan can be purchased for $ 179 USD as a standard edition (low-cost) or as a professional version for $ 3,499 USD. All the processes can be performed at different levels of accuracy and many parameters can be set to improve the final result (Brutto and Meli, 2012). Furthermore, this software is executable under Windows operating systems. Thus, all data remains with the user on the local personal computer, where this software can be operated. For the computation of large projects (100 images and more) a 64bit operating system with at least 6 GB RAM is recommended (Agisoft, 2012, Kersten and Lindstaedt, 2012).

Processing of images with PhotoScan includes the following main steps:

- Load photos into PhotoScan;
- Inspect loaded images, removing unnecessary images;
- Align photos;
- Build dense point cloud;
- Build mesh;
- Generate texture;
- Export results in a different format.

The list in table 11 represents the all the system requirements and recommended configuration needed for the construction of a textured 3D model from photos (Agisoft, 2014).

Table 11. Minimum and recommended hardware specifications for Agisoft PhotoScan

Minimum configuration	Recommended configuration
Windows XP or later (32 or 64 bit), Mac OS X Snow Leopard or later, Debian / Ubuntu (64 bit).	Windows XP or later (64 bit), Mac OS X Snow Leopard or later, Debian / Ubuntu (64 bit)
Intel Core 2 Duo processor or equivalent.	Intel Core i7 processor
2GB of RAM.	12GB of RAM

2.1.4 Statistical Analysis

Statistical analysis was performed using IBM SPSS 22 software. Correlation and frequency of the number of occurrences of repeating the measurements were analysed in groups of 20 cm e.g. (0-20), (20-40) for the total, and in groups of 5 cm for the small scene (0-5), (5-10). For the large scene was in groups of 15 cm (0-15), (15-30) (Figs. 35-38), (Appendix1, Table. 52). Descriptive statistics have been performed for all the samples clustered as a general, small and large (Table. 30). Intraclass Correlation Coefficient between the real and obtained measurements of the skull was calculated (Table 29). In addition, linear regression was used to analyse the observed and reconstructed measurements of different models (Figs 39, 40). In addition, the reliability of measurements was used to analyse the measurements obtained three times one of them was obtained by another operator (S.Vanin) (Fig. 42).

2.2 Carrion Decomposition Experimental Setup

The aim of these experiments was to document the carrion decomposition, focusing on the morphological transformations with a 3D reconstruction, and on the insect colonization and the bacterial communities associated with the carrion. Six rabbit's carcases, three with fur (F) and three without fur (NF) were exposed and their decomposition was studied in 2014 and in 2015 (Fig. 26). This allowed the comparison of the results between seasons and the evaluation of the effect of the fur on the decomposition process. The reconstruction of all the stages of decomposition using a new 3D reconstruction method was used to document the experiments.

2.2.1 Site Description and Experimental Design

Rabbit's carrion decomposition was studied in Huddersfield, West Yorkshire, United Kingdom (53°38'36.5'' N, 1°46'40.1''W). Carcases were sampled during the summer season, from 25 June 2014 until 27 October 2014, and spring season from 18 March 2015 until 15 July 2015.

The location was a suitable site identified within the University of Huddersfield, on the roof of the School of Applied Sciences (Fig. 24). This site was with special entrance and fence on two sides. This site allows following the transformation of six carcasses located in the same environment and to allowing exposed to the same condition because the aims of this experiment were mainly the possibility to reconstruct and follow the decomposition. For this reason, a reduction of the variables, (e.g. sand instead of soil, plastic box instead of an open field, and the effect of the location (roof instead of ground) did not affect the project. Laboratory work was performed at the University of Huddersfield, except the sequencing samples analysis.

In each year experiment (2014 and 2015), rabbit carcases ranging from 2.20 to 3.20 kg (Tables.12, 13), were purchased from a pet food company (Kiezebrink, https://www.kiezebrink.co.uk/category/64-rabbit/). Because animals were sold for animal consumption, no ethical approval was required. Carcases were transported to the field using special delivery. Carcases were randomly placed at a minimum of 7m between each other (Fig 25). Fur was removed using a specific animal hair trimmer (WAHL, 870/6791). Each rabbit was placed in a plastic box (60cm length, 25cm height, and 40cm width) with lid. Boxes contained holes along the sides to allow insects and air to entry normally, and to prevent disturbance by large vertebrate scavengers. Small holes were created on the bottom side of the box to allow water to leak out. All carcases were placed on a 4cm bed of clean and sterile sand

purchased from a children toys shop. Carcases boxes were numbered and covered by the boxes lids to protect the specimens from the direct rain (Fig. 25).

Figure 24. Experiments location. University of Huddersfield (UK) and placement of carcases in plastic boxes to start decomposing at day zero. Outside of the location was captured in the photograph.
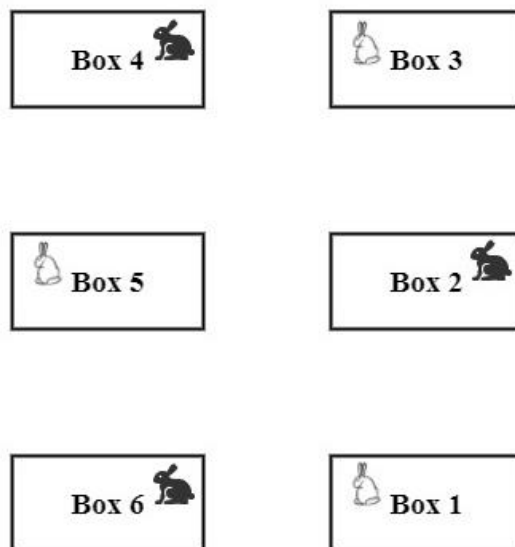
Figure 25. The position of the carcases at the location for the duration of the research. Animals in boxes 1, 3 and 5 were rabbits without fur (NF), boxes 2, 4 and 6 were rabbits with fur (F).

Figure 26. Example of rabbits with and without fur were exposed at day 0 in summer 2014 and spring 2015.

<table>
<tr><td colspan="3">Table 12. Starting weight of rabbits, Exp.1- 2014–Average (2.34kg).</td></tr>
<tr><td></td><td>**Weight (Kg)**</td><td>**Carcass**</td></tr>
<tr><td>BOX1</td><td>2.40</td><td>with fur (F)</td></tr>
<tr><td>BOX2</td><td>2.60</td><td>without fur (NF)</td></tr>
<tr><td>BOX3</td><td>2.15</td><td>with fur (F)</td></tr>
<tr><td>BOX4</td><td>1.95</td><td>without fur (NF)</td></tr>
<tr><td>BOX5</td><td>2.60</td><td>with fur (F)</td></tr>
<tr><td>BOX6</td><td>2.35</td><td>without fur (NF)</td></tr>
</table>

<table>
<tr><td colspan="3">Table 13. Starting weight of rabbits, Exp.2- 2015-Average (3.18kg).</td></tr>
<tr><td></td><td>**Weight (Kg)**</td><td>**Carcass**</td></tr>
<tr><td>BOX1</td><td>3.10</td><td>with fur (F)</td></tr>
<tr><td>BOX2</td><td>3.45</td><td>without fur (NF)</td></tr>
<tr><td>BOX3</td><td>2.75</td><td>with fur (F)</td></tr>
<tr><td>BOX4</td><td>3.50</td><td>without fur (NF)</td></tr>
<tr><td>BOX5</td><td>2.85</td><td>with fur (F)</td></tr>
<tr><td>BOX6</td><td>3.45</td><td>without fur (NF)</td></tr>
</table>

2.2.2 Meteorological Data Collection

Data loggers (DS1922L iButton® temperature logger from msI Measurement System Ltd) were inserted into the rabbit's mouth in order to record the internal temperature (carcass-associated) over the period of the experiment in one hour intervals. Whereas, environmental temperature was obtained from the meteorological weather stations placed on the same roof of the experiment. Temperature data were later converted into the Accumulated Degree Days (ADD) appendix 2 (Tables. 55, 56). Thermal summation models were used with a base temperature of 0 °C, which accounts for temperature variation over decomposition (Megyesi *et al*. 2005). This measure is commonly used in forensic applications when extrapolations are made from experimental (i.e., lab) to field data of carrion under different or highly variable thermal environmental conditions (Pechal *et al*. 2013a).

2.2.3 Weight Record

Digital scale (LAGUTE Digital Luggage Scale) and metal net with the handle was used to measure the loss of weight during the decomposition process (Fig. 27). The scale was calibrated using a bottle of water of known weight. Weight was recorded daily during the first week of each experiment and twice for the second week, then once a week until the final stage of the decomposition which was the end of October 2014 (Experiment 1) and June 20105 (Experiment 2) Appendix 2 (Tables. 53, 54).
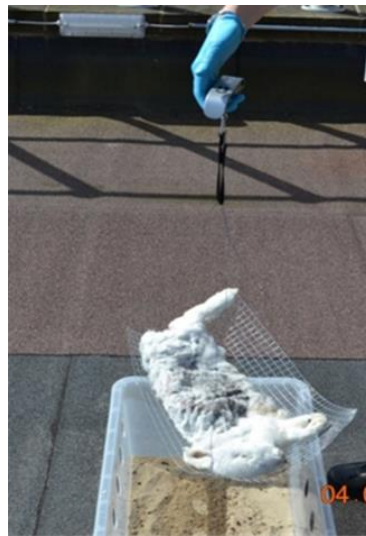
Figure 27. Carrion weight recorded daily during the first week of the experiment and twice for the second week then once a week until the final stage of the decomposition process using a digital scale.

2.2.4 Decomposition Process Monitoring

To document the decomposition stages of rabbits' carrions, and to record the changes over time pictures for all carrions over decomposition process were taken daily during the first week of the experiments. Then three times a week for two weeks, and once a week for a long time to check other possible changes, using Nikon D3100 digital camera, in addition, to using these pictures to reconstruct 3D models for carrion decomposition stages.

2.2.5 Entomological Analysis

2.2.5.1 Collection and Preparation Entomological Samples

Insects, developed on rabbits' carcases, were collected between June and August 2014 for the summer season, and between March and June 2015 for the spring season. Flies larvae and pupae samples were collected daily during the first week of the experiment; and then three days a week for second and third weeks; then twice a week for the fourth week then once a week, until the last stage of decomposition. Eggs samples were collected using a wet paintbrush. Eggs were then killed and preserved in 70-95% ethanol and placed in small vials labelled with the name and data. Larvae samples were collected by tweezers, spoon and paintbrush depending on their number and size.

All larvae samples were killed in hot water not boiling water (about 80C°); after immersion for 30 s and then washing with fresh water specimens were stored in vials with 70–95% ethanol as recommended by the EAFE (Amendt *et al*. 2007). Samples were then labelled with all data and time until further morphological or molecular investigations.

Pupae were collected using tweezers and spoon with a sieve, then placed in glass jars with wet tissue in them, closed with laboratory-paper, and stored at room temperature until adults emerged.

Adults samples present on the carcasses were collected using an entomological hand net, after that they were killed by placing into a vial, put into a freezer for 1 hour; then, dead samples were stored in 70–95% ethanol until further morphological or molecular investigations (Fig. 28). Some samples were investigated using an initial morphological approach eventually confirmed by molecular analysis based on sequencing techniques.

Figure 28. Insect samples collected from the rabbit carcasses and prepared for analysis and storage.

2.2.5.2 Morphological Identification

Morphological identification was performed for about 250 adult flies and about 100 larvae using an optical microscope Leica DME and a stereomicroscope Leica M60 equipped with a DFC425C camera. Pictures of some adult samples difficult to identify at species level were taken. LAS (Leica) software was used to take measurements in length of flies after manual calibration by the metric slide. Morphological identifications were performed using specific identification keys (Gennard, 2012) or descriptive articles (Table. 14).

Table 14. Identification keys used for the determination of the entomological samples collected from cadavers.

Taxon	Reference
Diptera: Family	McAlpine 1981
Diptera: Calliphoridae	Smith 1986; Szpila 2010
Diptera: Muscidae	Skidmore 1985; Seguy 1923
Hymenoptera: Pteromalidae	Turchetto *et al*. 2003
Coleoptera: Cleridae	Porta (1923-1934); Porta 1949

However, due to the lack of complete identification keys, the classical morphological identification method was not always possible, especially for insects in an immature stage of the development. For this reason, molecular identification was used to confirm the morphological data identification.

2.2.5.3 Molecular Analysis

To confirm the morphological identification data, molecular analysis was performed on adults' samples belonging to Muscidae, Sciaridae, and Piophilidae family. 15 samples from both seasons including 12 adults and 3 larvae were selected in order to perform DNA extraction, partial amplification of COI gene and sequencing. In both experiments, adults and larvae were chosen from the same carrion box in order to check the species compatibility between two different stages of development. 5 puparia from "season 1" experiment and 6 puparia and 6 pupae from the "season 2" experiment, were also randomly selected to collect further information about species colonising rabbits' carrions.

The experimental protocol, which is usually performed in order to identify the species at a molecular level, consists of DNA Extraction, DNA Amplification via PCR, and DNA Sequencing.

2.2.5.3.1 DNA Extraction

DNA was extracted from samples using the QIAamp DNA Mini Kit (QIAGEN) for total DNA extraction following the manufacturer's instructions for all insects collected from both experiments during all stages. Samples were first mechanically dismembered using plastic pastels to improve the subsequent enzymatic digestion. A partially modified protocol 'DNA Purification from Tissue' (QIAGEN) was used in order to increase the quality of the reaction by adding 4 µl of RNAse A (4mg/ml) purchased from Promega (Madison, Wisconsin, USA) after digestion by Proteinase K (100µg/ml) (Promega) which took three hours. Samples were left at room temperature for 5 min and incubated at 37°C for 30 min. RNAse was then inactivated at 70°C for 10 min. AL Buffer was added and successive steps were undertaken according to the manufacturer's instructions. Sterile deionized water was used to elute DNA.

The quality of each extraction was monitored by standard gel electrophoresis at a constant voltage of 100 V and using 1% w/v agarose/TBE gels, stained with Ethidium Bromide.

2.2.5.3.2 DNA Amplification

Polymerase Chain Reaction was carried out on mitochondrial COI gene, widely used for invertebrate species identification. Because of its evolutionary important role, COI is a well-conserved gene commonly used as a molecular target for insects' barcoding, i.e. the molecular identification of the species of interest. The primer pair listed below (Table. 15) consistently amplify a 710 bp fragment of COI across the broadest array of invertebrates.

Table 15.Universal primer pair used for COI gene amplification.

Primer	Sequence	Reference
LCO-1490 Fw	5'-GGTCAACAAATCATAAAGATATTGG-3'	(Folmer and Vrijenhoek, 1994)
HCO-2198 Rv	5'-TAAACTTCAGGGTGACCAAAAAATCA-3'	(Folmer and Vrijenhoek, 1994)

Additionally, two other different specific primer pairs have been designed to amplify COI gene belonging to *Hydrotaea* genus (Diptera; Muscidae) (Table. 16).

Table 16. The Primer pair used for Hydrotaea COI gene amplification.

Primer	Sequence
Op111 Fw	5'-TCGCAACAAATGGTTATTCTCT-3'
Rv	5'-TCAATTACCRAATCCTCCAAT-3'
Op211 Fw	5'-GTAATTGTAACAGCTCATGC-3'
Rv	5'-AACCAGTACCAGCTCCGTTT-3'

GoTaq® Flexi Polymerase protocol (Promega) was followed in order to prepare a master mix reaction of 20 µl final volume (Table. 17). Including 4 µl of Colorless GoTaqFlexi Buffer (5x), 2 µl of MgCl2 (25 mM), 0.5 µl of each primer (10 pmol/µl), 0.5 µl of Nucleotide Mix (10 mM), 0.25 µl GoTaq DNA Polymerase (5u/µl) and 2 or 4 µl of DNA template according to the quality of previous extraction. Have all been carefully prepared and collectively mixed.

Table 17. PCR volumes in master mix reaction.

Reagent	Concentration	Volume (µl)
Colourless GoTaq®Flexi Buffer	5x	4
MgCl2	25 mM	2
Primer FW	10 pmol/µl	0.5
Primer RV	10 pmol/µl	0.5
Nucleotide Mix	10 mM	0.5
GoTaq®DNA Polymerase	5 u/µl	0.25
DNA Template		4
Sterile Water		8.25
Total		20

The amplification program was set up on BioRad C1000 Thermal Cycler (Bio-Rad Laboratories, Inc.) (Table. 18). Initial heat activation step at 95°C for 10 min, 35 cycles at 95°C for 1 min, 1 min at the annealing temperature, 72°C for 1 min and a final extension step at 72°C for 10 min. Annealing temperature was 49.8°C using universal primers or 47°C using newly designed primers. Amplifications were confirmed by standard gel electrophoresis using 1.5% w/v agarose/TBE gels stained as previously described.

Table 18. Amplification program on BioRad C1000 Thermal Cycler.

Step	Time (min)	Temperature °C
Initial heat activation	10	95
Denaturation	1	95
Annealing	1	49.8 universal primers 47 Hydrotaea primers
Extension	1	72
Final extension	10	72

Thirty-five cycles of amplification have been performed in total. Every reaction was confirmed by standard gel electrophoresis as previously described.

2.2.5.3.3 DNA Sequencing

Fifteen μl of PCR products were purified using QIAquick PCR Purification kit®, following the manufacturer's protocol except for the elution step where deionized sterile water was used instead of Tris Buffer solution. The sequencing process based on standard Sanger method and Purified DNA samples were sent to an external Laboratory of Eurofins Genomic Operon, Eurofins MWG GmbH (Germany).

2.2.5.3.4 Analysis of Sequences

The obtained FASTA sequences were used for identification purposes performing an alignment with already known sequences kept in nucleotide databases as Gene Bank. BLAST-n® (Altschul *et al*. 1990) was used in order to check the identity among DNA sequences.

2.2.6 Microbiome Analysis

To assess the bacterial community functional during both seasonal trials, microbial samples were collected from three different body regions: Oral cavity, Skin, and Interface-sand carrion. In addition, sand samples were collected once a week from under the carcases (Tables 19, 20).

2.2.6.1 Microbiome Samples Collection

Microbial samples were aseptically collected using single sterile cotton swabs at three points over the decomposition process. During both seasonal trials, bacterial samples for each carcass were collected from three different body regions: (1) Oral cavity (internal region), (2) Skin (superior side exposed to the environment), and (3) Interface sand-carrion. Triplicate samples were collected for each body region using sterile cotton swab applicators for a total of 54 samplings at a time (Tables. 19, 20): two sets of 18 samples each were stored at -20°C until subsequent molecular processing such as DNA extraction and 16S rRNA analysis of the bacterial post-mortem communities. One set was used immediately at the same day of the collection in order to assess the phenotype of the microbial communities by BIOLOG EcoPlates™ as described below. Sampling swabs were carried out on the first 5 days started on the day of placement, and then once a week until the dry stage of the decomposition process.

Table 19. Total number of samples collected for each body region for (with and without fur carcases) during summer experiment 2014.

Sample type	Samples collected	Samples processed by Ecoplate	Samples storage at -20°C
Oral cavity swabs	108	36	72
Skin swabs	108	36	72
Interface – Sand swabs	108	36	72
Sand samples under the body	123	0	123
Insects	483	0	0
Sum	930	108	339

Table 20. Total number of samples collected for each body region for (with and without fur carcases) during spring experiment 2015.

Sample type	Samples collected	Samples processed by Ecoplate	Samples storage at -20 °C
Oral cavity swabs	216	72	144
Skin swabs	216	72	144
Interface – Sand swabs	216	72	144
Sand samples under the body	72	0	72
Insects	119	0	0
Sum	839	216	504

2.2.6.2 Samples Preparation

The Biolog EcoPlate was created especially for community analysis and microbial ecology studies. The characteristics of the microbial community functional diversity evaluation based on the community-level physiological profiling approach by Biolog EcoPlate with a mixed culture of microorganisms or environment samples (Gryta *et al*. 2014).

BIOLOG Ecoplates™ was used to investigate the phenotype of the microbial communities sampled as a function of their ability in using different carbon sources as growth sources. In this study, the following protocol was carried out according to manufacturer's instructions (Weber and Legge, 2010).

2.2.6.3 Functional Characterization of the Post-mortem Microbial Communities

The samples were prepared as follows:

All swab samples that collected from each body region of rabbits were placed into sterile test tubes with lids directly to avoid contaminated by unwanted bacteria from hands or other sources. Swabs labelled with sample name at the experiment location. Each swab Sample shacked in 15 ml of 0.9 % NaCl sterile physiological solution and mixed gently and labelled with sample name. The obtained microbial suspension was mixed gently and 150 µl of each sample was inoculated into each well of 96 wells of the BIOLOG EcoPlates™. Eighteen plates were prepared a time and then incubated at 25 °C temperatures on the sampling day.

EcoPlates' reading was performed every 24 hours for 120 hours (5 days) using microplate reader SPECTRO Star NANO spectrophotometer (BMG LABTECH). Absorbance in each well was read automatically at a wavelength of 590 nm at a constant temperature of 25°C to avoid any changes in growth conditions. Plates' reading was performed also the same day of the inoculum. All EcoPlates were inoculated in the same lab and then examined every day until the colour began to change. The metabolic fingerprint was recorded for each plate from the first day of the colour change and for four subsequent days.

2.2.6.4 Functional Evaluation of the Bacterial Community

In order to evaluate the bacterial functional diversity, of the samples, collected from the carrion, the positive plates defined by colour changing were noted and richness values of bacterial functionality index were calculated for each sample as follows:

% Functional Diversity = 100 * number of positive (purple/pink) carbon source wells
                                                Total number of carbon source wells (31)

This value varies from 0 to 100% with 0 being low diversity and 100% being a high diver.

% Variation of Results within Sample =   100* i /31

i = the number of carbon sources in which the three replicates were not all positive or all negative. On Table 2, i = sum of everywhere there is a 1 or 2 (but not 3 or 0).

The water is not a carbon source.

If the two samples give identical "fingerprints" on the EcoPlates, the value will be 100. If the two samples give exactly opposite "fingerprints", the value will be 0 (Mulcahy, 2007).

2.2.6.5 Molecular Analysis

Together with functional characterization, microbial communities developed on rabbits' carcases were also investigated using a molecular approach encompassing total DNA extraction, 16s rRNA gene amplification and Pyrosequencing.

2.2.6.5.1 DNA Extraction

Microbial DNA was extracted from individual swabs samples using the Fast Stool DNA Mini Kit (QIAGEN). Following the manufacturer protocol. The extremity of each swab was cut and put in a 2 ml collection tube then kept in ice to avoid DNA damage due to a sudden thermal shock. 1 ml of Inhibited Buffer was added and each suspension was left at room temperature for four hours and mixed by overtaxing every 60 minutes to improve the quality of the cellular suspension. The subsequent steps were performed according to the manufacturer's instructions.

Summer season experiment 2014 (June-October 2014)

Among all the swabs collected from three different body regions (Oral cavity, Skin, and interface sand), 8 samples belonging to the first season experiment (2014) were chosen depending on their Ecoplate positive results. In addition, they were chosen from two main points of the decomposition process, at the beginning of the decomposition (active decay stage) and the end of the decomposition process (dry stage). For each point, two different carrions, with fur (F) and without fur (NF) were selected in order to investigate a different post-mortem microbial pattern depending on the presence or absence of carrion covering (fur) over decomposition stages. All samples' information is shown in table 21.

Table 21. Samples of the summer season 2014. Two kinds of samples with Fur (F) and without Fur (NF) were selected.in order to investigate the different of post-mortem microbial pattern depending on the presence of Fur from three different body regions. (M) Mouth (oral cavity), (S) Skin, and (U) Under (interface carrion-sand). ADD (Days °C) were calculated by sum the daily average temperature.

NF Sample	Date	ADD (°C)	Functional Activity (%)	F Sample	Date	ADD (°C)	Functional Activity (%)
1M	02 / July	135.6	100.00	2M	02 / July	135.6	96.77
1S			0.00	2S			29.03
1U			96.77	2U			93.54
1M	27/ October	1901.3	54.83	2M	27/ October	1901.3	3.22
1S			48.38	2S			3.22
1U			100.00	2U			90.32

Spring season experiment 2015 (March-June 2015)

In order to perform molecular analysis for this season, 18 swab samples were selected. Three groups of six were chosen from three points of the decomposition process, (active decay, advanced decay, and dry stage). For each stage, two types of carcases with fur (F) and without fur (NF) were chosen for the purposes described above. For each carrion, three body region samples were selected depending on positive EcoPlate results, in order to evaluate the potential different distribution of the bacterial population in quantity and quality. All samples' information is shown in table 22.

Table 22. Samples of the spring season 2015. Two kinds of samples, with Fur (F) and without Fur (NF) were selected, and from three different body regions. (M) Mouth (oral cavity), (S) Skin, and (U) Under (interface carrion-sand. ADD (Days °C) were calculated by sum the daily average temperature.

NF Sample	Date	ADD (°C)	Functional Activity (%)	F Sample	Date	ADD (°C)	Functional Activity (%)
5M	25/ March	50.1	87.10	6M	25/ March	50.1	100.00
3S			45.16	6S			25.81
5U			83.87	6U			77.42
5M	20/ April	294.1	22.58	2M	20/ April	294.1	70.97
5S			3.23	2S			3.23
5U			54.84	2U			58.06
3S	18/ May	586.3	3.23	2M	18/ May	586.3	87.10
3U			6.45	2S			0.000
3M			12.90	4U			64.52

2.2.6.5.2 PCR

DNA amplification was carried out on 16S rRNA gene, which is largely used as a molecular marker to identify microorganisms at a taxonomic level. In fact, it consists of nine variable regions, different among the species, and flanked by well-conserved regions, which can be used to designed specific primers to amplify the region of interest. Universal Gray28 FW and Gray519 RV primers (Pechal *et al*. 2013) specific to amplify V1-3 genic region were modified by adding Junior-FLX adaptors as recommended by Roche in order to perform the one-step PCR prior Pyrosequencing analysis (Fig. 29). A complete list is shown in table 28. Original specific sequences for bacterial 16s rRNA gene amplification and the complete list of designed modified primers are reported in (Table 23). The first twelve fusion primers were used for Experiment 1-2014, while all the eighteen were used for Experiment 2-2015.
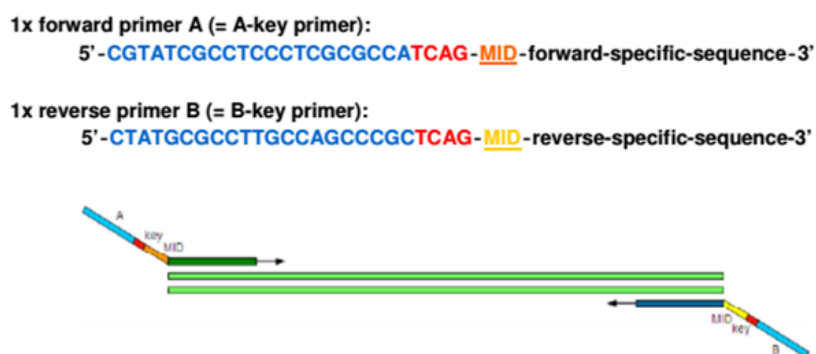

Figure 29. Roche design Pyrosequencing primers. Upper strand = Forward sequence, lower strand = reverse sequence. Same MID on both sides of the amplicon (mandatory for bidirectional sequencing) was required to distinguish different amplicons in a single PCR pool (Picture by Eurofins Genomic Operon).

Table 23. Specific primers used to amplify V1–3 regions of 16S rRNA gene.

Primer Name	Original Sequence	Reference
Gray28 Fw	5'-TTTGATCNTGGCTCAG-3'	(Pechal *et al*., 2013a)
Gray519 Rv	5'-GTNTTACNGCGGCKGCTG-3'	(Pechal *et al*., 2013a)

2.2.6.5.3 Universal Primers

Total DNA samples extracted from both seasons were first used as template in a PCR using 16S Gary 28 FW and 16S Gary 519 RV universal primers in order to detect microbial DNA in the starting samples (Pechal *et al*., 2013a). HotStarTaq Master Mix (QIAGEN) was used preparing a master reaction of 50 µl for each of the DNA template. Following volumes were added: 25 µl of a ready-to-use mixture containing HotStarTaq DNA Polymerase (5u/ µl), a modified form of Taq DNA Polymerase which provides high specificity in hot-start PCR, QIAGEN PCR Buffer, and dNTPs; 1.5 µl of each primer (10 pmol/ µl); 5 µl of total extracted DNA and 17 µl of H_2O RNAse free (Table. 24).

Table 24. HotStarTaq mixture. Volumes used to perform one-step PCR for a final volume of 50µl.

Reagents	Volume (µl)
Master Mix	25
H_2o RNAse free	17
16SBact Fw Primer	1.5
16SBact Rv Primer	1.5
Bacterial DNA Template	5
Total volume	50

The amplification program was set on BioRad C1000 Thermal Cycler (Bio-Rad Laboratories, Inc.) as follows: initial heat activation at 95°C for 15; denaturation at 94°C for 1min; primers' annealing at 52.3°C for 1min; primers' elongation step at 72°C for 1min and a final extension at 72°C for 10 min (Table. 25). The quality of amplification reaction was confirmed by electrophoresis gel 1.5% w/v agarose/TBE.

Table 25. Amplification program on BioRad C1000 Thermal Cycler.

Step	Time(min)	Temperature (°C)
Initial heat activation	15	95
Denaturation	1	94
Annealing	1	52.3
Extension	1	72
Final extension	10	72

Thirty-five cycles of the amplification reaction were enough to efficiently amplify a V1-3 variable region of 16S rRNA gene in each bacterial DNA sample as shown by electrophoresis gel 1.5% w/v agarose/TBE.

2.2.6.5.4 Generation of Sequencing Library

Bacterial DNA detection and amplification with universal 16S rRNA gene was correctly assessed, the initial generation of the sequencing library occurred with a one-step PCR using HotStarTaq Master Mix (QIAGEN) (Andreotti *et al*. 2011) as described above and using modified fusion primers' sequences. Same volumes were also used except for increasing primer's volume and doubling amount of DNA template (Table. 26).

PCR conditions were the same previously described except the annealing temperature was increased at 58°C considering the longer oligo's sequences. The quality of amplification reaction was confirmed by electrophoresis gel 1.5% w/v agarose/TBE.

Regarding samples resulted negative after setting up the above conditions a new PCR was carried out increasing the amount of total DNA template from 10 μl to 12 μl and increasing the number of amplification's cycles from 35 to 38 in order to improve the quality of the amplification reaction.

Table 26. HotStarTaq mixture. Volumes used to perform one-step PCR and generation of the sequencing library.

Reagents	Volume (μl)
Master Mix	25
H2O RNAse free	11
16SBact FW Primer	2
16SBact RV Primer	2
Bacterial total DNA Template	10
Total volume	50

2.2.6.5.5 DNA Purification and Quantification

All amplicons were purified using QIAquick PCR Purification Kit (QIAGEN) following the manufacturer's instructions. They were eluted in 30 µl of Elution Buffer (EB) to increase DNA concentration. EB contains Tris Buffer/EDTA that was requested by the external company Eurofins Genomics in order to perform the pyrosequencing analysis. Quantification of purified DNA was carried out on 1 µl of each sample by Nano DropTM 2000 (DNA detection spectrophotometric method at 260 nm as length wave); (Thermo Fisher Scientific, Waltham, Massachusetts, USA), following manufacturer's instructions. The concentrations are listed in tables 27 and 42.

Table 27. Concentrations of purified DNA samples eluted in 30 µl EB for pyrosequencing analysis.

Sample Name	Primer used	Concentration (ng/µl)
1	16SBact01	34.2
2	16SBact02	21.0
3	16SBact03	31.8
4	16SBact04	96.4
5	16SBact05	18.6
6	16SBact06	90.4
7	16SBact07	13.0
8	16SBact08	11.6
10	16SBact10	102.7
11	16SBact11	64.2
13	16SBact13	63.1
14	16SBact14	51.3

2.2.7 Pyrosequencing

Purified and quantified samples were sent to NGS Laboratory of Eurofins Genomic Operon. The sequencing was performed by a GS-Junior Pyrosequencing reaction with Titanium Series as part of 454 Roche sequencing system.

Table 28. Modified specific bacterial primers used for pyrosequencing analysis.

Name	Modified sequence with FLX adaptors
16SBact01FW_MID-01	CGTATCGCCTCCCTCGCGCCATCAGACGAGTGCGTTTTGATCNTGGCTCAG
16SBact 01RV_MID-01	CTATGCGCCTTGCCAGCCCGCTCAGACGAGTGCGTGTNTTACNGCGGCKGCTG
16SBact 02FW_MID-02	CGTATCGCCTCCCTCGCGCCATCAGACGCTCGACATTTGATCNTGGCTCAG
16SBact 02RV_MID-02	CTATGCGCCTTGCCAGCCCGCTCAGACGCTCGACAGTNTTACNGCGGCKGCTG
16SBact 03FW_MID-03	CGTATCGCCTCCCTCGCGCCATCAGAGACGCACTCTTTGATCNTGGCTCAG
16SBact 03RV_MID-03	CTATGCGCCTTGCCAGCCCGCTCAGAGACGCACTCGTNTTACNGCGGCKGCTG
16SBact 04FW_MID-04	CGTATCGCCTCCCTCGCGCCATCAGAGCACTGTAGTTTGATCNTGGCTCAG
16SBact 04RV_MID-04	CTATGCGCCTTGCCAGCCCGCTCAGAGCACTGTAGGTNTTACNGCGGCKGCTG
16SBact 05FW_MID-05	CGTATCGCCTCCCTCGCGCCATCAGATCAGACACGTTTGATCNTGGCTCAG
16SBact 05RV_MID-05	CTATGCGCCTTGCCAGCCCGCTCAGATCAGACACGGTNTTACNGCGGCKGCTG
16SBact 06FW_MID-06	CGTATCGCCTCCCTCGCGCCATCAGATATCGCGAGTTTGATCNTGGCTCAG
16SBact 06RV_MID-06	CTATGCGCCTTGCCAGCCCGCTCAGATATCGCGAGGTNTTACNGCGGCKGCTG
16SBact 07FW_MID-07	CGTATCGCCTCCCTCGCGCCATCAGCGTGTCTCTATTTGATCNTGGCTCAG
16SBact 07RV_MID-07	CTATGCGCCTTGCCAGCCCGCTCAGCGTGTCTCTAGTNTTACNGCGGCKGCTG
16SBact 08FW_MID-08	CGTATCGCCTCCCTCGCGCCATCAGCTCGCGTGTCTTTGATCNTGGCTCAG
16SBact 08RV_MID-08	CTATGCGCCTTGCCAGCCCGCTCAGCTCGCGTGTCGTNTTACNGCGGCKGCTG
16SBact 10FW_MID-10	CGTATCGCCTCCCTCGCGCCATCAGCTCGCGTGTCTTTGATCNTGGCTCAG
16SBact 10RV_MID-10	CTATGCGCCTTGCCAGCCCGCTCAGCTCGCGTGTCGTNTTACNGCGGCKGCTG
16SBact 11FW_MID-11	CGTATCGCCTCCCTCGCGCCATCAGTGATACGTCTTTTGATCNTGGCTCAG
16SBact 11RV_MID-11	CTATGCGCCTTGCCAGCCCGCTCAGTGATACGTCTGTNTTACNGCGGCKGCTG
16SBact 13FW_MID-13	CGTATCGCCTCCCTCGCGCCATCAGCATAGTAGTGTTTGATCNTGGCTCAG
16SBact 13RV_MID-13	CTATGCGCCTTGCCAGCCCGCTCAGCATAGTAGTGGTNTTACNGCGGCKGCTG
16SBact 14FW_MID-14	CGTATCGCCTCCCTCGCGCCATCACGAGAGATACTTTGATCNTGGCTCAG
16SBact 14RV_MID-14	CTATGCGCCTTGCCAGCCCGCTCAGCGAGAGATACGTNTTACNGCGGCKGCTG

2.2.8 Statistical Analysis

All statistical analyses were performed using Excel (Windows) and IBM SPSS 22.0 software (IBM® SPSS® Statistics, Armonk, NY). The significant threshold was set at 5%. Chi-square(X^2) was performed to analyse the microbial distribution difference in different cases (Fur and without fur, decomposition stages, boy regions and the humidity and environmental effect).

3. Results

3.1 3D reconstructions using 123D Catch software

3.1.1 Number of Photos Required

In order to determine the required number of photos to create a complete model, experiments were performed using a simple object (box) (Fig. 30). The quality of the models in these experiments varied according to the number of pictures used. Some 3D reconstructed models had incomplete parts or inexplicable deformities, reconstructions seemed to fail completely when only five photos are used. In addition, using 10 photos to perform the 3D reconstructions did not give any acceptable results, and only incomplete 3D models were obtained. Whereas, the best 3D models were achieved when the number of photos was higher than 25 (Fig. 30). Moreover, measurements were performed from each experiment in order to confirm the number of photos required to have an acceptable accuracy (Fig. 31). In addition to the number of the pictures as well the lighting conditions were considered, they showed a significant effect on the 3Dreconstructions. The best reconstructions were obtained when the objects were well illuminated with constant lightning and had a strong contrast with the background.
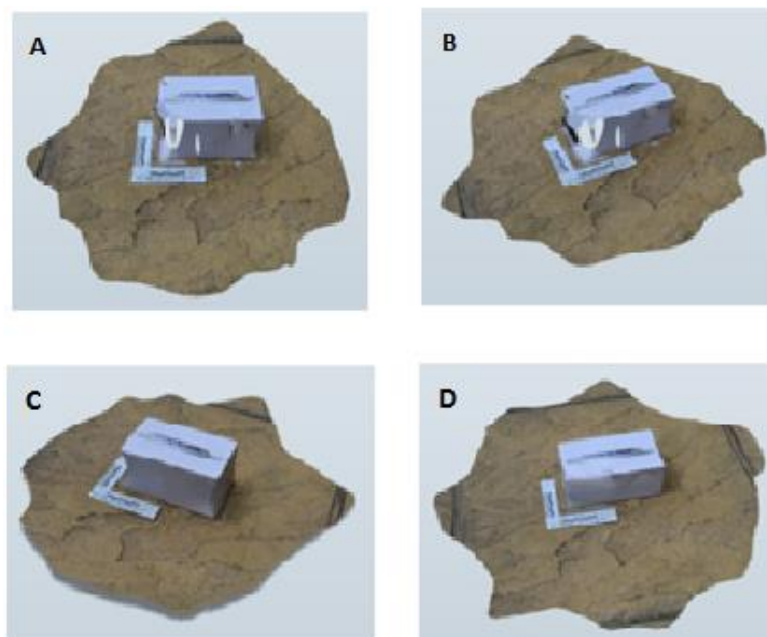

Figure 30. 3D models of box reconstructed using 123D Catch software with a different number of photos. (A) 10 photos, (B) 15 photos, (C) 25 photos and (D) 30photos.
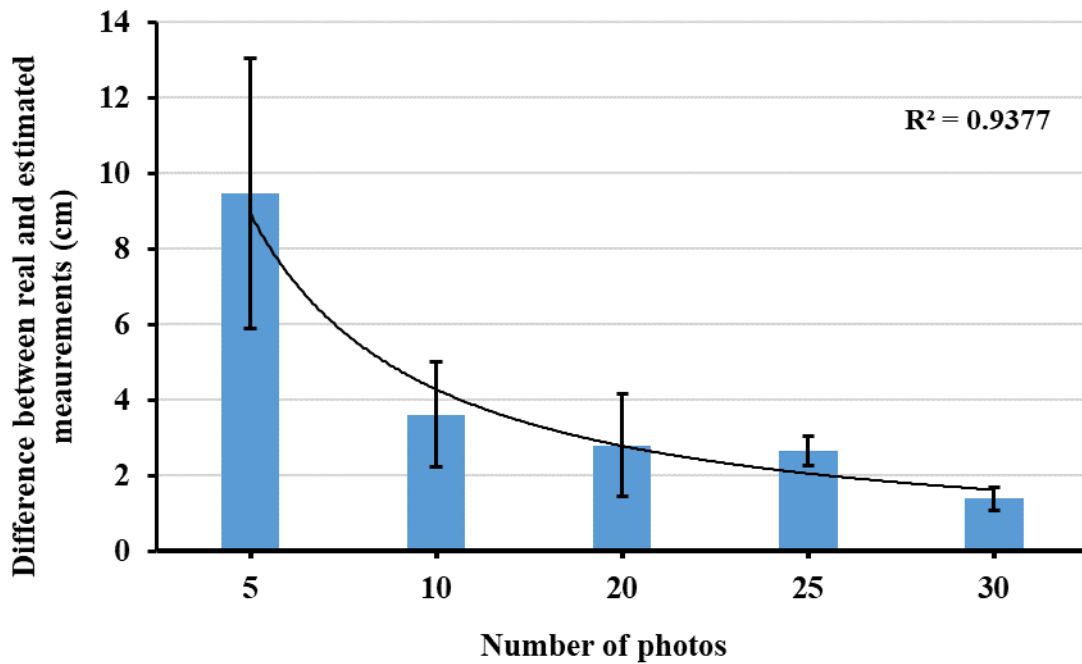
Figure 31. Differences between the control (original measurement) and the measurements obtained from the 3D reconstruction using a different number of photos.

3.1.2 Evaluation of the Method and Measurements

The number of photos required for the complete models was identified in the previous step. A further set of experiments were performed in order to investigate how the number of photos can be optimised working with different types of objects and in different conditions. The number of photos was defined between 20 to 30 photos depending on the size of the object or the scene, and the level of detail requested in a crime scene investigation. With a number of pictures between 20 and 30, the obtained results were complete (Figs. 33, 34). In fact, in a more complicated scenario where a skull, a cutter and a plier were present in the peripheral scene, this elevated the level of detail in the scene, and the reconstructed 3D model did not show any inaccuracy, missing part or deformation even in the peripheral details (Fig. 32). In addition, to identify the possibility to collect accurate measurements directly from the 3D reconstruction models, measurements of three skull regions (teeth and nose) (Fig. 32) were collected. This dataset was compared with the original measurements of the skull regions. The measurements collected from the 3D reconstructed models were repeated three times using a 3D reconstruction based on a minimum of 25 pictures. Measurements based on the reconstructed model showed a very strong agreement ($\sigma \sim 1.00$) in comparison to the measurements collected from the original objects (Table. 29).

115
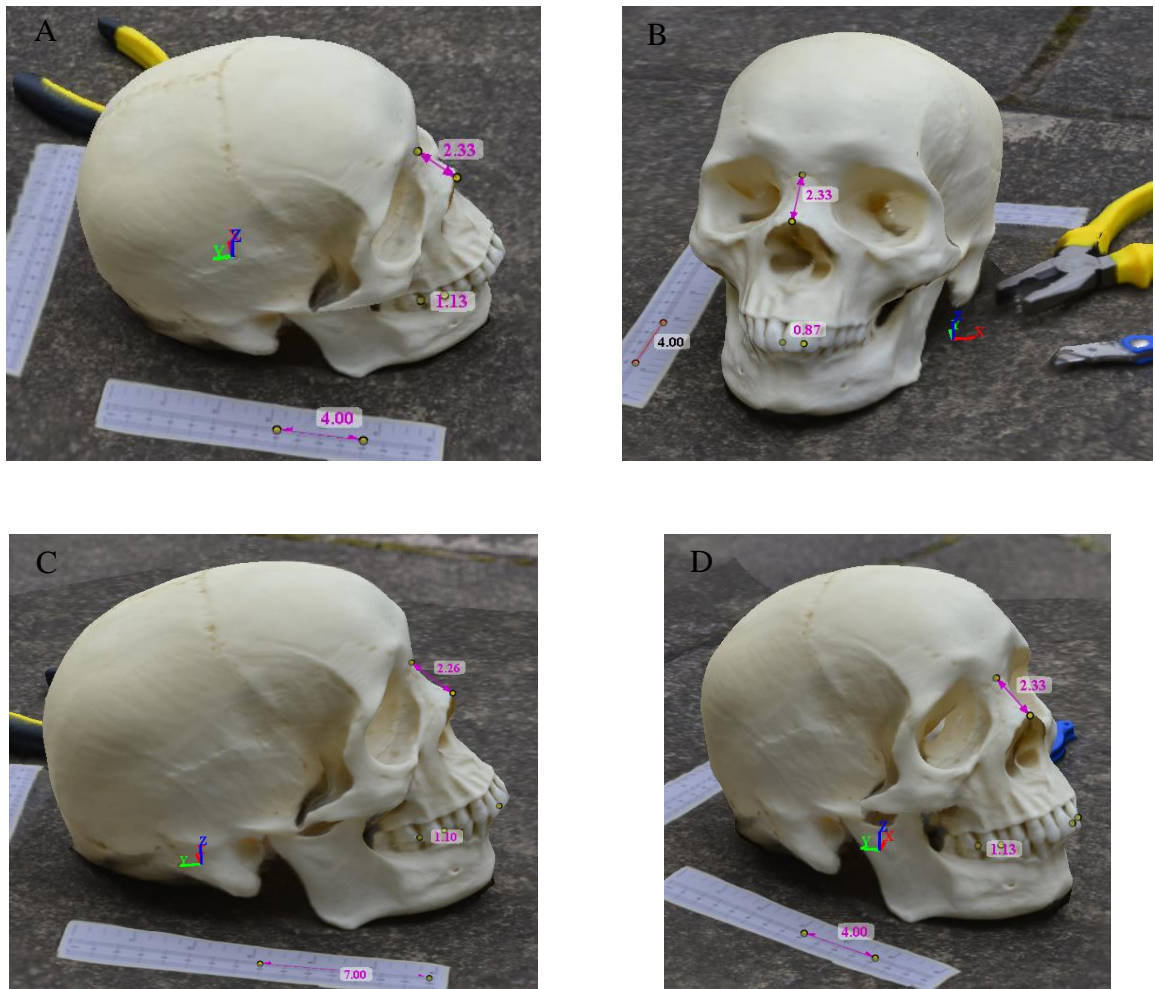
Figure 32. 3D reconstruction views of a skull created by 123D Catch using 20-30 photos. (A) upper lateral, (B) frontal 3D view, (C) lateral and (D) lateral.

Table 29. Intraclass Correlation Coefficient between the real and obtained measurement from the skull (Fig. 32). Two-way mixed effects model where people effects are random and measures effects are fixed were used.

	Intraclass Correlation	95% Confidence Interval	
		Lower Bound	Upper Bound
Single Measures	.995	.968	1.000
Average Measures	.999	.992	1.000
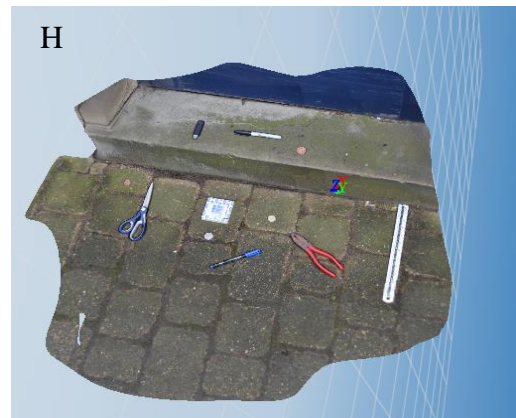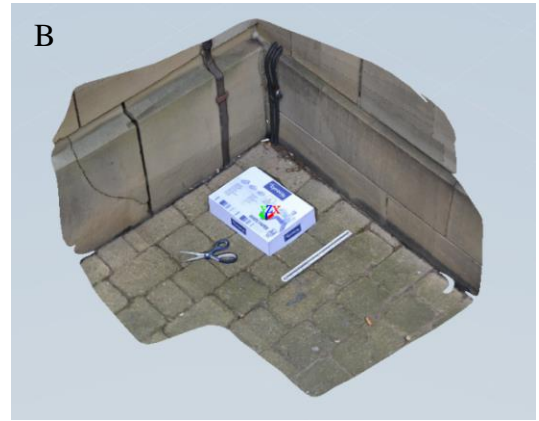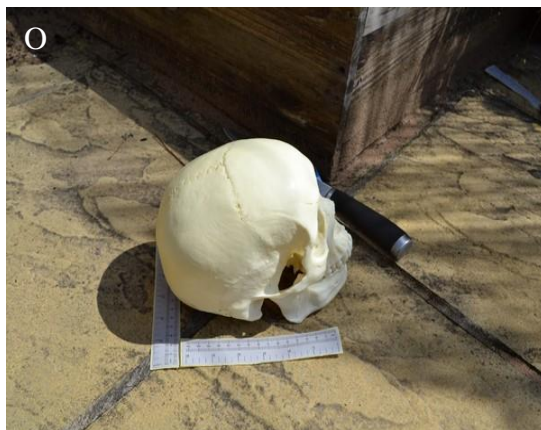
Figure 33. Different 3D reconstruction models created by 123D Catch using 20-30 photos for different scenario were created to have a wide range of distances from a micro (A, B, G, H, O and P) to a macro (C, D, E, F, I, J, K, L, M and N) crime scene.
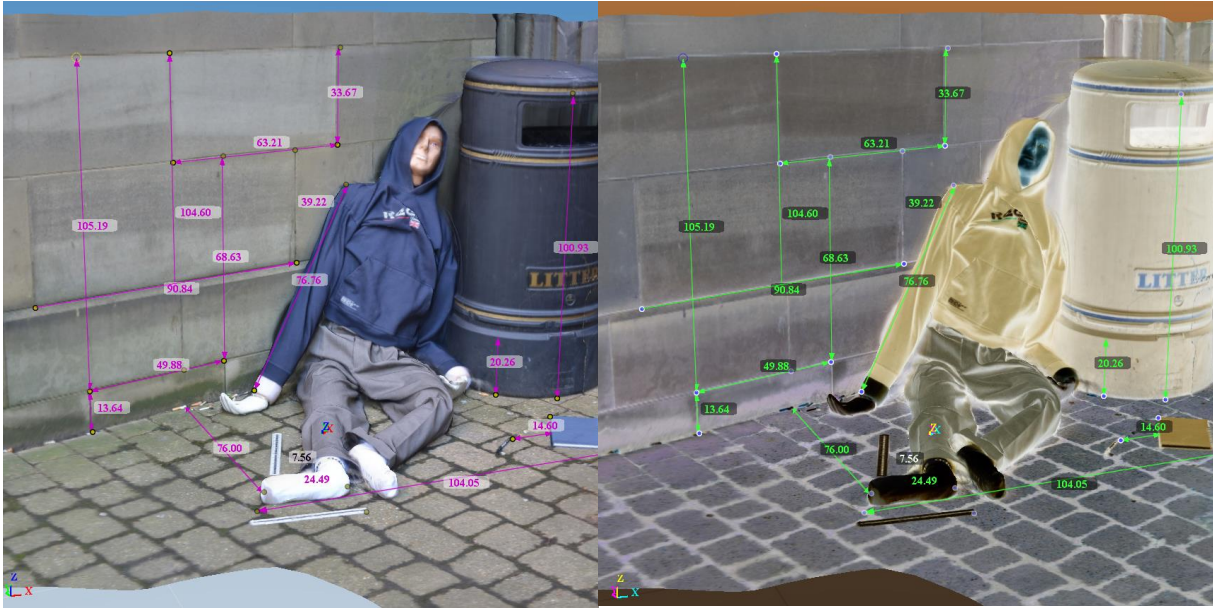
Figure 34. 3D reconstruction models created by 123D Catch using 20-30 photos with some measurements of two different scales of the crime scene.

3.1.3 Accuracy of Reconstructed Models

In order to evaluate the accuracy of the reconstruction models, validation experiments were performed for scenes of different sizes (small and large scale). In the small scenes, measurements and distances were smaller than 50 cm while in the large scene, all measurements and distances were bigger than 50 cm. All measurements of the objects at the sce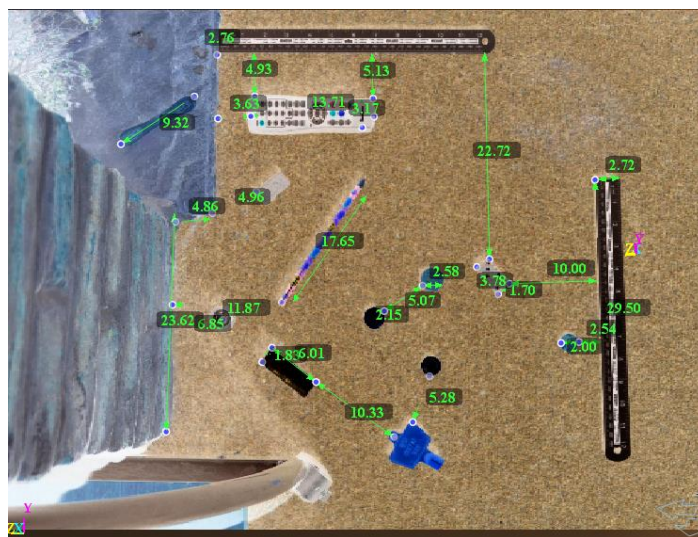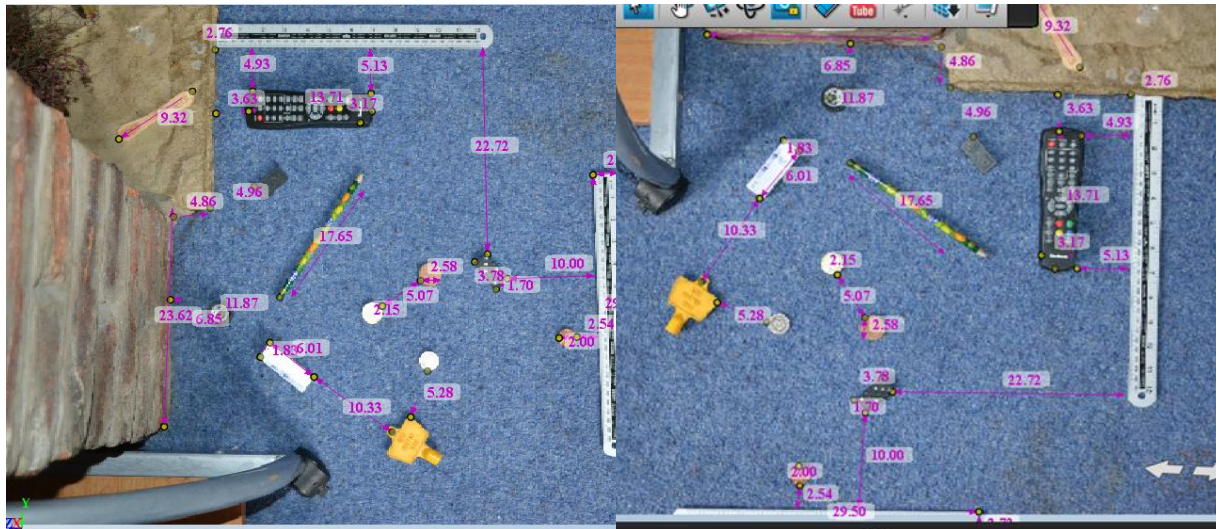ne and the distances between specific points were taken, to compute the difference between the measurements of 3D reconstruction models that were obtained by the 123D Catch software of three times measuring. These measurements were compared to the original measurements and the results of the correlation coefficient for a small-scale scene was 0.995 based on 155 measures. Whereas the large-scale scene correlation was 0.997 based on 73 measures. Consider the 228 measurements the correlation was 0.999. The results show the strength of the association between the two variables (real measurements and estimated measurements) (Figs. 39-41).

The visual examination of the graphs did not show any peculiar abnormality in the relationship between the real and estimated measurements, and the intraclass correlation showed a strong agreement (1.000) for the two class of measurements (real measurements vs estimated measurements). In addition, the frequency of the occurrences number of repeating the measurements showed the same pattern for real and estimated measurements, and there was no difference between real and estimated measurements for small and large scale scenes (Figs. 35-38).
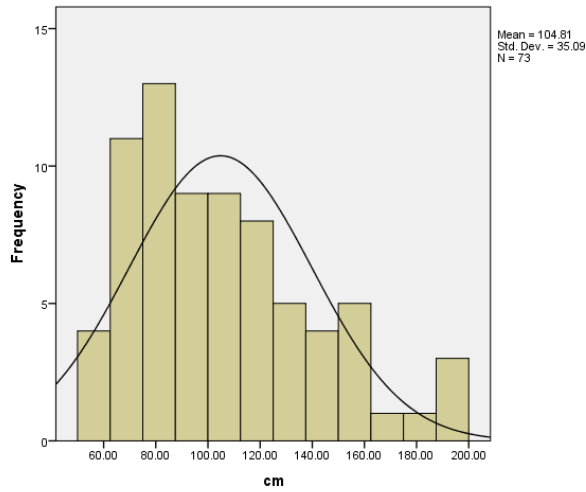
Figure 35. Frequency of real large scale-scene
measurements > 50 cm.
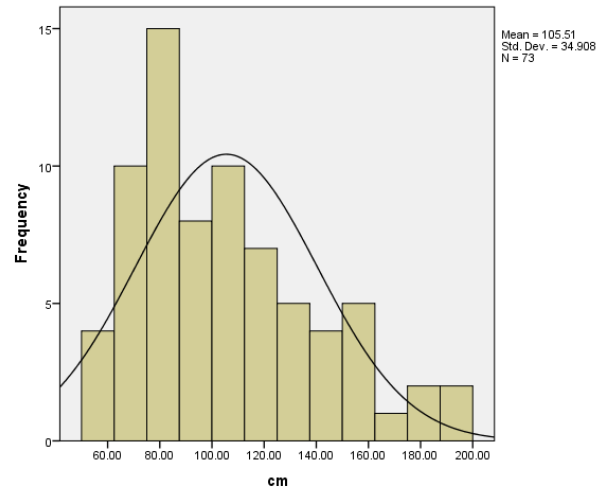
Figure 36. Frequency of estimated large-scale scene
measurements > 50 cm.
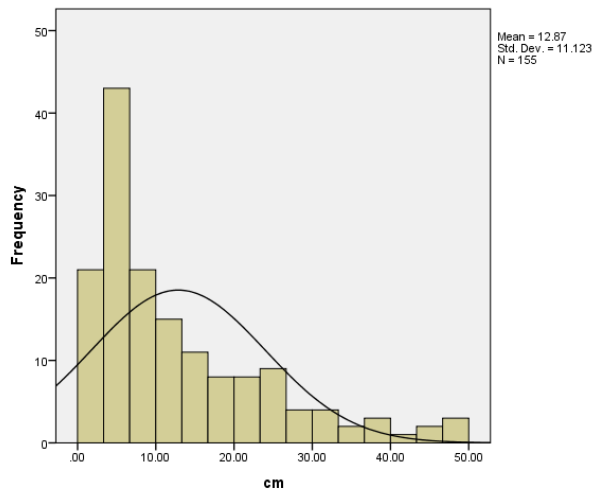
Figure 37. Frequency of real small scale scene
measurements < 50 cm.
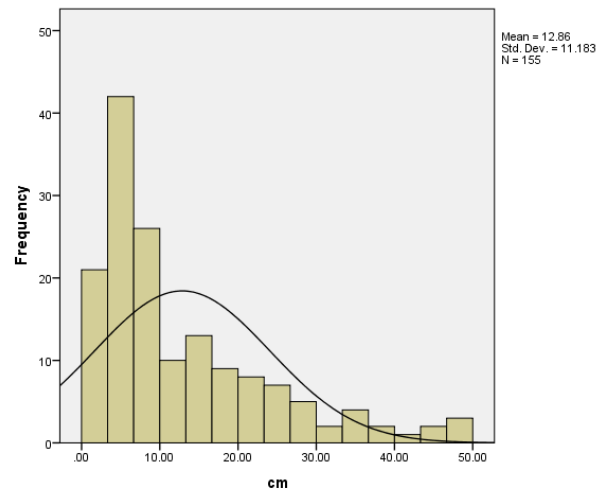
Figure 38. Frequency of estimated small scale scene
measurements < 50 cm.

Table 30. Summary table of N, Min, Max, Mode, Median, Average, and SD for total, small and large-scale
scenes.

	N	Min	Max	Range	Average	SD	Median	Mode
Total	228	1.80	192.00	190.20	42.30	48.20	18.00	10.00
<50cm	155	1.80	49.00	47.20	12.90	11.20	8.10	10.00
>50cm	73	53.00	192.00	139.00	104.80	35.10	97.00	83.00

122
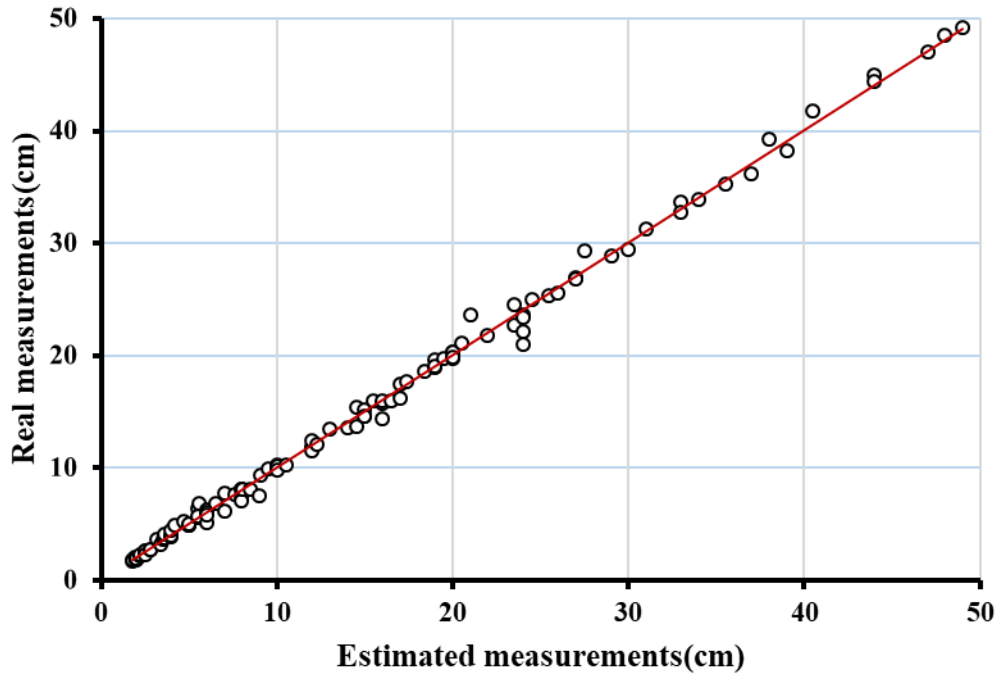
Figure 39. Correlation between estimated and real measurements of small scene <50cm. (R²=0.995), the red line is the linear correlation line.
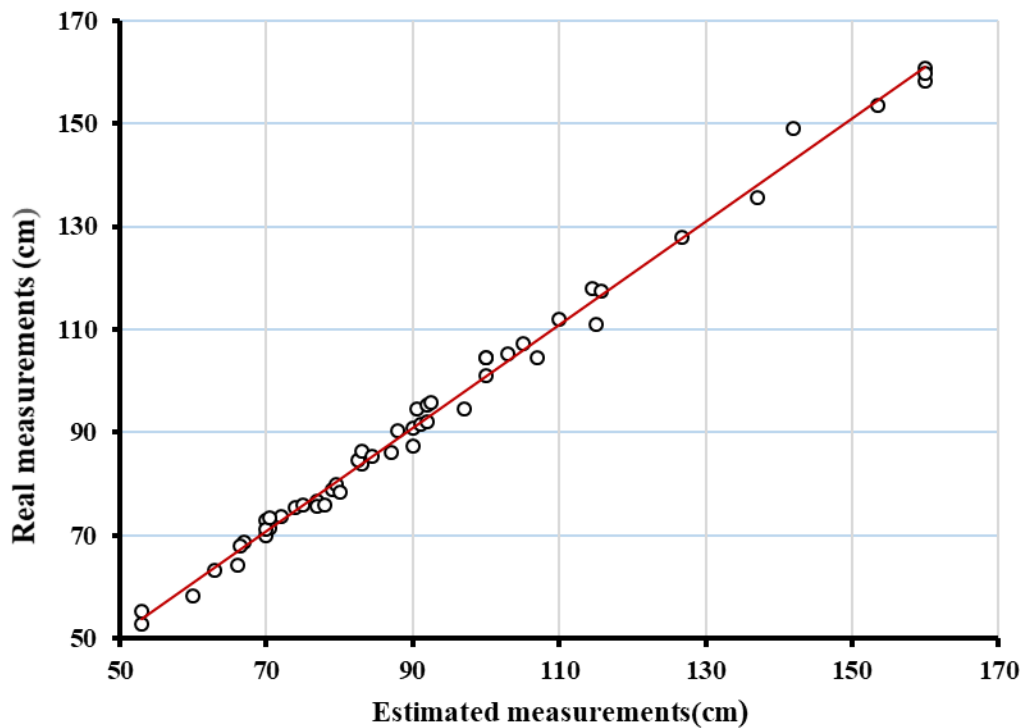
Figure 40. Correlation between estimated and real measurements of large-scale scene >50cm. (R²=0.997) the red line is the linear correlation line.
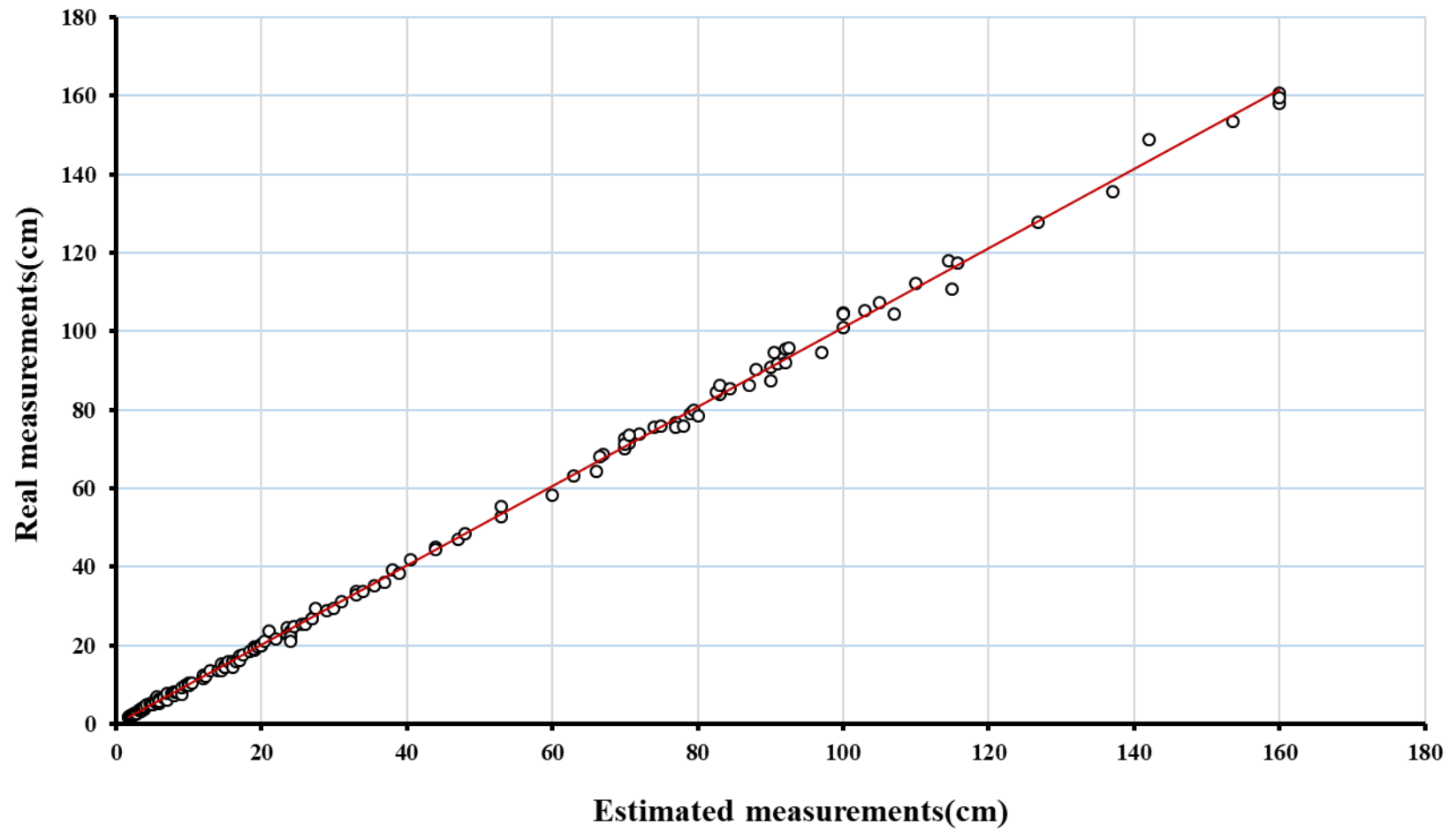
Figure 41. Correlation between estimated and real measurements of the total of small and large scales. (R²=0.999), the red line is the linear correlation line

3.1.4 Evaluation of Reliability for Measurements

The following experiment was performed in order to evaluate the consistency of the obtained reconstruction when performed by different users or in different times, this is a fundamental point in order to guarantee the reproducibility of the results and their consistency. To do that two measurements were performed in the different time by the same operator whereas a third one was performed by another operator. The experiment was done with different types of objects and the measurements were taken twice, and an additional time by another operator (S. Vanin) (Fig. 42). The reliability was analysed statistically and the result showed a strong agreement Intraclass Correlation Coefficient =1.00, p=<0.01, n= 50, and there were no significant individual differences concerning the real and obtained measurements.
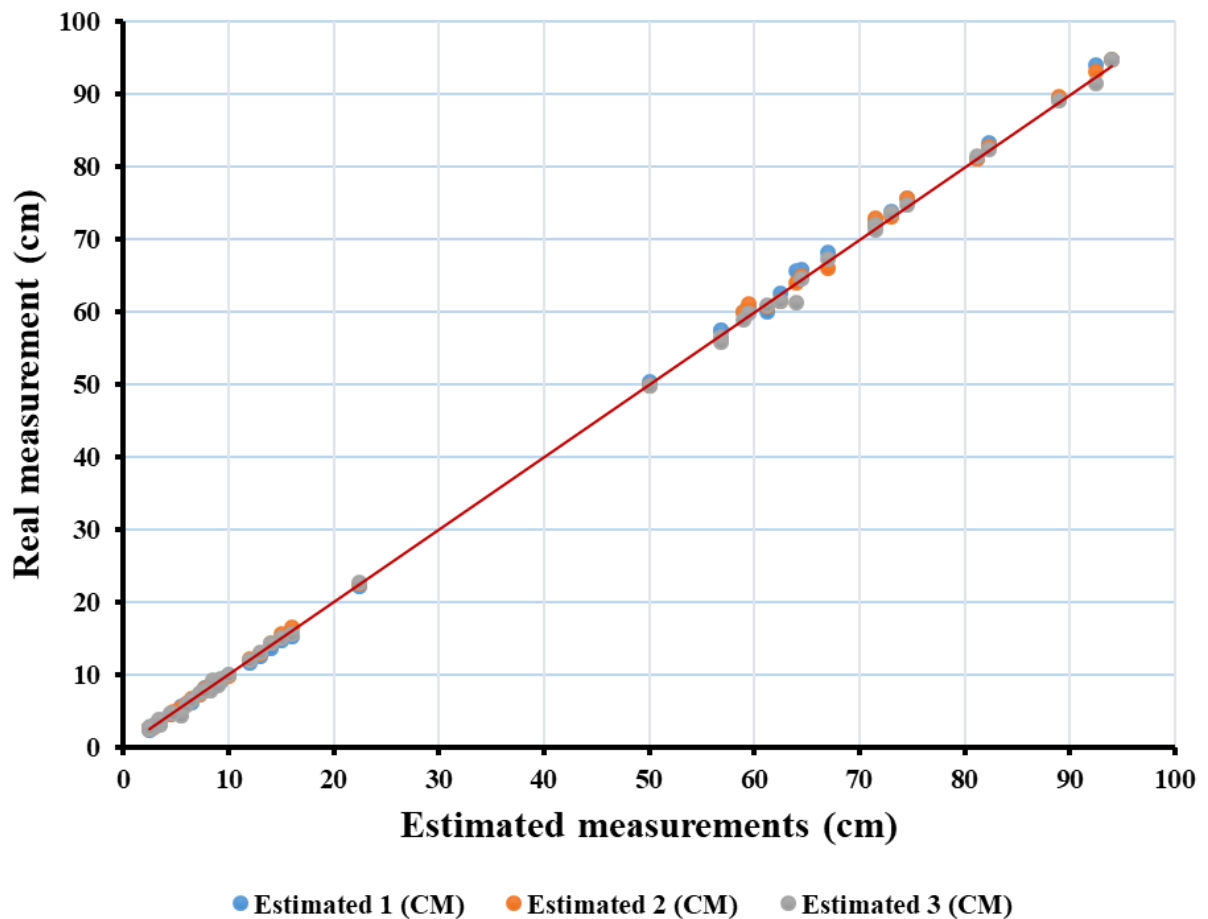
Figure 42. Correlations between the real measurements and the estimated measurements. Blue and orange dots indicate the reconstructs the estimated measurements performed by one operator, and grey dots reconstruct the estimated measurements performed by another independent operator (S. Vanin), (R²=0.9997, Intraclass Correlation Coefficient =1.00).

3.1.5 Comparison and Evaluation
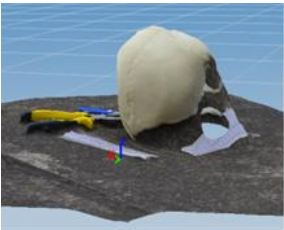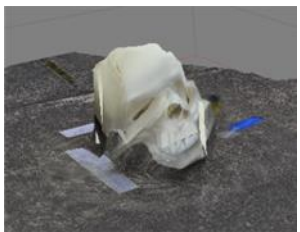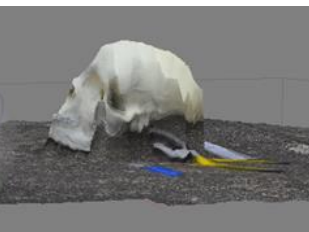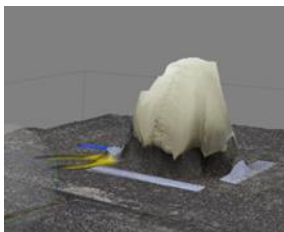
In order to evaluate the accuracy and time needed to obtain the 3D models using different methods, a comparison was performed using the open source software. Autodesk123D catch, Agisoft Photo-scan and Photosynth. 3D reconstruction tests were performed on four datasets. Each dataset was composed of a series of images of the same scene captured by the same camera, 10, 20, 35, and 50 images were used for the 3D reconstructions. The simple geometry of the scene allows evaluating the quality of reconstructing the surfaces and the angles. The test was used also to compare the processing time needed for each experiment.
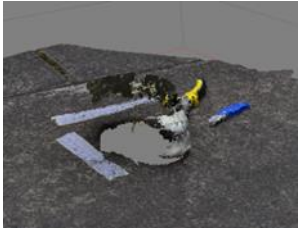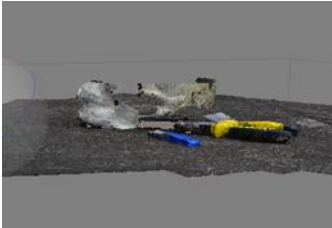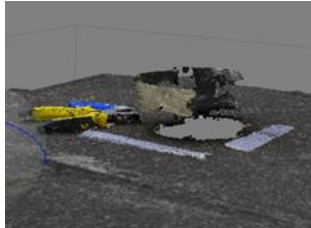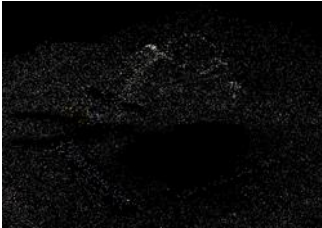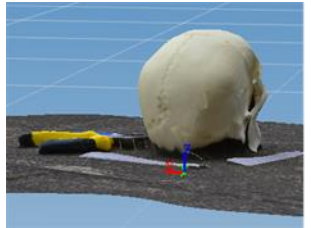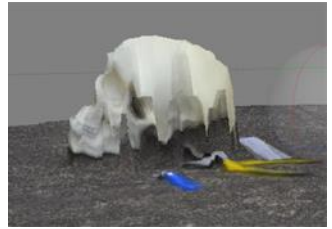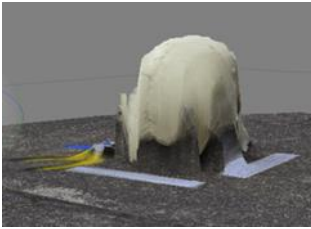
The quality of the reconstructed models was remarkable in some of the reconstructions, whereas, in some others, it was of low quality or incomplete depending on the number of photos. Reconstructions performed by Agisoft Photo-scan and Photosynth using the function "Texture" showed a very low quality, while in cloud format they were more detailed, accurate, and complete when more than 20 photos were used. Furthermore, the processing time was variable between the methods. Difference between some methods was 107 Minutes with 50 photos, and 34 Minutes with 35 photos. Some of the methods were faster in loading images but the result was incomplete and very low quality. Table (31) summarizes the results of running quality and time on all models by using different methods.
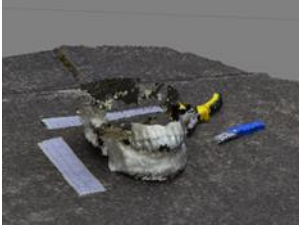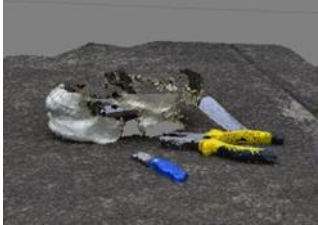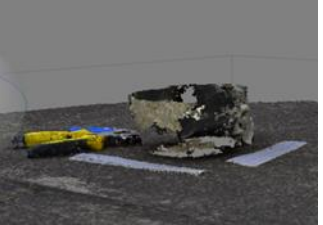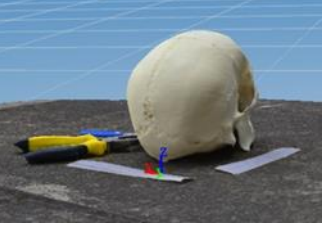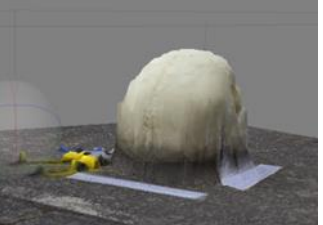
Indeed, the research showed that these methods create 3D models with different resolutions and in different processing time. The reconstruction was easy to be performed and obtained at a low cost.

The results indicated that 123D Catch software is a helpful and accurate method, which allowed the officers and investigators to document and reconstruct the crime scene, using such a powerful low-cost tool, and easy to use and move to different conditions of the crime scenes to capture the crime scene in its entirety, which considerably reduces the time.
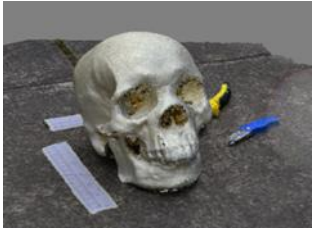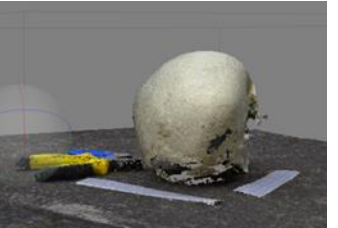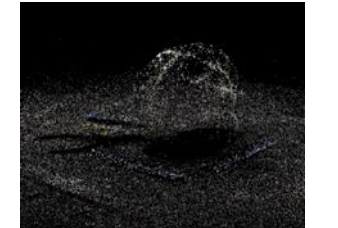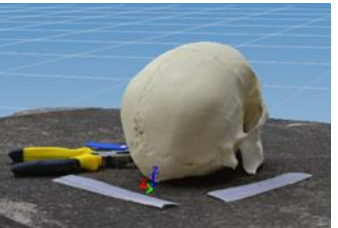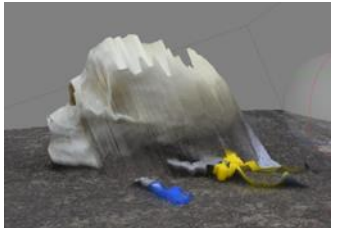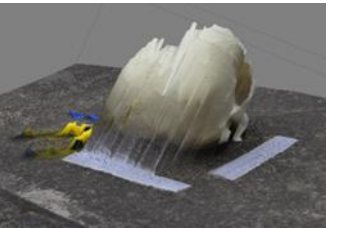
Table 31. Comparison of 3D models of a skull created by 123D Catch, PhotoScan, and Photosynth software's in general resolution and processing time required depending on the number of photos used. Which was on four data sets: 10, 20, 35, and 50 photos. Three sample images of each data set (frontal view, lateral view, and posterior view) are shown reconstruction results of each software. The evaluation was performed using a subjective scale considering the quality of the reconstruction.
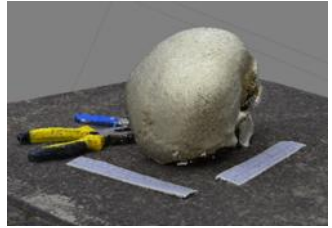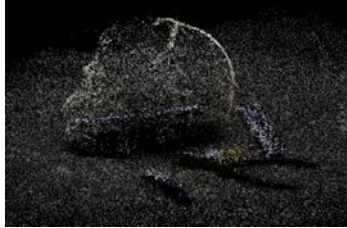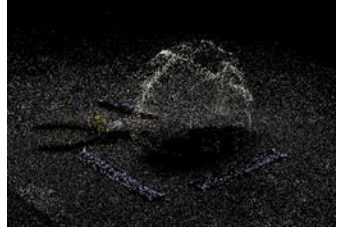
Software	No of photos	Time (Min)	Evaluation %	Frontal View	Lateral View	Posterior View
Autodesk 123D Catch	10	12	35			
Agisoft PhotoScan "Texture"	10	13	25			

Agisoft PhotoScan "Cloud"	10	13	8			
Photosynth "Cloud"	10	4	0			
Autodesk 123D Catch	20	21	100			
Agisoft PhotoScan "Texture"	20	25	40			

Agisoft PhotoScan "Cloud"	20	25	10			
Photosynth "Cloud"	20	10	5			
Autodesk 123D Catch	35	36	100			
Agisoft PhotoScan "Texture"	35	70	50			

Agisoft PhotoScan "Cloud"	35	70	70			
Photosynth "Cloud"	35	13	5			
Autodesk 123D Catch	50	38	100			
Agisoft PhotoScan "Texture"	50	145	40			

Agisoft PhotoScan "Cloud"	50	145	80			
Photosynth "Cloud"	50	15	7			

Agisoft PhotoScan   Photosynth   Autodesk 123D Catch

Large size pictures from the previous comparison with 50 photos created by Agisoft PhotoScan, Photosynth and Autodesk 123D Catch to emphasise differences in resolution

131

3.2 Decomposition Process Analysis

The 3D reconstruction using a cheap and easy tool was the first step to the document the decomposition process in an accurate way (Fig. 43). In fact, this approach allows the collecting and analysing of the decomposition process of rabbits with and without fur, in order to detect the carrion variations and associate them with the entomology and bacterial communities that play a key role in the decomposition process. The 3D reconstruction allows highlighting several details, for example, the reduction of the abdominal volume not visible in a 2D photo.

Experiment days	Rabbits without fur (NF)	Rabbits with Fur (F)
Day 0		
Day 4		
Day 5		

Day 7

Day 21
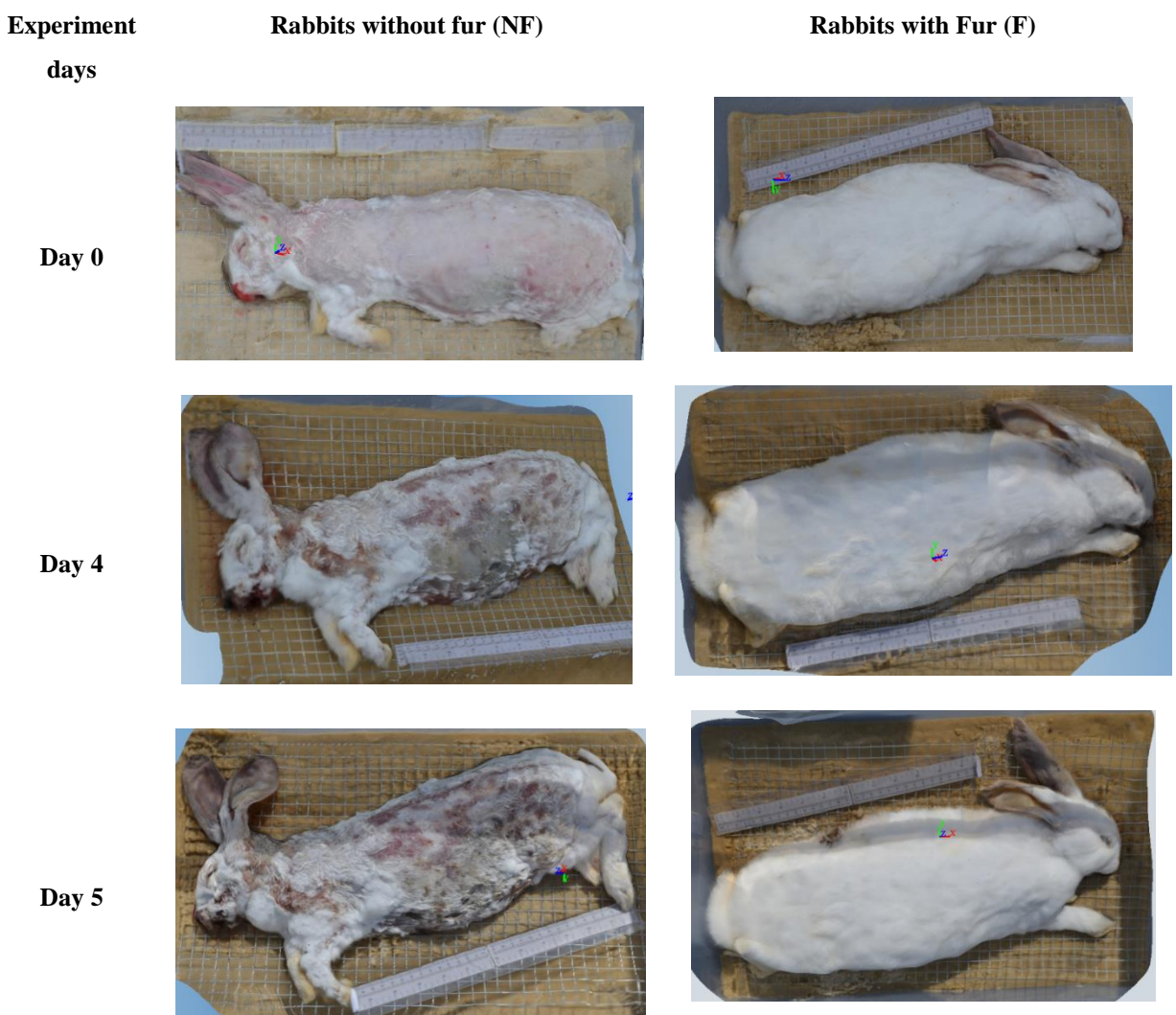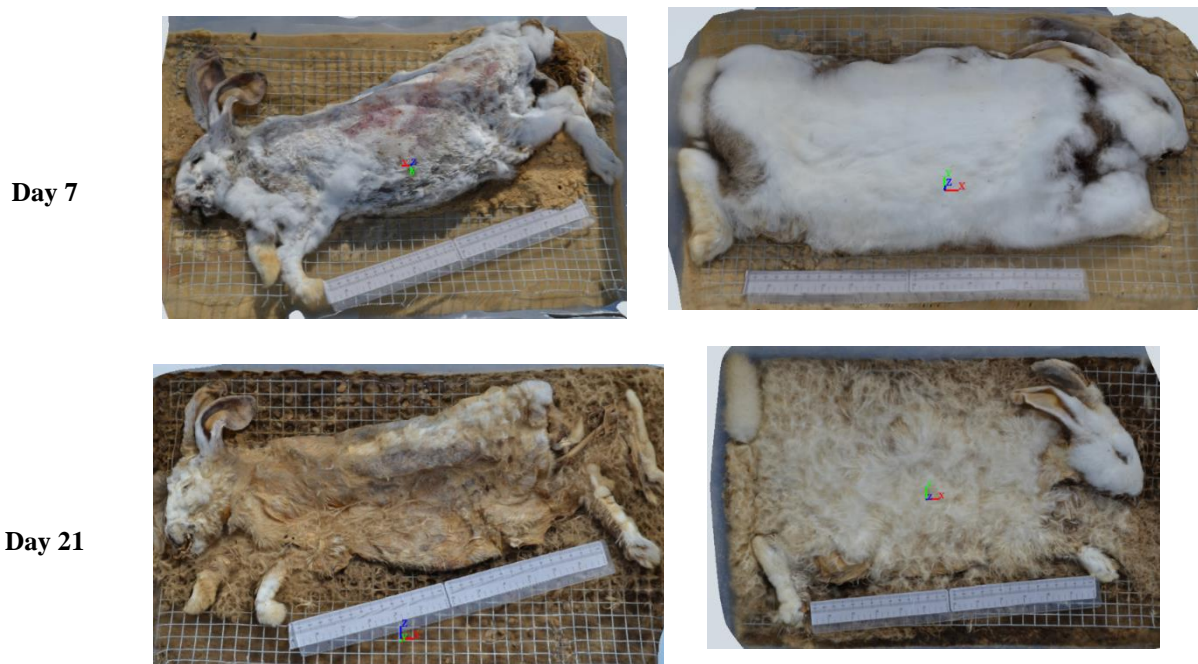
Figure 43. 3D reconstruction of rabbits' carcasses decomposition process during the summer seasonal trial (2014) using 123D Catch. The reconstruction is based on 25 photos.

3.2.1 Decomposition Stages

To identify the decomposition stages of the samples, photos were taken of all the rabbits' carrions every day for the first week and then three times a week for two weeks. Subsequently, twice a week to observe the changes that occurred, and notes were taken on the most important changes (Fig. 44). Carcasses consumption took 45 days to be completed in the summer season (experiment performed in 2014 see Material & Methods), while it took 82 days during the spring season (experiment performed in 2015 see Material & Methods). Five general stages were identified to describe the process of decomposition of invertebrate animals: fresh, bloat, active and advanced decay, and dry/remains. During the spring seasonal trial, the bloating stage was observed after two days from the day of placement (Day 0). In addition, in both seasons, skeletonisation stage was not reached. Photos for each rabbit carrion changes over the decomposition process is listed in Appendix 2 (Tables 57, 58).

Experiment days	Sample of rabbits without fur (NF)	Sample of rabbits with fur (F)
Day 0		
Day 2		
Day 7		
Day 19		
Day 29		
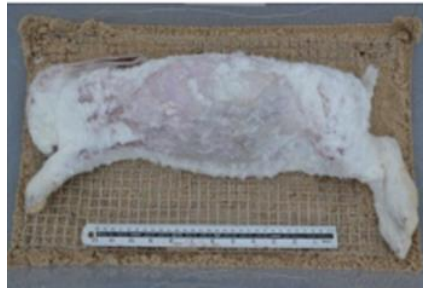
Day 36

Day 43

Day 82
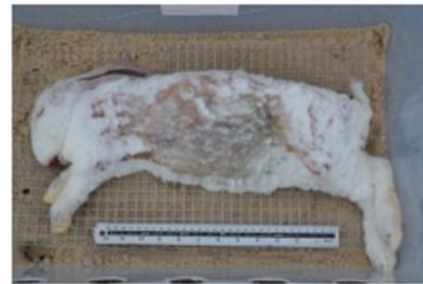
Figure 44. Carcasses decomposition process during the spring seasonal trial (2015).Because of the different environmental conditions, this experiment was carried out for a longer period compared to the 2014 experiment.

Moreover, insect colonisation started prior to carcasses without fur as larvae appear. Starting from day 22 puparia were collected and a maximum amount was observed on day 36. From day 43 the amount of collected entomological material decreased significantly and progressively until the end of the decomposition process (day 82).

3.2.1.1 Temperature Data

Summer experiment (First seasonal trial June-October 2014)

The local mean of the daily ambient temperature among carcasses between June and October 2014 was of 15.0 ± 2.7ºC, (Fig. 45). Over the entire period, maximum temperature value was 28.1ºC while the minimum value of temperature recorded was 7.9 ºC. The average

precipitations were 0.85 ± 2.22mm (Fig. 45). Temperature data were converted to Accumulated Degree Days (ADD) as shown in Appendix 2 (Table. 55).

Spring Experiment (Second seasonal trial March-June 2015)

Between March and June 2015, the local mean temperature recorded was 10.4 ± 2.8 ℃ (Fig. 46). Maximum temperature was 24.3 ℃; the minimum observed temperature was 0.2 ℃. During the spring season, the average of precipitations was 1.2 ± 4.0 mm (Fig. 46). Temperature data converted Accumulated Degree Days as shown in Appendix 2 (Table. 56).
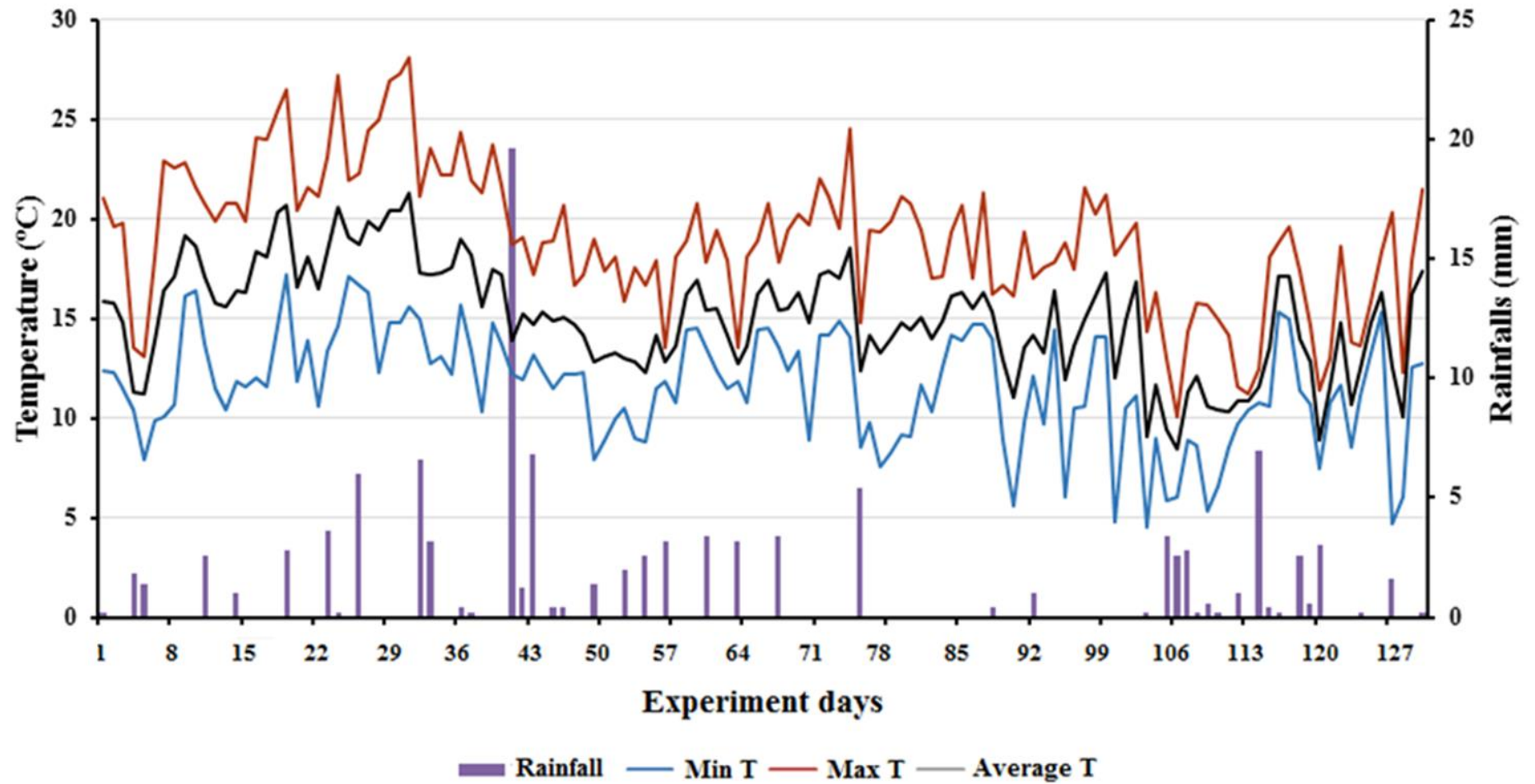
Figure 45. Meteorological data, recorded during the summer experiment (June-October 2014) by the University of Huddersfield station. (Red line) is maximum temperature, (Black line) is an average of temperature, the (Blue line) is minimum temperature, and the column is rainfalls (mm).
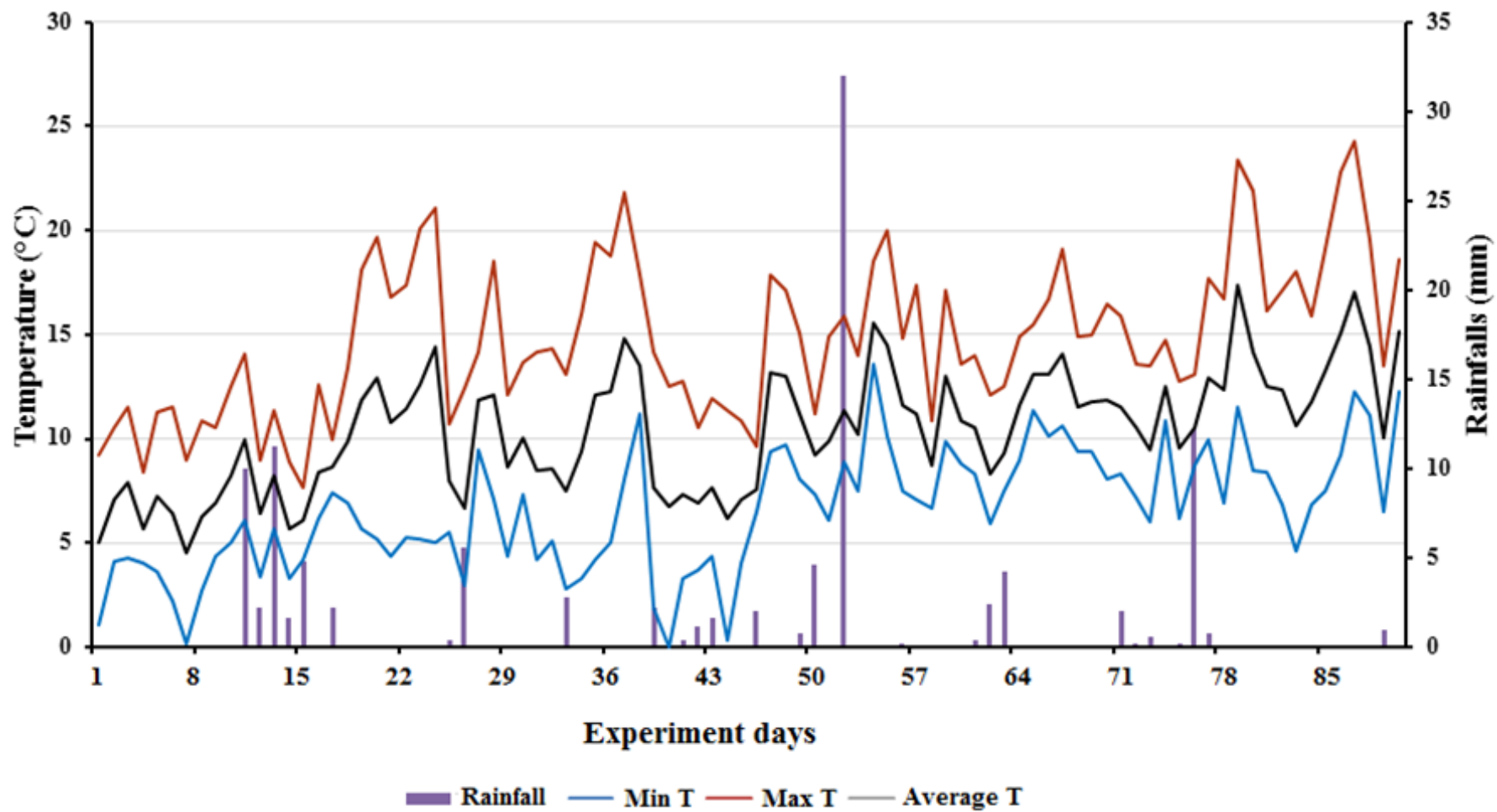
Figure 46. Meteorological data, recorded during the summer experiment (March-June 2015) by the University of Huddersfield station. (Red line) is maximum temperature, (Black line) is an average of temperature, the (Blue line) is minimum temperature, and the column is rainfalls (mm).

3.2.1.2 Animal Mass

The carcasses' weight was recorded during the experiments period, using a digital scale. The carcasses weight loss followed the same pattern in each experiment and the average of weight was used to follow the change across time (Figs. 47, 48). The carcasses have a slight loss of mass during the early stage of the decomposition process (Fresh stage). The loss of weight continued until the start of the colonisation stage at the third week in active decay stage where the carcasses lost the most of the weight. Finally, at the advanced decay stage, the carcasses lost more weight until dry stage, and then the weight was stable.
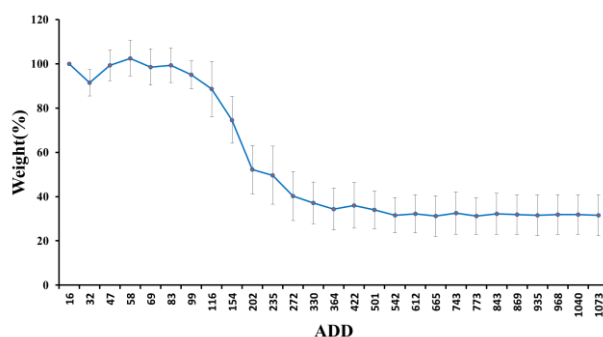
Figure 47. Average of the body mass of six rabbits' carcasses during the summer experiment (2014).
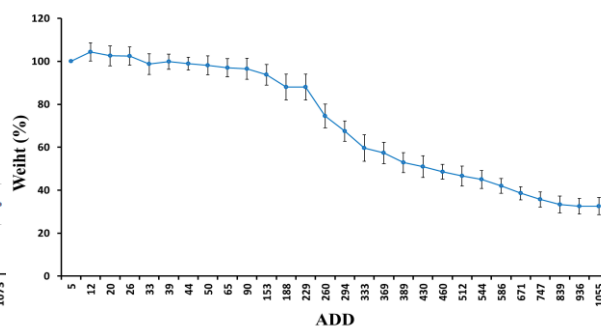
Figure 48. Average of the body mass of six rabbits' carcasses during the spring experiment (2015).

Summer experiment (First seasonal trial June-October 2014)

The average of the weight of the carcasses slightly decreased as the fresh stage occurred. After few days, the weight was slightly increased when bloat stage of the decomposition process occurred. In three weeks later, 70% of the body mass was lost on average, where active decay stage was occurring. In the same period, an active insect activity was also observed. One week after the beginning of the advanced decay stage, the body mass weakly changed until reaching a constant value. The weight was constant during the rest of the decomposition process as carcasses were totally dried (Figs. 47, 49).

139
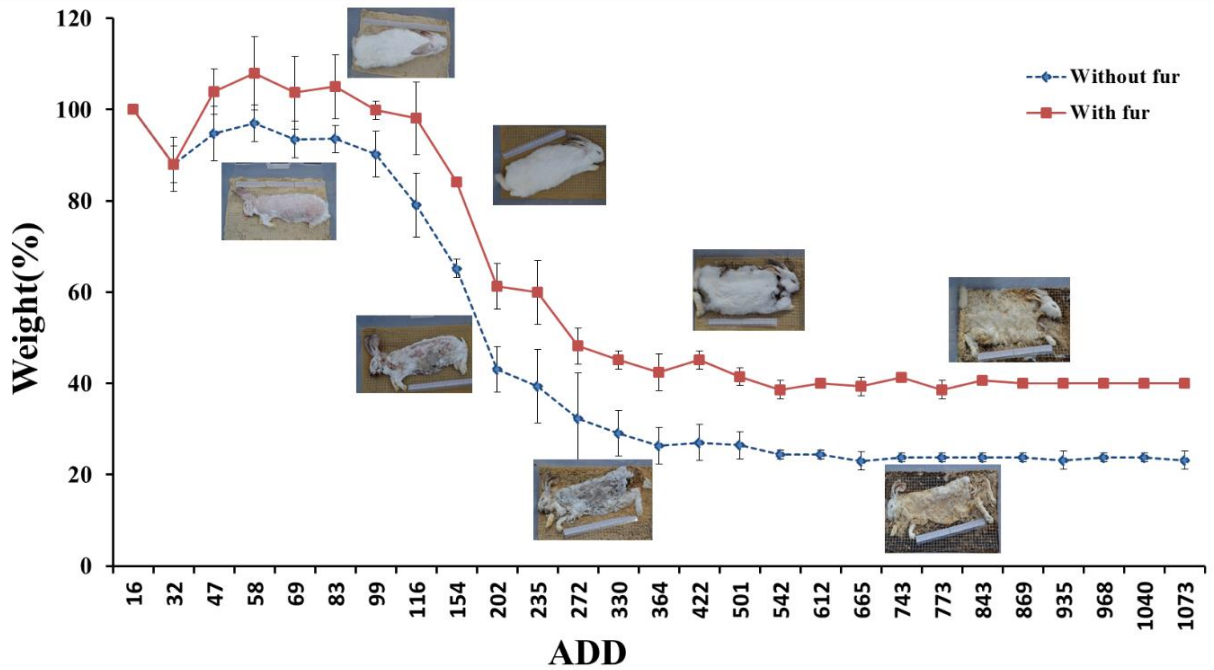
Figure 49. Average of the body mass of the total of three rabbits' carcasses during the summer experiment (2014). (Red line) is with fur carrion and (Blue line) is without fur carrions.

Spring Experiment (Second seasonal trial March-June 2015)

After the first week, initial increasing of all carcasses weight was observed due to the bloat stage. Thereafter, the average of the weights was decreased very slowly during the bloat stage. After three weeks, the weight loss was around only 10%. Reduction of 50% of the carcasses weight was observed after the week seven. The significant weight loss during this period is relevant to the advanced decay stage. After that, the body mass gradually declined at the end of the advanced decay stage. The stabilisation of the average of weight value occurred at the beginning of the dry stage (Figs. 48, 50).
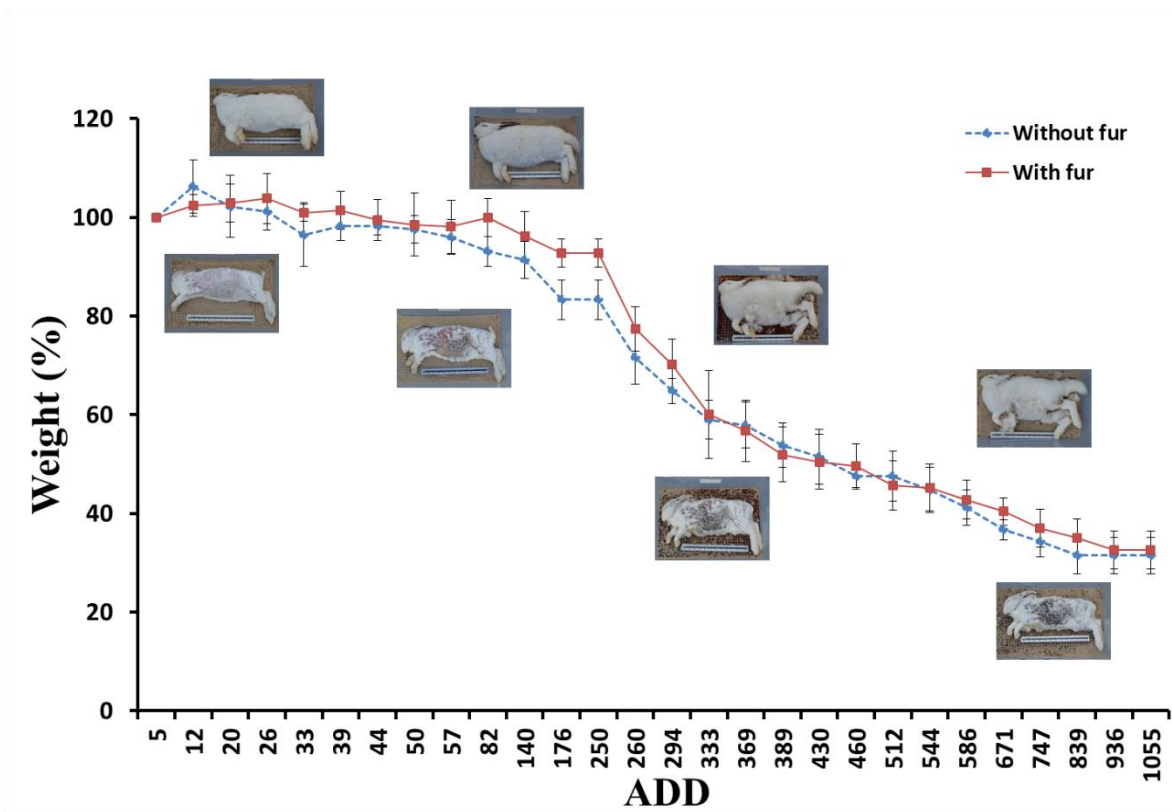
Figure 50. Average of the body mass of the total of three rabbits' carcasses during the spring experiment (2015). (Red line) is with fur carrion and (Blue line) is without fur carrions.

3.2.2 Entomo-Fauna Associated with the Carrion

All insects' samples (adults, eggs, larvae and puparia) during both summer and spring season's experiments were collected and identified. A difference in colonisation time was observed only in spring experiment: animals without fur were colonised two days before the animals with fur. No significant differences were observed in the summer experiment.

3.2.2.1 Morphological Identification

Summer experiment (First seasonal trial June-October 2014)

According to the morphological analysis carried out on more than 100 adult samples collected from carcasses, four families of flies (Diptera) identified Calliphoridae, Sphaeroceridae, Muscidae and Piophilidae. Dermestidae (Coleoptera) and Pteromalidae (Hymenoptera) were also observed. Among Calliphoridae, *Lucilia sericata* (Meigen, 1826) was the most abundant species followed by *Calliphora vicina* Robineau-Desvoidy,1830 and *Protophormia terraenovae* Robineau-Desvoidy, 1830. Among Sphaeroceridae, the following species were identified: *Leptocera caenosa* (Róndani, 1880), *Coproica vagans* (Haliday, 1833)*, Coproica hirticula* Collin, 1956*, Coproica hirtula* (Róndani, 1880) Specimens belonging to the Muscidae and Piophilidae family were identified as *Hydrotaea* Robineau-Desvoidy, 1830 *Ophyra* sp. and *Allopiophila Vulgaris* (Fallen, 1820) respectively. Among Dermestidae *Dermestes lardarius* Linnaeus, 1758 was the only beetle sampled in August. *Nasonia vitripennis* Ashmead, 1904 (Pteromalidae), commonly known as parasitic wasp was equally observed in all boxes over the entire collection period (Figs. 51, 52), (Table. 32).

Spring Experiment (Second seasonal trial March-June 2015)

Morphological analysis carried out on 100 adult samples collected from carcasses shown four families of flies (Diptera), i.e Calliphoridae, Muscidae, Piophilidae and Sciaridae. Pteromalidae (Hymenoptera) and Cleridae (Coleoptera) also observed. The most abundant species found was *Calliphora vicina* (Calliphoridae) confirming its preferential development during a spring-summer season in the United Kingdom. *Protophormia terranovae* were the second most abundant species belonging to Calliphoridae. Only one sample of *Lucilia sericata* (Calliphoridae) was found in box3 in June. *Nasonia vitripennis* (Pteromalidae) was also identified. *Necrobia rufipes* (Fabricius, 1781) and *Necrobia violacea* (Linnaeus, 1758) (Coleoptera: Cleridae) were sampled from box1 and box3 contain (NF) rabbits (Fig. 53) (Table. 33). For flies belonging to Muscidae, Piophilidae and Sciaridae family, species determination required further molecular analyses (Figs. 54 - 56).

Figure 51. Parasitic wasp (*Nasonia vitripennis*). Left lateral view.

Figure 52. *Allopiophila Vulgaris* (Piophilidae) was collected from (NF) box in August 2014. Adult left lateral view (left) and dorsal view (right). The orange colouration of the frons is one of the characters specific of this species.
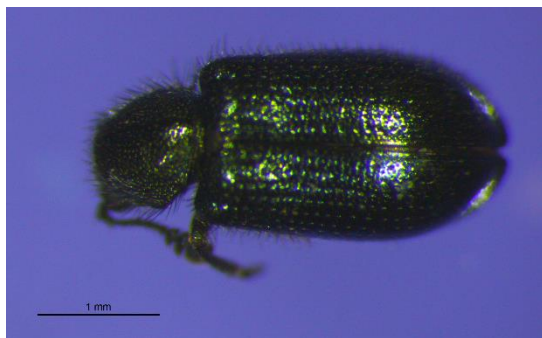
Figure 53. *Necrobia violacea* (left) and *Necrobia rufipes* (right). Adult samples collected from carcasses in (NF) BOX 1 and BOX 3 (April 2015). Both of them have a metallic blue body. *Necrobia rufipes* is easy to identify because of their red legs.

Figure 54. *Muscina prolapsa* (Muscidae) BOX3 11/05/2015. Adult sample, right lateral view (left). Thorax and right wing detail (right).

Figure 55. *Muscina prolapsa* (Muscidae) BOX5 18/05/2015. Adult sample, right lateral view (left). Dorsal view (right). The yellow spot on the scutellum is characteristic of the genus Muscina.

Figure 56. *Muscina prolapsa* (Muscidae) BOX6 18/05/2015. Adult left lateral view (left). Head details (right)

Table 32. Insects' morphological identification, summer experiment (2014).

	Month	Order	Family	Species
BOX1	June	Diptera	Calliphoridae	*Calliphora vicina, Lucilia sericata*
	July	Diptera	Calliphoridae	*C.vicina, L.sericata*
			Sphaeroceridae	*Leptocera caenosa*
		Hymenoptera	Pteromalidae	*Nasonia vitripennis*
	August	Diptera	Sphaeroceridae	*Coproica hirtula*
			Piophilidae	Gen. sp.
BOX2	July	Diptera	Calliphoridae	C. *vicina, L.sericata, Protophormia terranovae*
			Muscidae	Gen. sp.
			Sphaeroceridae	*Coproica vagans, C.hirticula,*
		Hymenoptera	Pteromalidae	*N. vitripennis*
	August	Diptera	Sphaeroceridae	*L.caenosa*
BOX3	July	Diptera	Calliphoridae	*C.vicina, L.sericata*
			Sphaeroceridae	*C. vagans, C.hirtula*
		Hymenoptera	Pteromalidae	*N. vitripennis*
	August	Diptera	Sphaeroceridae	Gen. sp.
			Piophilidae	Gen. sp.
		Coleoptera	Dermestidae	*Dermestes lardarius*
BOX4	July	Diptera	Calliphoridae	*P.terranovae*
			Sphaeroceridae	*L. caenosa*
		Hymenoptera	Pteromalidae	*N. vitripennis*
	August	Diptera	Sphaeroceridae	*L. caenosa*
			Muscidae	Gen. sp.
		Hymenoptera	Pteromalidae	*N. vitripennis*
BOX5	July	Diptera	Calliphoridae	*C.vicina, L.sericata, P.terranovae*
			Muscidae	*Hydrotaea sp.*
		Hymenoptera	Pteromalidae	*N. vitripennis*
	August	Diptera	Calliphoridae	*L.sericata*
		Hymenoptera	Pteromalidae	*N. vitripennis*
BOX6	July	Diptera	Calliphoridae	*C.vicina, L.sericata, P.terranovae*
			Muscidae	Gen. sp.
			Sphaeroceridae	*C.vagans, C. hirtula*
		Hymenoptera	Pteromalidae	*N. vitripennis*
	August	Diptera	Sphaeroceridae	*C. hirtula*

Table 33. Insects' morphological identification, spring experiment (2015)

	Month	**Order**	**Family**	**Species**
BOX1	April	Diptera	Calliphoridae	*Calliphora vicina*
		Hymenoptera	Pteromalidae	*Nasonia vitripennis*
		Coleoptera	Cleridae	*Necrobia violacea*
	May	Diptera	Calliphoridae	*C.vicina, Protophormia terranovae*
		Coleoptera	Cleridae	*Necrobia rufipes*
BOX2	April	Diptera	Calliphoridae	*C. vicina*
			Piophilidae	Gen. sp.
		Hymenoptera	Pteromalidae	*N. vitripennis*
	May	Diptera	Calliphoridae	*C.vicina, P.terranovae*
			Muscidae	Gen. sp.
BOX3	April	Diptera	Calliphoridae	*C.vicina, P.terranovae*
		Coleoptera	Cleridae	*N.rufipes*
	May	Diptera	Muscidae	Gen. sp.
			Sciaridae	Gen. sp.
		Hymenoptera	Pteromalidae	*N. vitripennis*
	June	Diptera	Calliphoridae	*Lucilia sericata*
BOX4	April	Diptera	Calliphoridae	*C.vicina*
	May	Diptera	Calliphoridae	*C.vicina, P.terranovae*
			Muscidae	Gen. sp.
			Sciaridae	Gen. sp.
BOX5	April	Diptera	Calliphoridae	*C.vicina*
	May	Diptera	Calliphoridae	*C.vicina*
			Muscidae	Gen. sp.
BOX6	April	Diptera	Calliphoridae	*C.vicina*
	May	Diptera	Calliphoridae	*C.vicina, P.terranovae*
			Muscidae	Gen. sp.
			Sciaridae	Gen. sp.

3.2.2.2 Molecular Identification

The obtained sequences were used for identification purposes performing an alignment with already known sequences kept in nucleotide databases as Gene Bank.

BLAST-n® is the bioinformatics tool used in order to check the identity among DNA sequences. Results are shown in the table (34) confirmed the previous morphological analysis, the most abundant species that colonised rabbits' carcasses in both spring and summer season is *Calliphora vicina*. *Muscina prolapsa* found in box 2 and box 6 at different stages of development and *Hydrotaea and leucostoma* in box 3, both belonging to Muscidae family, clearly demonstrate that the molecular approach is necessary for taxonomic characterisation at the species level. In fact, the initial morphological characterisation often allowed the family or genus identification only (Table. 34).

Table 34. Molecular identification of the insects taxonomic. (Adult, pupa, larva) that were collected in summer and spring experiments

Sample	Origin	Date of collection	DNA fragment size	BLAST Query cover	BLAST max ID Value %	Species
larva	BOX 6	May 2015	649 bp	99%	99%	*Muscina prolapsa*
larva	BOX 3	June 2014	197 bp	94%	99%	*Hydrotaea leucostoma*
pupa	BOX1	July 2014	652 bp	100%	99%	*Calliphora vicina*
pupa	BOX2	April 2015	646 bp	99%	99%	*Calliphora vicina*
pupa	BOX3	April 2015	650 bp	99%	99%	*Calliphora vicina*
pupa	BOX4	April 2015	646 bp	100%	99%	*Calliphora vicina*
pupa	BOX5	April 2015	654 bp	99%	99%	*Calliphora vicina*
pupa	BOX6	April 2015	649 bp	99%	99%	*Calliphora vicina*
pupa	BOX 5	July 2014	626 bp	98%	98%	*Calliphora vicina*
pupa	BOX1	June 2015	601 bp	99%	99%	*Calliphora vicina*
pupa	BOX2	June 2015	588 bp	99%	99%	*Calliphora vicina*
pupa	BOX3	June 2015	585 bp	98%	99%	*Calliphora vicina*
pupa	BOX4	June 2015	472 bp	100%	100%	*Calliphora vicina*
pupa	BOX5	June 2015	657 bp	95%	99%	*Calliphora vicina*
pupa	BOX6	June 2015	646 bp	95%	99%	*Calliphora vicina*
Adult	BOX2	May 2015	647 bp	99%	99%	*Muscina prolapsa*

3.2.3 Microbiome Associated with Cadavers

3.2.3.1 Functional Activity Characterisation

Differences in the post-mortem microbial communities between rabbits with and without fur were investigated using a functional approach based on the source of carbon used by the microorganisms. For each animal, the microbial pattern was analysed considering three different body regions. The average of functional activity and functional variation index calculated among three carcasses with and without fur per each day of sampling and for each body region. The functional variation index is reported as the error bars. Data for each rabbit condition and for each body region are listed in appendix 2 (Figs. 110-121).

Summer experiment (First seasonal trial June-October 2014)

The first observation about the functional activity of the microbial communities on all carcasses was the big variability depending on the stages of decomposition in addition to the body region as well (Oral cavity, Skin, Interface-sand-carcasses).

Oral cavity. The functional activity of the microbial communities had nearly the same pattern for both rabbits with and without fur in summer experiment. High functional activity was noticed in the first four weeks, and then there was no activity for two weeks during the decomposition until the last week when a slight increase occurred again (Fig. 57).

The average of microbial functional activity was calculated among three rabbits without fur (NF) at day one (fresh stage) (5.52%). Then increased on day four to reach (90.32%). For one week, this value was constant, and it was ranging between 90% and 92%. After two weeks of carcasses placement day, the functional activity average dramatically decreased to (6.45%). thereafter, no further action was detected over the decomposition process. The activity was observed during the advanced dry stage in order to investigate any further potential changes in the post-mortem microbial functional activity; One case of three showed an increase of 54.83% appendix 2 (Fig. 110).

The same pattern was observed in rabbits with fur (F) with some difference noted. On day one, the average of functional activity was (16.13%). During the active decay stage, on day four the activity was raising (88.17% to 96.77%). Two weeks after placement day, bacterial

communities were still active by (48.38%) where only (6.45%) was observed in samples without fur. One month later, during the advanced decay, the average was (16.13%) but it significantly decreased to (1.07%) later (Fig. 57), appendix 2 (Fig. 111).

Skin samples. During the summer 2014 experiment, functional activity of bacterial community on skin samples for rabbits with and without fur had almost the same pattern of activity. It was detected at the active decay stage, which was the second week after the day of carcasses placement over just one week. Then there was no more activity recorded until the late day sampling at advanced dry stage (Fig. 57), appendix 2 (Figs. 112, 113).

Interface-sand-carrion. Is the place where the most of the microbial functional activity were positive in all the samples days, with simple relatively different results. The highest activity was in the middle of the decomposition process of rabbits with and without fur over the summer experiment (Fig. 57). The first signal of microbial functional activity between the skin of carcasses without fur and sand was detected three days after the placement day at the fresh stage. The average functional value was (48.38%), then after one week increased to (94.59%) at active decay stage. Two weeks later, the microbial activity slightly decreased to (66.66%) before increased again gradually during advanced decay, at this point activities of (70.96%) and (78.49%) were calculated. The average functional activity remained relatively high in the advanced dry stage (83.87%) (Fig. 57), appendix 2 (Fig. 114). The same pattern was observed on carcasses with fur, but the functionality values slightly varied. An initial activity of (65.59%) during fresh stage increased to (97.85%) during active decay. Then slightly decreased to (63.44%) before reaching again higher values during advanced decay (73.11%) and (82.79%). last samples during the advanced dry stage showed a relatively high average activity (67.74%) but lower than carcasses without fur (Fig. 57), appendix 2 (Fig. 115).

In 2014 experiment no significant difference was found between each of the two kinds of carcasses, depending on the presence or absence of fur (Independent samples t-test p >0.05) (Table. 35). No significant difference was found between conditions (NF and F) (two ways ANOVA p >0.05) while a significant difference was found comparing the three body regions (two ways ANOVA p =0.00). The interactions between the two conditions delete the effect of the fur on the microbial functional activity (two ways ANOVA p > 0.05) (Table. 36).

Table 35. Independent sample t-test results testing microbial community functional responses between three body regions 2014.

Body Region	t	d.f.	p
Oral cavity	-0.353	12	0.730
Skin	-0.354	12	0.729
Interface-sand-carrion	-0.650	12	0.949

Table 36. ANOVA- two ways results in testing microbial community functional responses between conditions F and NF 2014.

Source	F	p
NF / F	0.139	7.121
Body regions	-13.272	0.000
Interaction	0.0054	0.952
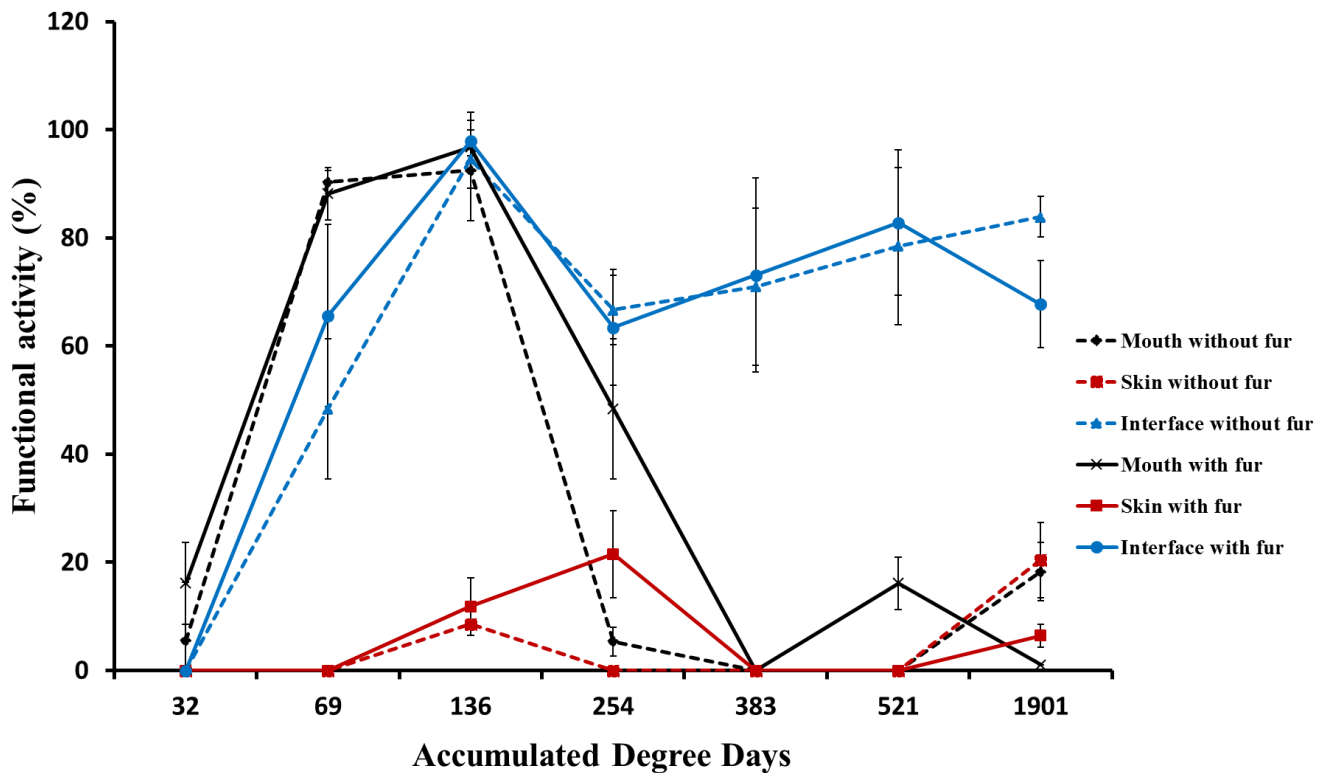
Figure 57. Average of microbial communities' functional activity for summer experiment 2014 of carcasses with and without fur (F, NF), in the different body region. Oral cavity (black line), Skin (red line), and Interface- sand (blue line) over accumulated degree-days (ADD), which was used as a surrogate of decomposition time. Average Functional Activity (%) was calculated among six carcasses with and without fur for each day sampling. Average Functional Variation (%) is reported as an error bar.

Spring Experiment (Second seasonal trial March-June 2015)

Oral cavity. During spring experiment, the functional activity was nearly the same in both rabbits with and without fur; it was high and variable during the decomposition process, until the last few days where it was increased slightly (Fig. 58).

The average of the microbial functional activity was (22.58%) at placement day and then increased to (88.17%) three days later at bloat stage. High values were observed during the active decay stage, and the highest value was (96.77%). During the advance decay, a decrease in the microbial functional activity observed. In the late stages of the advanced decay, constant values appeared between 30.11% and 34.11%. Once the dry stage occurred, a strong decreasing in mouth samples was observed. The average of the functional activity calculated for carrions with and without fur was very similar. The same functional activity pattern can be noted over all the stages of the decomposition process (Fig. 58), appendix 2 (Figs. 116, 117).

Skin samples. The bacteria functional activity had the same pattern in rabbits with and without fur. Generally, the activity started in the second week and lasted for three weeks, and then, no further action was recorded (Fig. 58), appendix 2 (Figs. 118, 119). Analysis showed the microbial communities' activity started a week after the day placement of the carcasses; at the active decay stage, and the average value recorded at this point was (29.03%). During the advance decay, the functional activity decreased and reached values lower than 10% in less than one week after the maximum level of the activity. Over the decomposition process, no more activity was detected, appendix 2 (Figs. 118, 119). A belt shape curve was observed in the functional microbial activity of carrion with fur. (31. 18%) was the maximum value reached during the active decay stage even if this resulted lower than previously described value for rabbits without fur (Fig. 58).

Interface-sand-carrions. The bacteria functional activity was positive, with variability in the value of the function in all samples of rabbits with and without fur during the decomposition process (Fig. 58), appendix 2 (Figs. 120, 121).

Microbial communities' functional activity was (36.56%) in the first three days at the bloat stage Appendix (Fig. 58). Once the active decay started, the microbial activity increased to (77.42%) until it reached a maximum value of (95.70%) during this stage. Then a mild decrease was initially observed at the advanced decay, followed by an increase to (43.01%). The maximum functional activity values were detected between the end and the beginning of the decomposition process. However, the average value progressively decreased and this pattern

was observed even for carcasses with fur (Fig. 58). From the maximum average level reached during the active decay (83.87%) a progressive decrease to (79.57% and 72.04%) was observed. The same pattern was in both (F and NF) conditions. In carcasses with fur, the last maximum value occurring during the late advance decay stage was higher (72.1%) if compared with the previous value in the same sampling day recorded for carcasses without fur (43.1%) (Fig. 58), appendix 2 (Figs. 120, 121).

In spring 2015, no significant difference was found between each of the two kinds of carcasses, depending on the presence of fur (Independent samples t-test p >0.05) (Table. 37). No significant difference was found between condition NF and condition F (two ways ANOVA p >0.05) while a significant difference was found comparing the three body regions (two ways ANOVA p =0.00). The interaction between the two conditions deletes the effect of the fur on the microbial functional activity (two ways ANOVA p > 0.05) (Table. 38).

Table 37. Independent sample t-test results testing microbial community functional responses between three body regions 2015.

Body Region	t	d.f.	p
Oral cavity	-0.610	22	0.952
Skin	0.411	22	0.685
interface sand/carrion	-0.654	22	0.520

Table 38. ANOVA- two ways results in testing microbial community functional responses between conditions F and NF 2015.

Source	F	p
NF - F	0.088	7.670
Body regions	16.504	0.000
Interaction	0.200	0.819
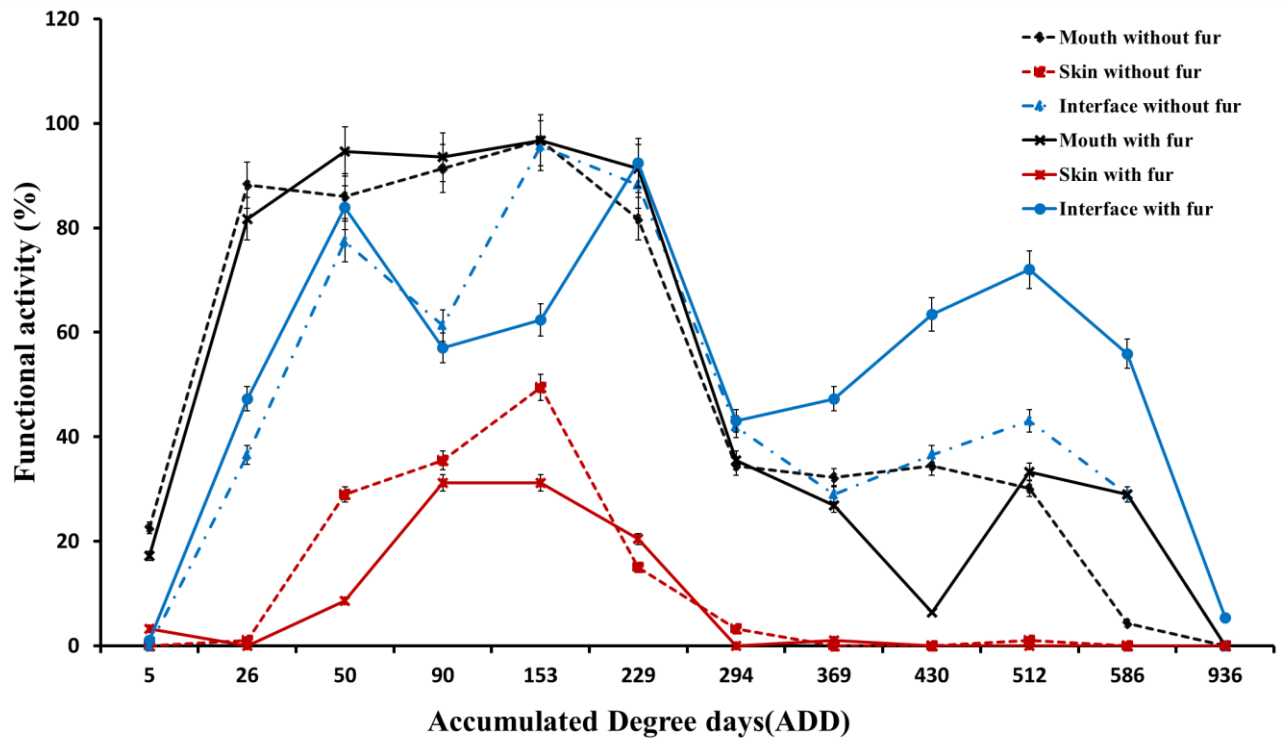
Figure 58. The seasonal average of microbial functional activity for spring experiment 2015, in the different body region. Oral cavity (black), Skin (red), and Interface- sand (blue) over accumulated degree-days (ADD), which used as a surrogate of decomposition time.

The results demonstrate that the fur does not affect the microbial community functional activity in the same season. However, significant changes in the functional activity were noted during decomposition stages both within and among seasons, which is similar to other studies conducted by Carter *et al* (2015) and Pechal *et al* (2013a).

3.2.3.2 Molecular Analysis

3.2.3.2.1 DNA Extraction from Swabs and PCR

DNA extraction was performed for 8 samples chosen for the summer trial (June-October 2014) (Table. 39) and 18 samples chosen for the spring trial (March-June 2015) (Table. 40).

Table 39. 2014 Samples origin source. (M' is for the mouth, I.e. oral cavity (body region 1). 'S' is for skin (body region 2). 'U' Is for under. I.e. interface carrion-sand (body region 3). 1-2 are Boxes number

PCR Sample	Origin Source	Collection Date
1	1M	2/July
2	1S	2/July
3	1U	2/July
4	2M	2/July
5	2S	2/July
6	2U	2/July
9	1U	27/October
12	2U	27/October

Table 40. 2015 Samples origin source. (M) Is for the mouth, i.e. oral cavity (body region 1). (S) Is for skin (body region 2). (U) Is for under, i.e. interface carrion-sand (body region 3). 3-5-6 are Boxes number.

PCR Sample	Origin Source	Collection Date	PCR Sample	Origin Source	Collection Date
1	5M	25/ March	10	2M	20/ April
2	3S	25/ March	11	2S	20/ April
3	5U	25/ March	12	2U	20/ April
4	6M	25/ March	13	3S	18/ May
5	6S	25/ March	14	3U	18/ May
6	6U	25/ March	15	3M	18/ May
7	5M	20/ April	16	2M	18/ May
8	5S	20/ April	17	2S	18/ May
9	5U	20/ April	18	4U	18/ May

3.2.3.2.1.1 Universal Primer Testing

Summer experiment (First seasonal trial June-October 2014)

A gradient PCR was performed in order to assess the annealing primer temperature showed an optimum of the amplification reaction at 52.3°C. Utilising PCR with universal primer pair was successful for all the selected samples.

Spring Experiment (Second seasonal trial March-June 2015)

PCR performed with a universal primer pair specific for a V1-3 region of bacterial 16S rRNA gene was successfully positive for all the samples (Fig. 59).
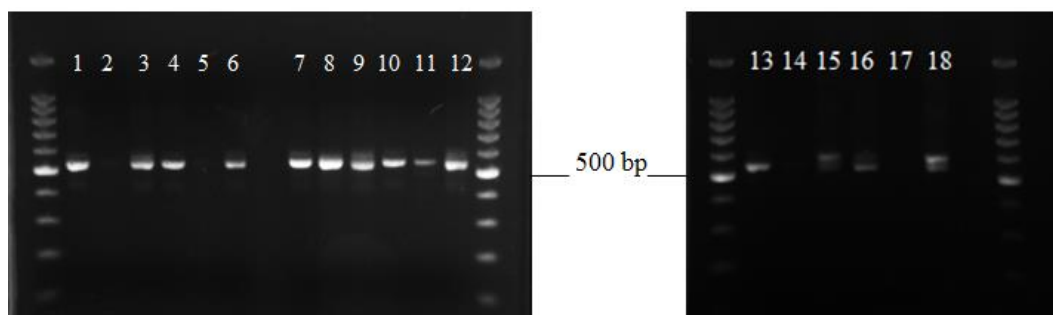
Figure 59. V1-3 16S rRNA gene Primer Testing PCR. DNA microbial samples from Exp.2 were amplified using unmodified universal primer 28FW and 519RV. Amplicons' size was about 500bp. DNA Ladder 100bp (Promega). Samples were numbered from 1 to 18.

3.2.3.2.1.2 Generation of Sequencing Library

PCR performed with modified fusion primers specific for a V1-3 region of bacterial 16S rRNA gene was successfully positive for all the samples chosen in both seasonal trials (Figs. 60, 61).

Summer experiment (First seasonal trial June-October 2014)
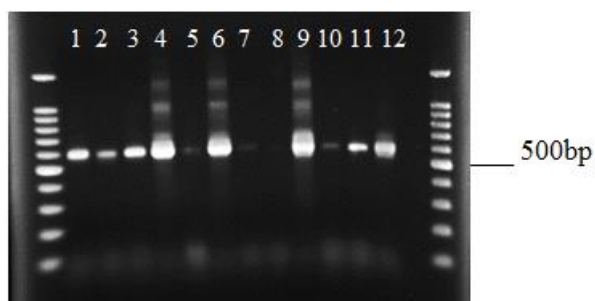
Figure 60. PCR with FLX-adaptors-fusion primers for pyrosequencing analyses. DNA microbial samples from Exp.1 were amplified using modified fusion primer FLX-28FW and FLX-519RV. DNA Ladder 100bp (Promega). Samples were numbered from 1 to 6 and 9, 12. Their origin source has been previously reported in table 39.

Spring Experiment (Second seasonal trial March-June 2015)
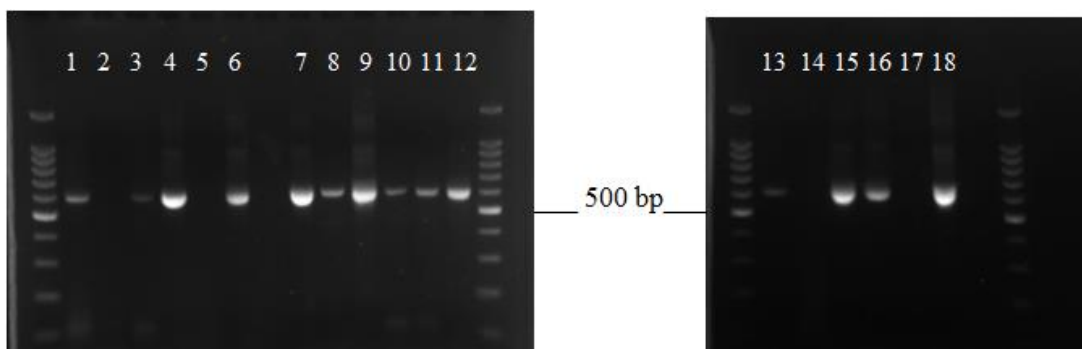
Figure 61. PCR with FLX-adaptors-fusion primers for pyrosequencing analyses. DNA microbial samples from Exp.2 were amplified using modified fusion primer FLX-28FW and FLX-519RV. DNA Ladder 100bp (Promega). Samples were numbered from 1 to 18. Their origin source has been previously reported in table 40. Sample 2-5-14-17 resulted positive only after performing another PCR increasing DNA template volume from 10 µl to 21 µl and amplification cycles from 35 to 38 (data not shown).

3.2.3.2.2 DNA Quantification

Summer experiment (First seasonal trial June-October 2014)

An amplicon of DNA concentrations was measured using NanoDrop are reported below in (Table. 41).

Table 41. DNA concentration (ng/µl) detected via spectrophotometric method at 260 nm with NanoDropTM 2000/2000 C.

Sample ID	Concentration (ng/µl)
1	34.2
2	21.0
3	31.8
4	96.4
5	18.6
6	90.4
9	102.7
12	51.3

Spring Experiment (Second seasonal trial March-June 2015)

An amplicon of DNA concentrations was measured using the Qubit® 3.0 are reported below in (Table. 42).

Table 42. DNA concentration (ng/µl) detected via a fluorometric method with Qubit® 3.0 fluorometer (Thermo Fisher Scientific).

Sample ID	Concentration (ng/µl)
1	39.0
2	21.0
3	23.0
4	44.4
5	22.0
6	54.5
7	45.5
8	38.0
9	58.0
10	22.0
11	28.6
12	45.0
13	22.0
14	15.0
15	51.0
16	52.0
17	27.5
18	46.0

3.2.3.2.3 Pyrosequencing Analysis

Summer experiment (First seasonal trial June-October 2014)

Pyrosequencing analysis of V1-3 region of the bacterial 16S rRNA gene was successfully performed on eight samples. SILVA taxa analysis carried out referring to SSU (Small Subunit rRNA Database) Ref NR 123 dataset (http://www.arb-silva.de/projects/ssu-ref-nr/). 108394 DNA sequences were read throughout decomposition from the samples of the two chosen carrions combined. 13099 sequences identified as the longest reference sequences of an OTU (Operational Taxonomic Units) with 98% identity threshold. 76313 were clustered, i.e. members of an OTU having <100% identity to OTU reference, 21301 were replicates, i.e. identical OTU member's sequences having 100% identity to OTU reference or OTU member

sequence. In addition, 3424 low-quality sequences including 3421 bad lengths, 1 bad alignment and 2 homopolymers were sorted out during quality control and have not entered classification steps. All read sequences were divided in (Classified) or (No Relative) if no match in the database was found because of too short length or because they were chimeric sequences (Table. 43).

Spring Experiment (Second seasonal trial March-June 2015)

Pyrosequencing analysis of V1-3 region of bacterial 16S rRNA gene successfully performed on 18 samples. SILVA taxa analysis carried out referring to SSU Ref NR 123 dataset (http://www.arb-silva.de/projects/ssu-ref-nr/).86562 DNA sequences read throughout decomposition from the samples of the two chosen carrions combined and 13690 sequences identified as the longest reference sequences of an OTU (Operational Taxonomic Units) with 98% identity threshold. 58744 were clustered, i.e. members of an OTU having <100% identity to OTU reference, 7552 were replicates, i.e. identical OTU member's sequences having 100% identity to OTU reference or OTU member sequence. In addition, 6576 low-quality sequences including 6548 bad lengths, 15 bad alignment identity, 8 bad alignment quality, 3 ambiguous and 2 homopolymers were sorted out during quality control and have not entered classification steps. All read sequences divided in (Classified) or (No Relative) if no match in the database was found because of too short length or because they were chimeric sequences. Low-quality sequences have not entered classification step Classified No Relative (Table. 44).

Table 43. Analysis results. The final status of sequences. A number of reads classified as a reference, clustered, replicate and low quality shown. Data refer both to total project and to each sample. ID sample is the same as listed in table 39.

sample ID	total no. of reads	reference	% of total reads	clustered	% of total reads	replicate	% of total reads	low quality	% of total reads
Total project	108394	13099	12.08	76313	70.40	15558	14.35	3424	3.16
1	16095	954	5.9	12561	78.0	2523	15.7	57	0.4
2	14600	1751	12.0	10958	75.1	1686	11.6	205	1.4
3	13940	770	5.5	10179	73.0	2819	20.2	172	1.2
4	17804	1558	8.8	12109	68.0	3933	22.1	204	1.2
5	7051	605	8.6	3441	48.8	423	6.0	2582	36.6
6	13018	1300	10.0	8747	67.2	2849	21.9	122	0.9
9	12695	3575	28.2	8385	66.1	685	5.4	50	0.4
12	13191	2586	19.6	9933	75.3	640	4.9	32	0.2

Table 44. Analysis results. The final status of sequences. A number of reads classified as a reference, clustered, replicate and low quality shown. Data refer both to total project and to each sample. ID sample is the as same listed in Table. 40.

sample ID	total no. of reads	reference	% of total reads	clustered	% of total reads	replicate	% of total reads	low quality	% of total reads
Total project	86562	13690	15.8	58744	67.9	7552	8.7	6576	7.6
1	5534	541	9.8	4139	74.8	463	8.4	391	7.1
2	4657	546	11.7	3426	73.6	539	11.6	146	3.1
3	4505	839	18.6	3375	74.9	257	5.7	34	0.8
4	4248	381	9.0	3287	77.4	559	13.2	21	0.5
5	6381	618	9.7	3953	62.0	445	7.0	1365	21.4
6	4575	1217	26.6	3039	66.4	249	5.4	70	1.5
7	4647	715	15.4	3506	75.5	393	8.5	33	0.7
8	4909	913	18.6	3316	67.6	217	4.4	463	9.4
9	4855	1349	27.8	3105	64.0	377	7.8	24	0.5
10	5300	638	12.0	3312	62.5	672	12.7	678	12.8
11	3801	553	14.6	2543	66.9	211	5.6	494	13.0
12	4526	764	16.9	2997	66.2	237	5.2	528	11.7
13	4810	525	10.9	3402	70.7	856	17.8	27	0.6
14	6194	1084	17.5	2803	45.3	148	2.4	2159	34.9
15	4385	965	22.0	3059	69.8	284	6.5	77	1.8
16	4914	470	9.6	3547	72.2	880	17.9	17	0.4
17	4461	436	9.8	3370	75.5	635	14.2	20	0.5
18	3860	1136	29.4	2565	66.5	130	3.4	29	0.8

3.2.3.3 Microbial Community Classification

3.2.3.3.1 Phylum Level Analysis

Summer season 2014 experiment

Looking at the phylum level, there was a significant difference in taxon relative abundance of bacterial communities among active decay stage (135.60 ADD) and body region. Four main phyla of bacterial communities were found among the analysed carrion samples throughout decomposition using 454-pyrosequencing. The Phylum relative abundance of these four groups was calculated regardless of cadavers' condition (NF or F) and body regions. The phyla represented higher than 2% of the total of the relative abundance were included, Proteobacteria was the dominant phylum (67%), followed by Firmicutes (16%), Bacteriodetes (12%), and Actinobacteria (5%). Whereas, the phyla which presented less than 2% (Rare taxa) accounted for 1 % of the total relative abundance across active decay stage of the decomposition (Fig. 62).
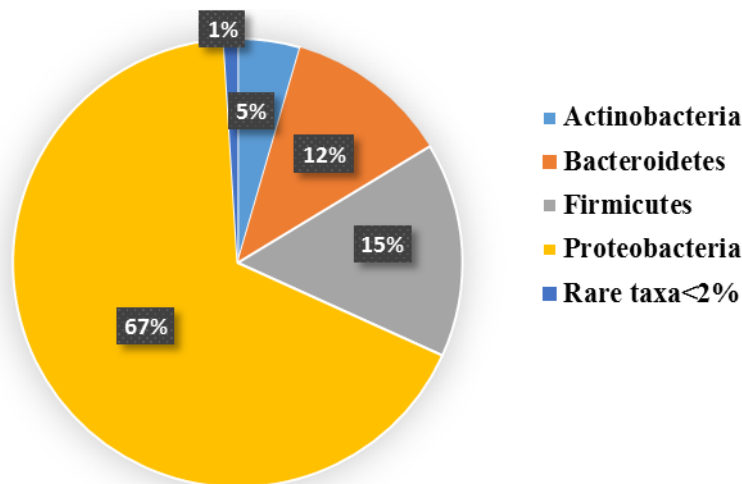
Figure 62. Bacterial community-relative abundance at a phylum taxonomic level with rare taxa at <2 %. Relative abundance on decomposing rabbit carcasses over active decay (ADD 135.60).

The effect of fur was investigated as a factor affecting the post-mortem microbial communities as follows; first, potential differences in post-mortem microbial communities were observed according to the absence or the presence of the fur. The analysis results of studied body regions were combined aiming to compare between with fur and without fur carrions during the active decay stage. The Pattern distribution among the four main phyla was kept as previously

162

described only in F condition, Proteobacteria was the most abundant phylum (71%). The second most abundant bacterial group was constituted of Firmicutes (18%) followed by Bacteroidetes (6%) and the less abundant group was Actinobacteria (5%). Whereas in NF condition the most dominant phylum was Proteobacteria (63%), followed by Bacteroidetes (18%), Firmicutes (13%) and Actinobacteria (5%) (Fig. 63). The results of this analysis showed that there was no significant difference between bacterial communities' distribution between F and NF conditions at phylum level in the same stage of the decomposition (X^2 = 7.279, df =4, p=0.121).

Figure 63. Absolute effect of the fur on post-mortem bacterial communities' distribution at phylum taxonomic level. Condition (NF) refers to carrions without fur, (F) refers to carrion with fur, and both were analysed for active decay stage, at ADD (135.60).

The comparison between the bacterial communities' distribution depending on the body region during the active decay stage of the carrions decomposition showed the almost absence of Actinobacteria in the oral cavity and the interface-sand-carrion regions. This taxon appeared only in skin samples (Fig. 65). Proteobacteria was the most abundant taxon in all the three-body regions oral cavity, skin and interface-sand samples with (66%, 55% and 81%) respectively. In the oral cavity, Bacteroidetes was the second phylum (18%) followed by Firmicutes (16%).

On the contrary, in the interface-sand-carrion samples, Firmicutes was the second phylum (10%), followed by Bacteroidetes (9%). Firmicutes also was the second abundant phylum in skin samples (21%), followed by Actinobacteria (14%), and Bacteroidetes was presented in a

163

relatively low level (9%) (Fig. 64). The statistical analysis result showed difference in bacterial communities' distribution pattern at the phylum level between body regions ($X^2 = 51.082$, df $=8$, p=0.000).
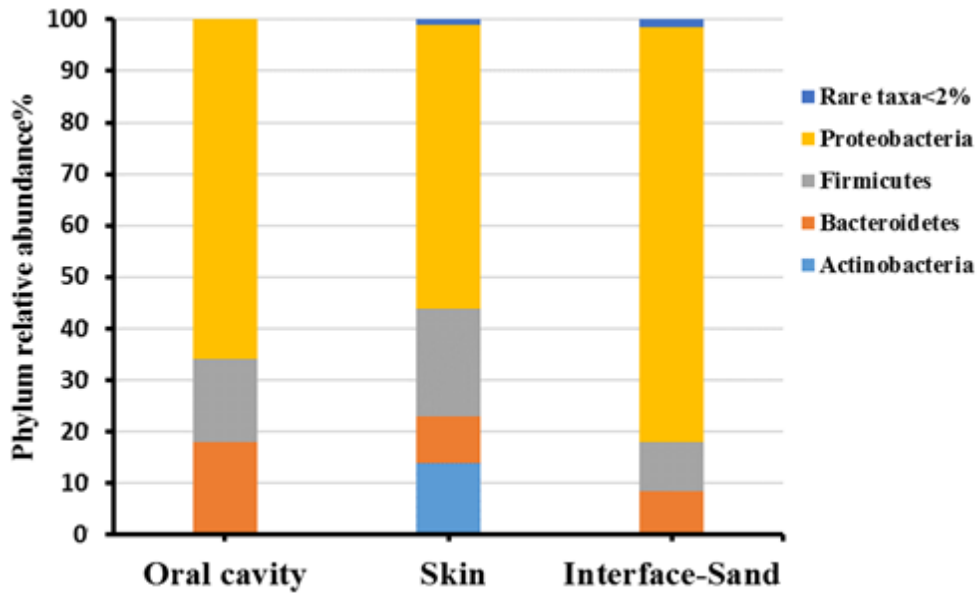
Figure 64. Phylum relative abundance during active decay stage, clusterisation is shown depending on the body region in carrions with and without fur, which was considered together in each region

Furthermore, two combined conditions were analysed in order to evaluate the effect of the humidity and the environment outside the carrions bacterial distribution. In the first case, relative abundances of phyla detected in the oral cavity and interface-sand-carrions samples were considered together as wet environment condition. They were then compared to the relative abundance of the same phyla found in skin samples renamed as a dry environment condition (Fig. 65). While in the second case the relative abundances of phyla detected in oral cavity were renamed as an Internal region, which was compared to the relative abundance of the same phyla found in skin and interface-sand-carrions samples that were considered together as an External region (Figs. 67, 68).

The results showed that a high degree of humidity negatively affected Actinobacteria development in a context such as animal decomposition, especially during active decay stage. On the contrary. The presence of the fur does not seem to affect phyla distribution within the same decomposition stage. There was no difference found between bacteria distribution colonising the carrions F and NF conditions at the phylum level, whereas, humidity (=water content) could cause the absence of some phyla within the same season (Fig. 65).

164

The statistical analysis result showed significant differences of the phylum relative abundance between wet and dry conditions over the decomposition process (X² = 18.845, df =4, p=0.000) (Fig. 66).
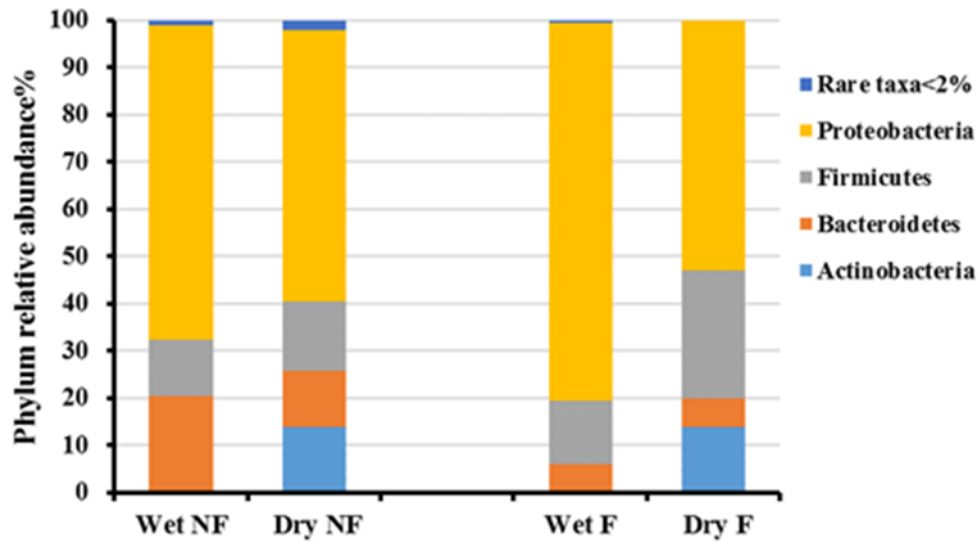
Figure 65. Humidity effect on phylum relative abundance. Phylum relative abundance clusterisation shown depending on both body region and the presence of the fur. Condition (NF) refers to carrions without fur condition, (F) refers to carrion with fur. Wet environment= bacteria developed in the oral cavity and under the carrions at the interface. Dry environment= bacteria developed in the skin.
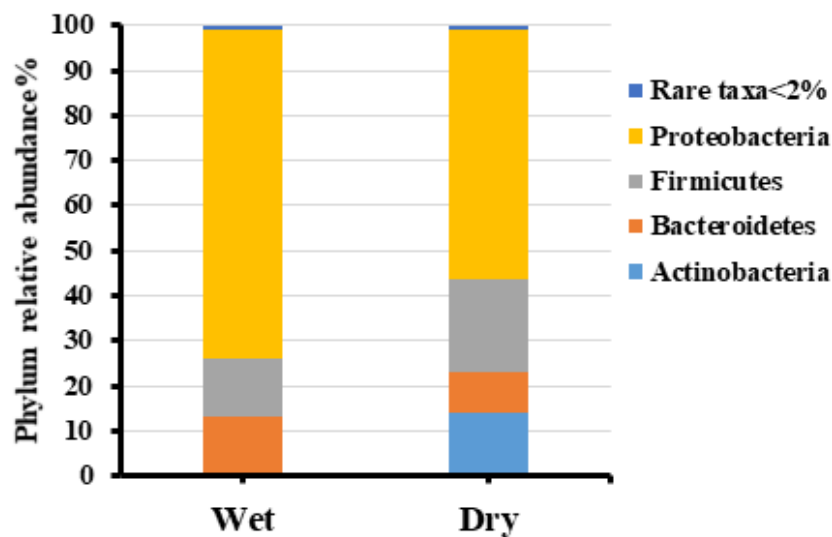
Figure 66. Humidity effect on phylum relative abundance. Phylum relative abundance clusterisation shown depending on the environmental condition. Wet environment= bacteria developed in the oral cavity and under the carrions at the interface-sand. Dry environment= bacteria developed in the skin.

In order to investigate the environment influence on the bacterial communities' development on decomposing animal carrions during the active decay, in the sample of carrions with fur

Proteobacteria was the most abundant phylum in both internal and external conditions with (78%), (53%) respectively. In NF conditions. Proteobacteria was also the most abundant phylum in internal and external samples with (54%), (58%) respectively.

Internal NF samples contain (22%) of Firmicutes, which is 7% more than the percentage of Firmicutes developed outside of the same animal (15%). On the contrary, in F condition Firmicutes were (27%) in external, whereas, were (10%) in internal samples. Bacteroidetes were 24%, 12% in NF and F in internal condition samples respectively, whereas, in an external condition, Bacteroidetes were decreased in NF and F to 12% and 6% respectively. A different phyla distribution pattern was observed during the active decay due to the condition of samples. Actinobacteria were found to colonise only the external body region of the animals with and without fur with (12% each) (Fig. 67).

The results showed that the environmental conditions could have important effects on the presence of some bacterial communities in places that exposed to the environment conditions (Skin+ interface-sand-carrion) than others. Statistical analysis showed significant differences between internal and external environment Phylum relative abundance during the decomposition stages ($X^2 = 19.49$, df =4, p=0.000) (Fig 68).
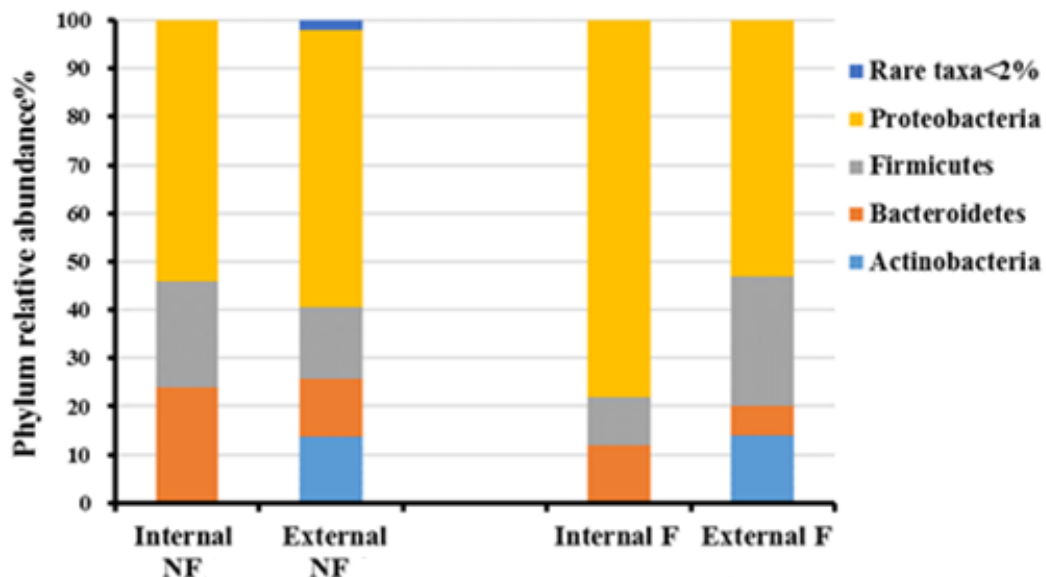
Figure 67. Environment effect on phylum relative abundance. Phylum relative abundance clusterisation shown depending on both body region and the presence of the fur. Condition (NF) refers to carrions without fur condition, (F) refers to carrion with fur. Internal region = bacteria developed in the oral cavity. External region = bacteria developed on the skin and under the carcasses at the interface with sand.

166
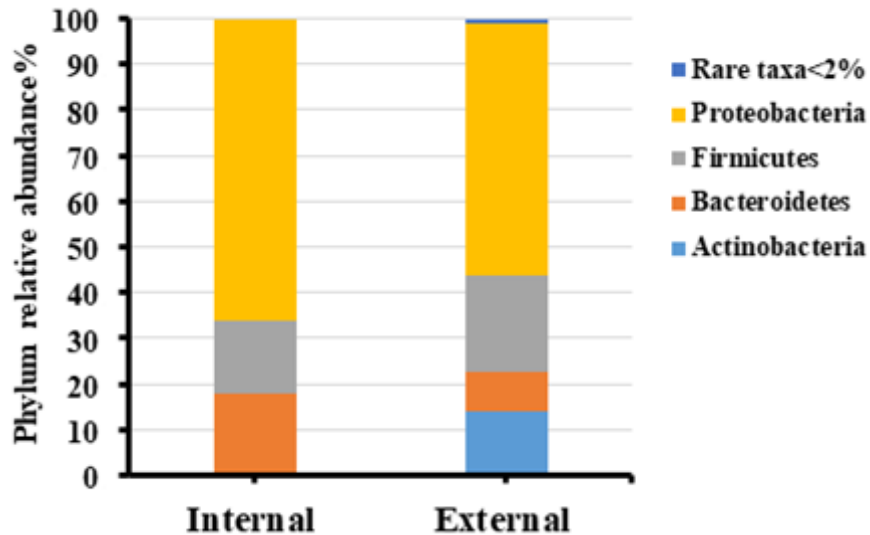
Figure 68. Average of phylum relative abundance clusterisation shown depending on the body region. Internal region = bacteria developed in the oral cavity. External region = bacteria developed on the skin and under the carcasses at the interface with sand.

Also, for more information about the changes in microbial community distribution during the decomposition stages. Two samples from the interface-sand-carrion for both F and NF conditions at the end of the decomposition process (dry remains stage) were analysed to compare with the same location samples in the early stage of the decomposition process (Active decay stage) (Fig. 69). The results showed significant differences in the distribution pattern of the bacterial communities at the phylum level of each stage samples regardless of fur condition ($X^2 = 89.322$, df =4, p=0.000) (Fig. 70).
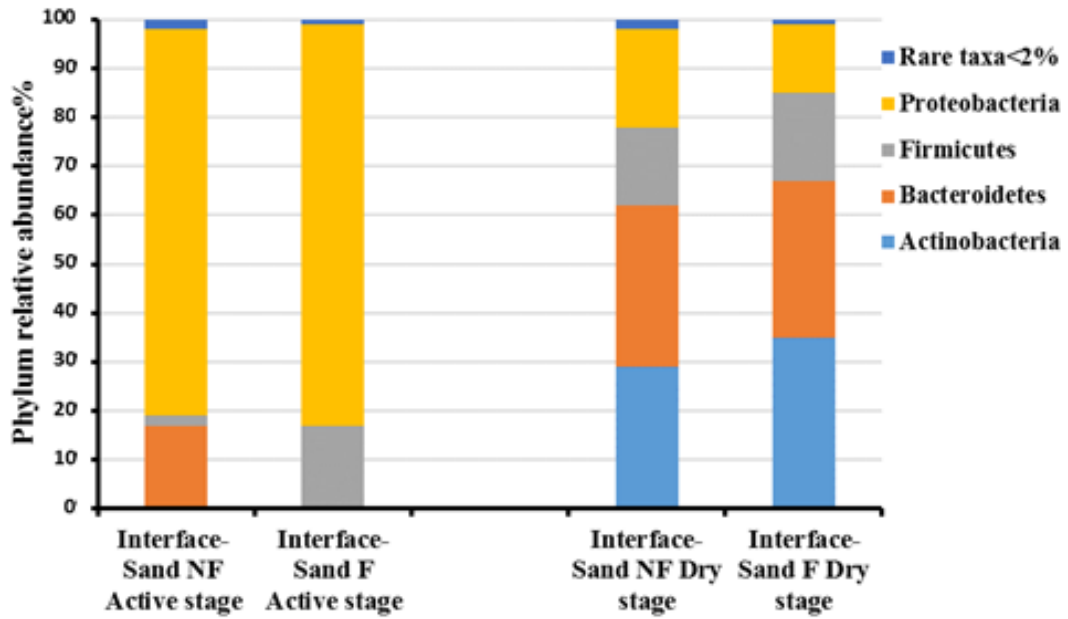
Figure 69. Bacterial communities at the phylum level. Values are shown for interface-sand carrion F and NF samples over active decay (135.6 ADD) and the advanced dry stage of the decomposition (1901.3 ADD).
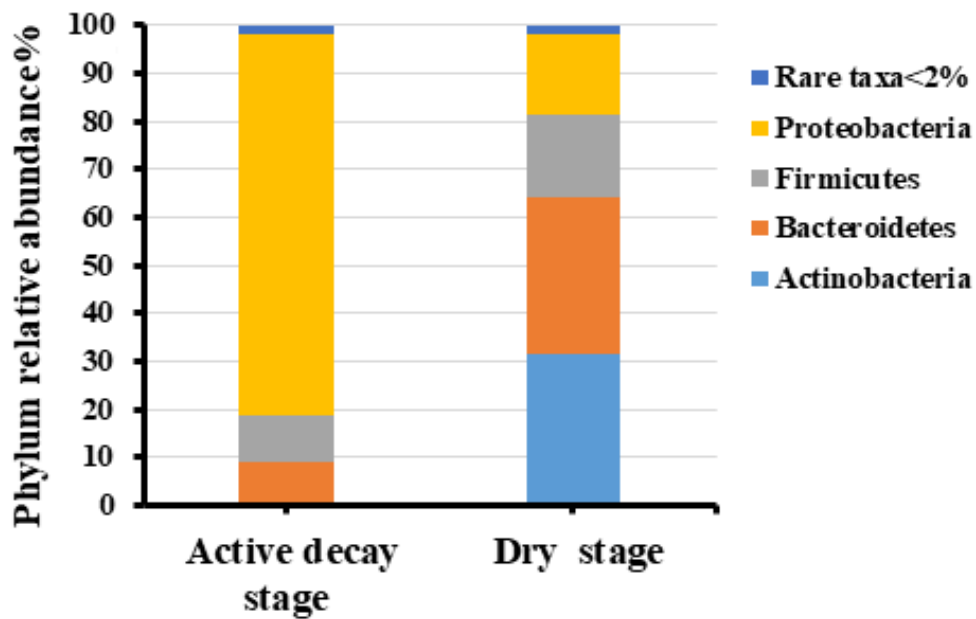
Figure 70. Average of bacterial communities' distribution at phylum level of the interface-sand- carrion samples regardless of F or NF conditions during active decay stage (135.6 ADD) and dry stage (1901.3 ADD).

168

Spring season 2015 experiment

The experiment carried out in spring 2015 and the sampling days were at three main points during the decomposition process, at active decay stage (50.10 ADD), advanced decay stage (294.10 ADD) and dry remains stage (586.30 ADD) as a variation was observed between the stages in the experiment carried out in summer 2014.

The major phyla associated with the cadaver samples detected throughout decomposition process using 454-pyrosequencing were Proteobacteria as the most abundant phylum (43%), Firmicutes (41%) the second abundant phylum, Bacteroidetes (14%) and Actinobacteria (3%). These phyla were represented 2% higher than of the total relative abundance, and there were no rare taxa (Fig. 71).
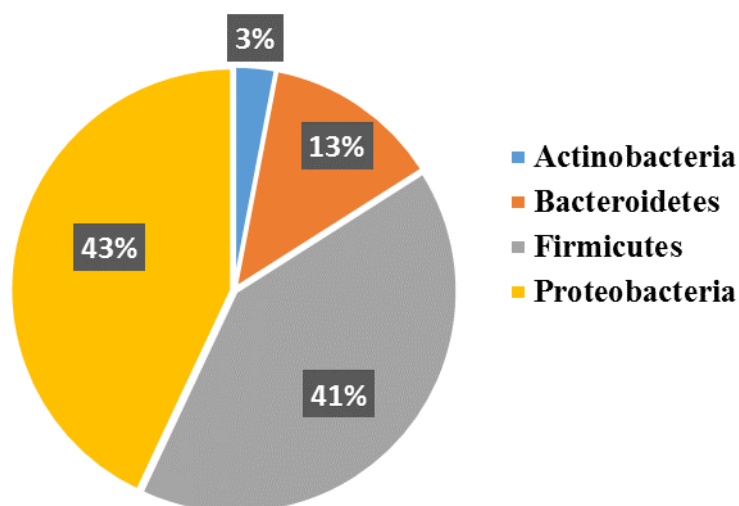
Figure 71. Phylum distribution over the decomposition process during spring 2015 experiment.

The effect of fur on the phylum distribution during the carrions decomposition process was investigated, (Fig. 72) and the statistical analysis showed no difference due to the presence or absence of the fur was found (X^2 = 8.284, df =4, p=0.081).
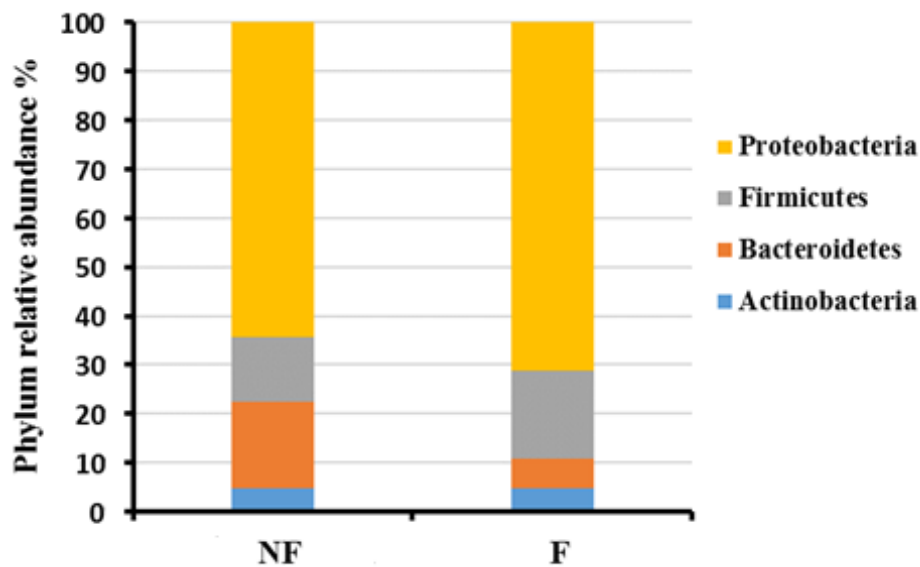
169
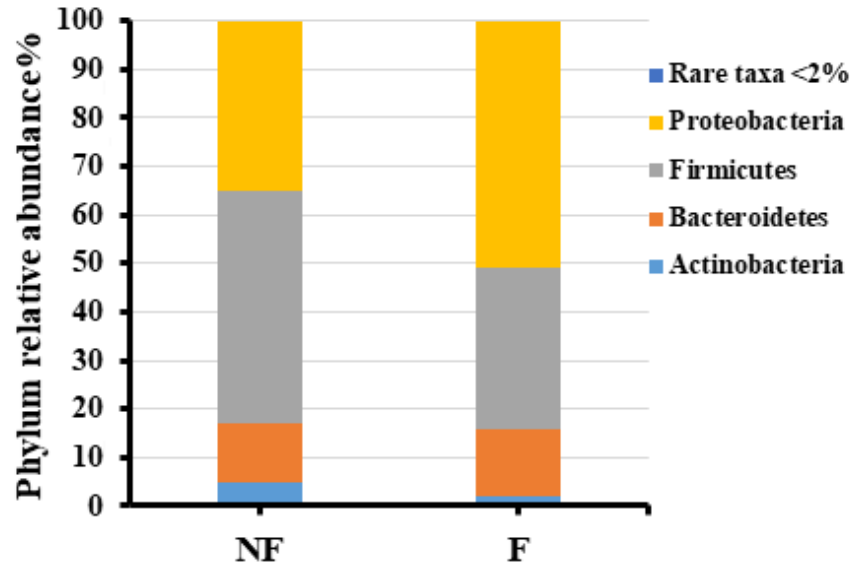
Figure 72. Absolute effect of the fur on post-mortem bacterial communities' distribution at phylum taxonomic level. Condition (NF) refers to carrions without fur, (F) refers to carrion with fur.

Figure (73) shows the phylum relative abundance of these four groups regardless of the carrions conditions (F or NF) and body region. All the other minority taxa were represented less than 2% of the total were considered as rare taxa. During the active decay stage of the decomposition, Proteobacteria was the most abundant phylum (68%), followed by Firmicutes (16%), Bacteriodetes (9%), and Actinobacteria (6%). Whereas over the advanced decay stage Actinobacteria was absent, Firmicutes increased to be the most abundant phylum (40%), followed by Proteobacteria (38%), and Bacteroidetes slightly increased to (11%). During the dry remains stage of the decomposition. Actinobacteria represented with low level (3%), Firmicutes still the most abundant phylum (66%), Proteobacteria decreased (16%) than the previous stage, but still the second abundant phylum and Bacteroidetes decreased to (8%).

There was a difference in the bacterial communities' distribution at phylum level among decomposition stages. Proteobacteria was the most abundant phylum at the earliest stage of the decomposition and then decreased over the decomposition process to the lowest level at the last stage. On the contrary. Firmicutes increased over the decomposition process to be the most abundant phylum at the last stage of the decomposition. In addition, Actinobacteria which was completely absent in advanced decay. The statistical analysis showed significant differences in the bacterial communities' distribution at the phylum level during the decomposition stages $(X^2 = 71.684, df = 8, p=0.000)$ (Fig. 73).
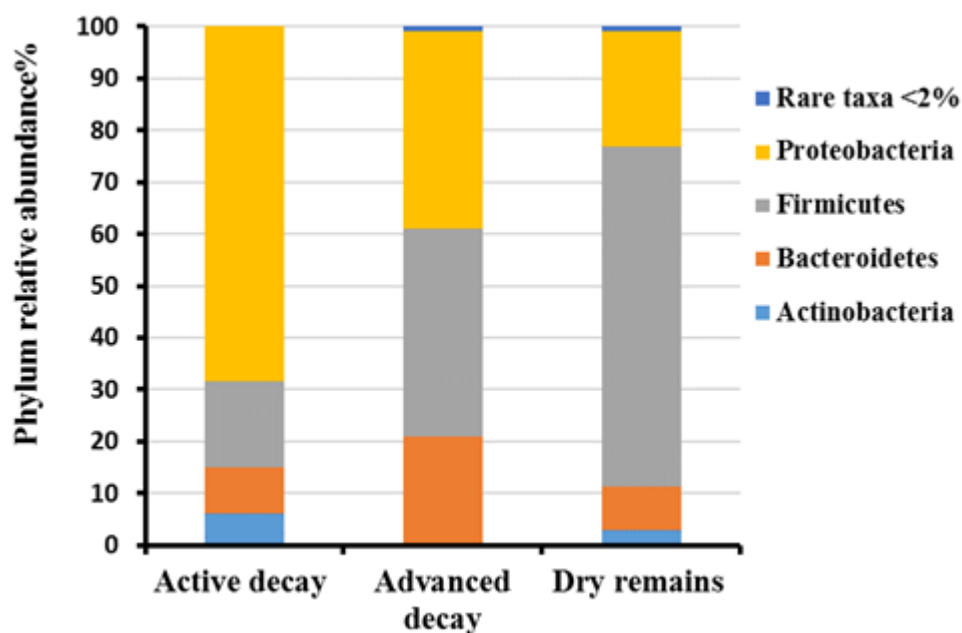
Figure 73. Post-mortem bacterial communities' distribution at phylum level was analysed for active decay stage, at ADD 50.10, advanced decay stage; ADD 294.10 and dry remain stage; ADD 586.30.

The effect of fur was investigated as a factor affecting the post-mortem microbial communities as follows; first, potential differences in post-mortem microbial communities were observed according to the absence or the presence of the fur. Pattern distribution among the four main phyla was kept as previously described only in NF condition. During the active decay actually, the dominant phylum was Proteobacteria (66%), followed by Firmicutes (17%). Bacteroidetes (9%) and Actinobacteria (8%) (Fig. 74). In F condition, Proteobacteria remained the most abundant phylum (71%); Firmicutes was the second most abundant bacterial group (16%), followed by Bacteroidetes (9%). The lowest level abundant group remained Actinobacteria (4%). On the other hand, during the advanced decay stage Actinobacteria was absent in both NF and F conditions.

The most abundant bacterial group on NF condition samples was Firmicutes (59%) followed by Proteobacteria (23%), and Bacteroidetes (17%). Whereas, in F condition samples, Proteobacteria was slightly decreased but it is still the most abundant phylum (53%), followed by Bacteroidetes (25%) and Firmicutes (21%). During the dry remains stage, Firmicutes was the most abundant bacterial group in both NF and in F conditions 68% and 63% respectively. Proteobacteria was the second abundant bacterial group also on both NF and F conditions (28%), (17%) respectively, followed by Bacteroidetes 9% and 8% in NF and F samples respectively. In addition, Actinobacteria were present only in NF samples (6%) (Fig. 74).

The Results showed that the fur does not affect the phylum distribution within the same stage except at dry stage where the Actinobacteria was found only in NF condition.
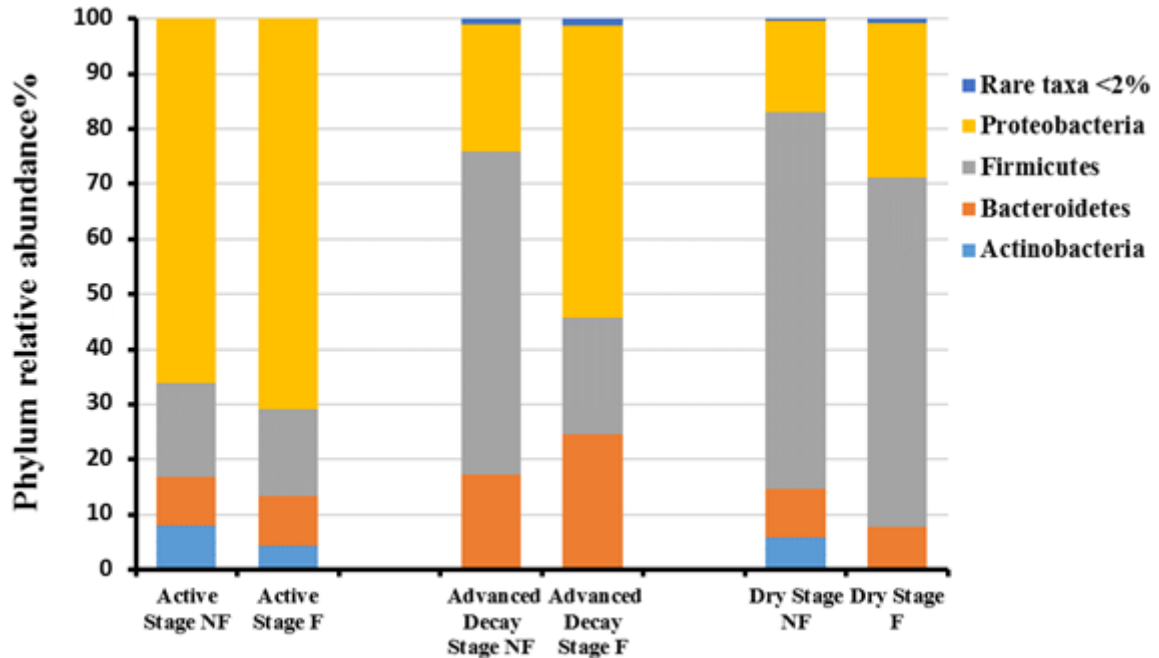
Figure 74. Absolute effect of the fur on post-mortem bacterial communities' distribution at phylum taxonomic level. Condition (NF) refers to carrions without fur. Condition (F) refers to carrion with fur was analysed at Active decay, advanced decay and Dry stage.

The phyla relative abundance was analysed in order to detect potential differences depending on the three different body regions keeping the two basic conditions of analysis (without and with fur) during the decomposition stages. The first noticed observation was the total or almost total absence of Actinobacteria in the oral cavity at all stages of the decomposition and in samples of the skin and interface between sand and carrions in F samples during the dry stage. There was a difference in phylum distribution with the presence of the fur among carrions during the initial phase of the decomposition process (Figs. 75, 76). Results showed that the fur does not significantly affect the phylum distribution within the same body region.
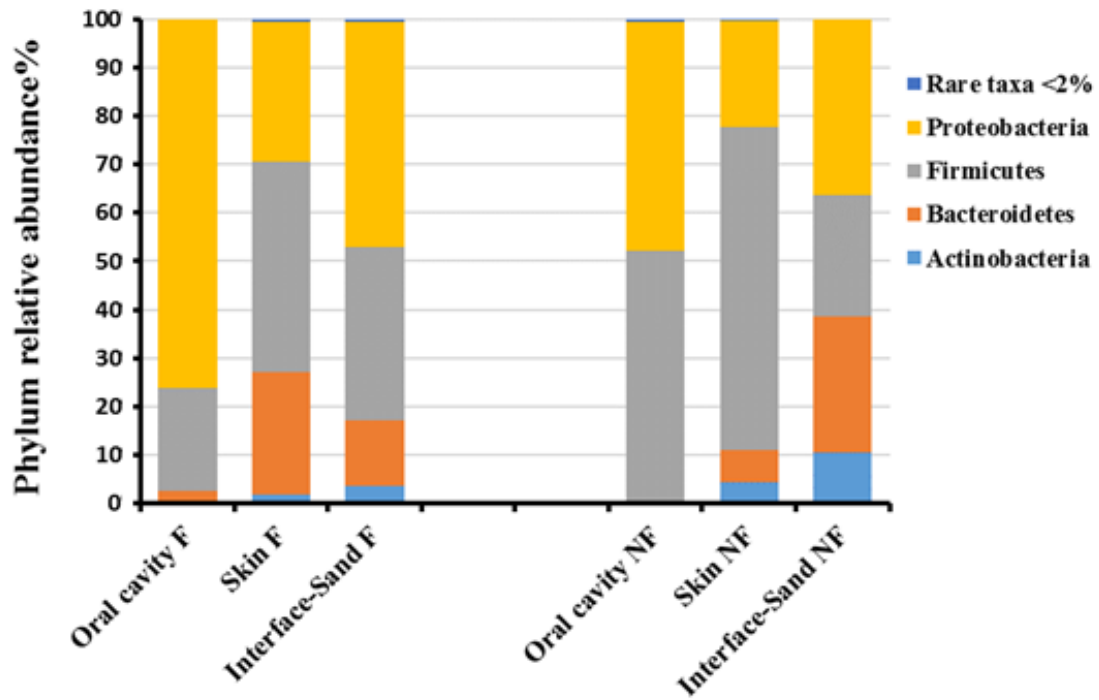
Figure 75. Effect of the fur on different body regions' microbial communities during the decomposition process. Phylum relative abundance clusterisation shown depending on both body region and the presence of the fur. (NF) refers to carrions without fur condition; (F) refers to the condition of carrions with and without fur.

The inter-seasonal comparison between the bacterial communities' distribution depending on the body regions during the decomposition stages of the carrions showed that Proteobacteria was the most abundant taxon in oral cavity and interface-sand- carrion regions with 62% and 42% respectively. Firmicutes followed as second abundant phylum with 37% and 30% respectively. While in skin region, Firmicutes was the most abundant taxon (55%), followed by Proteobacteria (25%). On the other hand, Bacteroidetes and Actinobacteria were represented only on the skin and interface-sand-carrion regions with 16%, 21% and 3% and 7% respectively (Fig. 76). The statistical analysis showed a significant difference in bacterial communities' distribution between body regions at phylum level ($X^2 = 52.047$, df =8, p=0.000).
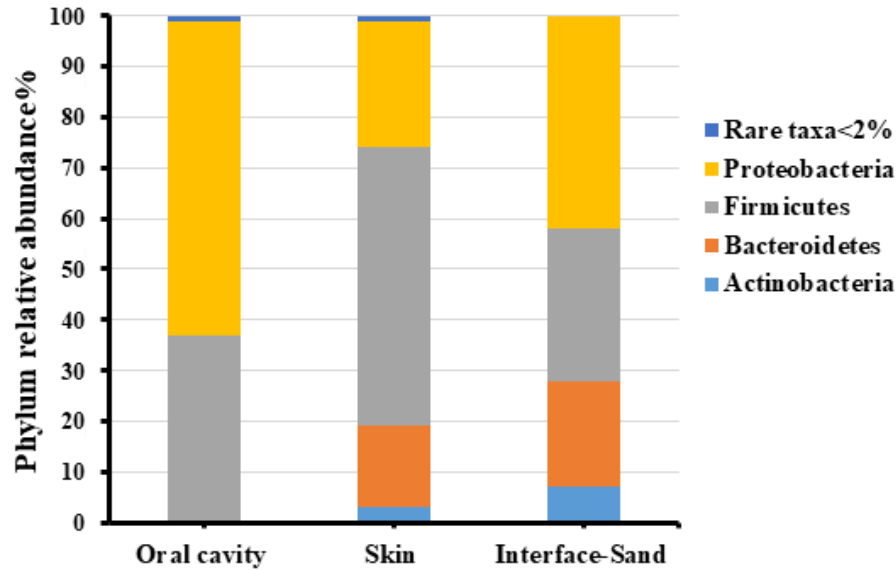
Figure 76. Phylum relative abundance during the decomposition stages clusterisation is shown depending on the body region of carrions with and without fur, which was considered to gather in each region.

In oral cavity samples, Proteobacteria was the most abundant taxon with (100%) over the active decay stage in both F and NF samples, there were not any other phyla presented. During the advanced decay stage, Proteobacteria decreased to (82%), and it remains the most abundant phylum in F samples, followed by Firmicutes by (18%). In contrast, Proteobacteria showed a significant reduction to 22% in NF samples with Firmicutes phylum being the most abundant (78%). However, in dry remains stage, Firmicutes phylum was (61%) still the most abundant in NF, followed by Bacteroidetes (22%), Proteobacteria (10%), and Actinobacteria (7%). While in F samples, Firmicutes and Proteobacteria were the most abundant with 46% and 47% respectively, followed by Bacteroidetes (7%), whereas Actinobacteria were not observed (Fig. 73).

In skin samples, at the active decay stage, the pattern of the distribution of the bacterial communities was converged between F and NF conditions. The most abundant taxon was Firmicutes 41% and 47% in F and NF respectively, followed by Proteobacteria 31% and 35% in F and NF, Bacteroidetes was present with 23% and 15% in F and NF, and Actinobacteria was represented in this region of the body with the lowest level 5% and 2% in F and NF respectively. In contrast, during the advanced decay stage, the pattern of the distribution of the bacterial groups was different in F and NF samples. Phyla presented in F samples were converged as following: Bacteroidetes (37%), Proteobacteria (34%) and Firmicutes (27%), and Actinobacteria was absence. In contrast to NF samples, Firmicutes was the most abundant

174

bacterial group with (89%), Proteobacteria (10%). Over the dry remains stage in F samples, Firmicutes was the most abundant with (61%), followed by Proteobacteria (21%) and Bacteroidetes (16%). On the other hand, in NF samples Firmicutes was the most abundant (65%), followed by Proteobacteria (20%), Actinobacteria (10%), and Bacteroidetes (5%) (Fig. 77).

In interface sand - carrion samples, Proteobacteria was the most abundant phylum with (82%), (63%) respectively in F and NF at active decay stage, followed by Actinobacteria (8%), (22%), Bacteroidetes (4%), (11%), and Firmicutes was the lower with (6%), (5%). During the advanced decay stage Bacteroidetes was the most abundant phylum with (36%), (52%) respectively in F and NF, followed by Proteobacteria as the second most abundant phylum with (42%), (37%) respectively in F and NF, Firmicutes (18%), (9%), and Actinobacteria was very low with (3%) in both F and NF samples. Whereas, at dry remains stage, the pattern was different; In F samples Firmicutes was the most abundant phylum with (83%), followed by Proteobacteria with (16%). No other phyla were presented. Whereas in NF samples Firmicutes was the most abundant phylum with (65%), followed by Bacteroidetes (22%). Proteobacteria (10%) and Actinobacteria appeared with 7% (Fig. 77).
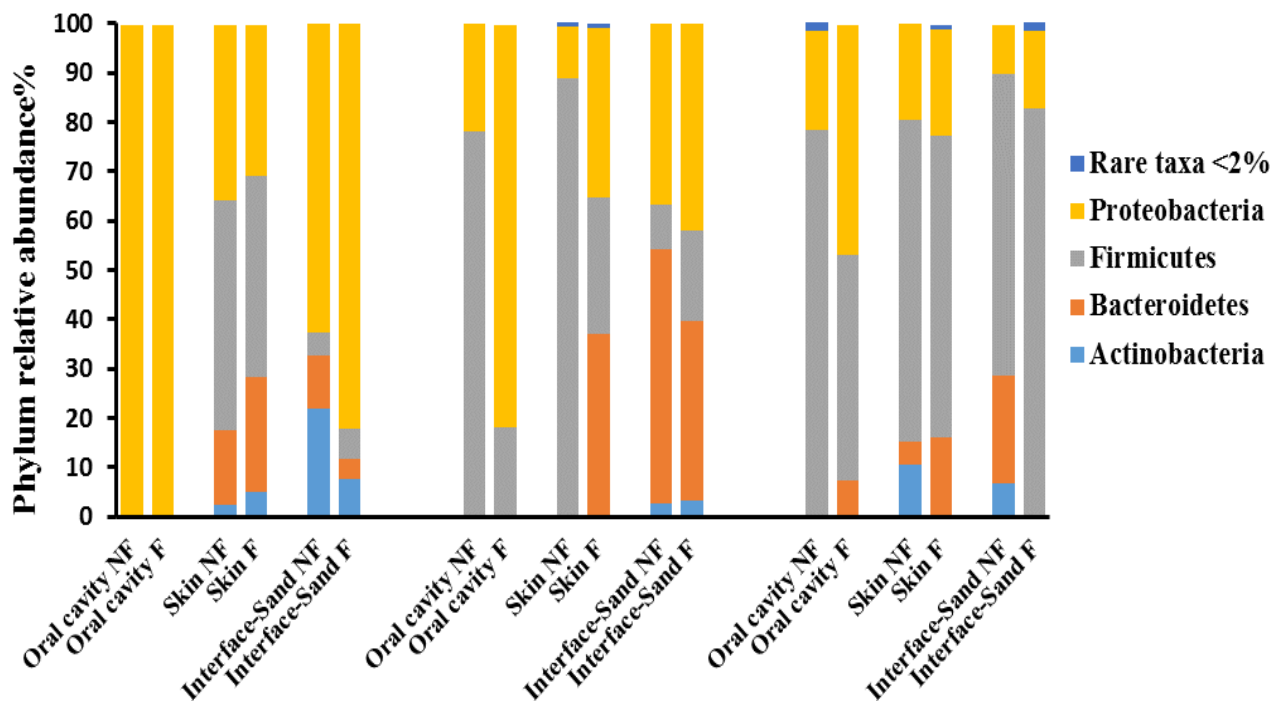
Figure 77. Identification of carcass microbial communities over decomposition using 454-pyrosequencing. The phyletic level taxonomic relative abundance of the microbial communities based on 454-pyrosequencing between two types of carrion with and without fur over decomposition days during 2015. Rare taxa include any phyla with, 2% of the total relative abundance.

In order to evaluate the effect of the humidity on the carrions, the relative abundances of phyla detected in the oral cavity and interface-sand-carrions samples were considered together as wet environment condition. They were then compared to the relative abundance of the same phyla found in skin samples which renamed as a dry environment.

The results showed that a high degree of humidity negatively affected Actinobacteria development in a context such as animal decomposition, specifically during advanced decay stage. On the contrary. The presence of the fur in this analysis did not affect phyla distribution within the same decomposition stage in most of the samples. However, there was a little difference was actually found between bacteria distribution colonising the two different types of carrions at advanced decay stage in dry samples Bacteroidetes phyla were absence on NF samples. In addition, at dry stage Actinobacteria only appeared in NF samples in both wet and dry samples (Fig. 78). The statistical analysis of the bacterial communities' distribution of wet and dry conditions during the decomposition process showed significant differences (Fig. 79) ($X^2 = 15.344$, df =4, p=0.004).
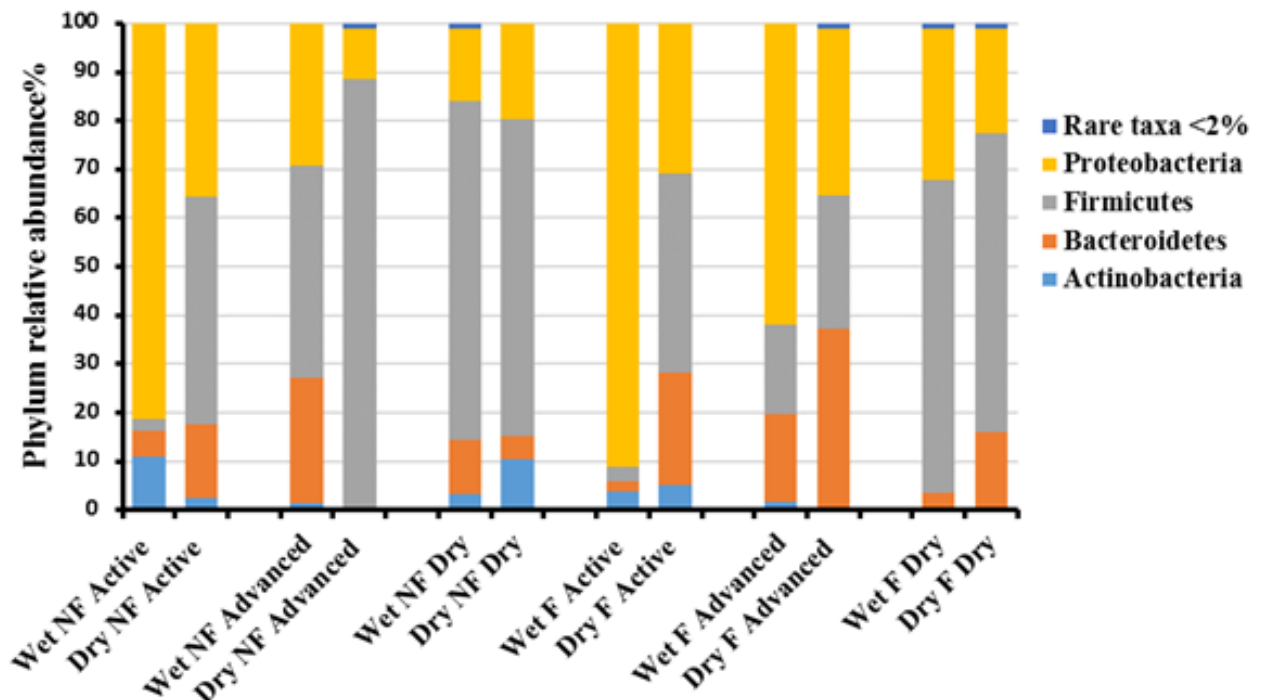
Figure 78. Humidity effect on phylum relative abundance. Phylum relative abundance clusterisation shown depending on both body region and the presence of the fur. Condition (NF) refers to carrions without fur condition, (F) refers to carrion with fur. Wet environment= bacteria developed in the oral cavity and under the carrions at the interface with sand. Dry environment= bacteria developed on the skin air exposed.
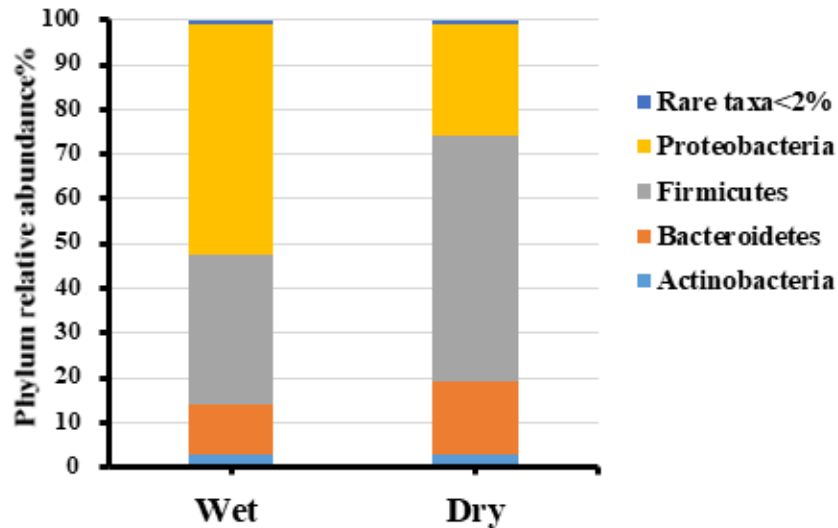
Figure 79. Humidity effect on phylum relative abundance. Phylum relative abundance clusterisation shown depending on the environmental conditions. Wet environment= bacteria developed in the oral cavity and under the carrions at the interface with sand. Dry environment= bacteria developed on the skin air exposed.

Furthermore, environmental conditions were analysed in order to evaluate the effect of the environment outside the carrions on the microbial communities. The relative abundances of phyla detected in the oral cavity, renamed as an internal region condition, were compared to the relative abundance of the same phyla found in skin and interface-sand-carrions samples, which were considered together as external region condition (Fig. 80).

Considering the environment influence on the bacterial communities' development on decomposing animal carrions during the active decay Proteobacteria were the most abundant phylum in both internal and external conditions in F and NF samples, it was (100% each) for the internal condition and (49%), (56 %) respectively in F and NF. External NF samples contain also (26%) of Firmicutes which were absent in the internal of the same animal. Bacteroidetes (13%) and Actinobacteria (12%). In external F condition, the pattern was the same where Firmicutes was (24%), Bacteroidetes (14%) and Actinobacteria (6%) (Fig. 80).

On the other hand, during the advanced decay stage, the pattern was completely different. In the internal condition of NF samples, Firmicutes were the most abundant phylum (78%), followed by Proteobacteria (22%), whereas, in the internal condition in F samples, Proteobacteria were the most abundant phylum (82%) and Firmicutes the second (18%). On the contrary, on external condition of NF samples Firmicutes were still the most abundant phylum (49%), followed by Bacteroidetes (26%), and Proteobacteria (24%), whereas, in external

condition of F samples Proteobacteria also were still the most abundant phylum (56%), followed by Firmicutes (24%). Bacteroidetes (14%) and Actinobacteria (6%) (Fig. 80).

During the dry stage, the microbial communities' distribution showed that Actinobacteria was presented only in external NF dry samples (9%). Firmicutes was the most abundant phylum in internal and external NF samples with 78% and 63% respectively, followed by Proteobacteria (20%) in internal condition. Whereas, in an external condition, Proteobacteria were the second phylum (15%), followed by Bacteroidetes (13%). On the other hand, in F samples in an internal condition, Proteobacteria and Firmicutes were the most abundant phylum with (47%), (46%) respectively, followed by Bacteroidetes (7%). Whereas in external condition Firmicutes were the most abundant phylum with (72%), followed by Proteobacteria (20%), and Bacteroidetes (8%) (Fig. 80).

A different phyla distribution pattern was observed during the decomposition stages due to the condition of samples. Actinobacteria were found to colonise only the external body region of the animals with and without fur with different values. The statistical analysis of the internal and external bacterial community distribution during the decomposition stages showed significant differences ($X^2 = 30.513$, df $=4$, p=0.000) (Fig. 81).

Figure 80. Environment effect on phylum relative abundance. Phylum relative abundance clusterisation shown depending on both body region and the presence of the fur. Condition (NF) refers to carrions without fur condition, (F) refers to carrion with fur Internal region= bacteria developed in the oral cavity. External region= bacteria developed on the skin and under the carcasses at the interface with sand.
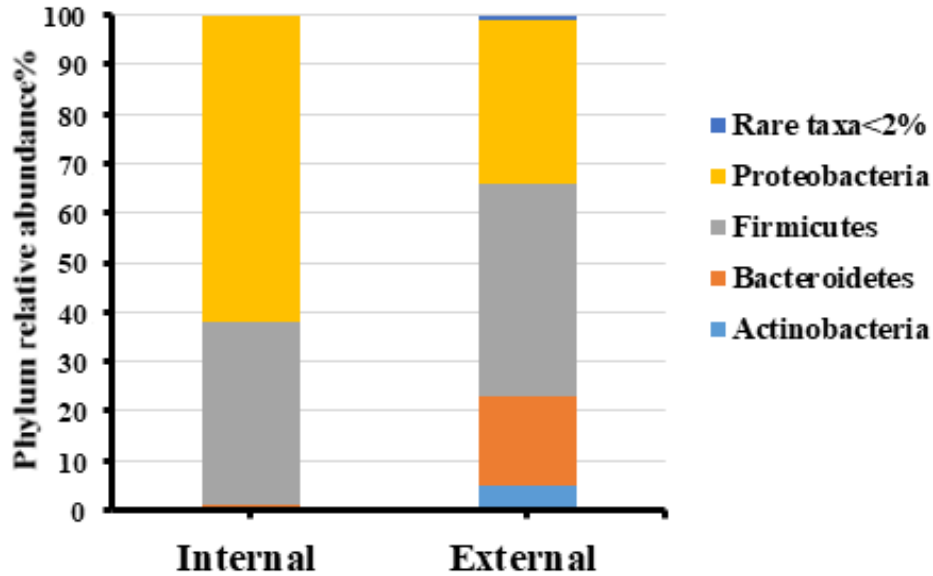
Figure 81. Environment effect on phylum relative abundance. Phylum relative abundance clusterisation shown depending on the regions. Internal region= bacteria developed in the oral cavity. External region= bacteria developed on the skin and under the carcasses at the interface with sand.

3.2.3.3.2 Family Level Analysis

Summer season 2014 experiment

Over the active decay stage, the 11 most abundant taxonomic families associated with the carrion samples detected using 454-pyrosequencing were Xanthomonadaceae (24%), Pseudomonadaceae (20%), Enterobacteriaceae (12%), Planococcaceae, Flavobacteriaceae (11% each) Moraxellaceae (6%), Enterococcaceae, (4%), and Brevibacteriaceae (2%). Rare taxa taken together represented the 10% out of the total (Fig. 82).

However, the distribution of the families during the decomposition stages showed Xanthomonadaceae (20%), Flavobacteriaceae (18%), Enterobacteriaceae (11%), Pseudomonadaceae (10%), Moraxellaceae (7%), Planococcaceae (6%), Sphingobacteriaceae (4%), Enterococcaceae, Microbacteriaceae, and Brevibacteriaceae (3% each) and Staphylococcaceae (2%). In addition, the rare taxa were accounted (13%) of the total (Fig. 83).

179
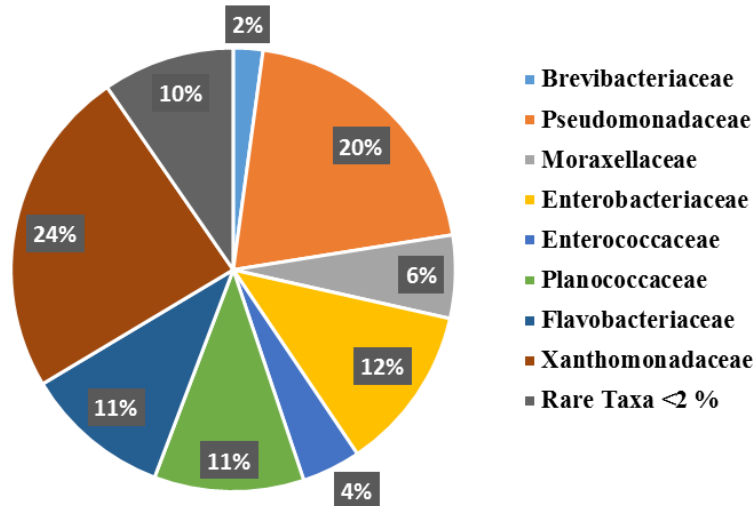
Figure 82. Families' distribution over the active decay of the decomposition process. Taxonomic groups including families presented higher than 2% and other groups considered as rare taxa. Each one of them represented less than 2% of the total.
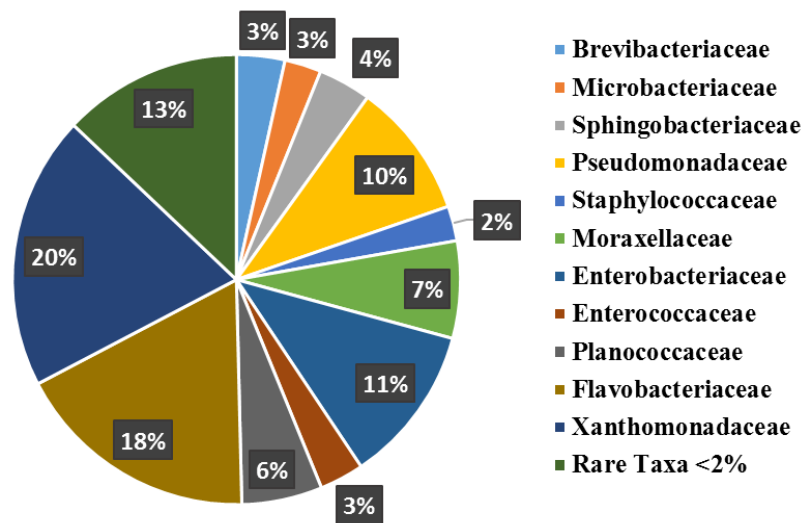
Figure 83. Families' distribution over the decomposition process (active decay with two samples of the interface-sand-carrion from the dry stage).

The effect of the fur was investigated as a factor affecting the post-mortem microbial communities as follows; firstly, investigating any potential differences resulting from the absence (NF) or presence (F) of the fur.

By observing the microbial communities' growth on the carrions within the same decomposition stage, four bacterial families were predominantly noted. During this analysis,

body region samples were considered together as part of a unique sampling. Over the active decay in NF samples, the most dominant families were Xanthomonadacee (32%), followed by Flavobacteriaceae (13 %), Planococcaceae and Enterobacteriaceae (11% each), Moraxellaceae (7%), Enterococcaceae and Pseudomonadaceae (4% each), Bacteroidaceae (3%), and Sphingobacteriaceae, Brevibacteriaceae (2% each). On the other hand, in F samples, Pseudomonadaceae was the most abundant family (34%). The second most abundant bacterial group was Xanthomonadacee (13%), followed by Enterobacteriaceae (12%), Planococcaceae (10%), Flavobacteriaceae (7%), Moraxellaceae (4%), Enterococcaceae (4%), and both Staphylococcaceae and Microbacteriaceae (3% each) and both were almost totally absent over the active decay in NF samples (Fig. 84).

Significant variations in the distribution of bacterial families during this stage in both conditions were noticed. For example, Bacteroidaceae and Enterococcaceae found only in NF, while Microbacteriaceae, Staphylococcaceae, and Sphingobacteriaceae appeared in F during the active decay. In addition, there was an increase in the level of Xanthomonadacee in NF compared to the condition F during the same stage. Furthermore, an increase in the Pseudomonadaceae's level was noted in F comparison to NF. These findings could be a helpful indicator for the estimation of PMI.

The statistical analysis showed significant differences between samples with and without fur at the family level (X^2 = 49.963, df =12, p > 0.05), (Fig. 84).
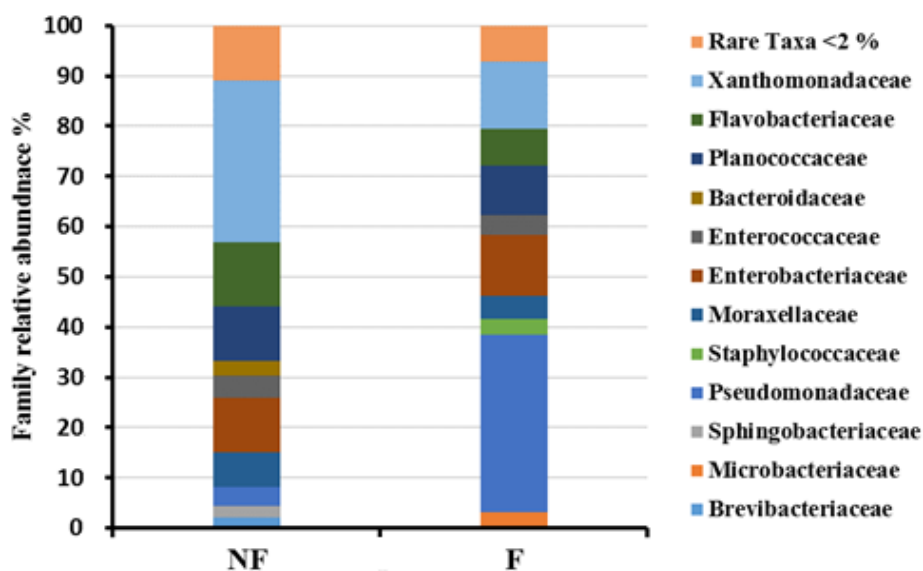
Figure 84. Absolute effect of the fur on microbial communities' distribution at family taxonomic level. During the active decay stage of the decomposition. Family relative abundance clusterisation is shown depending on the presence of the fur. Condition (NF) refers to carrions without fur condition (F) refers to carrion with fur. Rare taxa cut off was at <2 %.

The effect of fur on the family level of bacterial distribution was investigated in three different body regions during the active decay, the oral cavity of the carrion without fur was mainly colonised by Xanthomonadaceae (51%), Flavobaceriaceae (18%), Planococcaceae (18%), and 5.31% of Bacteroidaceae. On the contrary, in the same body region of the carrion with fur, Pseudomonadaceae was the most abundant family (54%), followed by Enterobacteriaceae (16%), Flavobaceriaceae (9%), Planococcaceae (6 %) and Moraxellaceae (6%) (Fig. 85).

At the interface between the sand in carrions without fur (NF), Xanthomonadaceae represented (78%) of the total population of bacteria and Flavobaceriaceae was (17%). On the contrary, in carrion with fur F samples Xanthomonadaceae represented only (13%) out of the total population and Enterobacteriaceae (36%) was the most abundant family, followed by the Moraxellaceae (26%). There was not any substantial difference in families' distribution based on the presence of the fur in the skin samples (Fig. 85).

The comparison among the body regions during the active decay stage showed that the level of Pseudomonadaceae changed dramatically between the body regions. It significantly decreased from (54%) in the oral cavity to (14%) in the skin and to (6%) in the interface- sand samples of carrions with fur. In contrast to carrions without fur, this family present only in the skin samples with (8%) (Fig. 85). Therefore, detection of Pseudomonadaceae could be used as an indicator for PMI estimation.

Active Decay stage day 9 (135.6 ADD)
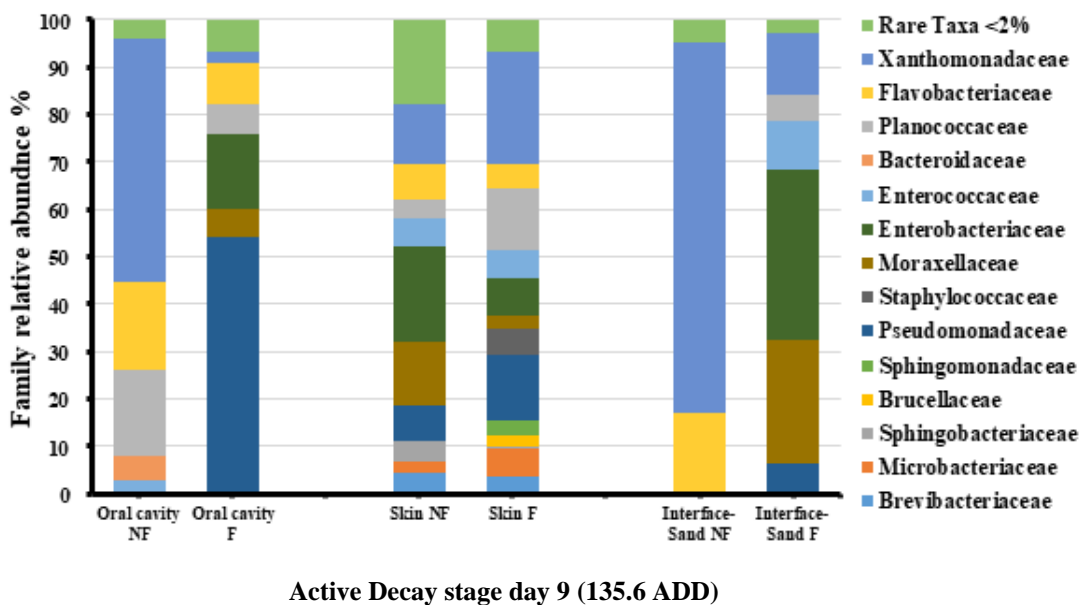
Figure 85. The effect of the fur on different body regions. Family relative abundance clusterisation is shown depending on both body region and the presence of the fur. Condition (NF) refers to carrions without fur condition, (F) refers to carrion with fur. Rare taxa cut off was at <2 %.

By investigating the distribution of families' level depending on the body regions during the active decay stage regardless of carrions condition (with or without fur), the results showed that Xanthomonadaceae was the most abundant in all body regions. Whereas, Bacteroidaceae detected only in oral cavity samples (3%). In addition, Brevibacteriaceae, Microbacteriaceae and Moraxellaceae appeared in the skin samples only. Enterobacteriaceae and Moraxellaceae were variable in different body regions, and their highest values were (18%) and (13%) in interface-sand samples. On the other hand, Planococcaceae and Pseudomonadaceae presented heist values in the oral cavity and much lower values in both the skin and interface samples (Fig. 86). The statistical analysis was performed and the result showed significant differences between body regions (X^2 = 101.712, df =24, p > 0.05).
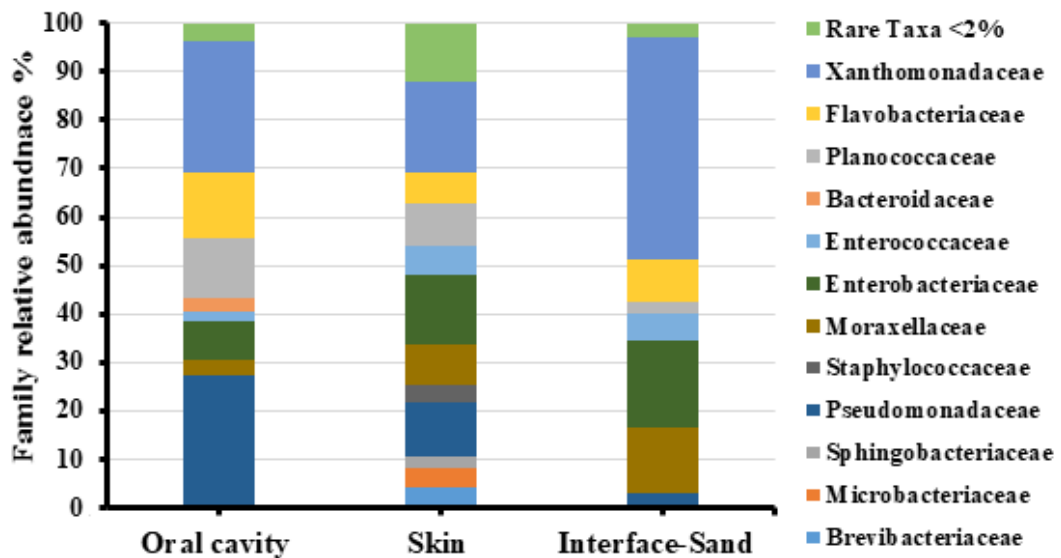
Figure 86. Bacterial communities at the family level in different body regions. Values are shown for the body region during active decay (135.6 ADD) of the decomposition process, F and NF conditions her were considered together in each body region.

By comparing the microbial community distribution in different stages of the decomposition process among the body regions over the active decay and the dry stage in Interface-sand samples, significant differences were observed. During the active decay, Xanthomonadaceae (78%) and Flavobaceriaceae (17 %) colonized carrions without fur. On the contrary, in carrion without fur in the same body region, the main families found were Enterobacteriaceae, Moraxellaceae, Xanthomonadaceae, and Enterococcaceae. In addition, Pseudomonadaceae appeared only in these samples (6 %) (Fig. 87).

Whereas, during the dry stage, the pattern of the bacterial distribution was different Sphingobacteriaceae, Flavobaceriaceae, Brevibacteriaceae, Microbacteriaceae, and Staphylococcaceae mainly dominated this stage, which was totally absent at the beginning of the decomposition process except for the Flavobaceriaceae family which was only present with (17%) in NF samples. In addition, Planococcaceae found only in F condition (4%) and Xanthomonadaceae strongly decreased in NF carrions over the decomposition process in interface-sand-carrion from (78%) to (5%) (Fig. 87).

The statistical analysis was performed using the average of the microbial community distribution in different stages regardless of the F or NF conditions (Fig 88). The result showed differences between different stages of the decomposition ($X^2 = 197.097$, df =15, p > 0.05).
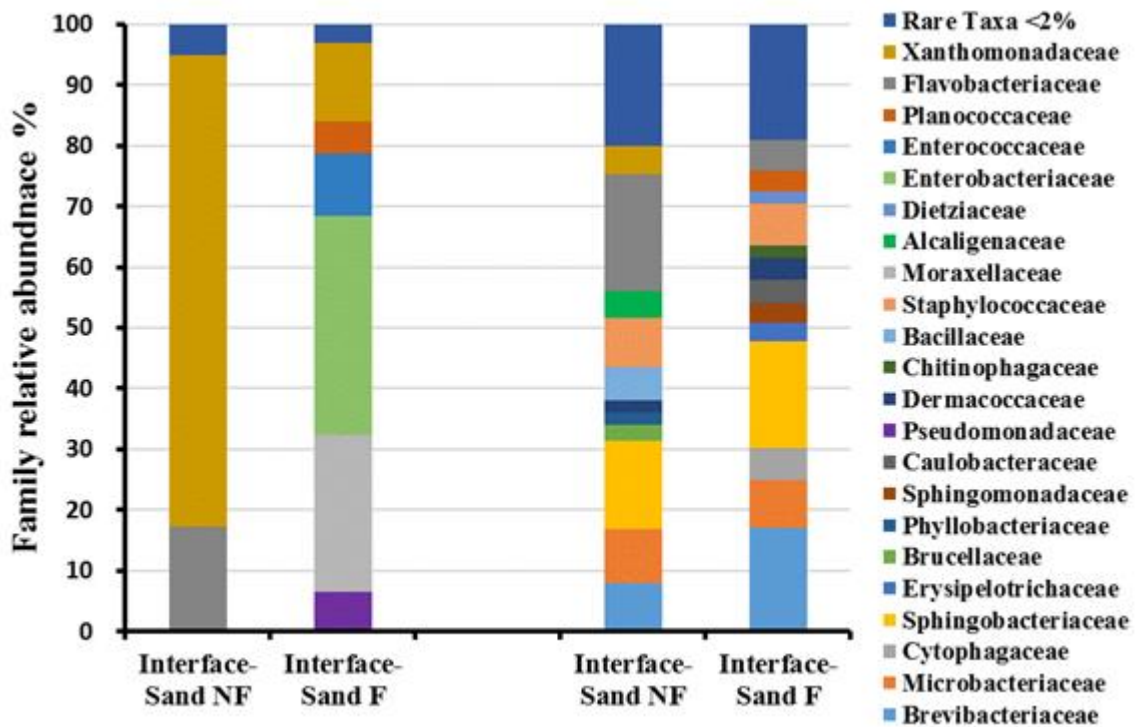
Active Decay. 135.6 ADD   **Advanced Decay.1901.3 ADD**

Figure 87. Bacterial communities at family level. Values are shown for interface-sand carrion F and NF samples over active decay and the advanced dry stages of the decomposition process.
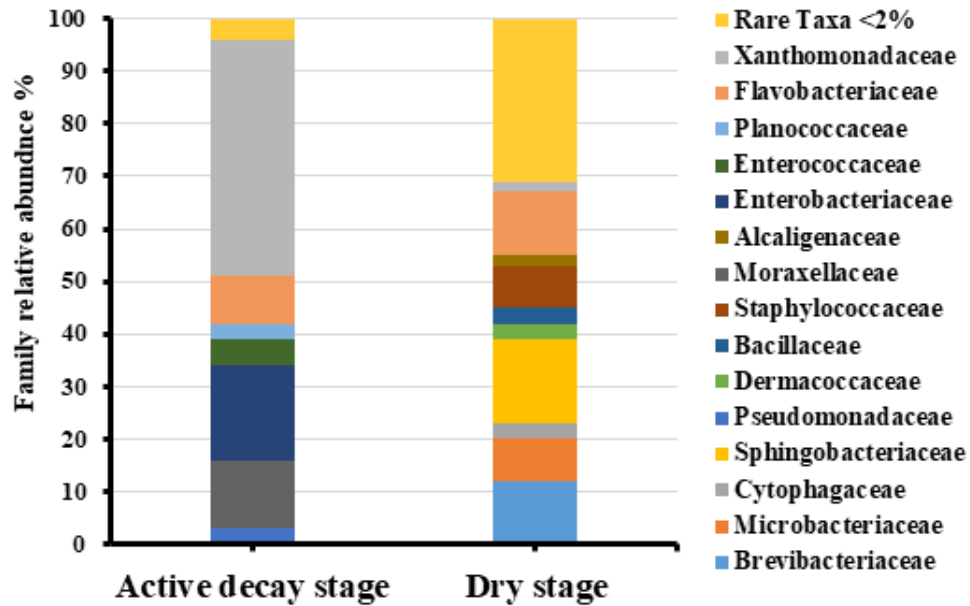
Figure 88. Bacterial communities' distribution at family level over two points of the decomposition process, active decay and dry stages.

Moreover, two conditions were analysed in order to evaluate the effect of the humidity and the environment outside the carrions. In term of humidity effect, the relative abundances of families detected in the oral cavity and interface-sand-carrions were considered together as a (wet condition). They were then compared to the relative abundance of the same families found in skin sampling renamed as (dry condition). The high degree of humidity negatively affected the development of Microbacteriaceae during the active decay phase (Fig. 89).

Results showed significant differences in the families' distribution between wet and dry conditions ($X^2 = 25.858$, df =11, p =0.006) (Fig. 90).
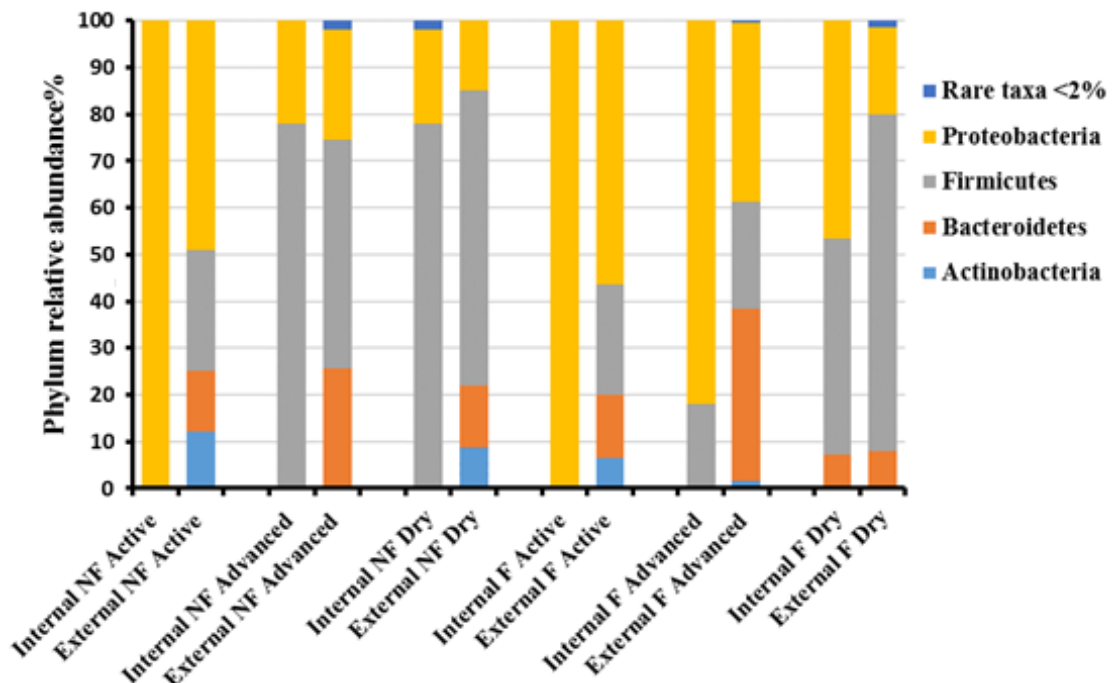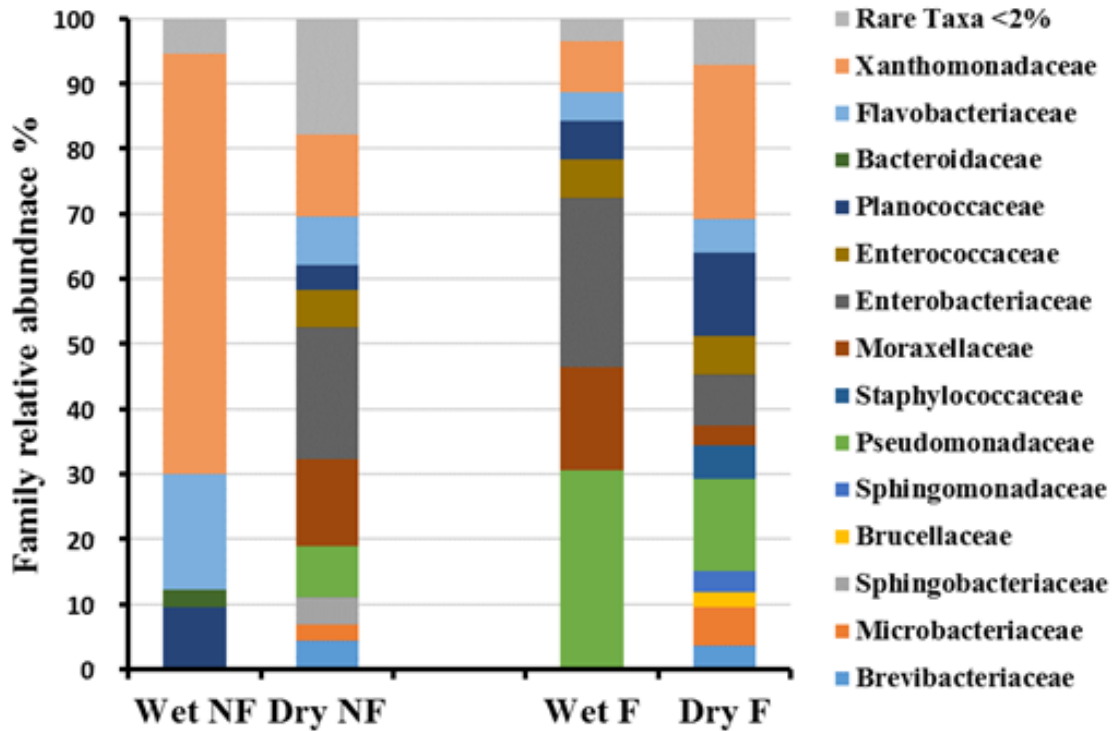
Figure 89. Humidity effect on family relative abundance. Family relative abundance clusterisation is shown depending on both body region and the presence of the fur. Condition (NF) refers to carrions without fur condition, (F) refers to carrion with fur. Wet environment= bacteria developed in the oral cavity and under the carrions at the interface with sand. Dry environment= bacteria developed on the skin air expose.
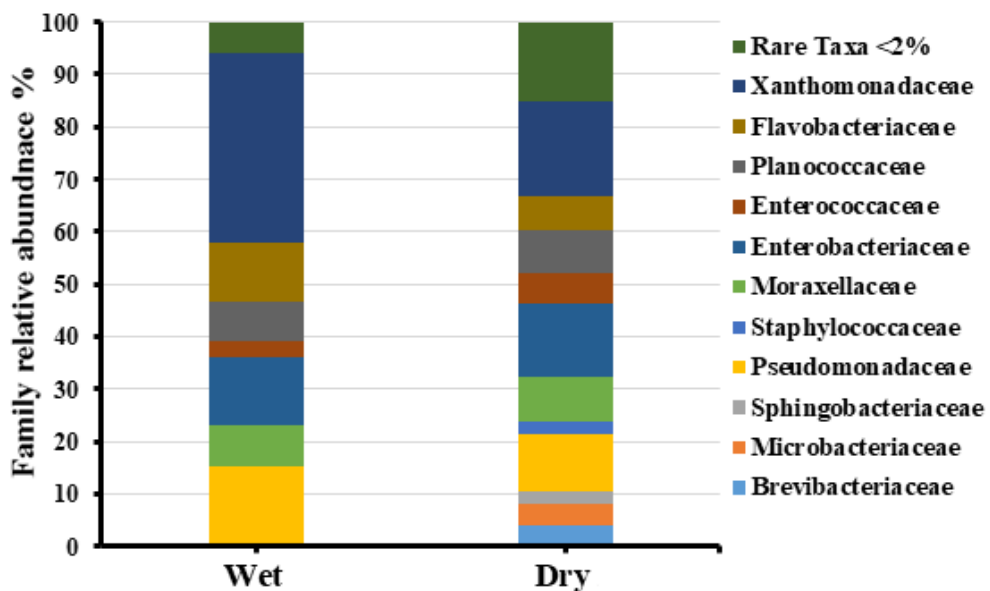
Figure 90. Average of family relative abundance clusterisation is shown depending on environment condition. Wet environment= bacteria developed in the oral cavity and under the carrions at the interface with sand. Dry environment= bacteria developed on the skin air expose.

Whereas, in the environment effect, the relative abundances of families detected in oral cavity renamed (Internal region) were compared to the relative abundance of the same families found in the skin and interface-sand-carrions samplings that were considered together as (External region) (Fig 91). By observing the environment influence on the bacterial communities' development during the active decay, it was noticed that the oral cavity of carrions without fur (Internal Region NF) contained (51%) of Xanthomonadaceae whereas it was (45%) outside the same animal. Bacteroidaceae was almost absent in the same two conditions in carrions without fur. On the other hand, a different family's distribution pattern was observed during active decay due to the presence of the fur. However, Brevibacteriaceae was found to colonise the external body region of the animal without fur only (Fig. 91). The statistical analysis was performed and the result showed significant differences between internal and external environmental samples ($X^2 = 34.972$, df =8, p =0.000) (Fig. 92).
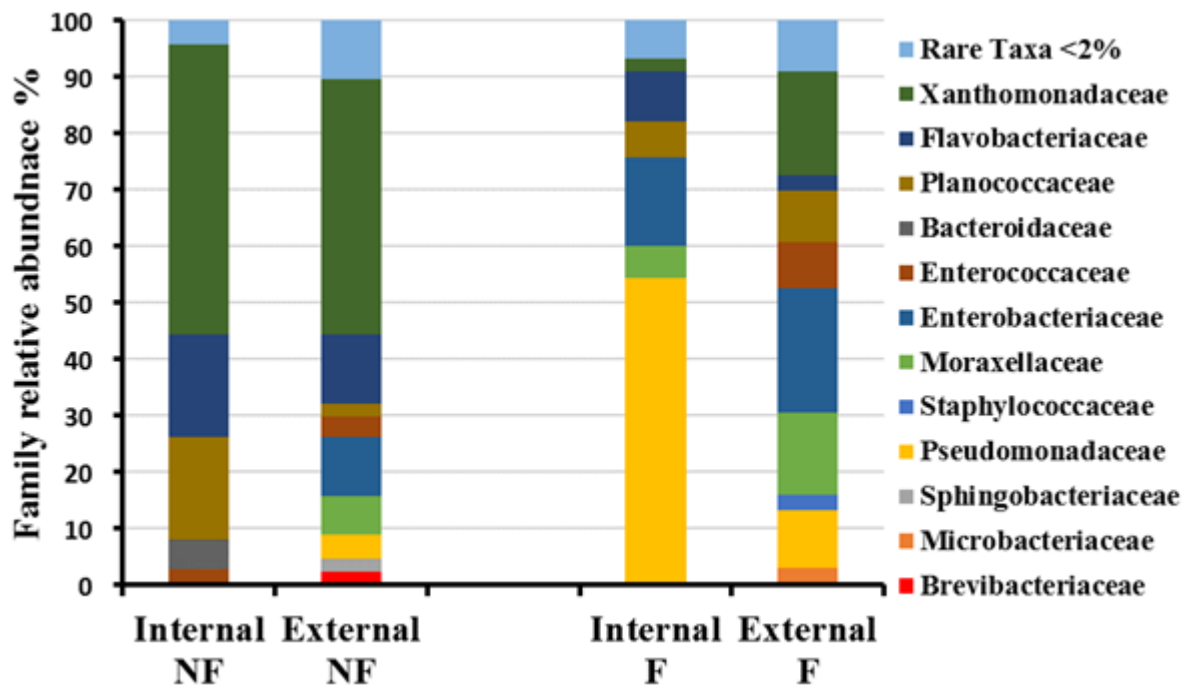
Figure 91. Environment effect on phylum relative abundance. Family relative abundance clusterisation is shown depending on both body region and the presence of the fur. Condition (NF) refers to carrions without fur condition, (F) refers to carrion with fur internal region= bacteria developed in the oral cavity. External region= bacteria developed on the skin and under the carcasses at the interface with sand.
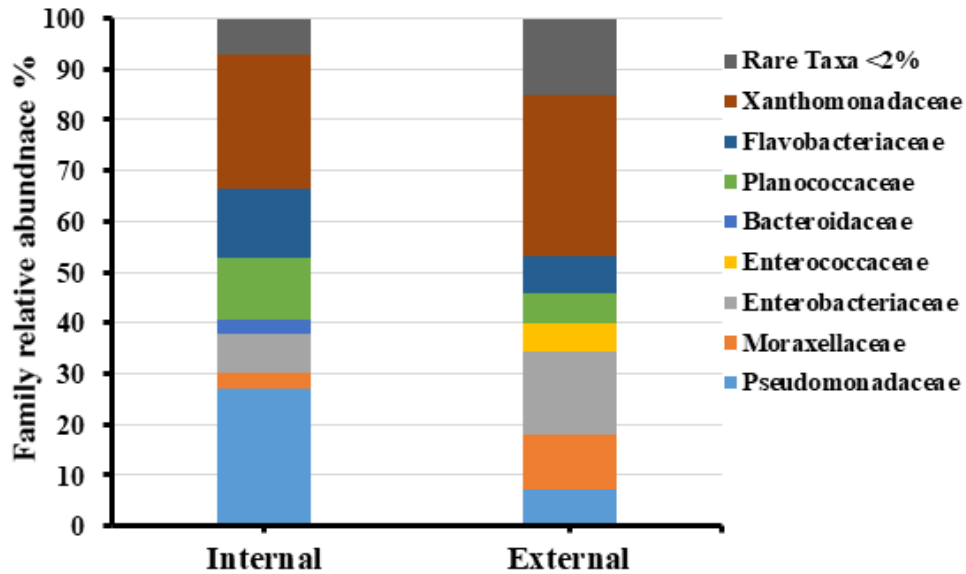
Figure 92. Environment effect on phylum relative abundance. Family relative abundance clusterisation is shown depending on both body region and the presence of the fur. Condition (NF) refers to carrions without fur condition, (F) refers to carrion with fur Internal region= bacteria developed in the oral cavity. External region= bacteria developed on the skin and under the carcasses at the interface with sand.

Spring season 2015 experiment

Over the decomposition, 85 families were taxonomically identified including other taxonomic families' groups were present less than 2% out of the total and were classified as a rare taxon. Rare taxa represented (15%) out of the total. The most seven abundant taxonomic families presented Percentage higher than 2% of the total relative abundance were Planococcaceae (31%), Pseudomonadaceae, (19%), Xanthomonadaceae, (16%), Flavobacteriaceae (11%), Bacillaceae, (4%) and both Micrococcaceae and Alcaligenaceae (2% each). Rare taxa taken together represented the (15%) out of the total (Fig. 93).
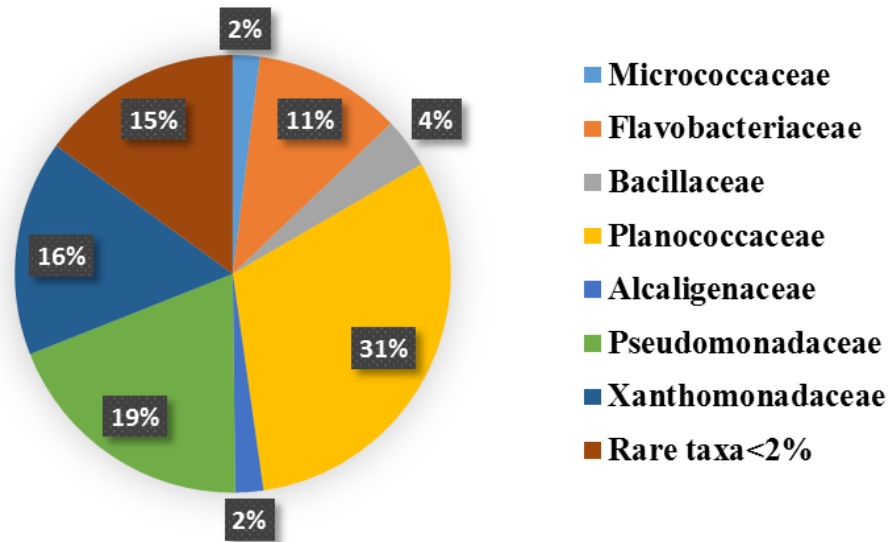
Figure 93. Taxonomic families' distribution over the whole decomposition process. 85 taxonomic group including other groups were clusterised as rare taxa. Each one of them represented less than 2% of the total.

During the active decay, Pseudomonadaceae was the most predominant family (54%) followed by Planococcaceae (11%), Flavobacteriaceae (7%), Micrococcaceae (5%), Xanthomonadacee (4%) and Enterobacteriaceae (3%). While during the advanced decay stage, Planococcaceae became the most abundant family (34%) followed by Xanthomonadacee (32%), Flavobacteriaceae (19%), Alcaligenaceae (3%) which was not present on the previous stage, and finally Enterococcaceae (3%). During the dry stage, Planococcaceae increased reaching (48%) and still the most abundant family, followed by Xanthomonadacee (12%), Bacillaceae as first present her in this stage (9%), Flavobacteriaceae (7%), Pseudomonadaceae (4%) which was the most abundant at the active stage then absent in advanced decay, Staphylococcaceae (3%), Alcaligenaceae and Microbacteriaceae (2%) each (Fig. 94). The statistical analysis showed significant differences in the families' distribution between the decomposition stages (X^2 = 205.645, df =22, p=0.121).
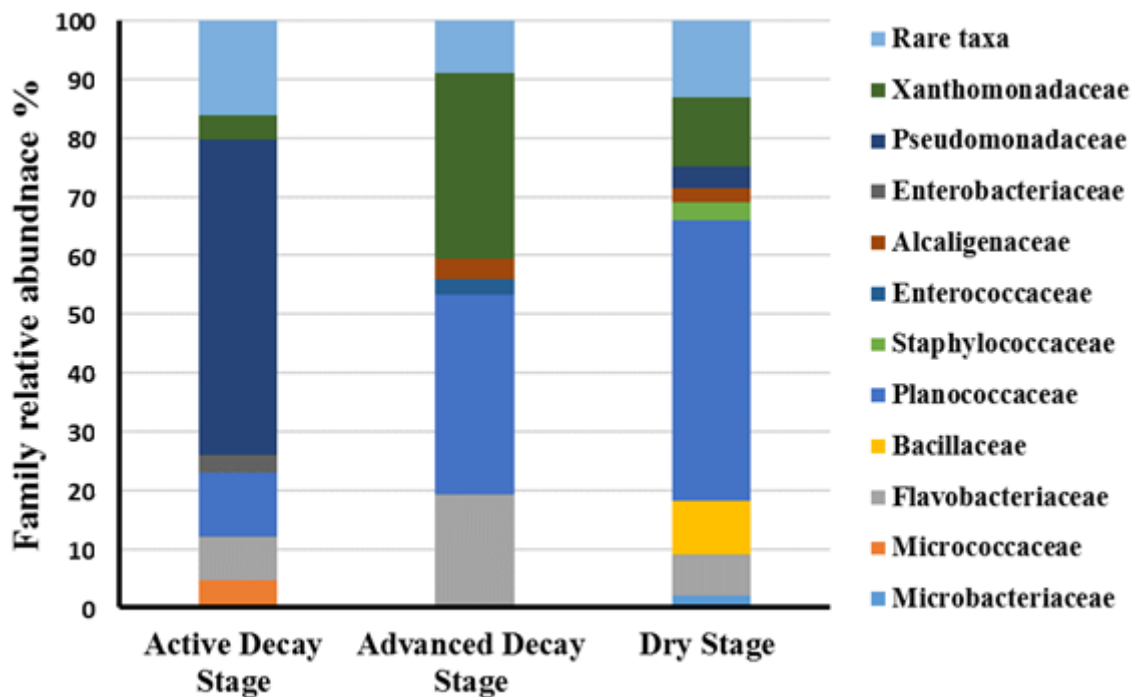
Figure 94. Family taxonomic level relative abundance distribution of microbial community, which presented higher than 2% over the stages of the decomposition, active decay (65.30 ADD), advanced decay (306.20 ADD), and dry stage (595.50ADD). Rare taxa cut off at <2 %.

Among the analysed material, 85 families were taxonomically identified, in addition to this number, some taxa have not been assigned to any family (~10). The results obtained by analysing the complete bacterial community allowed identifying 11 families with an occurrence bigger than 2%. Pseudomonadacea was the dominant taxon in the early phase of decomposition, whereas Planococcaceae abundantly present at the end of the observation. Xanthomonadaceae family seemed to appear only in the second and final phases of the decomposition. Micrococcaceae presented in the early phase whereas Flovobacteriaceae seemed to show a constant presence in the community during the decomposition process (Fig. 95).

The statistical analysis of the relative abundance of each kind of rabbits showed differences between fur and without fur conditions ($X^2 = 14.372$, df =7, p=0.044) (Fig. 96) despite they were not different at the phylum level.
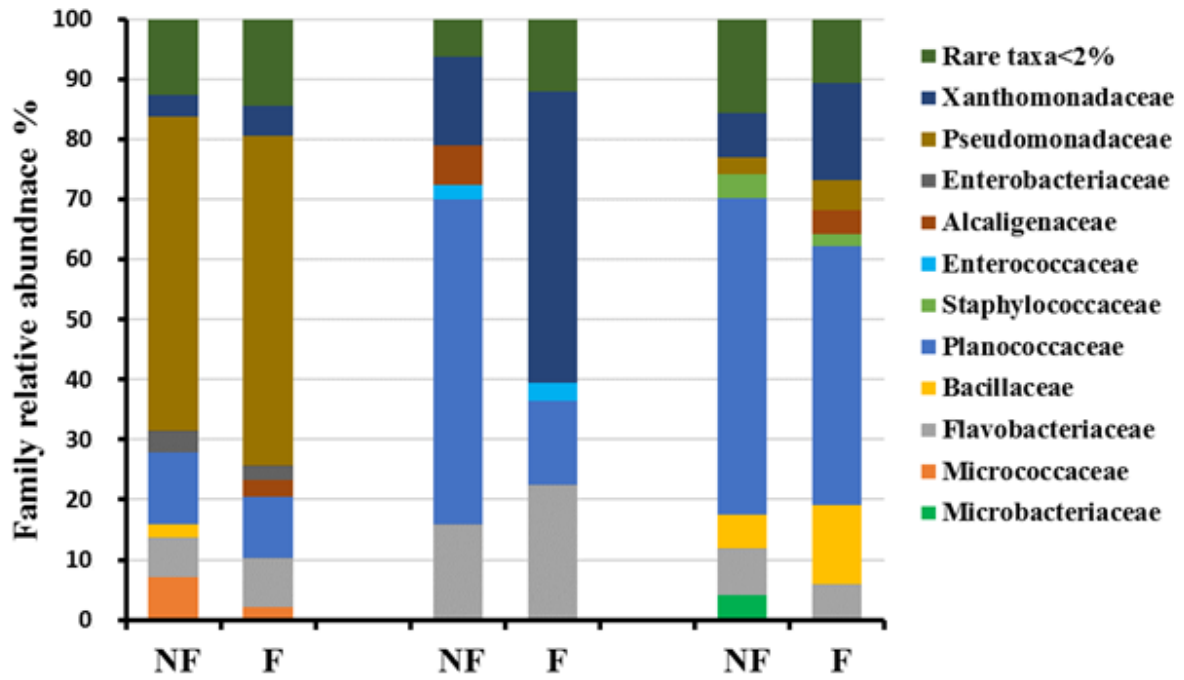
Figure 95. Absolute effect of the fur on post-mortem bacterial communities' distribution at a family taxonomic level during different stages of the decomposition. Family relative abundance clusterisation is shown depending on the presence of the fur. Condition (NF) refers to carrions without fur condition, (F) refers to carrion with fur. Rare taxa cut off was at <2 %.
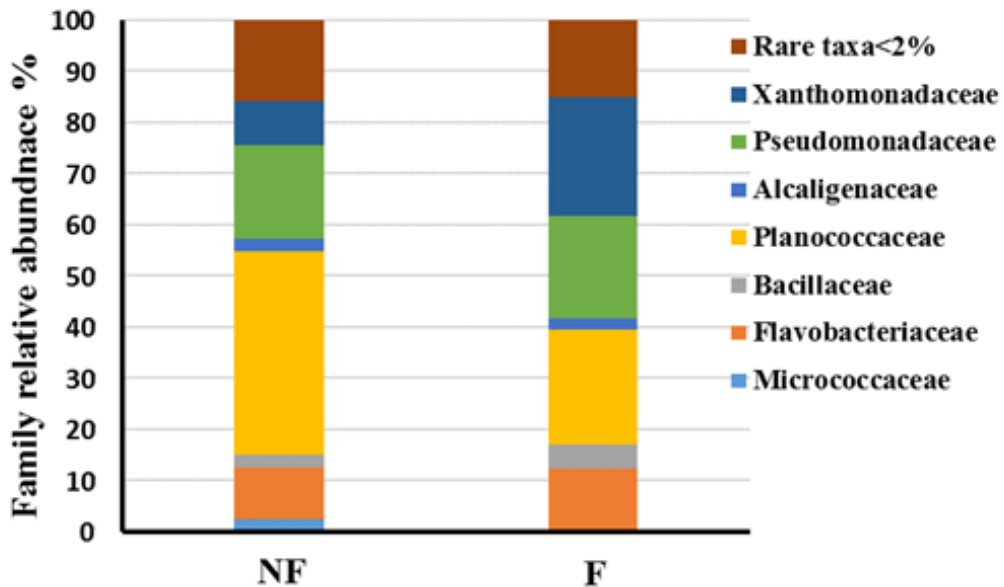
Figure 96. Absolute effect of the fur on post-mortem bacterial communities' distribution at a family taxonomic level over the whole of the decomposition. Family relative abundance clusterisation is shown depending on the presence of the fur. Rare taxa cut off was at <2 %.

By investigating the distribution of family-level depending on the body regions during the decomposition stages regardless of the fur presence. The results showed that Planococcaceae was the most abundant in Oral cavity and Skin regions (32%), (44%) respectively. Whereas it was the third abundant in interface-sand samples (17%), Pseudomonadacea was second abundant in the oral cavity and interface sand samples with 31% and 20% respectively, and with 6% in the skin region. In addition, Xanthomonadaceae were present with 24% and 13% and 12% respectively in the oral cavity, skin and interface sand samples.

On the contrary, Flovobacteriaceae appeared only in skin and interface samples with 14% and 18% respectively. Alcaligenaceae family was found only in the oral cavity and interface samples (3% each), Bacillaceae (4%), (7%) in the skin and interface samples. In addition, some families were present only in one body region; such as Micrococcaceae (5%) and Sphingobacteriaceae (2%) in interface-sand samples, Enterococcaceae (2%) and Enterobacteriaceae (3 %) in oral cavity region, Microbacteriaceae (2%) was found only in skin region (Fig. 97). The statistical analysis result showed difference in the distribution pattern of the bacterial communities between body regions ($X^2 = 95.192$, df =22, p > 0.05).
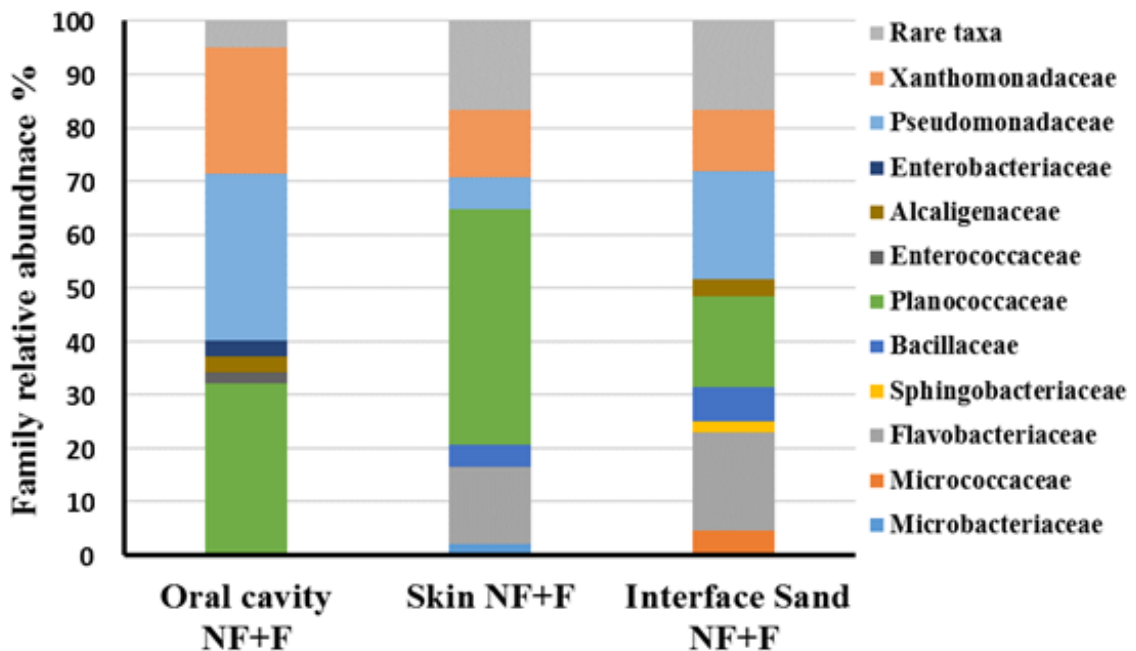
Figure 97. Bacterial communities' distribution at the family level in different body regions during the decomposition process. Values are shown for the body region, F and NF conditions her were considered together in each body region.

The analysis of the single body regions is partially consistent with the general analysis. In fact, in the early stage of the decomposition Pseudomonadacea was the dominant taxon only in the buccal level but despite being present in the other body regions. In contrast, Planococcaccae was the dominant taxon at the end of the process on the whole body. Xanthomonadacea shows a significant presence on the second and third collection points but they are more abundant in the oral cavity than in the other body parts.

In oral cavity samples, Pseudomonadaceae was the most abundant family at the active decay stage with (92%), (88%) respectively in F and NF conditions, followed by Enterobacteriaceae (7%), (11%) in F and NF conditions, and there were not any other families presented. During the advanced decay, the pattern was completely deferent in F condition; Xanthomonadaceae (80%) was the most abundant family, followed by Enterobacteriaceae (9%), and Planococcaceae (6%). On the other hand, in NF condition, Planococcaceae was the most abundant family (84%), followed by Alcaligenaceae (14%), Xanthomonadaceae (7%), and Enterococcaceae (4%).

During dry remains stage, the pattern was different, in F condition, Planococcaceae and Xanthomonadaceae were the most abundant with (39%), (35%) respectively, followed by Pseudomonadaceae (7%), Flavobacteriaceae (4%), Alcaligenaceae (3%), and Bacillaceae, Bacteroidaceae (2% each). However, in NF condition Planococcaceae was the higher level with (75%) and Xanthomonadaceae second (19%) (Fig. 98).

In skin samples, at the active decay stage, the pattern was quite similar in families presented with some differences in the values; Planococcaceae was the dominant taxon in F and NF samples with (31%), (36%) respectively. In F samples, Flavobacteriaceae was the second abundant (21%), followed by Xanthomonadaceae (15%), Pseudomonadacea (6%), Bacillaceae (4%), Alcaligenaceae (3%), Microbacteriaceae (3%), and Burkholderiaceae (2 %). Whereas, in NF samples the second abundant was Pseudomonadacea (17%), followed by Xanthomonadaceae, Flavobacteriaceae (11% each), Bacillaceae (7%), Sphingobacteriaceae (4%) and Burkholderiaceae (3%).

During the advanced decay stage, the pattern was different in F and NF, the families that presented in F samples was converged as following Flavobacteriaceae (36%), Xanthomonadaceae (28%), and Planococcaceae (23%). On the other hand, in NF samples Planococcaceae was the most abundant (84%), followed by Xanthomonadaceae 10.15% and Enterococcaceae (3%). In dry remains stage, the most abundant was Planococcaceae in both N

and NF samples with (42%), (49%) respectively. For the F samples, the second abundant presented was Flavobacteriaceae (14%), followed by Xanthomonadaceae (9%), Bacillaceae (7%), Staphylococcaceae (6%), Pseudomonadacea (5%) and Alcaligenaceae, Carnobacteriaceae (2% each). However, in NF samples the other families were presented as following, Microbacteriaceae (10%), Pseudomonadacea (8%), Bacillaceae (7%), Flavobacteriaceae (5%), Staphylococcaceae (4%), Xanthomonadaceae (3%), and Enterococcaceae, Paenibacillaceae (2% each) (Fig. 98).

In interface-sand-carrion, the pattern of F and NF conditions was the same. Pseudomonadaceae was the most abundant family over the active decay stage in F and NF conditions with 66.63%, (52%) respectively, followed by Micrococcaceae in both F and NF as second abundant (6%), (21%) respectively. Also, Moraxellaceae (5%), (6%) which only presented at this stage and in this body region. Flavobacteriaceae (39%), (9%), Carnobacteriaceae (3%), (4%), Oxalobacteraceae (2% each) (Fig. 98).

During the advanced decay, the pattern was completely different. Flavobacteriaceae clearly increased to become the most abundant family (31%), (48%) in F and NF respectively, followed by Xanthomonadaceae (38%), (26%), Planococcaceae (12%), (6%), Sphingobacteriaceae (4%), (3%) and Alcaligenaceae (6%) was found in NF samples only, whereas, Erysipelotrichaceae found in F samples only (Fig. 98).

At dry remains stage, Planococcaceae was the most abundant with (48%), (34%) in F and NF respectively, followed by Bacillaceae (30%) in F condition, Alcaligenaceae (6%), Xanthomonadaceae (5%) and Pseudomonadaceae (3%). On the other hand, in NF condition, Flavobacteriaceae was decreased to the second abundant (19%), followed by Bacillaceae (10%), and Staphylococcaceae (8%) which they were only found at this stage. In NF condition, Carnobacteriaceae (4%) found in the earliest stage (Active decay) and at the end of the decomposition (Dry stage); Sphingobacteriaceae and Microbacteriaceae (3% each) and Alcaligenacea showed a limited presence and decreased to (3%) (Fig. 98).
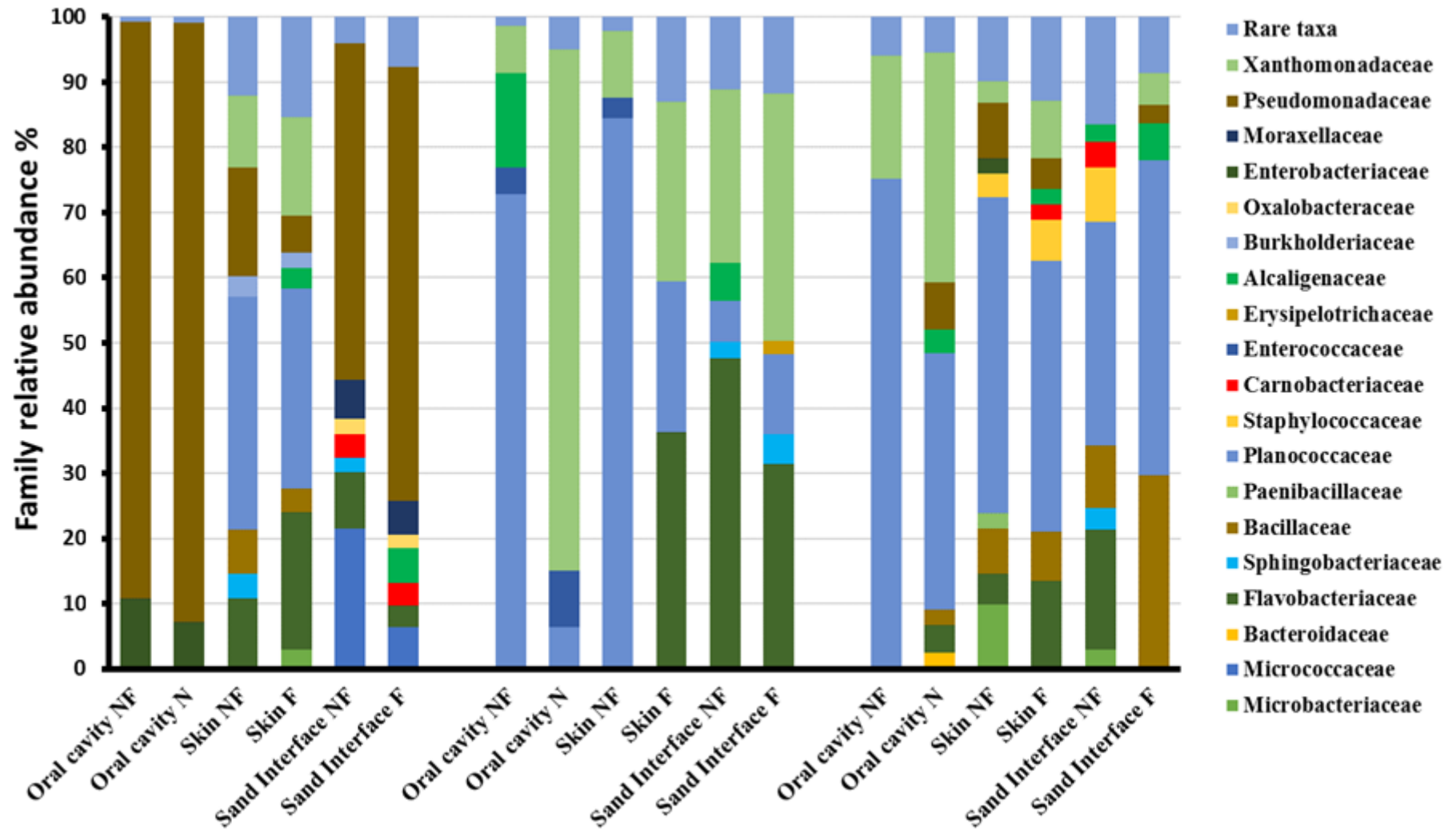
Figure 98. The effect of the fur on different body regions. Family relative abundance clusterisation is shown depending on both body region and the presence of the fur. Condition (NF) refers to carrions without fur condition, (F) refers to carrion with fur. Rare taxa cut off was at <2 %.

Furthermore, two conditions were analysed in order to evaluate the effect of the humidity and the environment outside the carrions on the families' distribution. In the first case, the relative abundances of the families detected in the oral cavity and interface-sand carrions were considered together as a (wet condition). They were then compared with the relative abundance of the same families found in skin samples referred as (dry condition) (Fig. 99).

In the environmental case, the relative abundances of families detected in oral cavity referred as (Internal region) were compared to the relative abundance of the same families found in the skin and interface-sand-carrions samples which were considered together as (External region) (Fig. 101). Results showed differences in the families' distribution according to the decomposition stages between rabbits with and without fur. In addition, a high degree of humidity negatively affected the development of Planococcaceae during the active decay phase. The presence of the fur in this analysis seemed to have no effect on the family distribution within the same decomposition stage except at advanced decay stage. The statistical analysis showed a significant difference of the relative abundances between the wet and dry conditions ($X^2 = 27.544$, df = 8, p = 0.000) (Fig. 100).
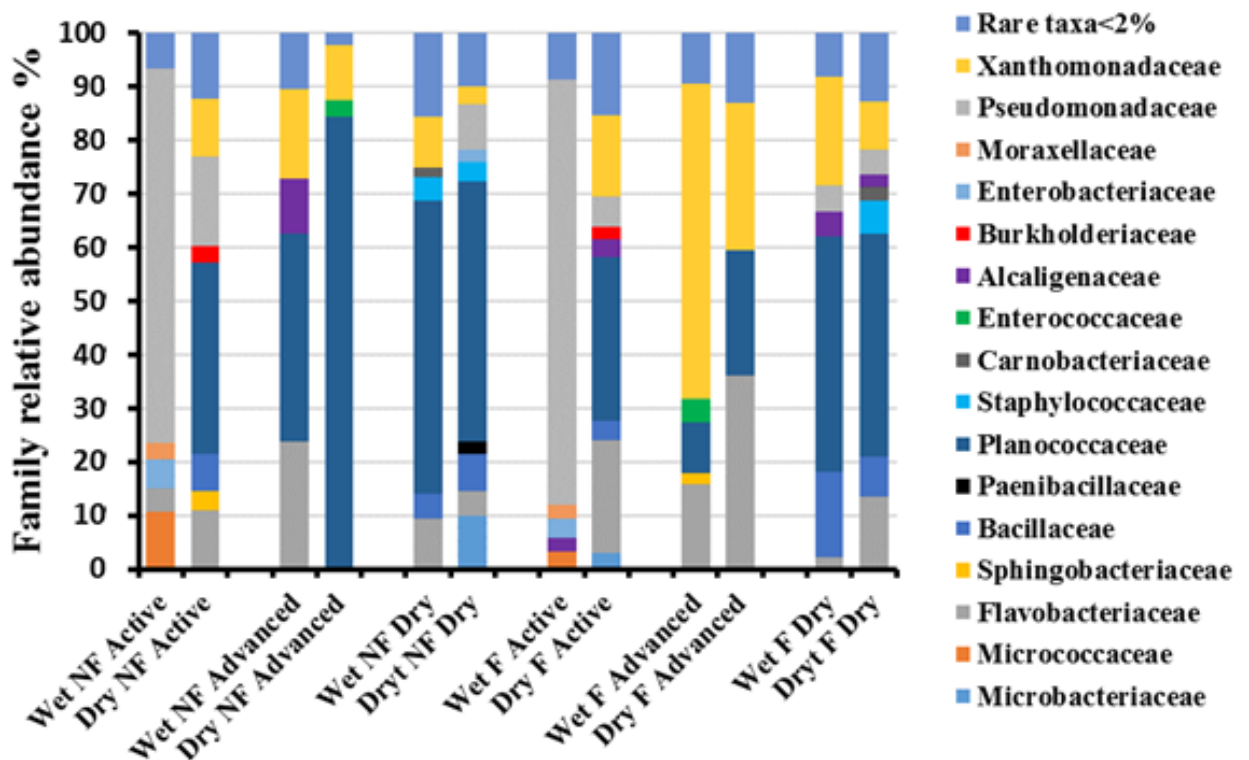
Figure 99. Humidity effect on family relative abundance. Family relative abundance clusterisation is shown depending on both body region and the presence of the fur. Condition (NF) refers to carrions without fur condition, (F) refers to carrion with fur. Wet environment= bacteria developed in the oral cavity and under the carrions at the interface with sand. Dry environment= bacteria developed on the skin air exposed.

196
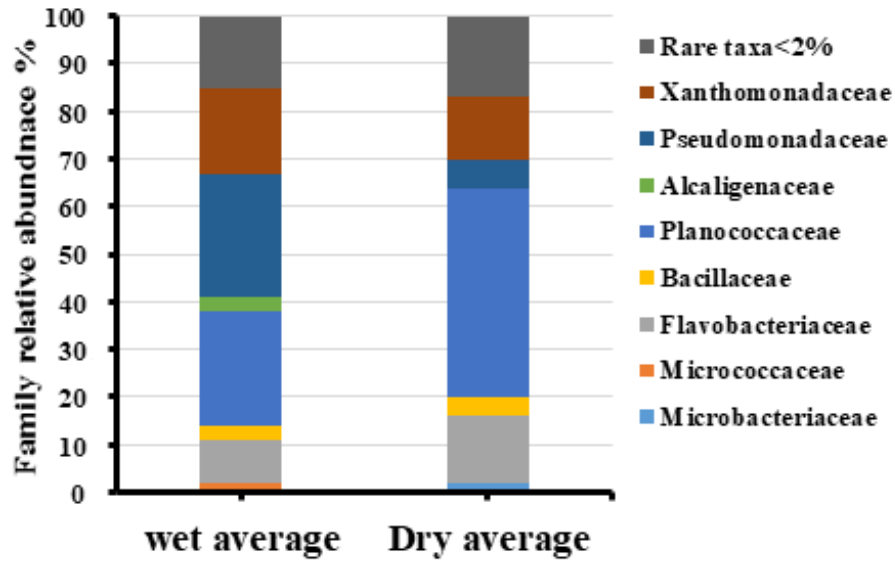
Figure 100. Average of family relative abundance clusterisation is shown depending on Environment condition. Wet environment= bacteria developed in the oral cavity and under the carrions at the interface with sand. Dry environment= bacteria developed on the skin air expose.

Considering the environment effect on the bacterial communities' development on decomposing animal carrions, the result showed significant differences over the decomposition stages between the two conditions NF and F, also between internal and external samples. For example, during the active decay the oral cavity of carrions without fur (internal region NF) Pseudomonadaceae was the most abundant taxon with 88% while it was 34% outside the same animal. In contrast, in an internal region F, Xanthomonadaceae was the most abundant family (80%) that was ten times more than the value outside the same animal (8%). Staphylococcaceae was almost totally absent in the two conditions (with and without fur) in active and advanced decay, while it presented in external condition only at a dry stage in NF and F samples. In addition, Moraxellaceae was found to colonise the external body region of the animal with and without fur at active decay stage only. A different family distribution pattern was observed during the decomposition stages due to the presence of the fur and state of samples (internal, external) (Fig 101). The statistical analysis showed significant difference between internal and external environmental samples ($X^2 = 53.132$, df = 9, p = 0.000) (Fig. 102).
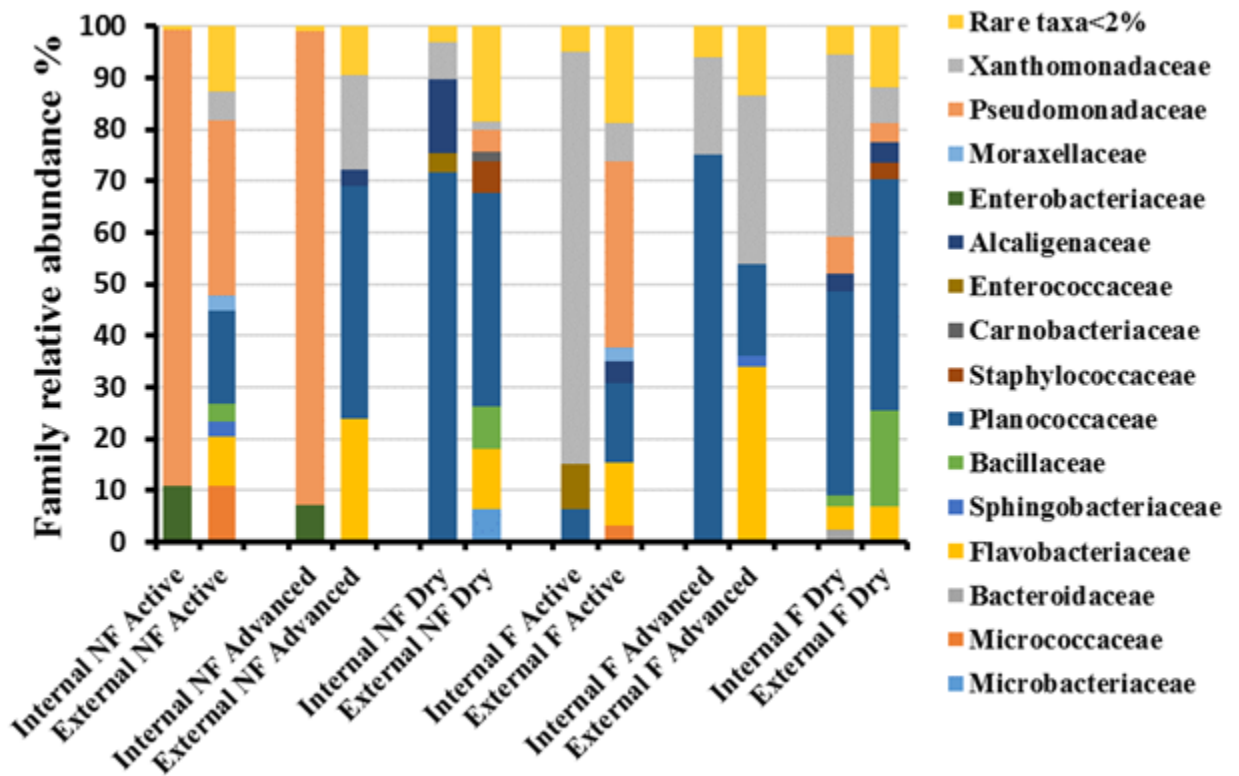
Figure 101. Environment effect on family relative abundance. Family relative abundance clusterisation is shown depending on both body region and the presence of the fur. Condition (NF) refers to carrions without fur condition, (F) refers to carrion with fur internal region= bacteria developed in the oral cavity. External region= bacteria developed on the skin and under the carcasses at the interface with sand.
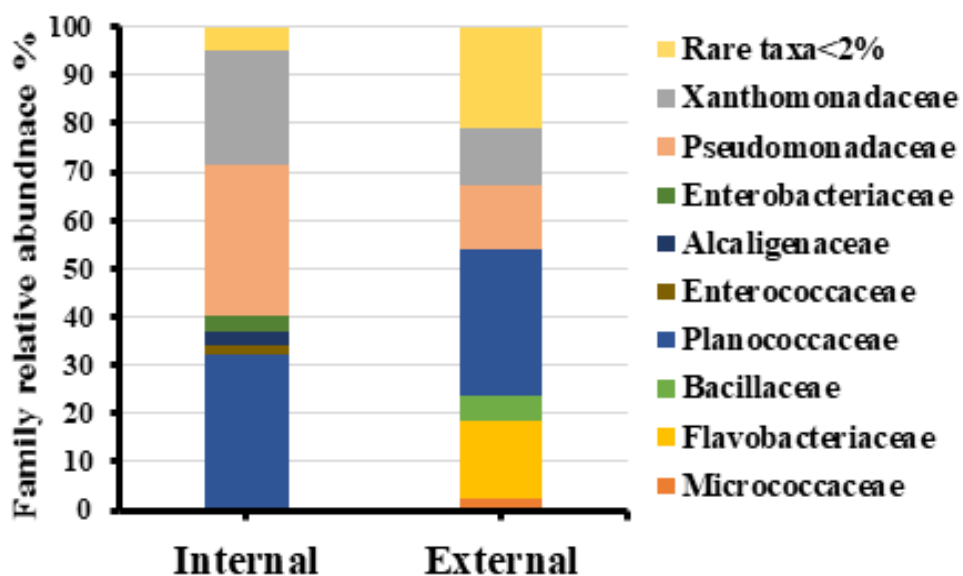
Figure 102. Family relative abundance clusterisation is shown depending on the body region. Internal region= bacteria developed in the oral cavity. External region= bacteria developed on the skin and under the carcasses at the interface with sand.

3.2.3.3.3 Comparison of microbial community distribution between seasons

The statistical analysis showed significant differences between summer and spring seasons at both levels, at the phylum level (X^2= 18.848, df =4, p = 0.000) (Fig. 103) and at family level (X^2= 62.461, df =14, p = 0.000) (Fig. 104).
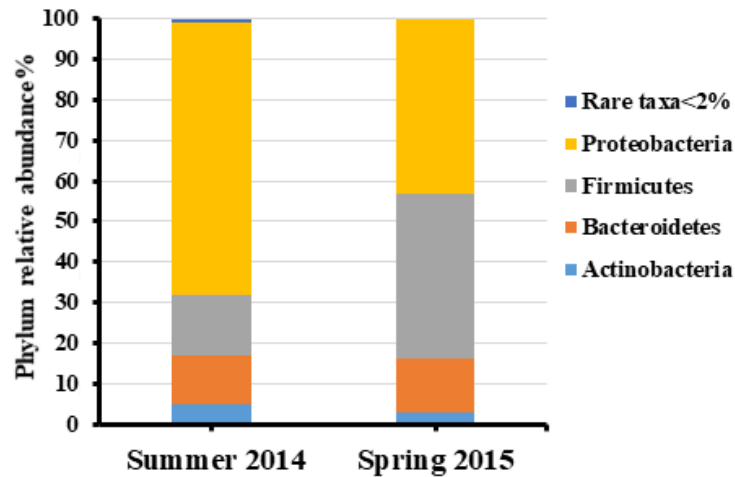
Figure 103. Season effect on phylum relative abundance. Phylum relative abundance clusterisation shown depending on the seasons during the decomposition process.
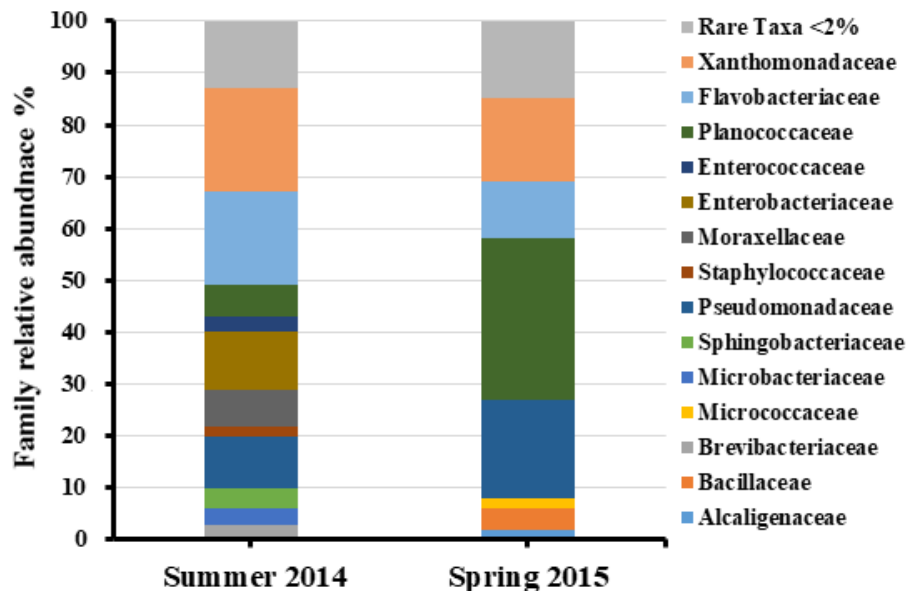
Figure 104. Season effect on family relative abundance. Family relative abundance clusterisation show depending on the seasons during the decomposition process.

4. Discussion

4.1. 3D reconstruction

Current 3D reconstruction and modelling methodologies for reality-based 3D documentation and recording of small and large objects in different aspects have been developed and optimised using different methods and approaches (Dustin *et al*. 2016, Schoning and Heidemann, 2015, Zancajo-Blazquez *et al*. 2015)(Gomez-Gutierrez *et al*. 2014, Niebner *et al*. 2013, Santagati *et al*. 2013, Brutto and Meli, 2012, Izadi *et al*. 2011). In regards to the crime scene investigation, traditional 3D reconstruction methods like laser scanner and total station are still unaffordable for a lot of police forces (e.g. developing countries) due to their costs, inflexible and often require specialised knowledge and personnel for processing the effective operations. In addition, there are problems with transportation at some crime scenes (e.g. high locations, caves) in which a power supply may be required with other accessories (Fig. 105) (de Leeuwe, 2017, Hołowko *et al*. 2016, Sheppard *et al*. 2017, Leipner *et al*. 2016, Barazzetti *et al*. 2012, Maksymowicz *et al*. 2009, Colwill, 2016, Clair *et al*. 2012). In terms of cost, a catalogue of different brands provided a range of costs between £3500 for old and £76000 for a new laser scanner and between £13000 and £31000 for the total station (Table. 45).

Recently, the realistic 3D models have been created and obtained from a small number of photos using photometry approaches and computer software such as 123D Catch software provided by Autodesk.

Figure 105. Laser scanner at a crime scene fixed on the tripod(A) with cables and power supply in the indoor scene (B) and outdoor scene (C).

Table 45. Cost of some kinds of total station and a laser scanner in Dec 2017.

Instrument	Price (£)	Information retrieved from
Leica Scan Station P40 3D Laser Scanner	76045.06	https://secure.fltgeosystems.com/laser-scanners-3d/leica-scanstation-p40-3d-laser-scanner-lca6009377/
Demo Leica P30 ScanStation 3D Laser Scanner (ea)	51069.48	https://secure.fltgeosystems.com/used-surveying-equipment/3d-laser-scanners/demo-leica-p30-scanstation-3d-laser-scanner-demo-p30/
FARO Scanner Freestyle 3D	8,310.00	http://surveyequipment.com/faro-scanner-freestyle-3d/
Leica Nova MS50 Multistation CS15	16774.65	https://surveyingepic.com/?88,leica-nova-ms50-1-multistation-cs15-used

Sokkia iX-1000 Series Robotic Total Station 1012302-53	15989.77	https://www.tigersupplies.com/Products/Sokkia-iX-1000-Series-Robotic-Total-Station__SOK1012302-53-.aspx

Topcon PS Robotic Total Station	13751.20	https://www.tigersupplies.com/Products/Topcon-PS-Robotic-Total-Station__TOP213067102.aspx

FARO Focus 3D S120 Laser Scanner	8610.98	http://www.directsurveystore.com/products.php?product=FARO-Focus-3D-S120-Laser-Scanner

FARO Laser Scanner LS 880 3D Scanner	3504.04	http://www.directsurveystore.com/products.php?product=FARO-Laser-Scanner-LS-880-3D-Scanner

Riegl LMS-Z420i Total Station	31669.99	http://shop.laserscanning-europe.com/Riegl-LMS-Z620-incl-accessories-camera-and-software

New technologies such as the digital camera and new software are available on the market, some of them are available online with no cost involved. These new tools can be applied in 3D reconstruction.

Among them, 123D Catch is one of the free software available which shows a lot of potential in 3D crime scene reconstruction. The limits of this software were tested in this study in order to verify how it can be used in crime scene investigation. The results demonstrated that the number of photos required to obtain the best result of 3D reconstruction models was specified to be from 20 to 30 photos as a minimum.

At the beginning of the research, a limited number of photos 5 and 10 have been used through the modelling process. Subsequently, the number of photos was increased step by step until a complete 3D model was achieved. At the beginning, the quality of the 3D model was not sufficient to provide a comprehensive platform for observing details, also, some holes and distortion of the model were noted.

Significantly, the increase in a number of photos used has led to the improvement of the 3D model in general and the associated details, which were more readily measurable. A first complete 3D model was achieved when 20 to 30 photos were used, and a high-quality 3D model was obtained. Also, the creation of complex objects may request the utilisation of more photos up to 70 depending on the object details or the size of the scene. According to a relevant study, the 123D Catch software can facilitate the assembling of individual photos up to 70 simultaneously in one 3D model (Butnariu *et al*. 2013).

Furthermore, the obtained results demonstrated that the quality of pictures and lighting condition play a critical role in the 3D reconstruction models. It has been observed that the difference in lighting degree between photos created mismatched linkage between the corresponding photos in a 3D model due the variability in light intensity and the clearances in photo sides. Accordingly, this emphasises the importance of flash lighting utilisation for maintaining the light consistency between photos in the concerned cases.

The photos were imported onto to the desktop application without any external adjustments or arranging, which is one of the useful features of 123D Catch in comparison with some other methods, which require calibration process of the photos in order to determine the camera orientation and position before uploading.

In addition, the results about the accuracy and reliability of both small and large scale provided an evaluation of the performance of 123D Catch approach. The level of accuracy achieved was acceptable which also were confirmed by the correlation analysis. Statistically, the intraclase agreement was close to one, on a small scale was 0.997 (N= 155); while in the large-scale was 0.999 (N=73). These results were certainly applicable to various aspects. This confirms another study conducted by (Erickson *et al.*, 2013) demonstrated that the mean position error was ranging between 0.7 mm to 8.5 mm with 1.70 m. In addition, other authors reported that the general differences with the control measurements were 3.5 mm, 1.7 mm, 3.4 mm in XYZ respectively with 9 m (Chandler and Fryer, 2013).

On the other hand, there are many other open source software available that can be downloaded or utilised online. 123D Catch was compared with other photometry methods based on images. The comparison was based on processing time and accuracy results. Agisoft PhotoScan and Photosynth were used to compare the outcomes with 123D Catch software results. The comparison demonstrated that the 123D Catch method produces highly detailed reconstruction in a short time using high-quality photos. A skull was used to validate this point. Photosynth software proved to be far less reliable than Autodesk 123D Catch and PhotoScan in terms of the level of the general result, as reported in the table (46). In fact, this was the only software that failed to produce complete 3D models with all number of the exploited photos. These results confirm a previous study conducted by (BartoA *et al.* 2014) which demonstrated that Microsoft Photosynth can provide an output of poor quality, contains many outliers and scattered. Also, the overall results were supported by another related study conducted by (De Reu *et al.* 2013, Kersten and Lindstaedt, 2012).

Table 46. Result of applications comparison (Agisoft PhotoScan Photosynth and 123D Catch).

Software	Speed	Quality
PhotoScan	Slow	Good
123D Catch	Fast	Very good
Photosynth	Very fast	Not good

Considerably, these obtained results by the 123D Catch software, as a new mobile technology of 3D crime scene reconstruction, were compared with another common method used for the

3D crime scene reconstruction, 3D laser scanner, as mentioned and demonstrated by some studies as seen in (Fig. 106).

Figure 106. Small-scale scene (skull) reconstructed by (A) laser scanner (Barazzetti *et al*. 2012) and (B) by 123D Catch.

Laser Scanning is a method used to obtain the 3D model of objects or surfaces in several applications, such as land surveying, archaeology, architecture, etc. The principle of its work is that the Laser Scanner sends out a massive number of rays to the scanned area and measures the distance of the first object on its path to create a 3D view of the scanned area with a surface accuracy up to 1 mm, depending on the selected frequency point, resolution, lighting and other factors. In some kinds for a complete image of all angles and sides, the scanner has to move around the object, because the instrument can only see what is visible. These different scans are connected after the scanning procedure in a computer program (Barber and Mills, 2007). In addition, two officers must operate the device. The device is mounted on a tripod at one part of the crime scene with one investigator operating it. Another investigator takes the rod-mounted prism and walks the scene placing the prism over evidence that needs to be measured (Loguidice, 2012).

 The 123D Catch software is considered to be a preferable selection in terms of cost-effectiveness in comparison to the laser scanner, the 123D Catch requires less number of operating personnel, only one person is required for operating all the software procedures (Butnariu *et al*., 2013, Chandler and Fryer, 2013). On the other hand, two or more persons are required for operating the laser scanner (Fig. 107). Also, the 123D Catch is a free software while the laser scanner is expensive as seen in (Table 45). Another point that makes 123D Catch software superior to the laser scanner in terms of cost-effectiveness is the lack of the presence

of trained or experienced personnel for conducting the operation, in contrary with the laser scanner instrument.

Figure 107. Two officers must operate the laser scanner or total station. one investigator operating with the main device. Another investigator with the rod-mounted prism moving and placing the prism over evidence that needs to be measured (A, B, C and D) (Galvin, 2011).

Additionally, the123D Catch is considered to be the time-saving approach, the total time needed for running this software is about 30-60 minutes while the laser scanner needs a prolonged time around 5 to 7 hours (Santagati and Inzerillo, 2013). Also, Erickson *et al*. (2013) reported that the time which was required for data collection and generation of the 3D model has been reduced in comparison to other methods such as total station survey and laser scanning.

The 123D Catch software is also considered to be more flexible as it can work with both small and large size crime scenes in different condition. In contrast, the use of laser scanner is limited to the small scale of the crime scenes while it is typically suitable for the crime scenes in the larger scale. In small scenarios where the scene developed in a planar area, photogrammetry method might provide more useful data (Barazzetti *et al*. 2012).

Ease of movement and operation of the 123D Catch are considered as added advantages for the use rather than the total station or laser scanner, the former technique is associated with higher complexity during the system operation and impose difficulties in movement and location shifting due to the presence of the associated appurtenances alongside with the prime instrument (Erickson *et al*. 2013).

Common conception, both methods the 123D Catch and the laser scanner are capable of taking measurements from the reconstructed 3D models with different degrees of accuracy, based on the conducted research, the results obtained by the 123D Catch software demonstrated a high level of accuracy around ±1 mm within 2 m, and according to another supportive study, the 123D Catch software provided accurate measurements with an accuracy of ±2 mm within 2 m (Gomez-Gutierrez *et al*. 2014, Dustin *et al*. 2016). While, the laser scanner provides more accurate measurements with ±2 mm within 25 m (Santagati and Inzerillo, 2013, Barazzetti *et al*. 2012).

In summary, the 123D Catch method is considered to be a cost-effective approach to be followed rather than the laser scanner in this scope. However, the laser scanner is considered to be preferable in terms of accuracy of measurements recorded within the crime scenes.

While 123D Catch approach better focuses on a small scale of scenes and details, laser scanning gives out a more comprehensive view of the geometry of whole crime scene. Thus, both techniques can be used together for recording a crime scene.

The 123D Catch method provides a general model of the survey area in a very quick time and in a very simple and inexpensive way. As demonstrated by the experiments carried out in this thesis, photometry can be used also to represent a cadaver or other body remains (e.g. skull). From this thesis, 20-30 pictures analysed with an appropriate software allow for detailed measures of the cadaver been taken.

This result opens the doors to the 3D representation of the decomposition of a body. As the output is an electronic file, it can be implemented with a lot of information from the body like body mass, injuries, insects species, decomposition phases and microbiological community, etc. In fact, during the decomposition, the body changes from the different point of view: shape, size, colour, the presence of animals and presence of microorganisms.

Organisms and insects have been investigated in recent years, in order to make an accurate estimation of the time since death.

4.2 Decomposition Process Analysis

4.2.1 Physical Transformation

Documenting and identifying the bacterial communities associated with carrion is the key point for applicability of the microbiome in forensic investigations. The microbiome can be used for the PMI estimation and as well for the evaluation of the body transfer.

The decomposition process and the microbial community associated with animal carcasses and human cadavers can be influenced by many factors such as environmental and individual characteristics of the bodies (Parmenter and MacMahon, 2009, Campobasso *et al.* 2001).

In general, there are normally five stages of the decomposition process, which are fresh, bloated, active decay, advanced decay and skeletal stage (Hau *et al.* 2014). Several environmental factors can affect the decomposition: temperature, humidity, clothing, scavengers, soil, arthropods and insects etc. (Campobasso *et al.* 2001, Dautartas, 2009).

Covering of the body is one of the factors, and Lowe *et al.* (2013) demonstrated that clothing could slow the rate of decomposition in pig carcasses. In addition, Stuart (2017) reported that the clothing and other body covering or wrappings have been observed to have a significant effect on the decomposition rate and on the estimation of the post-mortem interval with human cadavers. Dautartas (2009) also demonstrated that differences in the decomposition rate were noted in human cadavers between individuals, which were wrapped in different materials. As well as Capobianco (2017) demonstrated that, the clothing generally slowed the rate of decomposition in human cadavers placed on the same site.

In animals, fur can be considered as a cover as it can insulate, protect the animal and reduce the water evaporation.

According to the literature, a significant number of research groups conducted extensive studies focusing on the major factors, which are contributing to the microbial communities' proliferation during the decomposition process. There are no studies performed to investigate the effect of fur on the decomposition rate and on the microbial communities.

The results obtained in this thesis show similarity of the decomposition stages between animals with and without fur. The observed stages were including the fresh, bloated, active decay,

advanced decay, and dry remains for both summer and spring seasons with the minimum difference due to time variation.

Our decomposition stages followed the pattern observed by (Hau *et al*. 2014) in other models like pig and human.

The resulting data of this research was similar to a relevant scope study conducted under different models and conditions. Matuszewski (2008) reported five stages of decomposition were recognized in pig carcasses: fresh, bloated, active decay, advanced decay, and remains stage. Goff (1993) demonstrated that the pattern observed was following the division into five stages of the decomposition in human cadavers. Furthermore, Pechal *et al*. (2014) also stated that the decomposition progress was classified as fresh, bloat, active decay, advanced decay and dry stages in swine carrion. While Carter *et al* (2007) demonstrated the six stages (Fresh, Bloated, Active Decay, Advanced Decay, Dry, Remains) in pig carcasses. Moreover, (Kocarek, 2003) demonstrated that the stages of decomposition observed in rats have been divided into four stages: fresh, bloated, decay and dry.

Accordingly, some studies indicated that covering the body can affect the time interval of the decomposition rate, through shortening or prolonging the duration, as demonstrated in a conducted comparison of different corpses exposed to specified environmental conditions as elucidated by Centeno *et al.,* (2002) and Stuart and Ueland (2017).

Therefore, the aim of these experiments was to investigate the effects of fur as a contributing factor that can affect the decomposition rate and the count of microbial communities.

According to the results obtained, there were no significant differences observed in the rate of the decomposition process related to the fur factor, when compared to the previously mentioned studies, which were concerned in studying and scanning other kinds of covers e.g. clothing, bedding, plastic sheeting.

We can no longer consider the fur as a barrier towards the decreasing the rate of decomposition.

The season is another factor, which may affect the decomposition process; as it was demonstrated on both pig and human cadavers. Based on research conducted, the yielded results have shown that the decomposition of rabbits in spring season was prolonged due to the low temperature and the high moisture content in the environment. In contrast to the summer season, due to the elevated temperature in summer 2014, which on average was warmer than spring 2015, with lower relative humidity levels. Based on a relevant supportive study, the carcass

decomposition process in summer season was 3-7 times longer than in winter season, which supports what has been reported in other studies (Hyde *et al*. 2013, Johnson *et al*. 2013, Meyer *et al*. 2013). Moreover, the variation could be due to the differences observed in insect activity, which is affected drastically by the temperature degree and the relative humidity throughout the seasons.

In regards to the loss in body weight, the major attribution to this cascaded is due to the insect's activity and the rate of water evaporation and body fluid chemical deprivation. Additionally, flesh removal, which is a consequence of insects' activity or other scavengers. Accordingly, the boxes have been exploited during this research in order to exclude the factor of the flesh loss through preventing the proliferation of scavengers (bird activity). Wherefore, it is clear that the most of the weight loss during both seasons was due to the insects' activity during the active decay stage, and the rest of weight was lost during the dryness of the flesh and water evaporation.

There was no difference in weight loss observed between rabbits with and without fur, which both retained the same pattern in each experiment, conducted in each season. The carcasses lost the majority of their weight during the active decay stage as a result of insects' activity in both seasons. During the summer experiment, the carcasses have lost a minor amount of weight during the first week; and lost the majority of the weight during the active decay stage in the second and the third week, and the weight remained stable during the fourth week. While, in the spring season, the carcasses have slightly lost weight during the fresh stage until the start of the colonisation in the active decay stage, where the carcasses have lost most of their weight due to the insects' activity. Then at the advanced decay stage, the carcasses lost more weight until the dry stage, where the weight was stable because the carcasses became very dry as no more tissue or fluid was being lost. The decomposition and pattern of insect succession were not very different in both seasons (Kyerematen *et al*. 2006).

4.2.2 Insects Activity

Insects are the primary fauna associated with carrion and are considered most important in recycling this organic material back into the ecosystem. Species in the orders of Diptera and Coleoptera are the most important and abundant groups of insects associated with carrion. Insect colonisation of carrion is dependent on many factors. Each geographical region is

characterised by its season, temperature, humidity, habitat, vegetation, soil type and environmental conditions (Gill, 2005).

Entomological data that were collected during the summer and spring experiments were illustrated the same taxa nearly were present except (Diptera, Muscidae) *Hydrotaea* which was presented only throughout the summer experiment. Following a study performed by (Arnaldos *et al*. 2004), has confirmed that species in this genus are active between June and October.

Furthermore, only one sample of *Lucilia sericata* (Calliphoridae) was detected in the spring season, which is due to the low temperature on average. A supportive study by (Tarone *et al*. 2011), has reported that *L. sericata* has an increase growth rate during the higher temperatures. Also, (Pitts and Wall, 2005) demonstrated that 70–95 % of the *L. sericata*, larvae and pupae die over winter and spring seasons.

Entomological data for the first experiment revealed the presence of Diptera Calliphoridae (*Lucilia sericata, Calliphora vicina, Protophormia terraenovae*), Muscidae (*Hydrotaea*) Sphaeroceridae (*Leptocera caenosa, Coproica vagans, Coproica hirticula, Coproica hirtula*), and Piophilidae (*Allopiophila vulgaris*), Hymenoptera Pteromalidae (*Nasonia vitripennis*) and Coleoptera Cleridae (*Necrobia rufipes*) and Dermestidae (*Dermestes lardarius*).

During spring experiment, four families of Diptera (Calliphoridae, Muscidae, Piophilidae and Sciaridae), one of Hymenoptera (Pteromalidae) and one of Coleoptera (Cleridae) were collected. Among Calliphoridae *C.vicina*, and *P.terranovae* were sampled.

In fact, differences in colonisation times were observed only in the spring experiment, animals without fur were colonised two days before animals with fur. While no significant differences were observed in the summer experiment. The season could have affected the insect's activity and the spread of the decomposition volatiles. As expected, within years, insect succession patterns changed on a seasonal time scale influenced by climate change.

4.2.3 Metabolic Microbial Community Profiles (MMCPs)

The analysis of bacterial community functional diversity, metabolic potential, is extremely important for understanding the role of microbial communities in different environments. BIOLOG plates based on different carbon sources are now widely used to assess the functional diversity of microorganisms from environmental samples (Stefanowicz, 2006).

211

There were notable changes in the microbial community functional diversity during decomposition recorded under environmental factors. For describing the microbial community metabolic profiles throughout carrion decomposition. Biolog EcoPlates have different carbon sources (Pechal *et al*. 2013a), and the metabolic profiles were used as a potential surrogate for identifying the functional diversity of microbial community changes over time on carrion decomposition.

The experimental results showed differences in the functional diversity of bacterial community (p=0.000) within different body regions (oral cavity, skin and interface-sand-carrion). The microbial community was observed to be less active in skin samples during the decomposition in both rabbits with and without fur potentially due to the dry environment. Costello *et al*. (2009) demonstrated that the level of bacterial communities' diversity in human skin sites varies dramatically over time, and it is driven by differences in skin environmental characteristics. While across the oral cavity samples, it was higher and more variably active from the second week until the fourth week in rabbits with and without fur.

Whereas, in the interface-sand-carrion samples, more activity occurred during the process of the decomposition when compared with other samples collected from other regions, which could be due to the content of water present in this location as reported by Jordan and Tomberlin. (2017) and by Metcalf *et al*. (2016). The obtained results are in agreement with a study conducted by Hyde *et al*. (2013) which demonstrated the variation in communities' structure between different sample collection sites within the body and between the initial and the endpoints of the bloat stage for a specific body-sampling site.

In addition, this result is similar to the outcome of a study performed by Pechal *et al*. (2013a) which was reported, "There were significant differences in MMCPs over decomposition and between sampling regions (buccal and skin)".

Based on this conducted research, there were no differences found in a variety of results among the presence of fur during the seasons. In both summer and spring experiments, the functional diversity of the bacterial communities for (F) and (NF) rabbits' samples was followed the same pattern of activity and variety in each season. However, there were observable significant differences in functional diversity between the seasons. The period of activity of the spring season was slightly longer than the summer season associated with different levels of functional diversity.

The obtained results have been supported by findings of a relevant study (Pechal *et al*. 2013a) have concluded the absence of significant differences in MMCPs among seasons and the seasonal variation of microbial communities' functions, during the spring season was highly proliferative and more variable in comparison to the other seasons.

Furthermore, the analysis of the functional diversity of bacterial community showed a big variability depending on the decomposition stages. Limited functional diversity was observed at the beginning of the decomposition (fresh stage) and at the end of the decomposition process (dry stage) and the maximum level of the functional was recorded during the active decay stage. This is similar to the study by Pechal *et al*., (2013a) demonstrated significantly different metabolic profiles over decomposition stages for carrions in spring and summer seasons. In addition, a study by Metcalf *et al*. (2013) showed that the post-mortem microbial community changes are dramatic, measurable, and repeatable in a mouse model system over the decomposition. Also, Finley *et al*., (2014) reported that the bacterial community composition changes significantly and consistently over the course of decomposition of the mouse model. It is worth mentioning that the functional diversity of bacterial community associated with soil beneath human cadavers shows significant differences over the decomposition process (Finley *et al*. 2016).

It can be concluded that the obtained results in this thesis are in agreement with other studies by (Metcalf *et al*. 2016, Parkinson, 2009, Carter *et al*. 2015, Pechal *et al*. 2013b): significant differences in microbes' community functional diversity (MMCPs) were noted during the decomposition stages within and among seasons.

4.2.4 Bacterial Community Classification

Microbes' community plays a critical role in the organic matter decomposition, which contributes to energy and nutrient transformation in every ecosystem (Pechal *et al*. 2013a). As previously discussed the bacterial functional diversity during the decomposition process, between the summer and spring seasons on rabbits with and without fur has been conducted.

Further analysis was performed to investigate and classify the bacterial communities associated with the carrions. The bacterial communities collected during the summer and spring experiments were analysed at both phylum and family taxonomic levels as defined by (Wang

et al. 2007, Pechal *et al*. 2013b). Attention was paid to the different body regions of the rabbits e.g. mouth, skin, under the body and to the different stages of the decomposition.

4.2.4.1 Phylum Level Analysis

During the decomposition, the most four abundant phyla that have been detected included Proteobacteria, the dominant phylum, Firmicutes, Bacteroidetes and Actinobacteria. These phyla showed substantial shifts in relative abundance over the decomposition process with significant difference among sampling days and body regions over the decomposition process. Differences were observed as well as at the season's level (summer experiment vs spring experiment). The statistical analysis of the results showed significant differences in bacterial community distribution and relative abundance between summer and spring seasons ($X^2 = 18.848$, df $= 4$, p $= 0.000$) (Fig. 103).

The results from these experiments were compatible with the results obtained by Pechal *et al*. (2013b). According to this author, there was a significant difference between phylum taxon richness and relative abundance patterns over the decomposition. Proteobacteria was the most abundant phylum followed by Firmicutes, Bacteriodetes and Actinobacteria with significant differences between the stages of the decomposition on swine carrions. Pechal *et al*. (2013a), also have reported these phyla in another study. Furthermore, Hyde and colleagues. (2013, 2015) reported that the most similar phyla associated with human cadavers during the decomposition process were Proteobacteria, Firmicutes, Bacteroidetes and Actinobacteria.

Similar results were also obtained by another study by Pechal and Benbow. (2016) working on salmon carcasses. The authors showed that the main five phyla observed were Actinobacteria, Bacteroidetes, Firmicutes, Proteobacteria and Tenericutes, and the most common phyla among all individuals were Proteobacteria, Firmicutes and Bacteroidetes.

In addition, the effect of the environmental conditions analysis showed significant differences of bacterial communities in taxon richness and relative abundance patterns through the decomposition process between wet and dry conditions in each season (Tables. 47, 48). In addition, statistical analysis was performed for internal and external samples and the result showed a significant difference in each season (Tables. 49, 50).

Hyde *et al*., (2015) demonstrated that there was a change in community structure for all samples collection sites including the mouth samples, which is the internal region, and cheeks, which is the external region.

Table 47. Humidity effect on phyla distribution over the active decay stage in summer 2014.

Phyla	Wet	Dry
Actinobacteria	0	14
Bacteroidetes	13	9
Firmicutes	13	21
Proteobacteria	73	56
Rare taxa<2%	1	1
(X^2 = 18.845, df =4 and p=0.000)		

Table 48. Humidity effect on phyla distribution over the decomposition process in spring 2015.

Phyla	Wet	Dry
Actinobacteria	3	3
Bacteroidetes	11	16
Firmicutes	34	55
Proteobacteria	52	25
Rare taxa<2%	1	1
(X^2 = 15.344, df =4 and p=0.004)		

Table 49. Environment effect on phyla distribution over the active decay stage in summer 2014.

Phyla	Internal	External
Actinobacteria	0	14
Bacteroidetes	18	9
Firmicutes	16	21
Proteobacteria	66	56
Rare taxa<2%	0	1
(X^2 = 19.491, df =4and p=0.000)		

Table 50. Environment effect on phyla distribution during the decomposition in spring 2015.

Phyla %	Internal	External
Actinobacteria	0	5
Bacteroidetes	1	18
Firmicutes	37	43
Proteobacteria	62	33
Rare taxa<2%	0	1
(X^2 = 30.513, df =4 and p=0.000)		

On the other hand, the bacterial community associated with the soil under a decomposing of the human body showed significant differences in taxon richness at phylum level over the decomposition process. (Finley *et al*. 2016) detected the most important phyla in soil associated with decomposing human remains includes Proteobacteria, Firmicutes, Actinobacteria and Acidobacteria. The same author, Finley *et al*., (2014) reported that seven bacterial phyla were present in the grave soil, including Proteobacteria, Bacteriodetes, Firmicutes, Acidobacteria, Actinobacteria, Verrucomicrobia, and Planctomycetes, respectively by relative abundances.

Proteobacteria, Bacteriodetes, Firmicutes and Acidobacteria seem to be associated with a body, carrion decomposition in all the contexts (exposed, concealed bodies) and in different species (rabbits, pigs, mice, rats and humans).

4.2.4.2 Family Level Analysis

Over summer 2014 experiment, the most abundant taxonomic families that had been identified during the decomposition process, and detected in higher abundancy parentage more than 2% of the total relative abundance associated with the carrion samples were identified as following: Xanthomonadaceae, Flavobacteriaceae, Enterobacteriaceae, Pseudomonadaceae, Moraxellaceae, Planococcaceae, Sphingobacteriaceae, Enterococcaceae, Microbacteriaceae, Brevibacteriaceae and Staphylococcaceae. While, over spring 2015 experiment, the most abundant taxonomic families were Planococcaceae, Pseudomonadaceae, Xanthomonadaceae, Flavobacteriaceae, Bacillaceae, Micrococcaceae and Alcaligenaceae.

The obtained results (Fig. 104) showed significant differences in bacterial community families' distribution and relative abundance between summer and spring seasons (X^2= 62.461, df =14, p = 0.000). The Venn diagram (Fig. 108) and (Table. 51) clearly showed that only four families appear in both seasons. Seven families were exclusive of summer and three families were sampled only in spring.
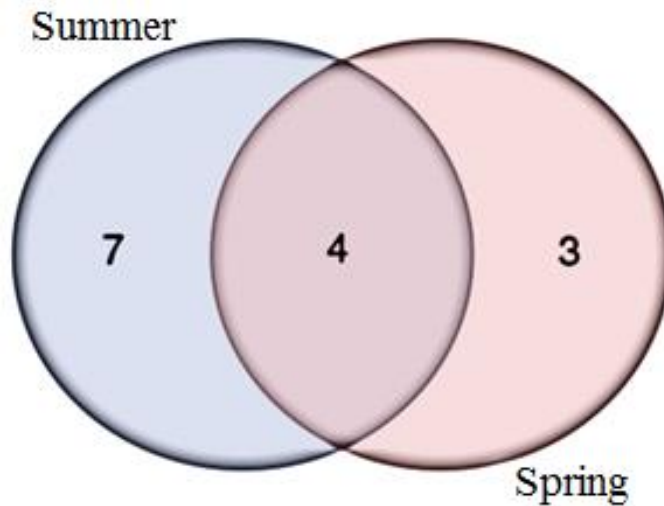
Figure 108. The similarity of the bacterial community families over the decomposition process during summer 2014 and spring 2015 experiments.

Table 51. Bacteria families' represented over decomposition process during summer 2014 and spring 2015 experiments.

Names	Total	Families
Spring Summer	4	Flavobacteriaceae Planococcaceae Pseudomonadaceae Xanthomonadaceae
Summer	7	Staphylococcaceae Enterobacteriaceae Microbacteriaceae Moraxellaceae Sphingobacteriaceae Brevibacteriaceae Enterococcaceae
Spring	3	Alcaligenaceae Micrococcaceae Bacillaceae

The results showed a significant difference in the bacterial community family distribution among the presence of fur and among the decomposition stages, with significant differences among the sampling regions and seasons. The obtained results were identical to documented results in a relevant study performed by Pechal *et al*. (2013b) using replicate swine carcasses that have demonstrated the presence of significant difference among the overall family richness during the decomposition. In addition, there was a significant difference between sampling regions (i.e., buccal and skin bacterial communities) and a significant interaction effect with the (ADD) of samples collections. Moraxellaceae was the most dominant family along with Pasteurellaceae, followed by Enterobacteriaceae, Aerococcaceae and Planococcaceae and Clostridiaceae.

According to the results obtained in this thesis, a variety of families was present at a specific time during the decomposition process. The variability of the families' distribution between the collected samples might be attributed to the variability of exposure to environmental factors surrounding the sampling site. The families of bacterial communities that exhibited the most substantial changes in abundance over time on rabbit's carrions were Planococcaceae, Pseudomonadaceae and Xanthomonadaceae. Whereas, the other studies using different models showed that the Xanthomonadaceae was the family changing the most on mouse carrions (Metcalf *et al*. 2013), while on pig corpses Planococcaceae and Xanthomonadaceae were the most substantial changes in abundance over time (Pechal *et al*. 2013b). In addition, Enterobacteriaceae, Xanthomonadaceae and Planococcaceae were the most changing families on salmon carrion (Pechal and Benbow, 2016). All these works suggest that Xanthomonadaceae may be the key contributors to the general process of the decomposition.

5. Conclusion

In this thesis, the possibility to reconstruct the crime scene and the decomposition process was investigated. A 3D model aiming to integrate the biological and thanatological information was generated. The thesis tried to combine the "software" analysis with the decomposition analysis. This is an attempt to produce in the future a multilayers software able to summarize the information about a cadaver/carcass transformation for investigative purposes and for court presentation. For logistic reasons, rabbits were used as a model.

5.1 General Conclusion of 3D reconstruction Approach

In order to develop an easy and cheap method as a substitute for more expensive technique (eg. Laser scan) in this thesis, 123D Catch software was investigated for documenting the small and large crime scene. This research presented an automated approach to document the spatial characteristics of crime scenes and for reconstructing a crime scene in 3D, in order to allow a better visualisation of the crime scene and so doing facilitating the investigation process.

This online free-of-charge software produces a 3D model of scene or object from 2D images captured at the crime scene. The crime scene was obtained in the form of 3D (cloud and Texture) after uploading all the images. Results showed an accurate 3D model and easily obtained using the 123D Catch approach.

Crime scene investigation is a key to reconstruct the nature of the crimes committed. The proposed approach provides a model that allows the investigators to better visualise the spatial relations in the crime scene and gain a better insight into the crime through an exit analysis.

In addition, about the court acceptance of the reconstructed scene as evidence, first, manually modelled reconstructions can consider as evidence. This work automatically reconstructs the crime scene from real photos, which are naturally accepted as evidence. Secondly, since this reconstruction is performed using digital camera calibration, the results are metric and photo realistic. Finally, the reconstruction is based on evidence, which is collected by law enforcement officers; hence, they shall be accepted by the court.

It can summarise the conclusions as follows:

- Photo-based 3D scanning using 123D Catch is a valid mode of reconstructing the geometry of a crime scene for the purposes of investigations.
- In comparison with other measurement methodologies, including Agisoft PhotoScan and Photosynth, 123D Catch requires less time to process the three-dimensional models of an object. Moreover, data collection using 123D Catch were more accurate than others with the same number of photos used.

The 123D Catch approach when compared with other methods, including total station and laser scanning, 123D Catch was inexpensive and requires less time to collect and process the 3D models of an object or the scene. In addition, data collection using 123D Catch can be performed by anyone with a digital camera and a computer.

More studies needed to investigate the 123D Catch software in more complex environments. In addition, the results can be merged with other software to show more details about the object or the body on the screen with one click.

5.2 Microbial Community General Conclusion

The decomposition is a dynamical physical, chemical and biochemical process driven by abiotic and biotic factors, which interact giving rise to the macroscopic transformations of a carrion or cadaver. Temperature and humidity mainly affect the arrival of necrophagous insects as well as the development of post-mortem microbial communities. Such a correlation has been confirmed during this experimental work using rabbits' carrions.

The effect of the fur in modulating the structure of the decomposing bacterial communities was investigated. No significant differences were found within the same seasonal trial between carcasses with and without fur, neither from a functional nor from primary molecular analyses based on a phylum level search. Furthermore, the functional microbial diversity showed the same pattern as the decomposition progressed and the identification of the microbial taxa at phylum level only did not allow for their substantial discrimination under the tested conditions.

On the contrary, the further analysis at family level showed differences in the main taxa colonising the carcasses, depending on the decomposition stage and the presence or absence of the fur. In addition, different bacterial families were found to colonise the three different body regions in all the carrions.

This experimental work confirms several previous observations about the usefulness of the study of the bacterial communities as 'death clock'. Furthermore, the analysis of the necrobiome allows for a deeper understanding of the ecology of the decomposition process.

Consequently, based on this analysis and the obtained result it can be summarised that the fur was not affecting the pattern of weight loss during the decomposition process. Whereas, seasonal variation can impose a higher control over the weight loss, and the insect's activity acquiring a major role in causing the weight loss during the decomposition process. In addition, the presence or absence of fur does not have an impact on the decomposition rate, whereas, the season played a key role in the decomposition rate.

On the other hand, the fur does not affect the bacterial community functional diversity; however, the functional diversity was influenced by the sampling location, seasons and decomposition process. Moreover, it was observed that the content of water drives the bacterial community activity. Delay in the development of the bacterial community on the exposed skin due to the dryness in this location.

Furthermore, the fur does not have an influence on the taxonomic richness and relative abundance patterns through the decomposition process at the phylum level. While the fur exhibited an impact on the family taxonomic classification level.

In addition, the relative abundance patterns and bacterial distribution were affected by the seasons and environmental conditions at phylum and family level.

The obtained results can enable the development and optimisation of forensic estimating approaches to estimate post-mortem interval based on the changes in the microbial communities over a time interval. Consequently, these results can permit the investigation team to perform the effective and the valid interpretation of the crime scene regarding the allocated decomposing bodies and their associated collected samples.

This study provides a baseline for making adjustments in the time since death estimates on animals. However, more research on this topic needs to be performed for other types of animals that also have fur like rats or mice or dogs etc.

The results and conclusion produced by the present work have to be considered as preliminary before to extrapolate them to a more general theory about necrobiome in animals with and without fur. In fact, further investigations need to be related to other environmental and seasonal

context. In order to draw the final picture of this topic, other variables and further analyses have to be included:

- Geographical region and location where the carcass/cadaver has been placed (soil has been reported to be the main source of the microbial decomposer communities both for the animal (mice) and human cadavers) (Metcalf *et al*. 2016).

- Season and climatic conditions. As demonstrated in this study and in some other studied (Carter et al. 2015) and (Pechal et al. 2014) that the seasons can effect on the decomposition rate and on the microbial community changes during the decomposition process.

- Presence and absence of micro (insect) and macro (vertebrate) scavenger. In fact, everybody after death is usually attacked by various types of animals and insects, which can have a main role in the breakdown of the cadaver thus, accelerating the decomposition rate.

- Internal organs (Can *et al*. 2014). In order to compare the microbial communities associated with the internal and the external organs.

- Pre-existing ante-mortem microorganisms, which colonize carcass/cadaver. In order to determine the role of the Pre-existing microorganisms on the body in the decomposition process.

- Wild vs domestic animals. To investigate how the habits and the lifestyle effect on the decomposition process and on the microbial community on the cadaver.

- Cause of death. For example, by hanging, poisons, accident, drowning and burning, etc. and how the cause of death can affect the decomposition rate or insects and bacteria colonization.

- Competition among bacterial taxa (toxins or antibiotics production).

We will only be able to provide accurate estimations of time since death if we thoroughly understand the most variables in the process of decomposition.

The integration of the thanatological information with the visual information obtained with an accurate 3D reconstruction will be helpful in reconstructing and studying cases related to human death (e.g. Homicides). In fact, it will provide a complete picture of the scene with all information and measurements in one-step, which is helpful for the investigators to make an accurate statement. Furthermore, it will be important in court presentation of the case overall, to allow a better understanding, thus a better judgment of the case.

6. Appendices

6.1. Appendix 1 3D reconstruction

Table 52. Frequency performed for all measurements real and estimated, frequencies were by 20cm and small measurements by 5 cm and large measurements by 15 cm.

Total		Small measurements <50cm		Large measurements >50cm	
cm	frequencies	cm	frequencies	cm	frequencies
0-20	119	0-5	37	50-65	5
20-40	30	5-10	48	65-80	16
40-60	8	10-15	18	80-95	15
60-80	19	15-20	16	95-110	9
80-100	16	20-25	15	110-125	9
100-120	15	25-30	6	125-140	6
120-140	8	30-35	5	140-155	5
140-160	5	35-40	4	155-170	3
160-180	4	40-45	3	170-185	2
180-200	4	45-50	3	185-200	3

6.2. Appendix 2 Decomposition and Microbial Analysis

Table 53. Carcasses weight recorded during summer 2014 experiment.

Date	Day	ADD	RB1	RB2	RB3	RB4	RB5	RB6	average	SEM	STDEV
25/06/2014	0	15.90	2.4	2.6	2.15	1.95	2.6	2.35	2.34	0.10	0.26
26/06/2014	1	31.70	2.15	2.35	1.8	1.8	2.35	2.4	2.14	0.11	0.28
27/06/2014	2	46.50	2.35	2.55	1.9	2.05	2.55	2.55	2.33	0.12	0.29
28/06/2014	3	57.80	2.4	2.6	2	2.25	2.55	2.55	2.39	0.09	0.23
29/06/2014	4	69.00	2.3	2.5	1.9	2.2	2.5	2.4	2.30	0.09	0.23
30/06/2014	5	82.90	2.3	2.6	1.95	2.2	2.45	2.4	2.32	0.09	0.23
01/07/2014	6	99.30	2.3	2.6	1.9	1.9	2.25	2.4	2.23	0.11	0.28
02/07/2014	7	116.40	2.1	2.35	1.65	1.9	1.9	2.5	2.07	0.13	0.32
04/07/2014	9	154.20	1.55	2.2	1.45	1.65	1.65	1.95	1.74	0.11	0.28
07/07/2014	12	202.07	1.05	1.5	0.8	1.3	1.25	1.4	1.22	0.10	0.25
09/07/2014	14	235.40	0.9	1.35	0.7	1.25	1.25	1.5	1.16	0.12	0.30
11/07/2014	16	271.90	0.65	1.15	0.55	1	1.15	1.15	0.94	0.11	0.27
14/07/2014	19	329.50	0.65	1.1	0.55	0.9	0.9	1.1	0.87	0.09	0.23
16/07/2014	21	364.10	0.6	1	0.5	0.9	0.8	1	0.80	0.09	0.21
19/07/2014	24	422.20	0.65	1.1	0.5	0.9	0.8	1.1	0.84	0.10	0.24
23/07/2014	28	500.60	0.7	1.05	0.5	0.85	0.7	0.95	0.79	0.08	0.20
25/07/2014	30	542.30	0.6	0.95	0.5	0.8	0.65	0.9	0.73	0.07	0.18
30/07/2014	35	611.70	0.6	1	0.5	0.8	0.65	0.95	0.75	0.08	0.20
01/08/2014	37	664.50	0.6	0.95	0.45	0.8	0.6	0.95	0.73	0.08	0.21
06/08/2014	42	743.00	0.6	1.05	0.5	0.8	0.6	1	0.76	0.09	0.23
08/08/2014	44	773.20	0.6	0.95	0.5	0.8	0.6	0.9	0.73	0.08	0.18
13/08/2014	49	843.10	0.6	1.05	0.5	0.8	0.6	0.95	0.75	0.09	0.22
15/08/2014	51	869.40	0.6	1	0.5	0.8	0.6	0.95	0.74	0.08	0.21
20/08/2014	56	935.10	0.6	1	0.5	0.8	0.55	0.95	0.73	0.09	0.21
22/08/2014	58	968.20	0.6	1	0.5	0.8	0.6	0.95	0.74	0.08	0.21
27/08/2014	63	1039.70	0.6	1	0.5	0.8	0.6	0.95	0.74	0.08	0.21
29/08/2014	65	1072.80	0.6	1	0.5	0.8	0.55	0.95	0.73	0.09	0.21

Table 54. Body mass for each carcass recorded during spring 2015 experiment.

Date	Day	ADD	RB1	RB2	RB3	RB4	RB5	RB6	average	SEM	STDEV
18/03/2015	0	5.00	3.10	3.45	2.75	3.50	2.85	3.45	3.18	0.14	0.33
19/03/2015	1	12.00	3.25	3.60	2.80	3.50	3.20	3.55	3.32	0.12	0.30
20/03/2015	2	20.00	3.15	3.50	2.65	3.50	3.10	3.70	3.27	0.15	0.38
21/03/2015	3	25.70	3.10	3.40	2.70	3.65	3.00	3.75	3.27	0.17	0.40
22/03/2015	4	32.90	2.95	3.45	2.50	3.50	2.95	3.55	3.15	0.17	0.42
23/03/2015	5	39.30	3.00	3.45	2.65	3.45	2.90	3.65	3.18	0.16	0.39
24/03/2015	6	43.90	3.05	3.35	2.65	3.40	2.85	3.60	3.15	0.15	0.36
25/03/2015	7	50.10	3.05	3.25	2.6	3.35	2.85	3.65	3.13	0.15	0.37
27/03/2015	9	57.00	2.9	3.25	2.6	3.35	2.85	3.6	3.09	0.15	0.37
30/03/2015	12	81.70	2.85	3.35	2.5	3.45	2.75	3.6	3.08	0.18	0.44
06/04/2015	19	140.40	2.85	3.15	2.4	3.35	2.7	3.5	2.99	0.17	0.42
09/04/2015	22	175.60	2.55	3.2	2.2	3.15	2.5	3.3	2.82	0.19	0.46
13/04/2015	26	250.00	2.55	3.2	2.2	3.15	2.5	3.3	2.82	0.19	0.46
16/04/2015	29	217.30	2.35	2.6	1.8	2.6	2.1	2.85	2.38	0.16	0.38
20/04/2015	33	383.00	2.1	2.5	1.75	2.25	1.8	2.55	2.16	0.14	0.34
23/04/2015	36	284.70	1.9	2.2	1.5	1.75	1.75	2.3	1.90	0.12	0.30
27/04/2015	40	361.20	1.85	2	1.45	1.75	1.75	2.15	1.83	0.10	0.24
30/04/2015	43	318.40	1.8	1.85	1.35	1.6	1.55	1.95	1.68	0.09	0.22
04/05/2015	47	417.00	1.75	1.8	1.25	1.55	1.5	1.9	1.63	0.10	0.24
07/05/2015	50	450.50	1.55	1.8	1.25	1.55	1.35	1.8	1.55	0.09	0.23
11/05/2015	54	497.50	1.6	1.65	1.15	1.4	1.4	1.7	1.48	0.08	0.21
14/05/2015	57	534.80	1.4	1.6	1.1	1.4	1.4	1.7	1.43	0.08	0.21
18/05/2015	61	577.90	1.4	1.5	1.05	1.35	1.15	1.6	1.34	0.09	0.21
25/05/2015	68	659.00	1.15	1.45	0.95	1.3	1.1	1.45	1.23	0.08	0.20
01/06/2015	75	828.50	1.15	1.3	0.85	1.15	1	1.4	1.14	0.08	0.20
08/06/2015	82	839.10	1.05	1.2	0.75	1.1	0.95	1.35	1.07	0.08	0.21
16/06/2015	89	935.80	1.05	1.15	0.75	1.05	0.95	1.3	1.04	0.08	0.19
24/06/2015	96	1054.80	1.05	1.15	0.75	1.05	0.95	1.3	1.04	0.08	0.19

Table 55. Conversion of the daily temperature in experiment 1 to Accumulated Degree Days (ADD, Days ºC).

Date	Exp Day	ADD	Date	Exp Day	ADD	Date	Exp Day	ADD	Date	Exp Day	ADD	Date	Exp Day	ADD
24/06/2014	1	**15.9**	20/07/2014	27	**460.8**	15/08/2014	53	**882.2**	10/09/14	79	**1273.6**	06/10/14	105	**1640.8**
25/06/2014	2	**31.7**	21/07/2014	28	**480.2**	16/08/2014	54	**894.5**	11/09/14	80	**1288.1**	07/10/14	106	**1649.2**
26/06/2014	3	**46.5**	22/07/2014	29	**500.6**	17/08/2014	55	**908.7**	12/09/14	81	**1303.2**	08/10/14	107	**1660.5**
27/06/2014	4	**57.8**	23/07/2014	30	**521.0**	18/08/2014	56	**921.5**	13/09/14	82	**1317.2**	09/10/14	108	**1672.6**
28/06/2014	5	**69.0**	24/07/2014	31	**542.3**	19/08/2014	57	**935.1**	14/09/14	83	**1332.0**	10/10/14	109	**1683.2**
29/06/2014	6	**82.9**	25/07/2014	32	**559.6**	20/08/2014	58	**951.3**	15/09/14	84	**1348.2**	11/10/14	110	**1693.7**
30/06/2014	7	**99.3**	26/07/2014	33	**576.8**	21/08/2014	59	**968.2**	16/09/14	85	**1364.5**	12/10/14	111	**1704.0**
01/07/2014	8	**116.4**	27/07/2014	34	**594.1**	22/08/2014	60	**983.6**	17/09/14	86	**1380.0**	13/10/14	112	**1714.9**
02/07/2014	9	**135.6**	28/07/2014	35	**611.7**	23/08/2014	61	**999.1**	18/09/14	87	**1396.3**	14/10/14	113	**1725.7**
03/07/2014	10	**154.2**	29/07/2014	36	**630.7**	24/08/14	62	**1013.3**	19/09/14	88	**1411.6**	15/10/14	114	**1737.3**
04/07/2014	11	**171.3**	30/07/2014	37	**648.9**	25/08/14	63	**1026.1**	20/09/14	89	**1424.5**	16/10/14	115	**1750.8**
05/07/2014	12	**187.1**	31/07/2014	38	**664.5**	26/08/14	64	**1039.7**	21/09/14	90	**1435.5**	17/10/14	116	**1767.9**
06/07/2014	13	**202.7**	01/08/2014	39	**682.0**	27/08/14	65	**1055.9**	22/09/14	91	**1449.1**	18/10/14	117	**1785.0**
07/07/2014	14	**219.1**	02/08/2014	40	**699.2**	28/08/14	66	**1072.8**	23/09/14	92	**1463.2**	19/10/14	118	**1799.1**
08/07/2014	15	**235.4**	03/08/2014	41	**713.1**	29/08/14	67	**1088.3**	24/09/14	93	**1476.5**	20/10/14	119	**1811.8**
09/07/2014	16	**253.8**	04/08/2014	42	**728.3**	30/08/14	68	**1103.8**	25/09/14	94	**1492.9**	21/10/14	120	**1820.7**
10/07/2014	17	**271.9**	05/08/2014	43	**743**	31/08/14	69	**1120.1**	26/09/14	95	**1504.8**	22/10/14	121	**1832.3**
11/07/2014	18	**292.2**	06/08/2014	44	**758.3**	01/09/14	70	**1134.9**	27/09/14	96	**1518.4**	23/10/14	122	**1847.0**
12/07/2014	19	**312.9**	07/08/2014	45	**773.2**	02/09/14	71	**1152.1**	28/09/14	97	**1533.4**	24/10/14	123	**1857.7**
13/07/2014	20	**329.5**	08/08/2014	46	**788.3**	03/09/14	72	**1169.5**	29/09/14	98	**1549.6**	25/10/14	124	**1870.2**
14/07/2014	21	**347.6**	09/08/2014	47	**803.0**	04/09/14	73	**1186.5**	30/09/14	99	**1566.8**	26/10/14	125	**1884.9**
15/07/2014	22	**364.1**	10/08/2014	48	**817.2**	05/09/14	74	**1205.0**	01/10/14	100	**1578.8**	27/10/14	126	**1901.3**
16/07/2014	23	**382.5**	11/08/2014	49	**830.0**	06/09/14	75	**1217.4**	02/10/14	101	**1593.8**	28/10/14	127	**1913.9**
17/07/2014	24	**403.1**	12/08/2014	50	**843.1**	07/09/14	76	**1231.6**	03/10/14	102	**1610.6**	29/10/14	128	**1924.0**
18/07/2014	25	**422.2**	13/08/2014	51	**856.4**	08/09/14	77	**1244.9**	04/10/14	103	**1619.6**	30/10/14	129	**1940.2**
19/07/2014	26	**440.9**	14/08/2014	52	**869.4**	09/09/14	78	**1258.8**	05/10/14	104	**1631.3**	31/10/14	130	**1957.6**

Table 56.Conversion of the daily temperature in Exp. 2 to Accumulated Degree Days (ADD, Days ºC).

Date	Exp Day	ADD	Date	Exp Day	ADD
18/03/2015	1	5.0	02/05/2015	46	403.9
19/03/2015	2	12.0	03/05/2015	47	417.0
20/03/2015	3	20.0	04/05/2015	48	430.1
21/03/2015	4	25.7	05/05/2015	49	441.2
22/03/2015	5	32.9	06/05/2015	50	450.5
23/03/2015	6	39.3	07/05/2015	51	460.4
24/03/2015	7	43.9	08/05/2015	52	471.7
25/03/2015	8	50.1	09/05/2015	53	481.9
26/03/2015	9	57.0	10/05/2015	54	497.5
27/03/2015	10	65.3	11/05/2015	55	512.0
28/03/2015	11	75.3	12/05/2015	56	523.6
29/03/2015	12	81.7	13/05/2015	57	534.8
30/03/2015	13	89.9	14/05/2015	58	543.5
31/03/2015	14	95.6	15/05/2015	59	556.5
01/04/2015	15	101.7	16/05/2015	60	567.4
02/04/2015	16	110.1	17/05/2015	61	577.9
03/04/2015	17	118.7	18/05/2015	62	586.3
04/04/2015	18	128.6	19/05/2015	63	595.5
05/04/2015	19	140.4	20/05/2015	64	607.2
06/04/2015	20	153.4	21/05/2015	65	620.2
07/04/2015	21	164.2	22/05/2015	66	633.4
08/04/2015	22	175.6	23/05/2015	67	647.4
09/04/2015	23	188.3	24/05/2015	68	659.0
10/04/2015	24	202.7	25/05/2015	69	670.8
11/04/2015	25	210.7	26/05/2015	70	682.7
12/04/2015	26	217.3	27/05/2015	71	694.2
13/04/2015	27	229.2	28/05/2015	72	704.7
14/04/2015	28	241.4	29/05/2015	73	714.1
15/04/2015	29	250.0	30/05/2015	74	726.7
16/04/2015	30	260.1	31/05/2015	75	736.3
17/04/2015	31	268.6	01/06/2015	76	746.8
18/04/2015	32	277.2	02/06/2015	77	759.7
19/04/2015	33	284.7	03/06/2015	78	772.1
20/04/2015	34	294.1	04/06/2015	79	789.4
21/04/2015	35	306.2	05/06/2015	80	803.6
22/04/2015	36	318.4	06/06/2015	81	816.1
23/04/2015	37	333.2	07/06/2015	82	828.5
24/04/2015	38	346.8	08/06/2015	83	839.1
25/04/2015	39	354.4	09/06/2015	84	850.9
26/04/2015	40	361.2	10/06/2015	85	864.1
27/04/2015	41	368.5	11/06/2015	86	879.2
28/04/2015	42	375.4	12/06/2015	87	896.2
29/04/2015	43	383.0	13/06/2015	88	910.7
30/04/2015	44	389.2	14/06/2015	89	920.7
01/05/2015	45	396.3	15/06/2015	90	935.8
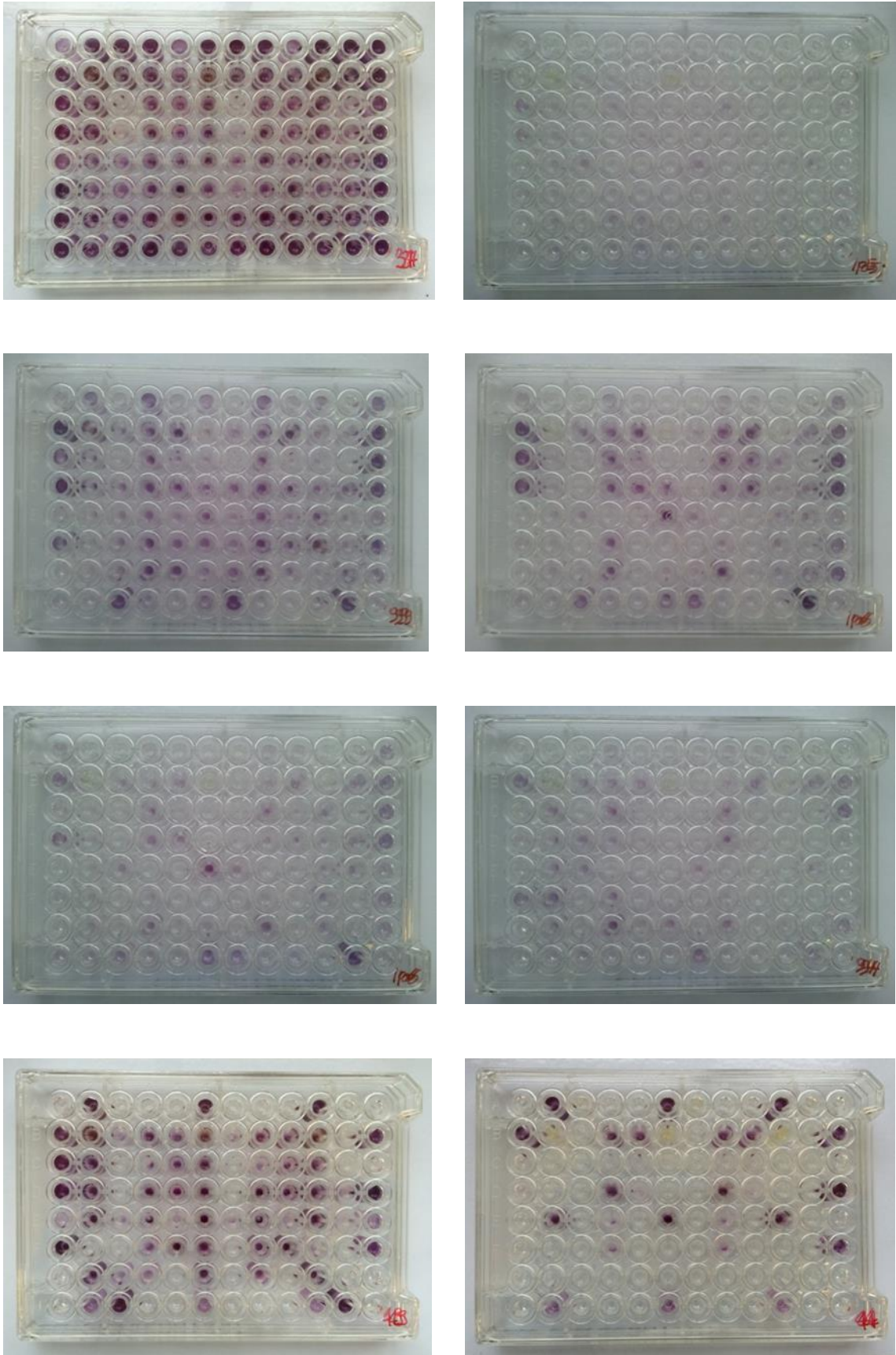
Figure 109. Pictures of some Biolog EcoPlates for different samples.

Figure 110. Microbial communities'activity in oral cavity sampling (M) of carcasses with fur (Exp. 1). Functional Activity (%) was calculated among each carcass without fur for each day sampling. Functional Variation (%) is reported as an error.
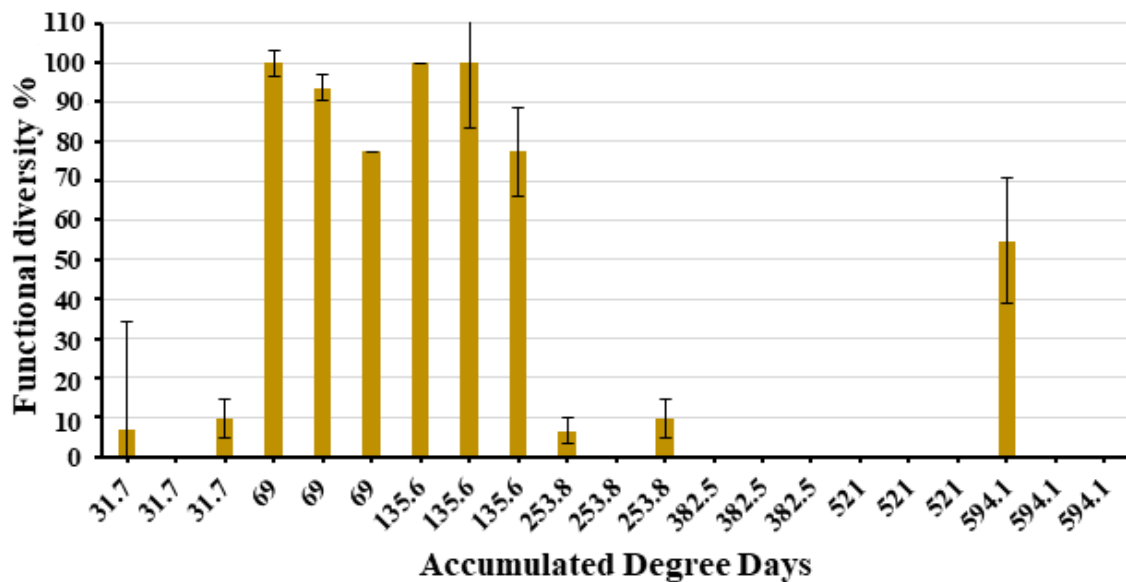
Figure 111. Microbial communities'activity in oral cavity sampling (M) of carcasses without fur (Exp. 1). Functional Activity (%) was calculated among each carcass without fur for each day sampling. Functional Variation (%) is reported as an error.
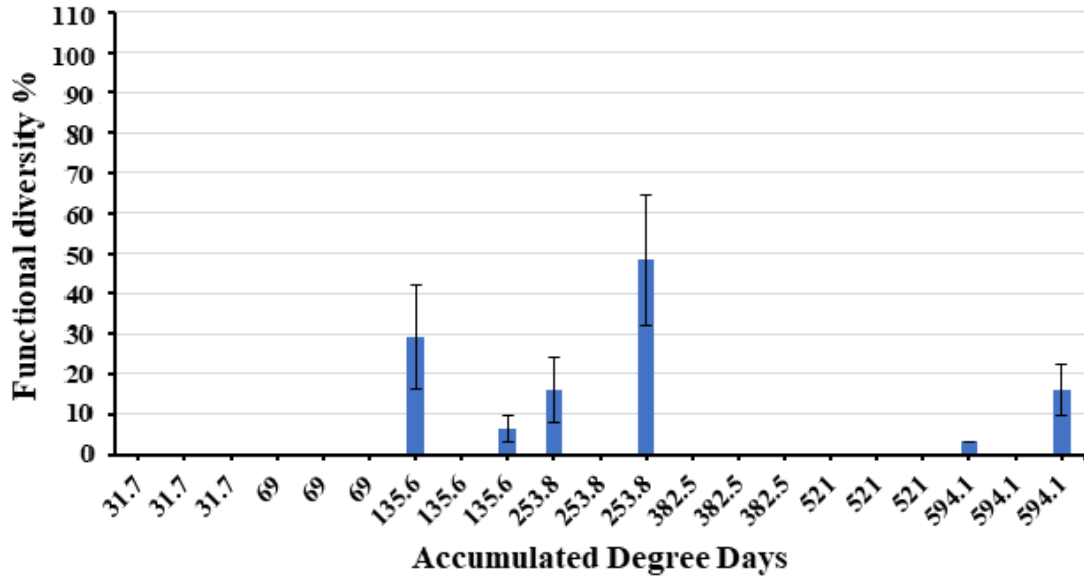
Figure 112. Microbial communities'activity in skin sampling (S) of carcasses with fur (Exp. 1). Functional Activity (%) was calculated among each carcass without fur for each day sampling. Functional Variation (%) is reported as an error.
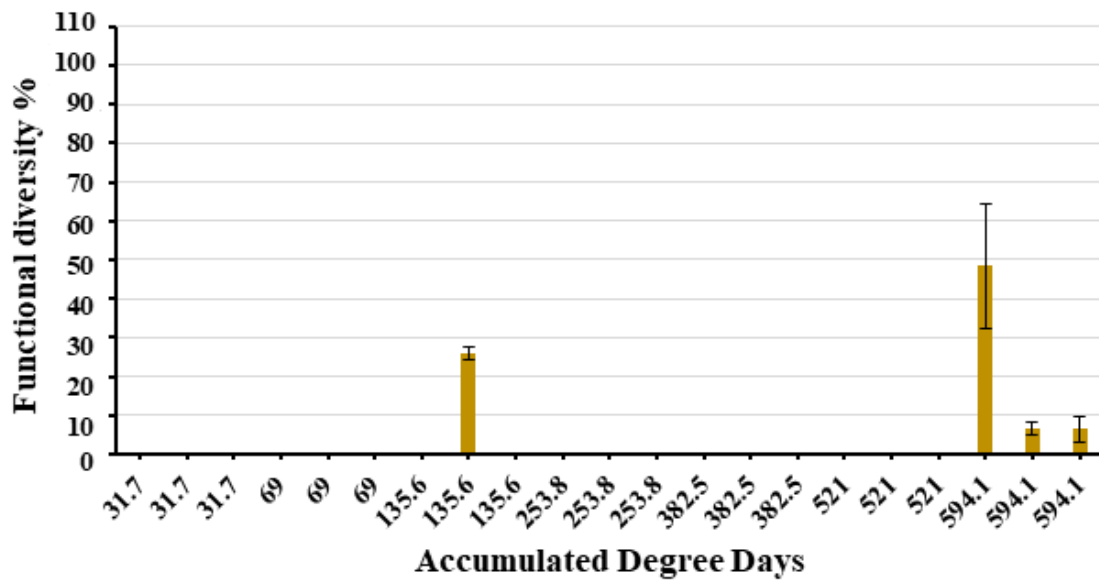
Figure 113. Microbial communities'activity in skin sampling (S) of carcasses without fur (Exp. 1). Functional Activity (%) was calculated among each carcass without fur for each day sampling. Functional Variation (%) is reported as an error.

229
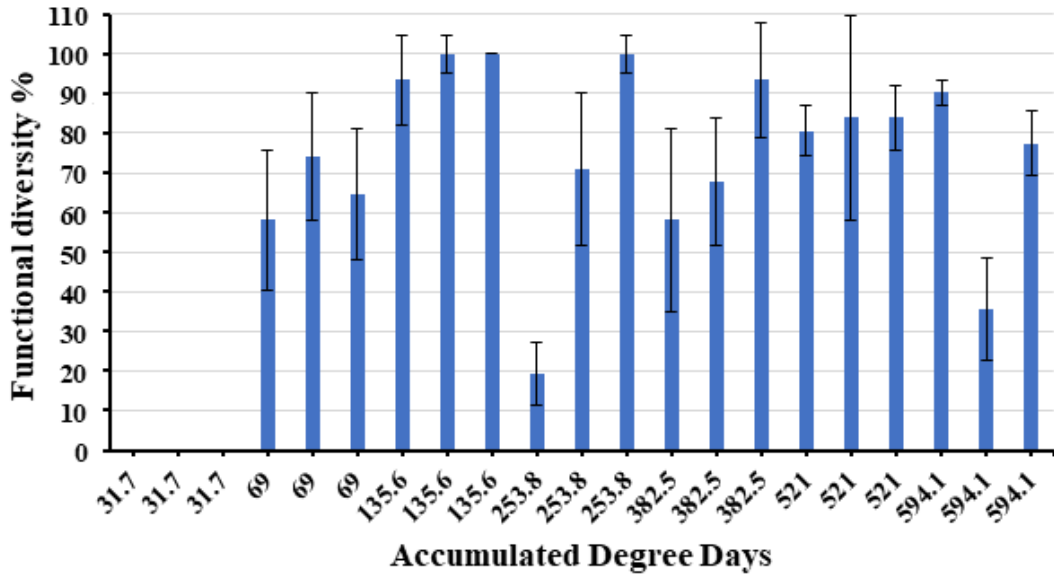
Figure 114. Microbial communities'activity in interface-sand-carrions sampling (U) of carcasses with fur (Exp. 1). Functional Activity (%) was calculated among each carcass without fur for each day sampling. Functional Variation (%) is reported as an error.
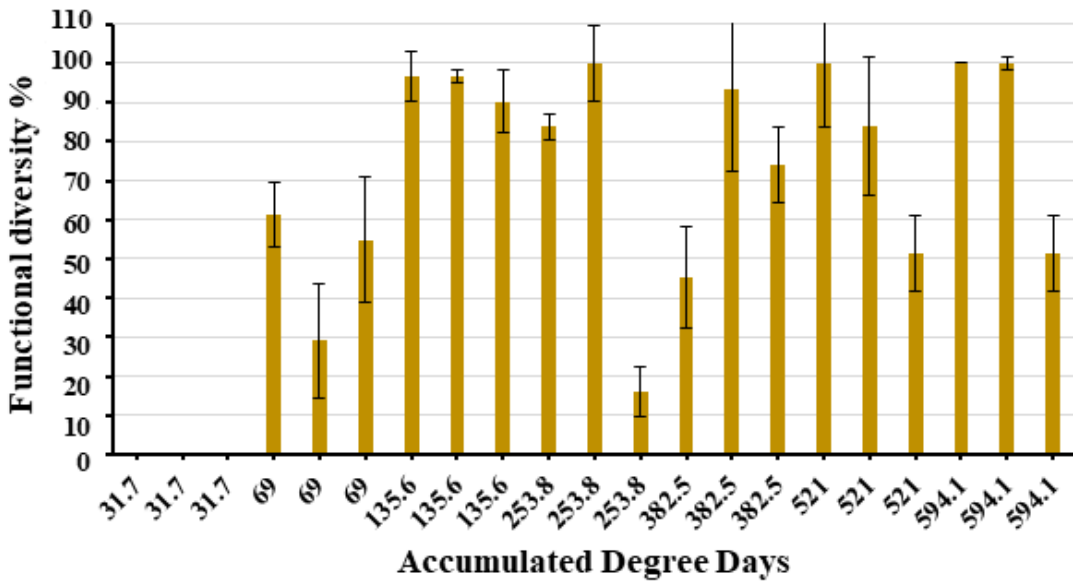
Figure 115. Microbial communities'activity in interface-sand-carrions sampling (U) of carcasses without fur (Exp. 1). Functional Activity (%) was calculated among each carcass without fur for each day sampling. Functional Variation (%) is reported as an error.

Characterisation of the microbial community functional diversity during spring 2015
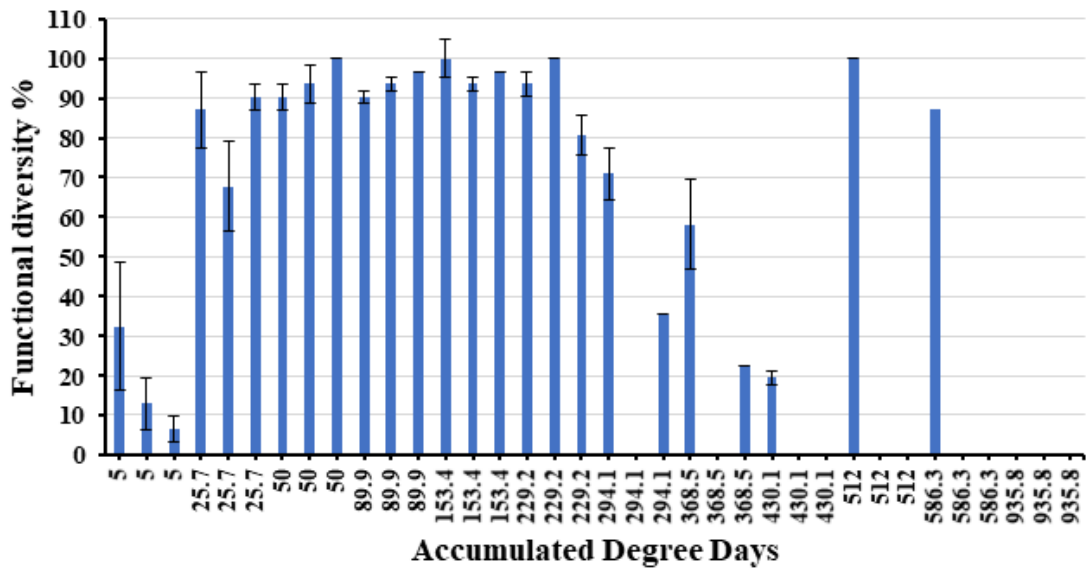
Figure 116. Microbial communities'activity in oral cavity sampling (M) of carcasses with fur (Exp. 2). Functional Activity (%) was calculated among each carcass without fur for each day sampling. Functional Variation (%) is reported as an error.
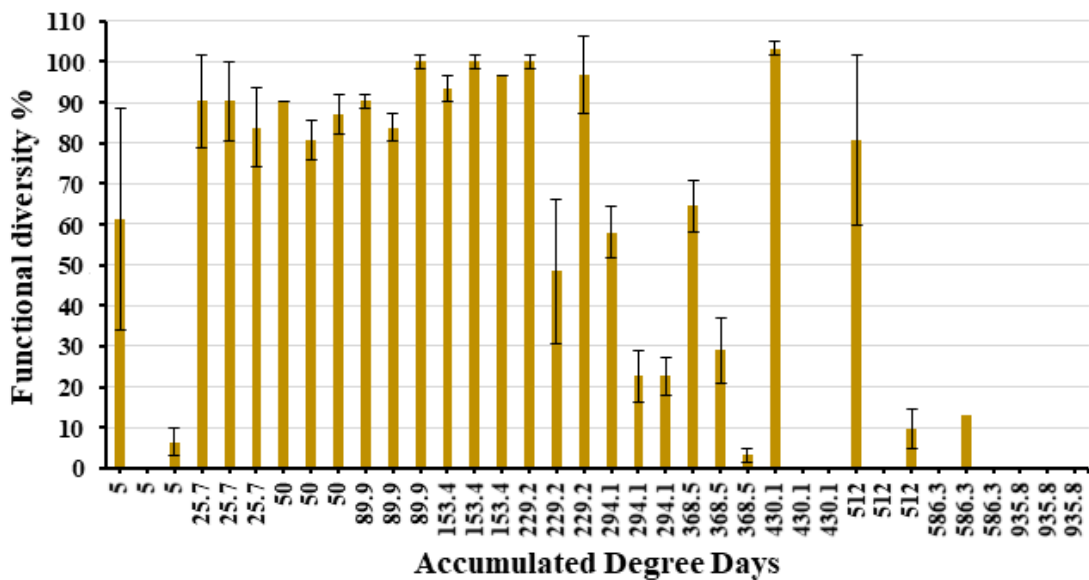
Figure 117. Microbial communities'activity in oral cavity sampling (M) of carcasses without fur (Exp. 2). Functional Activity (%) was calculated among each carcass without fur for each day sampling. Functional Variation (%) is reported as an error.
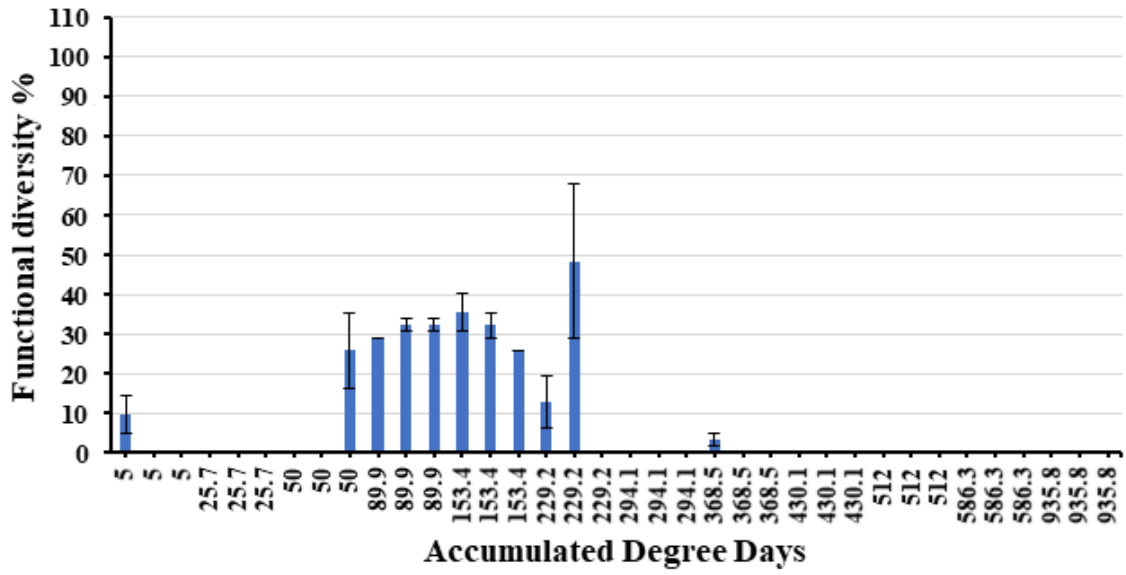
Figure 118. Microbial communities'activity in skin sampling (S) of carcasses with fur (Exp. 2). Functional Activity (%) was calculated among each carcass without fur for each day sampling. Functional Variation (%) is reported as an error.
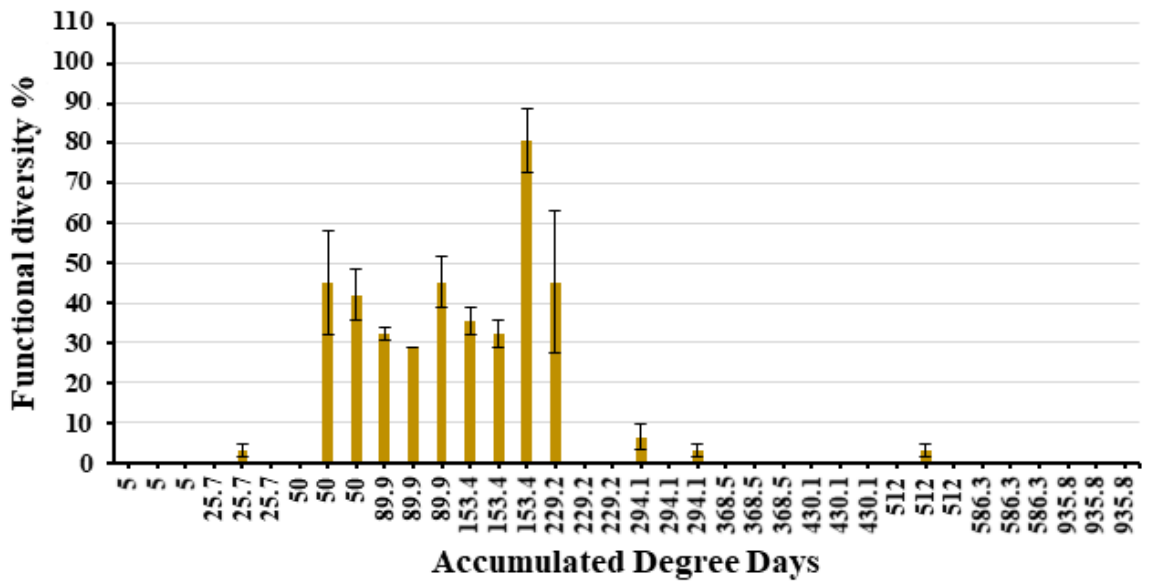
Figure 119. Microbial communities'activity in skin sampling (S) of carcasses without fur (Exp. 2). Functional Activity (%) was calculated among each carcass without fur for each day sampling. Functional Variation (%) is reported as an error.
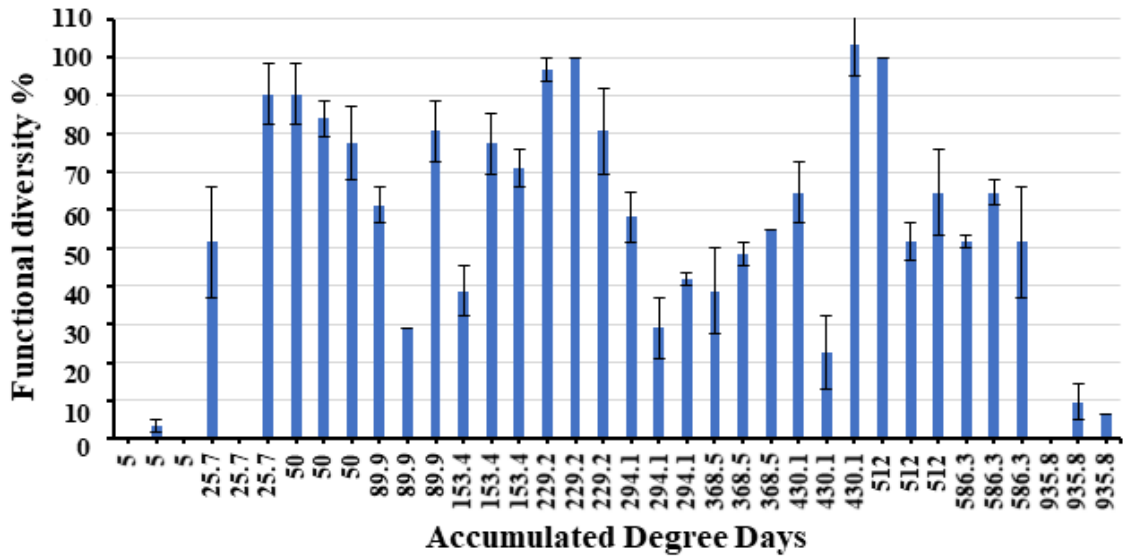
Figure 120. Microbial communities'activity in interface-sand-carrions sampling (U) of carcasses with fur (Exp. 2). Functional Activity (%) was calculated among each carcass without fur for each day sampling. Functional Variation (%) is reported as an error.
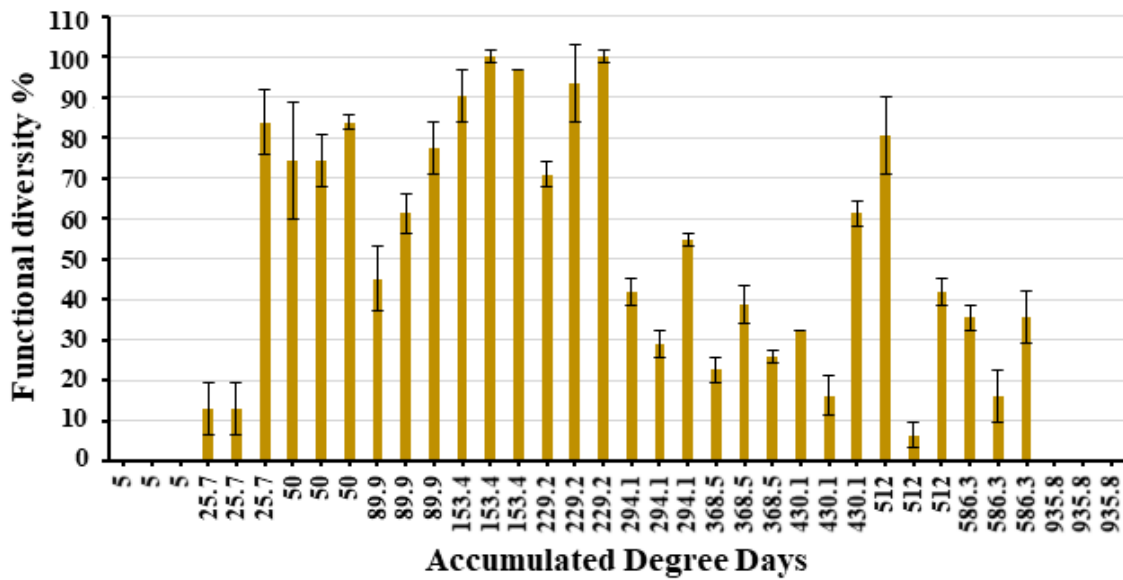
Figure 121. Microbial communities'activity in interface-sand-carrions sampling (U) of carcasses without fur (Exp. 2). Functional Activity (%) was calculated among each carcass without fur for each day sampling. Functional Variation (%) is reported as an error

Table 57. Collection of pictures for rabbits with and without fur during the decomposition stages in summer 2014 experiment (boxes 1,3 and 5 refer to rabbits without fur and boxes 2,4 and 6 referred to rabbits with fur).

Box 1

| Day 0 | Day 1 | Day 2 |

| Day 3 | Day 4 | Day 5 |

Day 6   **Day 7**   **Day 9**

Day 12   **Day 14**   **Day 16**

Day 19   Day 21   Day 24

Day 28   Day 30   Day 35

Day 37   **Day 42**   **Day 44**

Day 49   **Day 51**   **Day 56**

Day 58   **Day 63**   **Day 65**

BOX 2

Day 0

Day 1

Day 2

Day 3

Day 4

Day 5

Day 6 **Day 7** **Day 9**

Day 12 **Day 14** **Day 16**

Day 19

Day 21

Day 24

Day 28

Day 30

Day35

Day 37

Day 42

Day 44

Day 49

Day 51

Day 56

Day 58   **Day 63**   **Day 65**

BOX 3

Day 0   Day 1   Day 2

Day 3   Day 4   Day 5
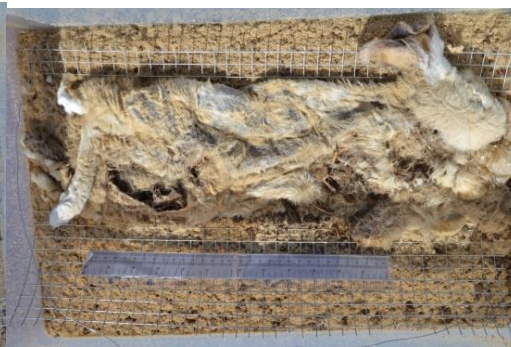
Day 6	**Day 7**	**Day 9**

Day 12	**Day 14**	**Day 16**

Day 19

Day 21

Day 24

Day 28

Day 30

Day35

Day 37   **Day 42**   **Day 44**

Day 49   **Day 51**   **Day 56**

Day 58   **Day 63**   **Day 65**

BOX 4

Day 0   Day 1   Day 2

Day 3   Day 4   Day 5

Day 6   **Day 7**   **Day 9**

Day 12   **Day 14**   **Day 16**

Day 19   **Day 21**   **Day 24**

Day 28   **Day 30**   **Day35**

Day 37   **Day 42**   **Day 44**

Day 49   **Day 51**   **Day 56**

| Day 58 | Day 63 | Day 65 |

BOX 5

Day 0

Day 1

Day 2

Day 3

Day 4

Day 5

Day 6

Day 7

Day 9

Day 12

Day 14

Day 16

Day 19   Day 21   Day 24

Day 28   Day 30   Day35

Day 37

Day 42

Day 44

Day 49

Day 51

Day 56

Day 58   **Day 63**   **Day 65**

BOX 6

| Day 0 | Day 1 | Day 2 |

| Day 3 | Day 4 | Day 5 |

Day 6

Day 7

Day 9

Day 12

Day 14

Day 16

Day 19   **Day 21**   **Day 24**

Day 28   **Day 30**   **Day 35**

Day 37

Day 42

Day 44

Day 49

Day 51

Day 56

Day 58   **Day 63**   **Day 65**

Table 58. Collection of pictures for rabbits with and without fur during the decomposition stages in spring 2015 experiment, (box 1 refer to rabbits without fur and box 2 refer to rabbits with fur).

Box1
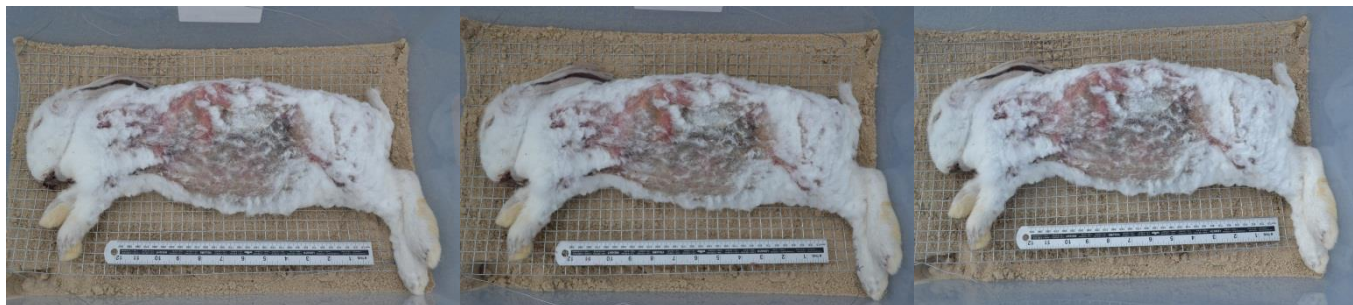
Day 0	**Day 1**	**Day 2**
Day 3	**Day 4**	**Day 5**

Day 6   **Day 7**   **Day 9**

Day 12   **Day 15**   **Day 19**

Day 22

Day 26

Day 29

Day 33

Day 36

Day 40

Day 43   Day 47   Day 50

Day 54   Day 57   Day 61

Day 64 **Day 75** **Day 82**

BOX 2

| Day 0 | Day 1 | Day 2 |

| Day 3 | day 4 | Day 5 |

Day 9   **Day 7**   **Day 6**

Day 12   **Day 15**   **Day 19**

Day 22   **Day 26**   **Day 29**

Day 33   **Day 36**   **Day 40**

Day 43   **Day 47**   **Day 50**

Day 54   **Day 57**   **Day61**

Day 64   **Day 75**   **Day 82**

7. References

ABU HANA, R. O., FREITAS, C. O., OLIVEIRA, L. S. & BORTOLOZZI, F. Crime scene classification. Proceedings of the 2008 ACM symposium on Applied computing, 2008. ACM, 419-423.

AGARWAL, A., GUPTA, M., GUPTA, S. & GUPTA, S. C. 2011. Systematic digital forensic investigation model. *International Journal of Computer Science and Security (IJCSS),* 5**,** 118-131.

AGISOFT, L. 2012. Agisoft PhotoScan user manual. Professional edition, version 0.9. 0. AgiSoft LLC.

AGOSTO, E., AJMAR, A., BOCCARDO, P., GIULIO TONOLO, F. & LINGUA, A. 2008. Crime scene reconstruction using a fully geomatic approach. *Sensors,* 8**,** 6280-6302.

AHMAD, I., AHMAD, F. & PICHTEL, J. 2011. *Microbes and microbial technology: agricultural and environmental applications*, Springer Science & Business Media.

AHMADIAN, A., EHN, M. & HOBER, S. 2006. Pyrosequencing: history, biochemistry and future. *Clinica Chimica Acta,* 363**,** 83-94.

ALTSCHUL, S. F., GISH, W., MILLER, W., MYERS, E. W. & LIPMAN, D. J. 1990. Basic local alignment search tool. *Journal of molecular biology,* 215**,** 403-410.

AMENDT, J., CAMPOBASSO, C. P., GAUDRY, E., REITER, C., LEBLANC, H. N. & HALL, M. J. 2007. Best practice in forensic entomology—standards and guidelines. *International journal of legal medicine,* 121**,** 90-104.

AMENDT, J., RICHARDS, C., CAMPOBASSO, C. P., ZEHNER, R. & HALL, M. J. 2011. Forensic entomology: applications and limitations. *Forensic science, medicine, and pathology,* 7**,** 379-392.

ANDREOTTI, R., DE LEON, A. A. P., DOWD, S. E., GUERRERO, F. D., BENDELE, K. G. & SCOLES, G. A. 2011. Assessment of bacterial diversity in the cattle tick Rhipicephalus (Boophilus) microplus through tag-encoded pyrosequencing. *BMC Microbiology,* 11**,** 6.

ARAYICI, Y. 2007. An approach for real-world data modelling with the 3D terrestrial laser scanner for built environment. *Automation in construction,* 16**,** 816-829.

ARAYICI, Y., HAMILTON, A., ALBERGARIA, P. & GAMITO, G. 2004. The scope in the intelcities project for the use of the 3D laser scanner. Fourth International Conference on Engineering Computational Technology, 7-9 September 2004, Lisbon, Portugal.

ARI, Ş. & ARIKAN, M. 2016. Next-Generation Sequencing: Advantages, Disadvantages, and Future. *Plant Omics: Trends and Applications.* Springer Cham. (pp. 109-135).

ARNALDOS, M., SANCHEZ, F., ALVAREZ, P. & GARCIA, M. 2004. A forensic entomology case from the Southeastern Iberian Peninsula. *Aggrawal's internet journal of forensic medicine and toxicology,* 5**,** 22-25.

AUTODESK. 2012. *Autodesk capturing and reality with 123d catch* [Online]. [Accessed].

BARAZZETTI, L., SALA, R., SCAIONI, M., CATTANEO, C., GIBELLI, D., GIUSSANI, A., POPPA, P., RONCORONI, F. & VANDONE, A. 3D scanning and imaging for quick documentation of crime and accident scenes. In Proceedings of SPIE, the International Society for optical engineering (vol. 8359, pp. 835910-1).

BARBER, D. & MILLS, J. 2007. *3D laser scanning for heritage: Advice and guidance to users on laser scanning in archaeology and architecture*, English Heritage.

BARLEY, S. 2009. Human microbes are picky about neighbourhoods on body. *New Scientist.* Scientist magazine. Journal reference: Science, DOI: 10.1126/science.1177486.

BARTOA, K., PUKANSKA, K. & SABOVA, J. 2014. Overview of available open-source photogrammetric software, its use and analysis. *International journal for innovation education and research,* 2**,** 62-70.

BARTON, P. S. 2015. The role of carrion in ecosystems. *Carrion ecology, evolution, and their applications.* CRC Press.

BENBOW, M., LEWIS, A., TOMBERLIN, J. & PECHAL, J. 2013. Seasonal necrophagous insect community assembly during vertebrate carrion decomposition. *Journal of Medical Entomology,* 50**,** 440-450.

BENSCHOP, C. C., QUAAK, F. C., BOON, M. E., SIJEN, T. & KUIPER, I. 2012. Vaginal microbial flora analysis by next-generation sequencing and microarrays; can microbes indicate vaginal origin in a forensic context? *International journal of legal medicine,* 126**,** 303-310.

BERGLUND, E. C., KIIALAINEN, A. & SYVANEN, A.-C. 2011. Next-generation sequencing technologies and applications for human genetic history and forensics. *Investigative Genetics,* 2**,** 23. Department of medical sciences, molecular medicine and science for life laboratory, Uppsala University, 751 85 Uppsala, Sweden.

BIOLOG 2012. Microbial Community Analysis with EcoPlates™.

BOISVERT, J., SHU, C., WUHRER, S. & XI, P. 2013. Three-dimensional human shape inference from silhouettes: reconstruction and validation. *Machine vision and applications,* 24**,** 145-157.

BORNEMISSZA, G. 1957. An analysis of Arthropod succession in Carrion and the effect of its decomposition on the soil fauna. *Australian Journal of Zoology,* 5**,** 1-12.

BOSTANCI, E. 2015. 3D Reconstruction of Crime Scenes and Design Considerations for an Interactive Investigation Tool. *arXiv preprint arXiv:1512.03156.* Ankara University, faculty of engineering, computer engineering department

BROOKES, P. 2001. The soil microbial biomass: concept, measurement and applications in soil ecosystem research. *Microbes and Environments,* 16**,** 131-140.

BRUSCHWEILER, W., BRAUN, M., DIRNHOFER, R. & THALI, M. J. 2003. Analysis of patterned injuries and injury-causing instruments with forensic 3D/CAD supported photogrammetry (FPHG): an instruction manual for the documentation process. *Forensic science international,* 132**,** 130-138.

BRUTTO, M. L. & MELI, P. 2012. Computer vision tools for 3D modelling in archaeology. *International Journal of Heritage in the Digital Era,* 1**,** 1-6.

BUCK, U., KNEUBUEHL, B., NATHER, S., ALBERTINI, N., SCHMIDT, L. & THALI, M. 2011. 3D bloodstain pattern analysis: ballistic reconstruction of the trajectories of blood drops and determination of the centres of origin of the bloodstains. *Forensic science international,* 206**,** 22-28.

BUCK, U., NAETHER, S., RASS, B., JACKOWSKI, C. & THALI, M. J. 2013. Accident or homicide–virtual crime scene reconstruction using 3D methods. *Forensic science international,* 225**,** 75-84.

BUDOWLE, B., CONNELL, N. D., BIELECKA-ODER, A., COLWELL, R. R., CORBETT, C. R., FLETCHER, J., FORSMAN, M., KADAVY, D. R., MARKOTIC, A. & MORSE, S. A. 2014. Validation of high throughput sequencing and microbial forensics applications. *Investigative Genetics,* 5,9. BioMed Central.

BUDOWLE, B., MURCH, R. & CHAKRABORTY, R. 2005. Microbial forensics: the next forensic challenge. *International journal of legal medicine,* 119**,** 317-330.

BUERMANS, H. & DEN DUNNEN, J. 2014. Next-generation sequencing technology: advances and applications. *Biochimica et Biophysica Acta (BBA)-molecular basis of disease,* 1842**,** 1932-1941.

BUTNARIU, S., GIRBACIA, F. & ORMAN, A. 2013. Methodology for 3D reconstruction of objects for teaching virtual restoration. *International journal of computer science,* 3**,** 16-21.

BUTTON, M., RODRIGUEZ, M., BRISSON, J. & WEBER, K. P. 2016. Use of two spatially separated plant species alters microbial community function in horizontal subsurface flow constructed wetlands. *Ecological engineering,* 92**,** 18-27.

BYCZKOWSKI, T. & LANG, J. A stereo-based system with inertial navigation for outdoor 3D scanning. Computer and Robot Vision, 2009. CRV'09. Canadian Conference on, 2009. IEEE, 221-228.

BYERS, S. N. 2015. *Introduction to forensic anthropology*, Routledge.

BYRD, J. H. & CASTNER, J. L. 2009. *Forensic entomology: the utility of arthropods in legal investigations*, CRC press.

CAMPOBASSO, C. P., DI VELLA, G. & INTRONA, F. 2001. Factors affecting decomposition and Diptera colonization. *Forensic science international,* 120**,** 18-27.

CAN, I., JAVAN, G. T., POZHITKOV, A. E. & NOBLE, P. A. 2014. Distinctive thanatomicrobiome signatures found in the blood and internal organs of humans. *Journal of microbiological methods,* 106**,** 1-7.

CAPOBIANCO, R. A. & CHRISTENSEN, A. M. 2017. The Effect of Clothing on the Decomposition of Human Remains. *Journal of forensic identification,* 67**,** 379.

CARD, A., CROSS, P., MOFFATT, C. & SIMMONS, T. 2015. The effect of clothing on the rate of decomposition and Diptera colonization on Sus scrofa carcasses. *Journal of forensic sciences,* 60**,** 979-982.

CARTER, D., METCALF, J. L., BIBAT, A. & KNIGHT, R. 2015. Seasonal variation of postmortem microbial communities. *Forensic science, medicine, and pathology,* 11**,** 202-207.

CARTER, D., YELLOWLEES, D. & TIBBETT, M. 2007. Cadaver decomposition in terrestrial ecosystems. *Naturwissenschaften,* 94**,** 12-24.

CAVAGNINI, G., SCALVENZI, M., TREBESCHI, M. & SANSONI, G. 2007. *Reverse engineering from 3D optical acquisition: application to Crime Scene Investigation*, Taylor & Francis Group: London, UK.

CENTENO, N., MALDONADO, M. & OLIVA, A. 2002. Seasonal patterns of arthropods occurring on sheltered and unsheltered pig carcasses in Buenos Aires Province (Argentina). *Forensic science international,* 126**,** 63-70.

CHANDLER, J. & FRYER, J. 2013. Autodesk 123D catch: how accurate is it. *Geomatics world,* 2**,** 28-30.

CHISUM, W. J. 2006. Crime Reconstruction. *In:* MOZAYANI, A. & NOZIGLIA, C. (eds.) *The Forensic Laboratory Handbook.* Humana Press.

277

CHOJNIAK, J., JAŁOWIECKI, Ł., DORGELOH, E., HEGEDUSOVA, B., EJHED, H., MAGNÉR, J. & PŁAZA, G. 2015. Application of the BIOLOG system for characterization of Serratia marcescens ss marcescens isolated from onsite wastewater technology (OSWT). *Acta Biochimica Polonica,* 62**,** 799-805.

CLAIR, E. S., MALONEY, A. & III, A. S. 2012. An introduction to building 3D crime scene models using SketchUp. *J Assoc Crime Scene Reconstr,* 18,29-47.

CLARRIDGE, J. E. 2004. Impact of 16S rRNA gene sequence analysis for identification of bacteria on clinical microbiology and infectious diseases. *Clinical microbiology reviews,* 17**,** 840-862.

CLEMENS, D. 1998. An introduction to crime scene reconstruction for the criminal profiler. *MAFS Newsletter,* 27(2). Crime and Clues. The Art and Science of Criminal Investigation

COETZEE, T. 2009. *The evidential value of crime scene investigation in child rape cases.* University of South Africa.

COLWILL, S. 2016. *Low-cost crime scene mapping: reviewing emerging freeware, low-cost methods of 3D mapping and applying them to crime scene investigation and forensic evidence.* Murdoch University.

CONSORTIUM, H. M. P. 2012. Structure, function and diversity of the healthy human microbiome. *Nature,* 486**,** 207-214.

COSTANDI, M. 2015. Life after death: The science of human decomposition. *Forensic science: neurophilosophy*. Mummified human remains at the Southeast Texas Applied Forensic Science.

COSTELLO, E. K., LAUBER, C. L., HAMADY, M., FIERER, N., GORDON, J. I. & KNIGHT, R. 2009. Bacterial community variation in human body habitats across space and time. *Science,* 326**,** 1694-1697.

COUNCIL, N. R. 2014. Findings and Conclusions: Initial Prioritized Science Needs for Microbial Forensics. National Research Council Washington. Doi 10.17226/18737.

CROSS, P. & SIMMONS, T. 2010. The Influence of Penetrative Trauma on the Rate of Decomposition. *Journal of forensic sciences,* 55**,** 295-301.

DANG, T. K., WORRING, M. & BUI, T. D. 2011. A semi-interactive panorama based 3D reconstruction framework for indoor scenes. *Computer vision and image understanding,* 115**,** 1516-1524.

DANG, T. K., WORRING, M. & BUI, T. D. 2015. Building 3D event logs for video investigation. *Multimedia tools and applications,* 74**,** 4617-4639.

DARLING, A. E., JOSPIN, G., LOWE, E., MATSEN IV, F. A., BIK, H. M. & EISEN, J. A. 2014. PhyloSift: phylogenetic analysis of genomes and metagenomes. *PeerJ,* 2**,** e243.

DAUTARTAS, A. M. 2009. The effect of various coverings on the rate of human decomposition. University of Tennessee, Knoxville. Trace: Tennessee Research and Creative Exchange

DE LEEUWE, R. 2017. The hiatus in crime scene documentation: Visualisation of the location of evidence. *Journal of Forensic Radiology and Imaging,* 8**,** 13-16.

DE REU, J., PLETS, G., VERHOEVEN, G., DE SMEDT, P., BATS, M., CHERRETTE, B., DE MAEYER, W., DECONYNCK, J., HERREMANS, D. & LALOO, P. 2013. Towards a three-dimensional cost-effective registration of the archaeological heritage. *Journal of archaeological science,* 40**,** 1108-1121.

DEBRUYN, J. M. & HAUTHER, K. A. 2017. Postmortem succession of gut microbial communities in human cadavers. *PeerJ Preprints,* 5**,** e2777v1.

DIAZ-VILARINO, L., KHOSHELHAM, K., MARTINEZ-SANCHEZ, J. & ARIAS, P. 2017. 3D modelling of building indoor spaces and closed doors from imagery and point clouds. *Sensors,* 15**,** 3491-3512.

DIAZ-VILARINO, L., KHOSHELHAM, K., MARTINEZ-SANCHEZ, J. & ARIAS, P. 2015. 3D modelling of building indoor spaces and closed doors from imagery and point clouds. *Sensors,* 15**,** 3491-3512.

DIX, J. & GRAHAM, M. 1999. *Time of death, decomposition and identification: an atlas*, CRC press.

DOUGLAS, J., BURGESS, A. W., BURGESS, A. G. & RESSLER, R. K. 2013. *Crime classification manual: A standard system for investigating and classifying violent crime*, John Wiley & Sons.

DRENOVSKY, R., VO, D., GRAHAM, K. & SCOW, K. 2004. Soil water content and organic carbon availability are major determinants of soil microbial community composition. *Microbial Ecology,* 48**,** 424-430.

DUSTIN, D., LISCIO, E. & ENG, P. 2016. Accuracy and Repeatability of the Laser Scanner and Total Station for Crime and Accident Scene Documentation. *J Assoc Crime Scene Reconstr***,** 20, 57-67.

DUTELLE, A. 2010. Documenting the Crime Scene. Evidence Technology Magazine. An excerpt from his book, (Volume 8, Number 1).

DUTELLE, A. W. 2016. *An introduction to crime scene investigation*, Jones & Bartlett Publishers.

ERICKSON, M. S., BAUER, J. J. & HAYES, W. C. 2013. The accuracy of photo-based three-dimensional scanning for collision reconstruction using 123D Catch (No. 2013-01-0784). SAE Technical Paper. SAE international 10.4271/2013-01-0784.

FAKRUDDIN, M. & CHOWDHURY, A. 2012. Pyrosequencing an alternative to traditional Sanger sequencing. *American Journal of Biochemistry and Biotechnology, 8(1), 14-20.*

FAKRUDDIN, M., CHOWDHURY, A., HOSSAIN, M. N., MANNAN, K. & MAZUMDA, R. 2012. Pyrosequencing-principles and applications. *International journal of life science and pharma research 2250-0480, vol* 2**,** 65-76.

FERNANDEZ-SARRIA, A., MARTINEZ, L., VELAZQUEZ-MARTI, B., SAJDAK, M., ESTORNELL, J. & RECIO, J. 2013. Different methodologies for calculating crown volumes of Platanus hispanica trees using terrestrial laser scanner and a comparison with classical dendrometric measurements. *Computers and electronics in agriculture,* 90**,** 176-185.

FIERER, N., LAUBER, C. L., ZHOU, N., MCDONALD, D., COSTELLO, E. K. & KNIGHT, R. 2010a. Forensic identification using skin bacterial communities. *Proceedings of the national academy of snciences of the United States of America (PNAS),* 107**,** 6477-6481.

FIERER, N., NEMERGUT, D., KNIGHT, R. & CRAINE, J. M. 2010b. Changes through time: integrating microorganisms into the study of succession. *Research in microbiology,* 161**,** 635-642.

FINLEY, S. J., BENBOW, M. E. & JAVAN, G. T. 2014. Microbial communities associated with human decomposition and their potential use as postmortem clocks. *International journal of legal medicine,* 129**,** 623-632.

FINLEY, S. J., BENBOW, M. E. & JAVAN, G. T. 2015. Potential applications of soil microbial ecology and next-generation sequencing in criminal investigations. ScienceDirect. Applied Soil Ecology, 88, 69-78.

FINLEY, S. J., PECHAL, J. L., BENBOW, M. E., ROBERTSON, B. & JAVAN, G. T. 2016. Microbial signatures of cadaver gravesoil during decomposition. *Microbial Ecology,* 71**,** 524-529. Springer US.

FISH, J. T., MILLER, L. S., BRASWELL, M. C. & WALLACE, E. W. 2013. *Crime scene investigation*, Routledge.

FISH, J. T., MILLER, L. S., BRASWELL, M. C. & WALLACE JR, E. W. 2014. Chapter 3 - Documenting the Crime Scene: Photography, Videography, and Sketching. *Crime Scene Investigation (Third Edition).* Boston: Anderson Publishing, Ltd.

FISHER, B. A. & FISHER, D. R. 2012. *Techniques of crime scene investigation*, CRC Press.

FOLMER, M. B., W. HOEH, R. LUTZ, AND & VRIJENHOEK, R. 1994. DNA primers for amplification of mitochondrial cytochrome c oxidase subunit I from diverse metazoan invertebrates. *Molecular marine biology and biotechnology,* 3**,** 294-299.

GALVIN, R. 2011. *Point of Beginning.* Point of Beginning: Burden of Proof.

GARDNER 2005. Practical crime scene processing and investigation: Practical aspects of criminal and forensic investigation series. Washington, DC: CRC Press.

GARDNER, R. 2011. *Practical crime scene processing and investigation*, CRC Press.

GARDNER, R. M. & BEVEL, T. 2009. *Practical crime scene analysis and reconstruction*, CRC Press.

GARLAND, J. L. & MILLS, A. L. 1991. Classification and characterization of heterotrophic microbial communities on the basis of patterns of community-level sole-carbon-source utilization. *Applied and environmental microbiology,* 57**,** 2351-2359.

GASSER, U., WEEKS, E. R., SCHOFIELD, A., PUSEY, P. & WEITZ, D. 2001. Real-space imaging of nucleation and growth in colloidal crystallization. *Science,* 292**,** 258-262.

GENNARD, D. 2012. Insects and decomposition. *Forensic entomology: an introduction* Second ed.: John Wiley & Sons.

GILL, G. J. 2005. *Decomposition and arthropod succession on above ground pig carrion in rural Manitoba*, University of Manitoba Winnipeg, Manitoba, Canada.

GOFF, M. 1993. Estimation of postmortem interval using arthropod development and successional patterns. *Forensic Science Review,* 5**,** 81.

GOFF, M. L. 2009. Early post-mortem changes and stages of decomposition in exposed cadavers. *Experimental and Applied Acarology,* 49**,** 21-36. In Current concepts in forensic entomology (pp. 1-24). Springer Netherlands.

GOMEZ-GUTIERREZ, A., DE SANJOSE-BLASCO, J. J., DE MATIAS-BEJARANO, J. & BERENGUER-SEMPERE, F. 2014. Comparing two photo-reconstruction methods to produce high-density point clouds and DEMs in the corral del Veleta Rock Glacier (Sierra Nevada, Spain). *Remote Sensing,* 6**,** 5407-5427.

GOODWIN, S., MCPHERSON, J. D. & MCCOMBIE, W. R. 2016. Coming of age: ten years of next-generation sequencing technologies. *Nature Reviews Genetics,* 17**,** 333-351.

GRYTA, A., FRĄC, M. & OSZUST, K. 2014. The application of the Biolog EcoPlate approach in the ecotoxicological evaluation of dairy sewage sludge. *Applied biochemistry and biotechnology,* 174**,** 1434-1443.

GUERRA, S. C. 2014. Qualifying and quantifying the rate of decomposition in the Delaware River Valley region.

GUNN, A. 2011. *Essential forensic biology*, John Wiley & Sons.

GUNN, A. & PITT, S. J. 2012. Review paper microbes as forensic indicators. *Tropical Biomedicine,* 29**,** 311-330.

HAGLUND, W. D. & SORG, M. H. 2001. *Advances in forensic taphonomy: method, theory, and archaeological perspectives*, CRC Press.

HASKELL, N. H., HALL, R. D., CERVENKA, V. J. & CLARK, M. A. 1997. On the body: Insects' life stage presence and their postmortem artifacts. *Forensic Taphonomy: The postmortem fate of human remains***,** 415-448.

HAU, T. C., HAMZAH, N. H., LIAN, H. H. & HAMZAH, S. P. A. A. 2014. Decomposition process and post-mortem changes. *Sains Malaysiana,* 43**,** 1873-1882.

HAWLENA, D., STRICKLAND, M. S., BRADFORD, M. A. & SCHMITZ, O. J. 2012. Fear of predation slows plant-litter decomposition. *Science,* 336**,** 1434-1438.

HEATHER, J. M. & CHAIN, B. 2016. The sequence of sequencers: The history of sequencing DNA. *Genomics,* 107**,** 1-8.

HEWADIKARAM, K. A. & GOFF, M. L. 1991. Effect of carcass size on rate of decomposition and arthropod succession patterns. *The American journal of forensic medicine and Pathology,* Europe PMC journal, 12**,** 235-240.

HOLOWKO, E., JANUSZKIEWICZ, K., BOLEWICKI, P., SITNIK, R. & MICHONSKI, J. 2016. Application of multi-resolution 3D techniques in crime scene documentation with bloodstain pattern analysis. *Forensic science international,* 267**,** 218-227.

HONEYCUTT, K. K. 2012. Fracture Patterns and Taphonomic Processes in a Mass Grave Environment: A Quantitative Analysis.

HOWARD, T. L., MURTA, A. D. & GIBSON, S. Virtual environments for scene of crime reconstruction and analysis. Electronic Imaging, 2000. International Society for Optics and Photonics, 41-48.

HSU, C.-H., VU, H.-H. & KANG, Y.-H. 2009. The rheology of blood flow in a branched arterial system with three-dimensional model: a numerical study. *Journal of mechanics,* 25**,** 21-24.

HUGENHOLTZ, P. 2002. Exploring prokaryotic diversity in the genomic era. *Genome biology,* 3**,** reviews0003. 1.

HUTTENHOWER, C., GEVERS, D., KNIGHT, R., ABUBUCKER, S., BADGER, J. H., CHINWALLA, A. T., CREASY, H. H., EARL, A. M., FITZGERALD, M. G. &

FULTON, R. S. 2012. Structure, function and diversity of the healthy human microbiome. *nature,* 486**,** 207.

HYDE, E. R., HAARMANN, D. P., LYNNE, A. M., BUCHELI, S. R. & PETROSINO, J. F. 2013. The living dead: bacterial community structure of a cadaver at the onset and end of the bloat stage of decomposition. *PloS one,* 8**,** e77733.

HYDE, E. R., HAARMANN, D. P., PETROSINO, J. F., LYNNE, A. M. & BUCHELI, S. R. 2015. Initial insights into bacterial succession during human decomposition. *International journal of legal medicine,* 129**,** 661-671.

IANCU, L., SAHLEAN, T. & PURCAREA, C. 2016. Dynamics of necrophagous insect and tissue bacteria for postmortem interval estimation during the warm season in Romania. *Journal of medical entomology,* 53**,** 54-66.

IZADI, S., KIM, D., HILLIGES, O., MOLYNEAUX, D., NEWCOMBE, R., KOHLI, P., SHOTTON, J., HODGES, S., FREEMAN, D. & DAVISON, A. KinectFusion: real-time 3D reconstruction and interaction using a moving depth camera. Proceedings of the 24th annual ACM symposium on User interface software and technology, 2011. ACM, 559-568.

JACKSON, A., MOUNTAIN, H. & BREARLEY, D. 2011. Forensic Science (3rd Edn). Pearson Education.

JANDA, J. M. & ABBOTT, S. L. 2007. 16S rRNA gene sequencing for bacterial identification in the diagnostic laboratory: pluses, perils, and pitfalls. *Journal of clinical microbiology,* 45**,** 2761-2764.

JAVAN, G. T., FINLEY, S. J., ABIDIN, Z. & MULLE, J. G. 2016a. The thanatomicrobiome: A missing piece of the microbial puzzle of death. *Frontiers in microbiology,* 7**,** 225.

JAVAN, G. T., FINLEY, S. J., CAN, I., WILKINSON, J. E., HANSON, J. D. & TARONE, A. M. 2016b. Human Thanatomicrobiome Succession and Time Since Death. *Scientific reports,* 6.

JENKINSON, D. 1977. Studies on the decomposition of plant material in soil. V. The effects of plant cover and soil type on the loss of carbon from 14c labelled ryegrass decomposing under field conditions. *European Journal of Soil Science,* 28**,** 424-434.

JOHNSON, A. P., MIKAC, K. M. & WALLMAN, J. F. 2013. Thermogenesis in decomposing carcasses. *Forensic science international,* 231**,** 271-277.

JORDAN, H. & TOMBERLIN, J. 2017. Abiotic and Biotic Factors Regulating Inter-Kingdom Engagement between Insects and Microbe Activity on Vertebrate Remains. *Insects,* 8**,** 54.

JULIAN, R., KELTY, S. & ROBERTSON, J. 2012. Get it right the first time: Critical issues at crime scene. *24 current issues crime just,* 24**,** 25.

KANG, Z. & MEDIONI, G. Progressive 3D model acquisition with a commodity hand-held camera. Applications of Computer Vision (WACV), 2015 IEEE Winter Conference on, 2015. IEEE, 270-277.

KARGER, B. 2009. Forensic Ballistics. *Forensic pathology reviews.* Springer.

KEITH W, S. 2015. A New Way to Capture Crime Scenes: How 3D Scanners, Laser Scanners and Advanced Cameras Are Revolutionizing Investigation as We Know It. *Law magazines.* HighBeam Research: Law Enforcement Technology.

KELLY, J. A., VAN DER LINDE, T. C. & ANDERSON, G. S. 2009. The influence of clothing and wrapping on carcass decomposition and arthropod succession during the warmer seasons in central South Africa. *Journal of forensic sciences,* 54**,** 1105-1112.

KERSTEN, T. P. & LINDSTAEDT, M. 2012. Image-based low-cost systems for automatic 3D recording and modelling of archaeological finds and objects. *Progress in cultural heritage preservation.* Springer.

KIELY, T. F. 2005. *Forensic evidence: science and the criminal law*, CRC Press.

KIRK, P. 2009. *Crime scene and physical evidence awareness for non-forensic personnel*, United Nations publication

KLINKNER, M. 2009. Forensic science expertise for international criminal proceedings: An old problem, a new context and a pragmatic resolution. *The International journal of evidence and proof,* 13**,** 102-129.

KNOX, M. A. 2012. A philosophy of crime scene reconstruction

KOCAREK, P. 2003. Decomposition and Coleoptera succession on exposed carrion of small mammal in Opava, the Czech Republic. *European journal of soil biology,* 39**,** 31-45.

KOMAR, D. & BEATTIE, O. 1998. Effects of carcass size on decay rates of shade and sun exposed carrion. *Canadian Society of forensic science journal,* 31**,** 35-43.

KYEREMATEN, R. A., BOATENG, B. A., HARUNA, M. & EZIAH, V. Y. 2006. Decomposition and insect succession pattern of exposed domestic pig (*Sus scrofa L*) carrion. J Agric Biol Sci, 8, 756-765.

LAND, M., HAUSER, L., JUN, S.-R., NOOKAEW, I., LEUZE, M. R., AHN, T.-H., KARPINETS, T., LUND, O., KORA, G. & WASSENAAR, T. 2015. Insights from 20 years of bacterial genome sequencing. *Functional & integrative genomics,* 15**,** 141-161.

LAYTON, J. 2006. How crime scene investigation works. HowStuffWorks newsletter of Science, Physical Science and Forensic Science. *Retrieved January* 13**,** 2008.

LEE, H. & PAGLIARO, E. 2013. Forensic evidence and crime scene investigation. *J Forensic Inv,* 1**,** 5.

LEE, H., PALMBACH, T. & MILLER, M. 2001. *Henry Lee's crime scene handbook*, Academic Press.

LEIPNER, A., BAUMEISTER, R., THALI, M. J., BRAUN, M., DOBLER, E. & EBERT, L. C. 2016. Multi-camera system for 3D forensic documentation. *Forensic science international,* 261**,** 123-128.

LEMAY, J. 2011. *CSI for the First Responder: A Concise Guide*, CRC Press.

LEWIS, A. & BENBOW, M. 2011. When entomological evidence crawls away: *Phormia Regina* en masse larval dispersal. *Journal of medical entomology,* 48**,** 1112-1119.

LIAO, G., ZHENG, Y., ZHAO, L. & WU, X. 2015. A novel plan for crime scene reconstruction.

Lin Liu, Yinhu Li, Siliang Li, Ni Hu, Yimin He, Ray Pong, Danni Lin, Lihua Lu, and Maggie Law. 2012. Comparison of next-generation sequencing systems. *Journal of Biomedicine and Biotechnology,* 2012, 11 pages.

LOGUIDICE, S. 2012. *Total station' technology helps police reconstruct accident and crime scenes quickly and precisely* [Online]. Syracuse Police department reconstructions accident and crimes in 3D Syracuse Media Group. [Accessed 2017].

LOUCAO, C. S. L. 2017. *Seasonal influence in the succession of entomological fauna on carrions of Canis familiaris in Lisbon, Portugal.* Universidade de Lisboa, Faculdade de Medicina Veterinária.

LOWE, A., BERESFORD, D., CARTER, D., GASPARI, F., O'BRIEN, R., STUART, B. & FORBES, S. 2013. The effect of soil texture on the degradation of textiles associated with buried bodies. *Forensic science international,* 231**,** 331-339.

MA, M., ZHENG, H. & LALLIE, H. 2010. Virtual reality and 3D animation in forensic visualization. *Journal of forensic sciences,* 55**,** 1227-1231.

MACKENZIE, B. W., WAITE, D. W. & TAYLOR, M. W. 2015. Evaluating variation in human gut microbiota profiles due to DNA extraction method and inter-subject differences. *Frontiers in Microbiology,* 6,130.

MAGNI, P., MASSIMELLI, M., MESSINA, R., MAZZUCCO, P. & DI LUISE, E. 2008. *Entomologia Forense–Gli insetti nelle indagini giudiziarie e medico-legali*, Minerva Medica.

MAKSYMOWICZ, K., ZOLNA, M., KOSCIUK, J. & DAWIDOWICZ, B. 2009. Documentation of course and results of crime scene reconstruction and virtual crime

scene reconstruction possibility by means of 3D laser scanning technology. *Archiwum medycyny sadowej i kryminologii,* 60**,** 292-297.

MANN, R. W., BASS, W. M. & MEADOWS, L. 1990. Time since death and decomposition of the human body: variables and observations in case and experimental field studies. *Journal of forensic science,* 35**,** 103-111.

MATUSZEWSKI, S., BAJERLEIN, D., KONWERSKI, S. & SZPILA, K. 2008. An initial study of insect succession and carrion decomposition in various forest habitats of Central Europe. *Forensic science international,* 180**,** 61-69.

MATUSZEWSKI, S., BAJERLEIN, D., KONWERSKI, S. & SZPILA, K. 2010. Insect succession and carrion decomposition in selected forests of central Europe. Part 1: Pattern and rate of decomposition. *Forensic science international,* 194**,** 85-93.

MEGYESI, M. S., NAWROCKI, S. P. & HASKELL, N. H. 2005. Using accumulated degree-days to estimate the postmortem interval from decomposed human remains. *Journal of forensic science,* 50**,** 618-26.

MENNELL, J. & SHAW, I. 2005. Science and technology at the crime scene. *Measurement and control,* 38**,** 75-78.

METCALF, J. L., PARFREY, L. W., GONZALEZ, A., LAUBER, C. L., KNIGHTS, D., ACKERMANN, G., HUMPHREY, G. C., GEBERT, M. J., VAN TREUREN, W. & BERG-LYONS, D. 2013. A microbial clock provides an accurate estimate of the postmortem interval in a mouse model system. *Elife,* 2**,** e01104.

METCALF, J. L., XU, Z. Z., WEISS, S., LAX, S., VAN TREUREN, W., HYDE, E. R., SONG, S. J., AMIR, A., LARSEN, P. & SANGWAN, N. 2016. Microbial community assembly and metabolic function during mammalian corpse decomposition. *Science,* 351**,** 158-162.

METHE, B. A., NELSON, K. E., POP, M., CREASY, H. H., GIGLIO, M. G., HUTTENHOWER, C., GEVERS, D., PETROSINO, J. F., ABUBUCKER, S. & BADGER, J. H. 2012. A framework for human microbiome research. *nature,* 486**,** 215.

MEYER, J., ANDERSON, B. & CARTER, D. O. 2013. Seasonal variation of carcass decomposition and gravel soil chemistry in a cold (Dfa) climate. *Journal of forensic sciences,* 58**,** 1175-1182.

MEYERS, M. S. & FORAN, D. R. 2008. Spatial and temporal influences on bacterial profiling of forensic soil samples. *Journal of forensic sciences,* 53**,** 652-660.

MICOZZI, M. S. 1996. Frozen environments and soft tissue preservation. *Forensic Taphonomy: The postmortem fate of human remains.* CRC Press.

MICROBE INOTECH LABORATORIES, I. 2009. *Microbial Identification Methods*.

MILLER, M. T. 2013. *Crime Scene Investigation Laboratory Manual*, Elsevier.

MULCAHY, M. P. A. H. M. E. 2007. Environmental microbial ecology. Pages 28-51.

MURPHY, B. L. & MORRISON, R. D. 2014. *Introduction to environmental forensics*, Academic Press.

MURTA, A., GIBSON, S., HOWARD, T., HUBBOLD, R. & WEST, A. Modelling and rendering for scene of crime reconstruction: A case study. Proceedings Eurographics UK, 1998. Citeseer, 169-173.

NIEBNER, M., ZOLLHOFER, M., IZADI, S. & STAMMINGER, M. 2013. Real-time 3D reconstruction at scale using voxel hashing. *ACM Transactions on Graphics (TOG),* 32**,** 169.

NIKOLAKI, S. & TSIAMIS, G. 2013. Microbial diversity in the era of omic technologies. *BioMed research international,* vol 2013,15 pages.

NOTTER, S. J. & STUART, B. H. 2012. The effect of body coverings on the formation of adipocere in an aqueous environment. *Journal of forensic sciences,* 57**,** 120-125.

OLIVEIRA, L. S., JUSTINO, E., FREITAS, C. & SABOURIN, R. The graphology applied to signature verification. 12th Conference of the International Graphonomics Society, 2005. 286-290.

OSTERBURG, J. W. & WARD, R. H. 2010. *Criminal investigation: A method for reconstructing the past*, Routledge.

PARKINSON, R. 2009. Bacterial communities associated with human decomposition. Victoria University of Wellington.

PARMENTER, R. R. & MACMAHON, J. A. 2009. Carrion decomposition and nutrient cycling in a semiarid shrub–steppe ecosystem. *Ecological monographs,* 79**,** 637-661.

PASTRA, K., SAGGION, H. & WILKS, Y. 2003. Intelligent indexing of crime scene photographs. *IEEE Intelligent systems,* 18**,** 55-61.

PATEL, J. B. 2001. 16S rRNA gene sequencing for bacterial pathogen identification in the clinical laboratory. *Molecular diagnosis,* 6**,** 313-321.

PAYNE, J. A. 1965. A summer carrion study of the baby pig *Sus scrofa* Linnaeus. *Ecology,* 46**,** 592-602.

PECHAL, J., CRIPPEN, T. L., TARONE, A. M., LEWIS, A. J., TOMBERLIN, J. K. & BENBOW, M. E. 2013a. Microbial community functional change during vertebrate carrion decomposition. *PloS one,* 8**,** e79035.

PECHAL, J., SCHMIDT, C. J., COUNTY, W., WARREN, D. & BENBOW, M. E. 2015. The first use of postmortem microbiomes in human death investigations. *Proceedings of the American Academy of forensic sciences 67th annual scientific meeting.* 2015 ed. Colorado AAFS.

PECHAL, J. L. & BENBOW, M. E. 2016. Microbial ecology of the salmon necrobiome: Evidence salmon carrion decomposition influences aquatic and terrestrial insect microbiomes. *Environmental Microbiology,* 18**,** 1511-1522.

PECHAL, J. L., BENBOW, M. E., CRIPPEN, T. L., TARONE, A. M. & TOMBERLIN, J. K. 2014. Delayed insect access alters carrion decomposition and necrophagous insect community assembly. *Ecosphere,* 5**,** 1-21.

PECHAL, J. L., CRIPPEN, T. L., BENBOW, M. E., TARONE, A. M., DOWD, S. & TOMBERLIN, J. K. 2013b. The potential use of bacterial community succession in forensics as described by high throughput metagenomic sequencing. *International Journal of Legal Medicine,* 128**,** 193-205.

PINHEIRO, J. 2006. Decay process of a cadaver. *Forensic anthropology and medicine: complementary sciences from recovery to cause of death***,** 85-116.

PITTS, K. & WALL, R. 2005. Winter survival of larvae and pupae of the blowfly, Lucilia sericata (Diptera: Calliphoridae). *Bulletin of entomological research,* 95**,** 179-186.

POLLEFEYS, M. 1999. *Self-calibration and metric 3D reconstruction from uncalibrated image sequences.* PhD thesis, ESAT-PSI, KU Leuven.

POLLEFEYS, M., KOCH, R., VERGAUWEN, M., DEKNUYDT, A. A. & VAN GOOL, L. J. Three-dimensional scene reconstruction from images. Electronic Imaging, 2000. International Society for Optics and Photonics, 215-226.

PRESTON-MAFHAM, J., BODDY, L. & RANDERSON, P. F. 2002. Analysis of microbial community functional diversity using sole-carbon-source utilisation profiles-a critique. *FEMS Microbiology Ecology,* 42**,** 1-14.

QUINCE, C., LANZEN, A., CURTIS, T. P., DAVENPORT, R. J., HALL, N., HEAD, I. M., READ, L. F. & SLOAN, W. T. 2009. Accurate determination of microbial diversity from 454 pyrosequencing data. *Nature methods,* 6**,** 639-641.

RAGURAM, C. W., JEN, Y.-H., DUNN, E., CLIPP, B., LAZEBNIK, S. & POLLEFEYS, M. 2010. Building Rome on a Cloudless day (ECCV 2010).

RAJSHEKAR, M., JULIAN, R., WILLIAMS, A.-M., TENNANT, M., FORREST, A., WALSH, L. J., WILSON, G. & BLIZZARD, L. 2017. The reliability and validity of measurements of human dental casts made by an intra-oral 3D scanner, with

conventional hand-held digital callipers as the comparison measure. *Forensic science international,* 278**,** 198-204.

RAMSEY, J. 1996. Crime-scene investigation and evidence collection, Jonbenet Ramsey cases.

RASTOGI, G. & SANI, R. K. 2011. Molecular techniques to assess microbial community structure, function, and dynamics in the environment. *In Microbes and microbial technology* (pp. 29-57). Springer, New York, NY.

REED JR, H. 1958. A study of dog carcass communities in tennessee, with special reference to the insects. *American Midland Naturalist***,** 213-245.

REMONDINO, F. 2011. Advanced 3D Recording Techniques for the digital documentation and conservation of heritage sites and objects. *Change over time,* 1**,** 198-214.

REMONDINO, F. 2013. Worth a thousand words–photogrammetry for archaeological 3D surveying. *Interpreting archaeological topography: airborne laser scanning, 3D data, and ground observation, occasional publication of the aerial archaeology research group***,** 115-122.

REUTER, J. A., SPACEK, D. V. & SNYDER, M. P. 2015. High-throughput sequencing technologies. *Molecular cell,* 58**,** 586-597.

RODRIGUEZ-ECHAVARRIA, K., MORRIS, D. & ARNOLD, D. Web-based presentation of semantically tagged 3D content for public sculptures and monuments in the UK. Proceedings of the 14th International Conference on 3D Web Technology, 2009. ACM, 119-126.

RODRIGUEZ, I., WILLIAM C 1996. Decomposition of buried and submerged bodies. *Forensic taphonomy: the postmortem fate of human remains.* CRC Press,1-7.

ROWLINSON, J. 2015. *Types of Forensics* [Online]. ExploreForensics: ExploreForensics. [Accessed http://www.exploreforensics.co.uk/ 2017].

SAFERSTEIN, R. 2013. *Criminalistics*, Pearson Education.

SANTAGATI, C. & INZERILLO, L. 2013. 123D Catch: efficiency, accuracy, constraints and limitations in the architectural heritage field. *International journal of heritage in the digital era,* 2**,** 263-289.

SANTAGATI, C., INZERILLO, L. & DI PAOLA, F. 2013. Image-based modelling techniques for architectural heritage 3D digitalization: limits and potentialities. *International archives of the photogrammetry, remote sensing and spatial information sciences,* 5**,** 555-560.

SAUTER, P. M. 2011. Introduction to crime scene reconstruction using real-time interactive 3D Technology. Pittsburgh, Pennsylvania. http://www.pmsmicro.com. 1-9.

SCHIRO, G. 2007. Collection and preservation of evidence. *http://www.crime-scene-investigator.net/csi-collection.html.*

SCHOFIELD, D. Animating and interacting with graphical evidence: Bringing courtrooms to life with virtual reconstructions. Computer graphics, imaging and visualisation, 2007. CGIV' 07. IEEE, 321-328.

SCHONING, J. & HEIDEMANN, G. Evaluation of multi-view 3D reconstruction software. International conference on computer analysis of images and patterns, 2015. Springer, Cham, 9257,450-461.

SCOTT, A. M. 2009. Crime scene documentation. *Wiley Encyclopedia of forensic science*.

SE, S. & JASIOBEDZKI, P. Instant scene modeller for crime scene reconstruction. 2005 IEEE Computer society conference on computer vision and pattern recognition, 23-123.

SE, S. & JASIOBEDZKI, P. Photo-realistic 3D model reconstruction. Proceedings 2006 IEEE International conference on robotics and automation. ICRA 2006, 3076-3082.

SE, S. & JASIOBEDZKI, P. 2008. Stereo-vision based 3D modelling and localization for unmanned vehicles. *International journal of intelligent control and systems,* 13**,** 47-58.

SHARANOWSKI, B. J., WALKER, E. G. & ANDERSON, G. S. 2008. Insect succession and decomposition patterns on shaded and sunlit carrion in Saskatchewan in three different seasons. *Forensic science international,* 179**,** 219-240.

SHEPPARD, K., CASSELLA, J. & FIELDHOUSE, S. 2016. How Technology is Revolutionising Crime Scene Capture and Presentation Visualising a Crime Scene using Novel Crime Scene Documentation Technology. *CSeye,* 2016**,** 16-24.

SHEPPARD, K., CASSELLA, J. P. & FIELDHOUSE, S. 2017. A comparative study of photogrammetric methods using panoramic photography in a forensic context. *Forensic science international,* 273**,** 29-38.

SIMMONS, T., CROSS, P. A., ADLAM, R. E. & MOFFATT, C. 2010. The influence of insects on decomposition rate in buried and surface remains. *Journal of forensic sciences,* 55**,** 889-892.

SINCLAIR, L., OSMAN, O. A., BERTILSSON, S. & EILER, A. 2015. Microbial community composition and diversity via 16S rRNA gene amplicons: evaluating the Illumina platform. *PloS one,* 10**,** e0116955.

SINGH, B. & CRIPPEN, T. L. 2015. Methodologies in forensic and decomposition microbiology. *Forensic entomology: international dimensions and frontiers***,** 263-282.

SNAVELY, N., SEITZ, S. M. & SZELISKI, R. 2008. Modelling the world from internet photo collections. *International journal of computer vision,* 80**,** 189-210.

SORG, M. H. & HAGLUND, W. D. 1996. *Forensic taphonomy: the postmortem fate of human remains*, CRC Press. Law - 668 pages.

STEFANOWICZ, A. 2006. The biolog plates technique as a tool in ecological studies of microbial communities. *Polish journal of environmental studies,* 15**,** 669.

STEUSSY, E. E., EISEN, J., IMWINKELRIED, E. J. & VANDAMME, A.-M. 2015. Microbial forensics: The biggest thing since DNA? University of California Davis legal studies research paper series, research paper No. 416.

STUART, B. H. & UELAND, M. 2017. Degradation of clothing in depositional environments. *Taphonomy of human remains forensic analysis of the dead and the depositional environment***,** 120. Medical - 542 pages.

SUBOCH, G. 2016. *Real-world Crime Scene Investigation: A step-by-step procedure manual*, CRC Press. Taylor and Francis group. International standard book number- 13:1-138-03212-5 (ebook- EPUB3).

SUTHERLAND, A., MYBURGH, J., STEYN, M. & BECKER, P. 2013. The effect of body size on the rate of decomposition in a temperate region of South Africa. *Forensic science international,* 231**,** 257-262.

TARONE, A., PICARD, C., SPIEGELMAN, C. & FORAN, D. 2011. Population and temperature effects on *Lucilia sericata* (Diptera: Calliphoridae) body size and minimum development time. *Journal of medical entomology,* 48**,** 1062-1068.

THALI, M. J., BRAUN, M., BUCK, U., AGHAYEV, E., JACKOWSKI, C., VOCK, P., SONNENSCHEIN, M. & DIRNHOFER, R. 2005. VIRTOPSY scientific documentation, reconstruction and animation in forensic: individual and real 3D data based geometric approach including optical body/object surface and radiological CT/MRI scanning. *Journal of forensic science,* vol. 50, No. 2.

THALI, M. J., BRAUN, M., KNEUBUEHL, B. P., BRUESCHWEILER, W., VOCK, P. & DIRNHOFER, R. Improved vision in the forensic documentation: forensic 3D/CAD-supported photogrammetry of bodily injury external surfaces combined with the volumetric radiologic scanning of bodily injury internal structures provides more investigative leads and stronger forensic evidence. V 3905, 28th AIPR Workshop: 3D visualization for Data exploration and decision making, 2000.Washington, DC, United States. International society for optics and Photonics, 213-221.

THOMAS, T., GILBERT, J. & MEYER, F. 2012. Metagenomics-a guide from sampling to data analysis. *Microbial informatics and experimentation,* 2**,** 3. BioMed Central Ltd.

TILSTONE, W. J., HASTRUP, M. L. & HALD, C. 2013. *Fisher's Techniques of Crime Scene Investigation*, CRC Press.

TREUILLET, S., ALBOUY, B. & LUCAS, Y. 2009. Three-dimensional assessment of skin wounds using a standard digital camera. *IEEE Transactions on medical imaging,* 28**,** 752-762.

TSOKOS, M. 2005. Postmortem changes and artifacts occurring during the early postmortem interval. *Forensic pathology reviews*. Humana Press, 3,183-238.

TUMER, A. R., KARACAOGLU, E., NAMLI, A., KETEN, A., FARASAT, S., AKCAN, R., SERT, O. & ODABAŞI, A. B. 2013. Effects of different types of soil on decomposition: an experimental study. *Legal medicine,* 15**,** 149-156.

TURCHETTO, M. & VANIN, S. 2004. Forensic entomology and climatic change. *Forensic science international,* 146, S207-S209.

VANIN, S., ZANOTTI, E., GIBELLI, D., TABORELLI, A., ANDREOLA, S. & CATTANEO, C. 2013. Decomposition and entomological colonization of charred bodies–a pilot study. *Croatian medical journal,* 54**,** 387-393.

VANLAERHOVEN, S. 2008. Blind validation of postmortem interval estimates using developmental rates of blowflies. *Forensic science international,* 180,76-80.

VASCONCELOS, S. D., CRUZ, T. M., SALGADO, R. L. & THYSSEN, P. J. 2013. Dipterans associated with a decomposing animal carcass in a rainforest fragment in Brazil: notes on the early arrival and colonization by necrophagous species. *Journal of insect science,* volume 13, Issue 1, 145.

VASS, A. A. 2001. Beyond the grave-understanding human decomposition. *Microbiology today,* 28**,** 190-193.

VASS, A. A. 2011. The elusive universal post-mortem interval formula. *Forensic science international,* 204**,** 34-40.

VENKATESH, S., GANESHKAR, S. V., AJMERA, S. & BANGALORE, K. 2012. Image-based 3D modelling: a simple and economical technique to create 3-D models of the face. *International journal of health sciences and research,* 2**,** 93-99.

VILLA, C., OLSEN, K. & HANSEN, S. 2017. Virtual animation of victim-specific 3D models obtained from CT scans for forensic reconstructions: living and dead subjects. *Forensic science international,* 278**,** e27-e33.

WANG, Q., GARRITY, G. M., TIEDJE, J. M. & COLE, J. R. 2007. Naive Bayesian classifier for rapid assignment of rRNA sequences into the new bacterial taxonomy. *Applied and environmental microbiology,* 73**,** 5261-5267.

WARLOW, T. 2016. *Firearms, the law, and forensic ballistics*, 3rd Edition. CRC Press, Law - 518 pages.

WEBER, K. P. & LEGGE, R. L. 2010. Community-level physiological profiling. *Bioremediation.* Springer. S.P. Cummings (ed.), Bioremediation, methods in Molecular Biology (Clifton, N.J.) 599, 263-281.

WHITE, P. 2010. *Crime scene to court: the essentials of forensic science*,3rd edition. Royal Society of Chemistry. RSCPublishing, Medical-569 pages.

WINTZINGERODE, F. V., GOBEL, U. B. & STACKEBRANDT, E. 1997. Determination of microbial diversity in environmental samples: pitfalls of PCR-based rRNA analysis. *FEMS microbiology reviews,* 21(3), 213-229. https://doi.org/10.1111/j.1574-6976.

ZANCAJO-BLAZQUEZ, S., GONZALEZ-AGUILERA, D., GONZALEZ-JORGE, H. & HERNANDEZ-LOPEZ, D. 2015. An automatic image-based modelling method applied to forensic infography. *PloS one,* 10 (3): e0118719. https://doi.org/10.1371/journal.